CONFERENCE ON

PLANETARY VOLATILES

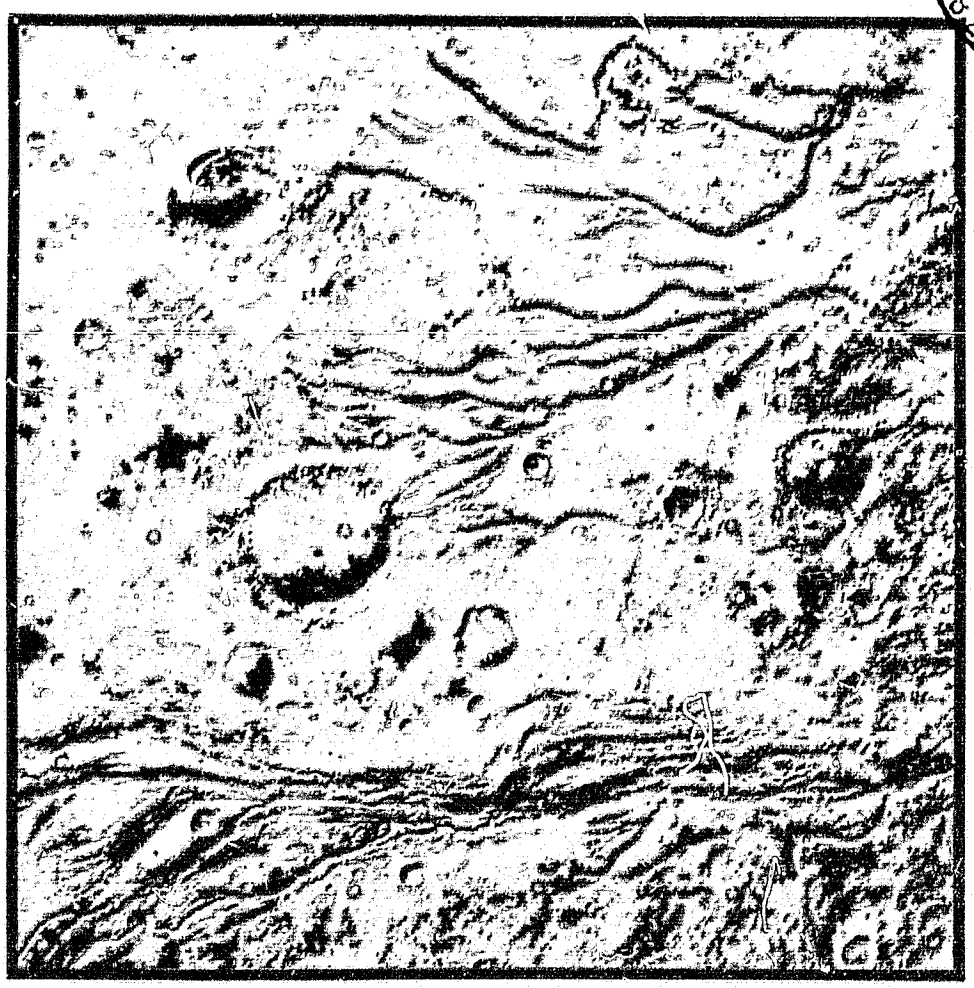

LPI Technical Report Number 83-01
LUNAR AND PLANETARY INSTITUTE 3303 NASA ROAD 1 HOUSTON, TEXAS 77058

CONFERENCE ON

PLANETARY VOLATILES

Compiled by:
Robert O. Pepin
and
Richard O'Connell

Sponsored by
The Lunar and Planetary Institute
National Aeronautics and Space Administration
National Science Foundation

A Lunar and Planetary Institute Topical Conference
Alexandria, Minnesota
October 9-12, 1982

Lunar and Planetary Institute 3303 NASA Road 1 Houston, Texas 77058

LPI Technical Report 83-01

Compiled in 1983 by the
LUNAR AND PLANETARY INSTITUTE

The Institute is operated by Universities Space Research Association under Contract NASW-3389 with the National Aeronautics and Space Administration.

This report may be cited as:
Pepin, R. O. and R. O'Connell (1983) *Conference on Planetary Volatiles*. LPI Tech. Rpt. 83-01, Lunar and Planetary Institute, Houston, 205 pp.

Papers in this report may be cited as:
Author A. (1983) Title of paper. In *Conference on Planetary Volatiles* (R. O. Pepin and R. O'Connell, eds.), p. xx-yy. LPI Tech. Rpt. 83-01, Lunar and Planetary Institute, Houston.

This report is distributed by:

LIBRARY/INFORMATION CENTER
Lunar and Planetary Institute
3303 NASA Road 1
Houston, TX 77058
Mail order requestors will be invoiced for the cost of postage and handling.

Program Committee

Authur L. Boettcher
University of California, L.A.

Sherwood Chang
NASA Ames Research Center

Richard O'Connell
Harvard University

Robert O. Pepin
University of Minnesota

James B. Pollack
NASA Ames Research Center

Norman H. Sleep
Stanford University

W. Randall Van Schmus
University of Kansas

Conference Support Staff

Bruce Barraclough, UCLA

Gary Huss, Univ. of Minnesota

Pamela Jones, LPI

Robert Luth, UCLA

Tina Masterson, Iowa St. Univ.

Scott Thieben, Iowa St. Univ.

LeBecca Turner, LPI

Production Staff, LPI

Sharon Adlis

Donna Chady

Renee Dotson

Carl Grossman

Karen Hrametz

Linda Kofler

Pam Thompson

Cover *Channels between Lunae Planum and Chryse Planitia Channels have been cut across old cratered terrain between the lava plains of Lunae Planum on the left and the plains of Chryse Planitia to the right. Three separate channel systems are visible, starting from the north: Vedra Vallis, Maumee Vallis, and Maja Vallis. Flow along the eastern edge of Lunae Planum converged to cut Maja Vallis. Numerous teardrop-shaped islands occur upstream of the main channel. Below the channel to the east (off the right side), the flow diverges across Chryse Planitia. (NASA photograph #211-5101.)*

Contents

Introduction

Volatile elements and their compounds are greatly depleted in inner solar system planets, and in most meteorites, relative to their cosmic abundances. The fractions that remain are the source of atmospheres surrounding these planets and have played an important role in the histories of their interiors. The nature of preplanetary carriers of volatiles, and how they were associated with the bulk of planetary matter, are subjects of active debate. But recent determinations of the atmospheric compositions of Mars and Venus, and recognition that primordial gases are still being released from the interior of the Earth, now provide data for comparing the volatile inventories of meteorites and the terrestrial planets with the predictions of different models for their origin and distribution.

Volatiles are a controlling factor in many of the details of planetary development. Initial distributions, abundances, and chemical compositions of these components may determine the evolutionary tracks taken by primitive planetary assemblages as they accrete and differentiate to form a core, mantle, crust, and hydrosphere-atmosphere. The types, time scales, and ultimate degrees of petrologic and tectonic processing in differentiation are sensitive to the influence of volatile species such as H_2O and CO_2 on mineral associations, chemical partitioning, and dynamics of heat and mass transport. Masses and compositions of planetary atmospheres (and hydrospheres, biospheres, and sedimentary columns, if they exist) provide lower limits on primordial volatile inventories. The challenge is to read the integrated record of volatile fluxes contained in these reservoirs for what they can reveal about the initial distribution of volatiles within planets, the rates and mechanisms of their transfer between planetary surfaces and interiors, and the physical states and chemical compositions of the species that took part in these exchanges during the geologic history of a planet. Knowledge of recycling processes along with understanding of irreversible transfers such as loss of atmospheric gases to space are essential elements of any comprehensive theory for the evolution of planetary atmospheres and hydrospheres. On Earth, the origin and development of the earliest biosphere must have been sensitively related to the chemical nature of its environment. One of the goals of paleobiology is to deduce the interre-

lations between evolving life and the physical and chemical properties of Earth's atmosphere, ocean, and crust.

Most of the papers presented at the Conference on Planetary Volatiles described research within three broad topical areas that collectively represent the principal focus of the study of volatiles in the terrestrial planets:

Initial and Present Volatile Inventories and Distributions in the Earth, Other Planets, Meteorites, and Comets

Initial conditions and processes (*preplanetary form, distribution and carriers of volatiles; how, when and where did planets accrete volatiles?; where, when, and to what extent did early fractionation and loss of volatiles from parent bodies and planets occur?*); present inventories, reservoirs and fluxes (*atmospheric, surficial, crustal, mantle, core*).

Observational Evidence on the Time History of Volatile Transfer among Reservoirs

Early catastrophic degassing of the terrestrial planets (*extent, energy sources*); the significance of continuing juvenile degassing; changes in the chemical compositions and masses of planetary atmospheres and hydrospheres with time (*astrophysical influences, oxidation states, greenhouse gases, climate impacts*); development of volatile element cycling among surficial and interior reservoirs (*geochemical, geological, and biological constraints; possible prebiotic cycles and the evolution of biological redox processes*); chemical and isotopic heterogeneity in planetary interiors, and relation of volatile reservoirs to chemical reservoirs.

Volatiles in Planetary Bodies, their Mechanisms of Transport, and their Relation to Thermal, Chemical, Geological and Biological Evolution

Thermal histories (*time variations of surface and interior temperatures, melting, differentiation*); transport mechanisms (*styles of mass transport, depths and modes of convection, relation of heat and volatile transport*); styles of outgassing (*point volcanism (Io mode) plate tectonics, flood volcanism, shield volcanism*); geochemistry of volatiles in planetary interiors (*solubility, diffusivity in mantle phases, stability and mobility of volatile-rich phases, oxidation and thermodynamic*

state of mantle); recycling of volatiles into planetary interiors (*incorporation of volatiles into solid phases, biological and nonbiological recycling mechanisms*); loss of volatiles to space (*mechanisms, past and present rates*).

The 96 conference participants represented the many different approaches, viewpoints, and disciplines necessary for a provocative and profitable discussion of volatiles in the solar system and their influence on planetary evolution. Abstracts of all papers given at the conference are included in this technical report. A number of these abstracts were expanded by their authors to include extended bibliographies and illustrations used by the speakers in the presentation of their talks.

Program

Saturday, October 9, 1982
8:30 a.m. - 12:00 noon

INTRODUCTION
Conveners: Richard O'Connell and Robert O. Pepin

SESSION I - PRESENT VOLATILE INVENTORIES

Chairmen: Fraser Fanale
John W. Morgan

Owen T.*
Current compositions of planetary atmospheres

Turekian K.*
What are the volatiles like inside the earth?

Morgan J. W.*
Planetary abundances of volatile elements: A datum from the Earth's upper mantle

Podosek F. A.* Bernatowicz T. J. Honda M. Kramer F. E.
The sedimentary inventory of atmospheric xenon

Jovanovic S. Reed G.*
Trapping of gases and low temperature volatiles in lunar samples

Moore C. B.*† Evans K. L. Tartar J. G.
Chlorine concentrations in chondrites

Gibson E. K.*
A review of distributions of sulfur in solar system objects

Duba A. G.* Shankland T. J.
High electrical conductivity in carbon-bearing rocks and meteorites: Implications for planetary interiors and asteroids

---

* - Speaker

† - Scheduled to speak but was unable to attend

Saturday, October 9, 1982
1:00 p.m. - 5:30 p.m.

SESSION II - VOLATILES IN EARTH'S INTERIOR

Chairmen: Arthur L. Boettcher
Richard O'Connell

Boettcher A.*
Progress in the experimental investigation of volatile components in vapors and silicate liquids at high pressures

Sato M.*
Redox state and stable distribution of volatiles in planetary interiors

Arculus R. J. Gust D. A. Holmes R. D.*
Oxidation states of the upper mantle and controls on evolved volatiles

Holmes R. D.* Arculus R. J.
Metal-silicate redox reactions: Implications for core-mantle equilibrium and the oxidation state of the upper mantle

Eggler D. H.*† Schneider M. E.
Geochemistry of fluids in the terrestrial upper mantle

Mathez E A.* Dietrich V. J. Irving A. J.
Carbon in rocks from the Earth's mantle

Des Marais D. J.* Sakai H. Moore J. G.
Stable carbon isotopes in midoceanic basaltic glasses

Nordlie B. E.* Theiben S. E. Burggraf D. R.
Equilibrium composition of the Mt. St. Helens magmatic volatile phase from the pyrrhotite-magnetite assemblage

Rutherford M. J.* Carroll M.
Volatile element transport from the mantle: Experimental solubility data for S-system

Ito E.* Anderson A. T., Jr.
Sources of volatiles in subduction zone magmas: Possible geologic cycling of chlorine and water

Smith S. P.*
Origin and circulation of hydrothermal fluids at Larderello: Clues from noble gases

Sunday, October 10, 1982
8:30 a.m. - 11:15 a.m.

SESSION III - SOURCES OF PLANETARY VOLATILES

Chairmen: A. G. W. Cameron
Patrick Cassen

Black D. C.*
Volatiles and solar-nebula models

Irvine W. M.*
Boundary conditions on the paleoenvironment: The chemical compositions of pre-solar nebulae

Cassen P. M.*
Models of the solar nebula: What determined the thermal structure?

Chang S.* Kerridge J. F.
Accretion of volatiles

Fegley B.*
A condensation-accretion model for volatile element retention

Ramadurai S.*†
Incorporation of noble gases in meteorites

Ashwal L. D.* Colucci M. T. Lambert P. · Henry D. J.
Gibson E. K., Jr.
Fluid inclusions in meteorites: Direct samples of extraterrestrial volatiles

Sunday, October 10, 1982
12:45 p.m. - 2:45 p.m.

SESSION IV - ORIGIN OF PLANETARY ATMOSPHERES

Chairman: Tobias Owen

Pollack J. B.* Black D. C.
Noble gases in planetary atmospheres: Implications for the origin and evolution of atmospheres

Lal D. Rao M. N.*†
Early volatiles accretion in inner planets

Cameron A. G. W.*
Compositional clues to the history of the terrestrial planet atmospheres

Mizuno H.*
The structure of the primordial atmosphere and the amount of grains

Tamhane A. S. Wetherill G. W.*
Bubble diffusion and composition of inert gases on Venus

Sunday Evening, October 10, 1982
8:00 p.m. - 9:30 p.m.

SESSION V - NEAR-SURFACE VOLATILE RESERVOIRS

Chairman: Everett K. Gibson

Fanale F.* Salvail J. R.
Ice-poor regolith development and destruction on small icy-dusty or icy-rocky objects

Clifford S. M.*
Mechanisms for the vertical transport of H_2O within the martian regolith

Jakosky B. M.*
Exchange of water between the regolith, atmosphere, and polar caps of Mars

Staehle R. L.*
Importance of non-terrestrial volatiles to future space operations

Brass G. W. Thurmond V. L. (Poster Presentation)
Brines at low temperatures

Monday, October 11, 1982
8:00 a.m. - 12:00 noon

SESSION VI - PLANETARY EVOLUTION AND DEGASSING I

Chairmen: V. Rama Murthy
George W. Wetherill

Lange M. A.* Ahrens T. J.
Accretion of water by the terrestrial planets

Lambert P.* Lange M. A.
Processes of shock dehydration on accreting planets

Weissman P. R.*
Cometary impacts on the terrestrial planets

Richardson S. M.* Reynolds R. T. Grossman A. S.
Pollack J. B.
Atmospheric evolution during accretion: A numerical model

Visconti G.*
Thermal and degassing histories of the Earth and Venus

Scott D. H.* (Poster Presentation)
Meander relicts: Direct evidence of extensive flooding in northern plains of Mars

Schultz P. H.* Rogers J. L.
Impact basins and the storage/release of volatiles on Mars

Condomines M.* Gronvold K. Hooker P. J. O'Nions R. K.
Osburgh E. R.
Comparison of He, Sr and Pb isotopic variations in the Icelandic 'hotspot'

Zindler A.* Goldstein S. Jagoutz E.
Mantle differentiation and crustal growth: An isotopic viewpoint

Fisher D. E.*
Homogeneity of argon and the ^{40}Ar-^{36}Ar ratio within the solid earth

Monday, October 11, 1982
1:00 p.m. - 3:15 p.m.

SESSION VII - PLANETARY EVOLUTION AND DEGASSING II

Chairman: Frank A. Podosek

Sarda Ph. Staudacher Th. Allègre C. J.*
Comparative Ar-Xe systematics in the Earth's mantle

Kurz M. D.* Allègre C. J.
Constraints on the evolution of the mantle from noble gas isotope ratios

Jenkins W. J.*
Terrestrial helium isotopic systematics

Prather M. J.*
Helium: Further evidence of a similar origin for Earth and Venus

Sabu D. D. Manuel O. K.*
The noble gas record of the primitive nebula and the Earth

Turner G.* Jones C. M. Butterfield A.
Ancient atmospheric argon in cherts

O'Nions R. K.*† Oxburgh E. R.
Relationships between heat and rare gas transport in the Earth

Monday Evening, October 11, 1982
8:00 p.m. - 10:15 p.m.

SESSION VIII - LOSS OF GASES TO SPACE

Chairman: James B. Pollack

Zahnle K.* Walker J. C. G.
Evolution of solar ultraviolet luminosity

Kasting J. F.* Pollack J. B.
Loss of a massive early ocean from Venus

Kumar S.* Hunten D. M. Pollack J. B.
Nonthermal escape of hydrogen and deuterium from Venus and implications for loss of water

Fox J.*
Escape of nitrogen from the Martian atmosphere

Strobel D.*
Chemistry and evolution of Titan's atmosphere

Hall P. K.*
Sputtering of volatile reservoirs

Tuesday, October 12, 1982
8:00 a.m. - 1:15 p.m.

SESSION IX - THERMAL STATES AND VOLATILE TRANSPORT

A. THERMAL EVOLUTION

Chairman: Norman H. Sleep

Peltier W. R.*†
Thermal history and convection

England P.* Bickel M.
Constraints on Archean geothermal regimes and their implication for Earth thermal history models

Phillips R.*
Interrelationships of volatile history, thermal evolution and tectonics in the terrestrial planets

O'Connell R.* Houseman G. Hager B. H.
Heat and volatile transport in planetary interiors

Sleep N. H.*
Volatile exchange with the mantle at mid-oceanic ridges and the thermal history of the Earth's interior

B. OXYGEN IN ATMOSPHERES

Chairmen: Sherwood Chang
James Kasting

Chang S.* Bar-Nun A.
Prebiotic carbon cycle: Photochemical reduction of CO in Earth's primitive atmosphere

Boston P. J.* Stoker C.
Microbial metabolism of organic molecules produced by chemical synthesis in a reducing atmosphere: Implications for the origin of life

Burke K.*
Was the Earth's atmosphere anoxic between 3.8 and 2.0 g.a. ago?

Baur M. E.* Hayes J. M. Walter M. R.
Implications of stable isotope variation in a banded iron formation for Precambrian volatile reservoirs

Schidlowski M.*
Early atmospheric oxygen levels: Constraints from Archaean photoautotrophy

Richardson S. M.* Grossman A. S.
Numerical experiments with the geochemical cycle for carbon

Broecker W.*†
What controls the CO_2 content of the atmosphere?

Veizer J.*
Geologic buffering of the hydrosphere-atmosphere system in post-Hadean times

Allègre C. J.*
The mantle-atmosphere-hydrosphere system and the geochemical cycle for volatile elements

ABSTRACTS

THE MANTLE ATMOSPHERE-HYDROSPHERE SYSTEM AND THE GEOCHEMICAL CYCLE FOR VOLATILE ELEMENTS.

C.J. Allègre, Laboratoire de Géochimie, Institut de Physique du Globe, 4 Place Jussieu-75230 Paris cedex 05-France.

Atmosphere and hydrosphere systems have been formed (at least partially) by outgassing mantle processes. On the other hand, subduction processes inject into the mantle some material coming from the surface of the Earth. The (mantle) + (atmosphere + hydrosphere) can therefore be modelled as a two-reservoir complementary-coupled system. On the other hand, atmosphere, hydrosphere and sediments are linked by a set of equilibrium conditions, and the mantle can be divided into upper and lower mantle. The overall cycle also has a leak, which is the transformation of sediments into continental crust. Such complex systems can be described by coupled differential equations, and the time evolution can be examined using phase plane techniques in both linear and non linear cases. We have treated successively the three important cases :

a) evolution of concentration of volatile elements
b) evolution of mantle isotope ratios
c) evolution of radiogenic isotopic ratios

The models have been applied to different types of volatiles including rare gases, carbon, nitrogen, water, and chlorine. We can then model quantitatively the evolution of the mantle and the earth's surface through geological time under various conditions. The different elements are described by their transfer functions and their residence time in both reservoirs; the modelling results lead to major distinctions between the geochemical cycles of the various elements.

OXIDATION STATES OF THE MANTLE AND CONTROLS ON EVOLVED VOLATILES.
R.J. Arculus, D.A. Gust* and R.D. Holmes, Research School of Earth Sciences, Australian National University P.O. Box 4, Canberra A.C.T. 2600, Australia.
*Current address: N.A.S.A., L.B.J. Space Center, Houston, TX 77058, U.S.A.

The oxidation state of the upper mantle reflects the variety of processes that have occurred since mantle formation about 4.5 byr ago. For example, protocore-mantle equilibrium, meteorite bombardment, magma extraction and infiltration, metasomatic fluxing and lithosphere recycling may have all combined to result in distinctive intrinsic oxygen fugacity (fO_2) signatures in specific mantle materials. The influence of oxidation state on evolved volatiles is important with respect to the nature of the degassed species and the possibility that there has been a secular change in these species through time. There is presently some controversy over the buffering agents in the upper mantle:- carbon-carbonate or ferrous-ferric equilibria being the rival contenders. Furthermore, the significance of electrochemical cell determinations of intrinsic fO_2 with respect to in situ oxidation states in the upper mantle and magma genesis are points of contention. We present some new data which bear on these general problems.

Recent measurements of the intrinsic fO_2's of (1) peridotites (and spinels separated therefrom), (2) megacryst spinels, (3) kimberlite-hosted megacryst ilmenite, (4) alkali basalt-hosted magnetite bearing cumulates have revealed dramatic variations in the redox state of these mantle-derived materials. These variations in fO_2 may exceed six orders of magnitude. Repeated determinations of the free energy of formation of standard oxides with stabilized, O_2-specific ZrO_2 electrolytes reveal no discrepancy with accepted data, so that erratic behaviour of the cells does not seem to be a problem in intrinsic fO_2 measurements.

Type 1 (chrome diopside type) spinel peridotites from widely dispersed localities in Australia, U.S.A., West Germany and Japan have intrinsic fO_2's close to the iron-wüstite (IW) buffer curve in T-fO_2 space. Other intrinsic fO_2 data consistent with a reduced upper mantle have been published for a marine-erupted Hawaiian basalt[1], the Bushveld[2] and Skaergaard[3] intrusions. Interestingly, where calculation of fO_2 for given peridotite assemblages have been made through application of equilibrium of the sort $6Fe_2SiO_4 + O_2 \rightleftharpoons 3Fe_2Si_2O_6 + 2Fe_3O_4$[4], oxidation states between IW and fayalite-magnetite-quartz (FMQ) have been determined. However, intrinsic and calculated fO_2's do not coincide with the former determinations being reduced by up to an order of magnitude or more. It is possible that defect structures in the spinel phase (cation excess) are responsible for this discrepancy in calculation (see also [5]).

Measurements of intrinisc fO_2 of rarer upper mantle-derived rock types and mineral species have revealed that oxidation states considerably higher than IW may exist in the upper mantle. For example, megacryst ilmenites associated with several southern African kimberlite pipes have intrinsic fO_2's close to the Ni-NiO (NNO) and FMQ buffers. These values are more oxidized than those calculated by Eggler[6] for olivine-orthopyroxene-ilmenite assemblages from kimberlites, and are not compatible with the stable existence of graphite or diamond in kimberlite fluids. Similar oxidized values have been obtained for megacryst ilmenite from the alnöitic breccia pipes in the Solomon Islands[7]. Type 2 (aluminous augite type) peridotites from San Carlos (U.S.A.) and magnetite in cumulates from alkaline rock types in eastern New South Wales (Australia) are also close to or more oxidized than the NNO buffer (e.g. $\log_{10} fO_2 \simeq -9.0$ at 1000°C).

Type 1 peridotites are regarded by most petrologists as representative of the major portion of the shallower upper mantle. However, the volumetrically minor portion represented by type 2 peridotites and sampled by kimberlitic and alkaline igneous activity points to the existence of strongly

oxidized source areas in the mantle. Because these oxidized sources are associated with volatile-rich magmatism, their influence on the composition of erupted volcanic gases may be considerable in spite of their limited volume. The important point is that a range of intrinsic fO_2's exists at present in the upper mantle, and the most important questions that need answering are 1) What are the relative proportions and significance of these various oxidation states? 2) What are the origins of these varied states? 3) How long has the dispersion in oxidation states persisted?

Possible explanations for the development of contrasted oxidation states in the upper mantle include: (1) long-term (1 Gyr) recycling of ancient, subducted lithosphere[8] and associated crustal layers previously exposed to hydrosphere-biosphere activity may result in localized oxidation[9]; (2) upward fluxing of volatiles derived from zones in the lower mantle where segregation of Fe^{3+}-bearing silicate-oxide assemblages from core-forming Fe metal (produced during Fe^{2+} disproportionation) may produce local oxidation; (3) the range of oxidation states may reflect the differential diffusion rate of H_2 with respect to other potential volatile species (in the system C-H-O-S). One might expect the first two processes to be important factors in large terrestrial planets such as Earth (and Venus?). Whereas the third process may operate in any planet with sufficient volatile complement, and subjected to variable internal heating. Finally, it is worth noting that both carbon-carbonate and Fe^{2+} - Fe^{3+} equilibria may be locally important, dependent on the relative molar concentrations involved.

References

1. Sato, M. (1972) Geol. Soc. Am. Mem., 135, 289-307.
2. Flynn, R.T., Ulmer, G.C. and Sutphen, C.F. (1978) J. Petrology, 19, 136-152.
3. Sato, M. and Valenza, M. (1980) Am. J. Sci., 280A, 134-158.
4. O'Neill, H.St.C., Ortez, N., Arculus, R.J., Wall, V.J. and Green, D.H. (1982) Terra Cognita, 2, 228.
5. Aragon, R. and McCallister, R.H. (1982) Phys. Chem. Minerals, 8, 112-120.
6. Eggler, D.H. (1982) Geophys. Res. Lett., in press.
7. Arculus, R.J. and Gust, D.A. (1981) IAVCEI Symp. Arc Volcanism, 14-15.
8. White, W.M. and Hofmann, A.W. (1982) Nature, 296, 821-825.
9. Arculus, R.J. and Delano, J.W. (1981) Geochim. Cosmochim. Acta, 45, 1331-1343.

FLUID INCLUSIONS IN METEORITES: DIRECT SAMPLES OF EXTRATERRESTRIAL VOLATILES. L.D. Ashwal [1], M.T. Colucci [1,2], P. Lambert [3], D.J. Henry[3], and E.K. Gibson, Jr.[3] (1) Lunar and Planetary Institute, Houston, TX (2) Rutgers Univ., New Brunswick, NJ (3) NASA Johnson Space Ctr., Houston, TX

Fluid inclusions have been found in 9 meteorites (both falls and finds) representing a wide variety of petrologic classes and types: diogenite ALHA 77256 and chondrites ALHA 77230 (L4), ALHA 77299 (H3), Bjurbole (L4), Faith (H3), Holbrook (L6), Jilin (H5), Peetz (L6), and St. Severin (LL6). Ample petrographic and other evidence exists to conclude that the inclusions are not artifacts introduced from terrestrial sources or during sample preparation (1).

Petrographic examination reveals that all these meteorites have experienced a complex sequence of events. For diogenite ALHA 77256 these include, from oldest to youngest: (A) crystallization and accumulation of orthopyroxene, (B) slow cooling in a plutonic environment, (C) shock induced fracturing, brecciation, and planar deformation ($P > 20GPa$), (D) thermal metamorphism ($T \simeq 900^{o}C$)(2), (E) mild shock ($P < 20GPa$). All chondrites examined show evidence of at least some shock and/or thermal effects possibly analogous to (C-E) of ALHA 77256. Fluid inclusions are generally restricted to large (1-2 mm), primary (?) orthopyroxene crystals in the diogenite, and to clear, transparent olivine in chondrules or chondrule fragments in the chondrites. Inclusions appear to be absent from mechanically deformed (i.e. highly fractured or brecciated) areas in all samples.

Two types of inclusions have been identified. Type 1 inclusions are most abundant and occur (in all 9 meteorites) either isolated or in small clusters. These inclusions have the following common properties: (a) variable shape and size (generally 5-10 μm or less; up to 100 μm), (b) presence of 2 phases (liquid + vapor) at T_{room}, (c) broad range of homogenization temperature (T_h) of L+V to L within individual meteorites (T_h = 30° - 300°C with no preferred value), (d) apparent difficulty in observing freezing phenomena, i.e. recognition of an observable crystalline phase at low (-180°C) temperatures, (e) continuous decrease in vapor bubble volume on heating from -180°C to T_h, and (f) strong fluorescence levels during laser Raman spectroscopic (LRS) analysis. Properties (a-c), along with an observed Raman vibration band at 3200-3600 cm^{-1} in ALHA 77256 (1) are consistent with an aqueous fluid, but the fluid cannot be pure H_2O because of (d-f). Warner et al. (1) inferred a large solute content, possibly salts, based on observations of change in vapor bubble morphology from deformed to spherical at -20° to -25°C. Recent work indicates that

complex hydrocarbons may be an important constituent of these fluids (3). Evidence includes: (i) fluorescence of the inclusions under UV excitation, (ii) precipitation of graphitic material within the inclusions during some LRS experiments, (iii) detection of a broad Raman band at about 2900 cm^{-1}, characteristic of C-H stretching. The broadness of this LRS signal suggests a higher aliphatic hydrocarbon than simple methane. Type 2 fluid inclusions, identified thus far in diogenite ALHA 77256 and L4 chondrite Bjürbole occur exclusively along healed fractures. In the diogenite, these are parallel to major shock-induced fractures produced during event (C) above. Preliminary microthermometry on type 2 inclusions suggests that their compositions may be different than type 1 inclusions.

IMPLICATIONS: (a) The similarity of fluid inclusions in the chondrites and the diogenite may have implications which bear on current theories as to where meteorites come from. Plausible sources of fluids available for interaction with meteoritic material include hydrous or carbonated minerals, such as are present in carbonaceous chondrite matrices, and ices. These fluids may have been released from either source by heating due to impact processes (4) or to radionuclide decay (possibly of short-lived radionuclides such as ^{26}Al (5,6)). The origins of these fluid inclusions must await further characterization of their chemical compositions and distributions. (b) Different generations of fluid inclusions can be identified in these meteorites despite their complex histories. It appears likely that such inclusions are able to survive (but perhaps not intact) moderate shock and thermal events. This is in agreement with fluid inclusion studies of terrestrial impactites (7), and with our observations of surviving fluid inclusions in microcline which had been experimentally shocked at about 20 GPa. (c) A better understanding of the relationship between the observed fluid inclusions and the shock and thermal events must await experiments which address the behavior of such inclusions during varying shock conditions.

REFERENCES: (1) Warner, J.L. et al. (1982) Proc. Lunar Planet. Sci. Conf. 13th, in J. Geophys. Res., in press. (2) Hewins, R.H. (1981) Lunar & Planet. Sci. XII, p. 445-446. (3) Adar, F. et al. (1982) Meteoritics, in press. (4) Lambert, P. and Lange, M.A. (1982), this volume. (5) Lee, T. et al. (1976) Geophys. Res. Lett. 3, 109-112. (6) Irvine, W.M. et al (1980) Nature 283, 748-749. (7) Pagel, M. et al. (1975) Fortschr. Mineral. 52, 479-489.

THERMAL AND DEGASSING HISTORIES OF THE EARTH AND VENUS I. Barigelletti and G. Visconti, Istituto di Fisica, Universita dell'Aquila, 67100 L'Aquila, Italy

Studies based on the morphology of the Venus surface have suggested the possibility that the evolution of the atmosphere is closely related to the thermal history and tectonics of that planet (Phillips et al.[1], Phillips and Malin[2]). On the other hand, the atmospheric temperature depends mainly on the amount and composition of the degassing material. Another possible influence of the atmosphere is through the amount of water vapor recycled in the asthenosphere. Thus it is of considerable importance to ascertain the epoch of possible destabilization of water on the surface of Venus.

We present the preliminary results of a model which takes into account the evolution of the atmosphere and the thermal history and lithosphere growth on Venus. Comparisons are also made with some cases calculated for the Earth.

Surface temperature is determined radiative code as suggested by Pollack[3]. The bases contributing to the radiative balance are carbon dioxide and water vapor and opacities are evaluated on 13 wavelengths intervals. The equilibrium temperature of the surface is obtained with a relaxation technique (Ramanathan[4]) imposing the equality of the net solar flux and IR flux at the top of the atmosphere. The thermal structure of the atmosphere is fixed with a constant lapse rate of 10^{o}/km, up to radiative equilibrium temperature (tropopause level). Above this altitude the temperature is assumed constant. The albedo through all epochs is fixed at 0.7 so that the surface temperature is 740^{o}K for the present atmospheric conditions. In this approximation surface temperatures were calculated for the degassing histories given by Walker[5]. Results are presented in Fig. 1. Early degassing of both carbon dioxide and water vapor is responsible for the high initial temperature while a continuous degassing of carbon dioxide up to 100 bars pressure gives high temperature between 0.5 and 2 b.y. Minimum mixing ratio for water vapor is assumed at 5×10^{-4}. Both scenarios presented by Walker include large amounts of oxygen which could influence surface temperature by absorbing UV solar radiation.

These temperatures were used as a boundary condition to calculate mantle cooling and lithosphere growth with a parameterized convection model as in Schubert et al.[6] This model includes a radioactive source decaying with time while spherical geometry is taken into account to calculate mantle heat balance.

For Venus we have used the same parameters as for the Earth except for R_m (the mantle outer radius) and R_c (the inner radius) which were taken 5951 km and 3310 km respectively. Fig. 2 shows examples of the cooling histories for the surface temperatures previously found. For comparison we also show a case calculated for the Earth. This case refers to a surface temperature of 273^{o}K while for both planets the initial mantle temperature is taken 3273^{o}K. Fig. 3 shows the lithosphere thickness for a constant surface temperature and for the temperature given by curve A in Fig. 1. Both lithosphere thickness and mantle temperature are very sensitive to the initial mantle temperature in the case of Venus (high surface temperature) showing even an initial temperature rise for mantle temperatures lower than 2000^{o}C. Also the influence of the surge in surface temperature between 0.5 and 2 b.y. is felt mainly by the lithospheric growth although the final value of the thickness is not affected. On the other hand mantle temperature is only marginally affected.

We plan to improve further our model by introducing a crust separated from the lithosphere as in [2] to study lithosphere stability. We also plan to consider

feedback between degassing and surface or mantle boundary heat flux.

1. Phillips, R. J., Kaula, W. M., McGill, G. E. and Malin, M. C. (1981) Science, 212, 879-899.
2. Phillips, R. J. and Malin, M.C. (1982), The interior of Venus and tectonic implications, Chap. 10 of Venus, to be published.
3. Pollack, J. B. (1969) Icarus, 10, 314-341.
4. Ramanathan V. (1976) J. Atmos. Sci., 33, 1092-1111.
5. Walker, J.C.G. (1975) J. Atmos. Sci., 32, 1248-1256.
6. Schubert, G., Stevenson, D., and Cassen, P. (1980), J. Geophys. Res., 85, 2531-2538.

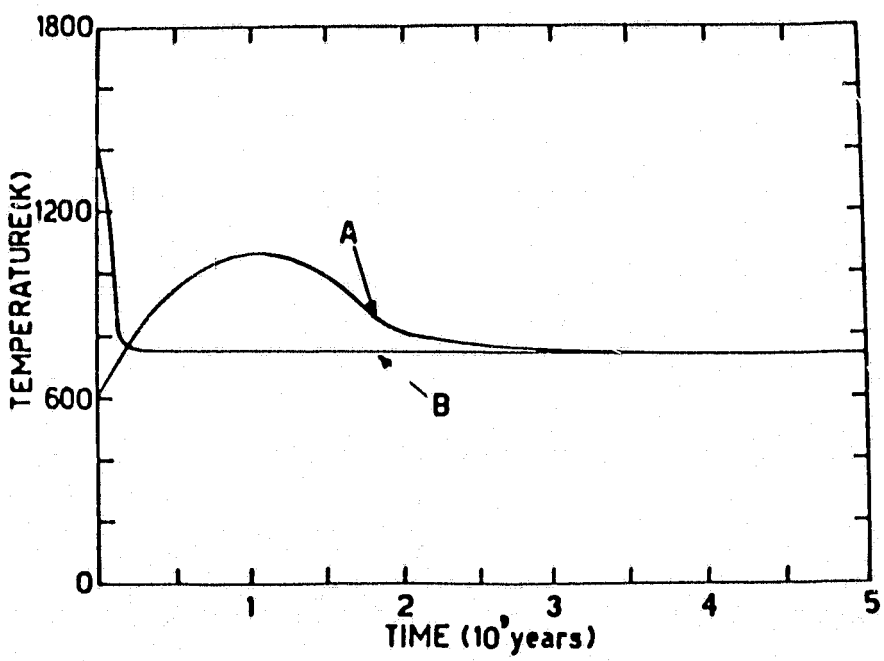

Figure 1. Surface temperature of Venus for the degassing scenarios suggested by Walker[5]. Curve A is for a continuous degassing of carbon dioxide and curve B is for early catastrophic degassing of water vapor.

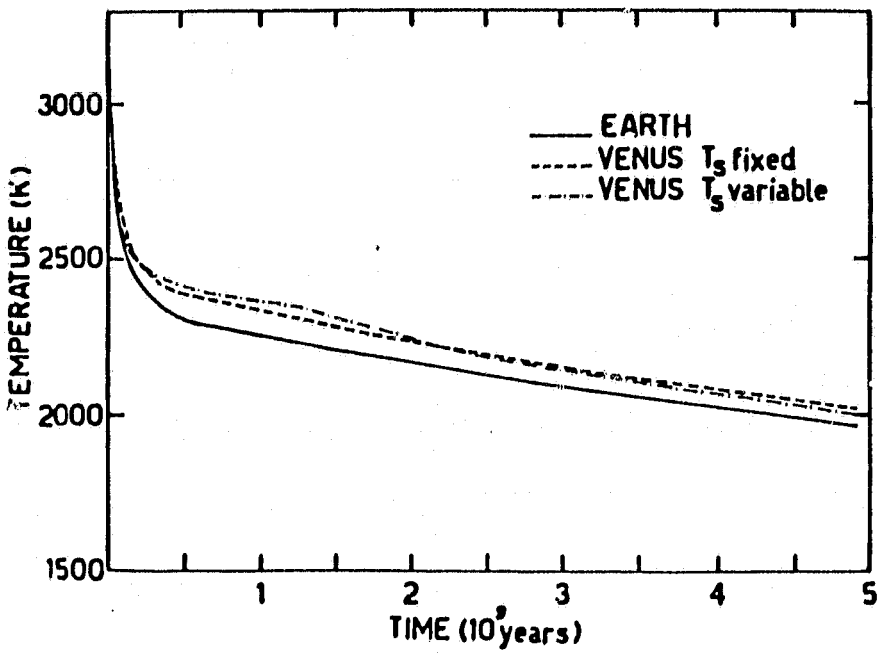

Figure 2. Mantle temperatures as a function of time for the Earth and Venus. Initial mantle temperature is 3272°K. The dashed line refers to a surface temperature of 740°K while the dashed-dotted line to a surface temperature as in case A in Fig. 1.

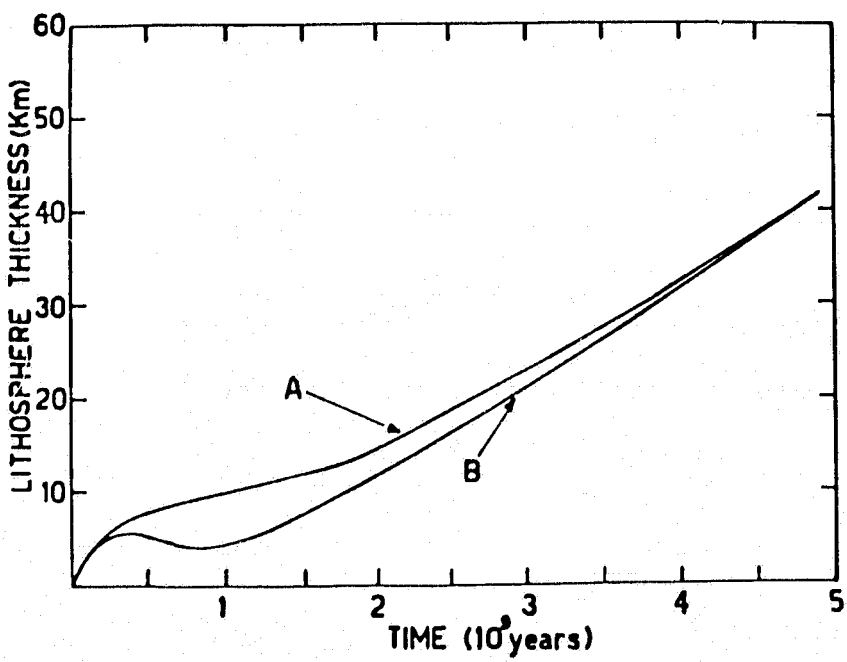

Figure 3. Lithosphere thickness for Venus for a fixed surface temperature (curve A) and changing surface temperature (curve B).

MODEL STUDIES OF O_2-BIOTA COUPLING IN THE PRECAMBRIAN

M. E. Baur, Department of Chemistry, University of California, Los Angeles, CA 90024

Microorganisms capable of O_2 respiration play an important role in setting the boundary between oxic and anoxic zones in present terrestrial soil and water environments. The division of environments into such zones indeed may reflect the markedly nonlinear behavior predicted by coupled kinetic equations for microbial growth and oxygen utilization in the presence of an initial mild O_2 gradient. If this type of kinetic model is applied to presumed Precambrian conditions, we reach the somewhat paradoxical conclusion that the development of fully anoxic zones could not occur until an O_2-dependent biota had evolved, that is, until atmospheric O_2 levels had reached some critical value in late Archaean or early Proterozoic time. Sequestering of reduced carbon in such anoxic zones may have acted in turn to accelerate atmospheric O_2 buildup, yielding a pronounced positive feedback effect between the rise in O_2 and the proliferation of O_2 respirers. If such a mechanism were indeed operative in late Archaean or Proterozoic time, then a quite rapid, even cataclysmic, rise in ambient O_2 levels may have occurred.

Implications of Stable Isotope Variation in a Banded Iron Formation for Precambrian Volatile Reservoirs

M. E. Baur, J. M. Hayes and M. R. Walter
Precambrian Paleobiology Research Group
University of California at Los Angeles
Los Angeles, California 90024

We discuss the mechanism of genesis of banded iron formations (BIF), common sedimentary structures of the early and mid Precambrian[1] in the context of recent advances in our understanding of Precambrian geochemistry and microbial ecology[2,3] based on carbon stable isotope analyses[4].

Extensive collections of data on the ^{13}C content of Precambrian sediments reveal no clear overall trend in $\delta^{13}C$ through Precambrian and Phanerozoic time, though large excursions from the mean seem more common in the Precambrian than subsequently. If the distribution width σ for the individual formations is plotted, however, it is seen that a clear break occurs somewhere between 1.5 and 2.0 Ga ago. This may reflect a decrease in ecosystem diversity following upon establishment of an O_2-rich atmosphere[2]; previous to this time CH_4 could have formed an important part of the terrestrial atmosphere and its presence could explain the existence of isotopically light carbon in many Precambrian sediments[3]. These trends are displayed in Fig. 1, in which $\delta^{13}C_{PDB}$ and σ are plotted as functions of time of deposition for Precambrian and Phanerozoic argillaceous sediments.

The specific BIF which we have studied are from the Hamersley Group of Western Australia[5]. The characteristic structural feature of BIF is a more or less thin lamination with iron-rich and iron-poor layers alternating. Powder samples milled from individual laminae for two BIF of the Hamersley Group, the Marra Mamba Iron Formation and Bruno's Band of the Mount Sylvia Formation, were analyzed for carbon and oxygen isotopic composition. We found a sharp and reasonably regular alternation of $\delta^{13}C$, iron-rich zones being isotopically lighter. The isotope trends are shown for the Marra Mamba sample in Fig. 2. We interpret these results to mean that two

distinct mobile carbon reservoirs were present in Hamersley time, contributing in varying proportion to the carbonate mineral deposited in sediment. One, presumably, was the hydrosphere CO_2 reservoir, with $\delta^{13}C$ near zero as on the present Earth. The other must have been biologically coupled and contained very light carbon; the most plausible candidate is that it consisted of methane, produced biogenically and oxidized to isotopically light carbonates in the sediments or anoxic part of the water column. The delicate balance between oxic and anoxic processes implied by this presumably could not exist after establishment of a massively oxygenic terrestrial atmosphere, and BIF formation ceased thereafter. The termination of BIF genesis in late Proterozoic time thus is consistent with the trends in overall Precambrian sedimentary $\delta^{13}C$ values.

References

[1] James, H. L. (1954) Sedimentary facies of iron-formation. Econ. Geol. 49, 235-294

[2] Baur, M. E. (1983) Diversity in Precambrian microbial communities. J. Geol. Soc. 140, xxx.

[3] Hayes, J. M. (1983) Geochemical evidence bearing on the origin of aerobiosis, a speculative interpretation. In: J. W. Schopf, ed., Origin and Evolution of Earth's Earliest Biosphere, Princeton University Press, Princeton, NJ, Chapter 12.

[4] Hayes, J. M., Kaplan, I. R. and Wedeking, K. W. (1983) Precambrian organic geochemistry preservation of the record. In: J. W. Schopf, ed., Origin and Evolution of Earth's Earliest Biosphere, Princeton University Press, Princeton, NJ, Chapter 5.

[5] Trendall, A. F. (1973) Precambrian iron-formation of Australia. Econ. Geol. 68, 1023-1034.

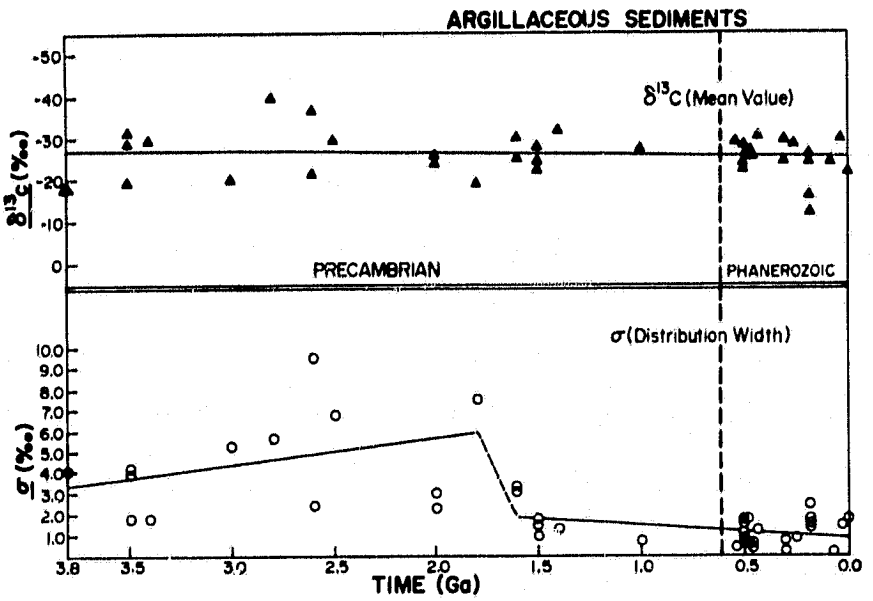

FIGURE 1

$\delta^{13}C_{PDB}$ and σ for Precambrian and Phanerozoic argillaceous sediments.

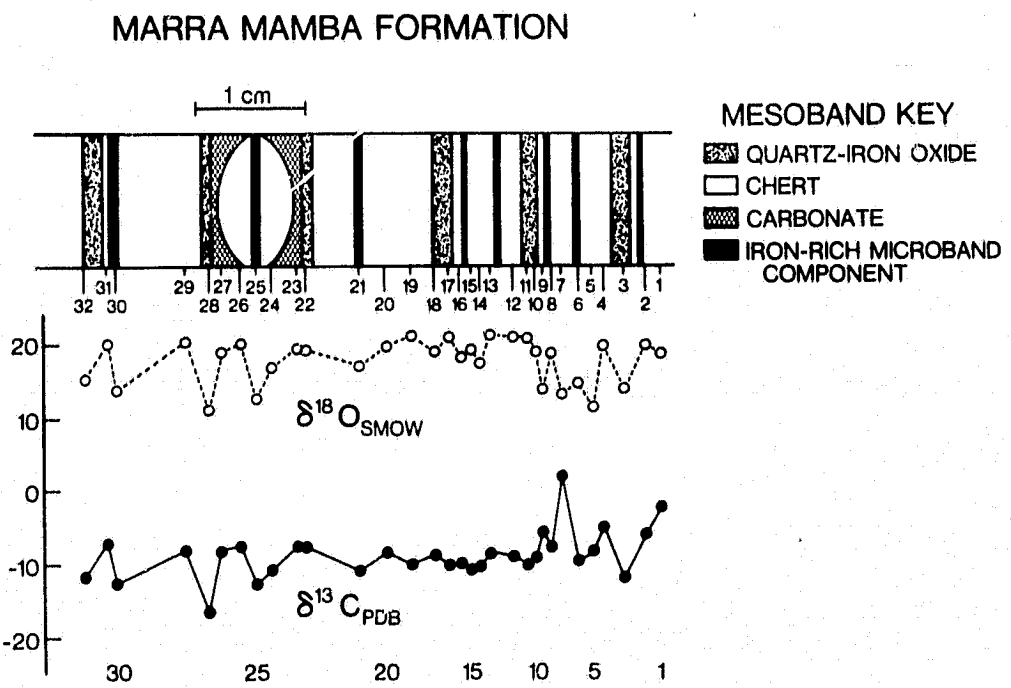

FIGURE 2

$\delta^{13}C_{PDB}$ and $\delta^{18}O_{SMOW}$ for a core from the Marra Mamba Iron Formation.

VOLATILES AND SOLAR-NEBULA MODELS. D.C. Black, NASA Ames Research Center, Moffett Field, CA

The study of planetary volatiles is a multi-faceted problem which can be divided into three general subproblems; the formation and evolution of the solar nebula, the interaction between planets and their environment, and the physical/chemical evolution of planets. These three are not mutually exclusive, but given the embryonic state of knowledge concerning planetary volatiles and the potential significance of enhanced knowledge in constraining our understanding of a variety of planetary and nebular phenomena, these subproblems are of heuristic value. The focus of this paper will be on the subproblem of the formation and early evolution of the solar nebula, emphasizing possible relationships between events/processes in that formation and evolution with the general problem of planetary volatiles.

Years of analysis of lunar, meteoritic, and terrestrial samples, and nearly two decades of spacecraft exploration of the solar system does not yet permit specification of even the more fundamental characteristics of the putative solar nebula. For example, there is no unequivocal evidence as to the mass of the nebula; was it massive ($\sim 1 M_{\odot}$) or was it a so-called "minimum-mass" nebula ($\sim 0.01\text{-}0.02 M_{\odot}$)? There is also no clear evidence as to the thermodynamic evolution of the nebula, although the past decade of meteoritic studies have shown rather clearly that an earlier paradigm in which a reasonable portion of the nebula was hot (i.e., $\geq$ 1500-2000K) is <u>not</u> consistent with available data.

One can identify at least four aspects of solar nebula formation and evolution which relate to the study of planetary volatiles. It would be useful to know how the elemental and isotopic composition of volatiles, in both the gas and solid (i.e., dust grains) phases varied in time and space as the nebula evolved. One would also like to know the evolution of physical conditions in the nebula in terms of the way(s) in which those conditions influence or control the process of planet formation. Finally, one would like to know the nature of planet-nebula interactions, specifically those which affect volatile inventories in planetary bodies.

The purpose of this paper is to present a brief review of competing models of the solar nebula, as well as to outline some rather general theoretical considerations which delineate generic nebular formation and evolution behavior. Possible consequences of those theoretical constructs for studies of planetary volatiles in general, and of the noble gases in particular, will also be discussed.

PROGRESS IN THE EXPERIMENTAL INVESTIGATION OF VOLATILE COMPONENTS IN VAPORS AND SILICATE LIQUIDS AT HIGH PRESSURES

Art Boettcher, Institute of Geophysics and Planetary Physics and Department of Earth and Space Sciences, University of California, Los Angeles, California 90024

In the mid-60's, we achieved the capability of routinely experimentally examining the role of H_2O and other volatile components in melting and other phase transformations at pressures > 10 Kbar, i.e., pressures equivalent to those in the mantle of the Earth. At these pressures, aluminosilicate magmas (e.g., basaltic) can dissolve > 15 wt% H_2O -- i.e., > 70 mole% (1). At pressures < ∿ 10 Kbar, H_2O-saturated fusion curves of silicate and aluminosilicate minerals have negative dP/dT slopes; at higher pressures, they become positive as a result of the increasing density of H_2O and also of minerals as the result of phase transformations (2). In 1970, we (3) demonstrated that CO_2 is quite soluble in basaltic liquids at > ∿ 15 Kbar, and this has been substantiated in many synthetic silicate and aluminosilicate systems (e.g., 4,5). Thus, at Earth-mantle pressures, anhydrous, as well as hydrous and/or carbonated, silicate systems have fusion curves with positive dP/dT slopes, but the latter are displaced to lower temperatures as the result of the solubility and negative free energy of mixing of the H_2O and/or CO_2 in the silicate liquids. Thus, when the proportion of H_2O and/or CO_2 is sufficient to saturate the system and form a vapor phase, the temperature of the beginning of melting and the composition of the first-formed liquids are functions of the ratio of H_2O/CO_2 (i.e., of the fugacities of these components) (6). However, when the proportions of CO_2 and H_2O are insufficient to make all of the potential hydrous and carbonate crystalline phases (e.g., amphiboles and dolomite), the values of μH_2O and μCO_2 are isobarically invariant, and the temperatures of the beginning of melting and the compositions of the first-formed liquids are independent of total H_2O/CO_2 (7).

The discovery that CO_2 reacts with olivines and pyroxenes to form carbonates at depths < 100 km (8) is significant because primary (Mg-rich) carbonate is extremely rare in mantle-derived samples, suggesting to me that the mantle may be more chemically reduced (9) than accepted by many petrologists, and reduced C-bearing species may be more important. Reactions similar to the carbonation of olivines and pyroxenes may also occur in silicate liquids at about 20 Kbars, explaining the remarkable increase in the solubility of CO_2 in these liquids above this pressure (3,10,11). That is, the abrupt increase in the solubility and freezing-point depression may result from an increase in the ratio of CO_3^{2-}/CO_2 in the liquid (1,4,11). However, the presence of CO_3^{2-} in liquids requires non-bridging oxygen ions (e.g., 4) as well as cations such as Ca or Na for charge balance, and no CO_3^{2-} is expected in melts of SiO_2 composition. Nevertheless, recent experiments in the system SiO_2-H_2O-CO_2 (12) reveal that CO_2 is very soluable in the liquid above ∿ 20 Kbar, suggesting that molecular CO_2 is the major, if not the only, carbon-bearing species in this liquid.

Our recent studies of the melting of silicate and aluminosilicate minerals in the absence of vapors (13) and in the presence of H_2O-CO_2

vapors (11,14) provide thermodynamic data for liquids and vapors at high pressures that previously were unobtainable. Nevertheless, problems occur with this approach because of a lack of knowledge of the absolute solubilities of carbon-bearing species in the liquids and of the effects of such solubilities on the values of γ_{H_2O}. For example, activity coefficients for H_2O determined experimentally in the systems albite-H_2O-CO_2 (11) and SiO_2-H_2O-CO_2 (12) yield values of γ_{H_2O} in the vapor that are strongly dependent on the ratio of H_2O/CO_2 in the vapor, whereas those determined in the system sanidine-SiO_2-H_2O-CO_2 are much more nearly those of ideal solutions (14). Despite these and other uncertainties, the experimental approach has enabled us to gain insight into the structures of silicate liquids and to derive thermodynamic parameters for them. This approach provides us with much more reliable fusion curves than those calculated from thermochemical data calorimetrically determined at atmospheric pressure and using metastable glasses rather than stable liquids. For example, our experimentally determined, vapor-saturated solidi in the presence of CO_2-rich vapors in the system albite-H_2O-CO_2 are hundreds of Kelvins lower than those previously calculated. Similarly, phase transformations in aluminosilicate liquids at high pressures (particularly the $Al^{IV} \leftrightarrows Al^{VI}$ transformation) result in fusion curves that depart markedly from those calculated from volumetric and thermodynamic data obtained at atmospheric pressure (13,15).

Continued experimentation at high pressures, coupled with calorimetric and spectrographic investigations of glasses and, preferably, liquids, will enable us to more nearly quantify our understanding of the processes in the interiors of planets that involve volatile components, including melting and the origins of atmospheres and hydrospheres.

REFERENCES

(1) Burnham, C. W. (1979) in H. S. Yoder, Jr., ed., The Evolution of the Igneous Rocks: Fiftieth Ann. Appraisal, Princeton Univ.Press, Princeton, N.J., p. 439-482.
(2) Boettcher, A. L. and Wyllie, P. J. (1969) Amer. J. Sci., v. 267, p. 875-909.
(3) Hill, R. E. T. and Boettcher, A. L. (1970) Science, v. 167, p. 980-982.
(4) Mysen, B. O. (1976) Amer. J. Sci., v. 276, p. 969-996.
(5) Eggler, D. H. and Rosenhauer, M. (1978) Amer. J. Sci., v. 278, p. 69-94.
(6) Mysen, B. O. and Boettcher, A. L. (1975) J. Petrol., v. 16, p. 520-548.
(7) Eggler, D. H. and Holloway, J. R. (1977) in Magma Genesis, State of Oregon, Dept. Geology and Min. Ind. Bull. 96, p. 15-36.
(8) Newton, R. C. and Sharp, W. E. (1975) Earth Planet. Sci. Lett., v. 26, p. 239-244.
(9) Arculus, R. J. and Delano, J. W. (1981) Geochim. Cosmochim. Acta, v. 45, p. 899-913.

(10) Wyllie, P. J. (1979) Amer. Mineralogist, v. 64, p. 469-500.
(11) Bohlen, S. R., Boettcher, A. L. and Wall, V. J. (1982) Amer. Mineralogist, v. 67, p. 451-462.
(12) Boettcher, A. L., in preparation.
(13) Boettcher, A. L., Burnham, C. Wayne, Windom, K. E. and Bohlen, S. R. (1982) J. Geology, v. 90, p. 127-138.
(14) Bohlen, S. R., Boettcher, A. L. and Wall, V. (1982) Abs., Geol. Soc. Amer. Ann. Mtg., in press.
(15) Burnham, C. Wayne (1982) in Rickard, D. and Wickman, F. E., eds., Chemistry and Geochemistry of Solutions at High Temperatures and Pressures, Pergamon Press, Ltd., p. 197-229.

MICROBIAL METABOLISM OF ORGANIC MOLECULES PRODUCED BY CHEMICAL SYNTHESIS IN A REDUCING ATMOSPHERE; IMPLICATIONS FOR THE ORIGIN OF LIFE

Penelope J. Boston, Dept. of Environmental, Population, and Organismic Biology, University of Colorado, Boulder, CO 80309
Carol Stoker, Dept. of Astro-Geophysics, University of Colorado, Boulder, CO 80309

Tholins, a class of complex organic solids, have been produced under laboratory conditions using a reducing mixture of gases including methane and ammonia (1). Tholin hydrolysis yields amino acids. Its pyrolysis products contain many other compounds of biological significance (2). The tar-like tholin (produced by sparking an equimolar mixture of NH_3 and CH_4 with 2.6% water vapor) is used as a carbon or energy source for these organisms.

We have isolated a variety of micro-organisms which are capable of metabolizing tholins. Isolations have been performed under both aerobic and anaerobic conditions. Using samples of several dry Colorado soils, anaerobic lake mud, and tarsands from Utah, aliquots were first enriched with tholin to encourage possible tholin metabolizers. Organisms which showed growth were then separated into pure culture by streaking or differential plating. Pure cultures were tested for tholin metabolism using basal salts-silica gel medium pairs with and without tholin. Light was excluded to inhibit phototrophs. If growth occurred in the no-tholin control, the organism was assumed to be fixing CO_2 and discarded. Strains growing in tholin medium as the sole carbon source were retained and identified to the genus level.

The majority of tholin-positive strains isolated under ambient oxygen conditions are actually microaerophiles (demonstrated by banding in oxygen gradient tubes) preferring reduced oxygen tensions. Several of these have been tested for tholin metabolism under anaerobic conditions. Some strains are capable of facultative anaerobic metabolism of tholin. However, growth is much slower (8-10 weeks) than under aerobic conditions (about one week).

Organisms isolated under strictly anaerobic conditions exhibit very long lag times before visible growth (8-10 weeks). The differences in growth rate between aerobes and anaerobes (either strict or facultative) are in keeping with the ralative efficiencies of aerobic versus anaerobic meabolism (3). Our organisms have been grown on tholin concentrations of 0.033%, 0.05%, 0.1%, and 0.5% (w/v).

Production of organic precursor compounds by inorganic chemical means is a salient feature of virtually every scenario for the origin of life (4). In some of these, notably the classic Oparin-Haldane (5) and Miller-Urey (6) scenarios, a highly reducing atmosphere including the constituents methane, ammonia, and water prevailed on the primitive Earth. Tholin compounds, which could have provided a source for either the molecular building blocks of life or potential precursors to them, are easily synthesized in such a reducing atmosphere (7).

Recently a case has been made based on the atmospheric photochemistry of ammonia (8) and geochemical evidence that the primordial atmosphere consisted primarily of H_2, CO_2, and N_2 (9). In such an atmospheric mix, however, it is difficult to produce the rich variety of organic compounds observed in tholins.

The demonstration of microbial growth on tholin has implications for the chemical environment that led to the origin of life and early cellular evolution on Earth. The results suggest that terrestrial organisms originated in a chemical environment in which tholins or similar substances were present as a source of energy and materials, either produced from <u>in situ</u> reservoirs of CH_4 and NH_3 or introduced by extraterrestrial means such as meteoritic infall.

To test the Oparin-Haldane view of early life in light of our microbiology results, using tholins as the abiologically produced food substance, we have considered a highly simplified picture of the primitive biosphere. We envision this as sometime after the origin of primitive entities or cells but befor the invention of any sort of autotrophy.

Let us consider the flux of organic carbon required to sustain a postulated primitive biosphere. A simple model has been calculated using the following assumptions:

Boston, P. J. and C. Stoker

(a) The bioactive zone, i.e. the area in which the microbes live, is restricted to the upper 10 m of the ocean, taken as global. This implies a volume of the bioactive zone V equal to the surface area of the Earth, 5.10×10^{18} cm^2 multiplied by 1000 cm, or $V = 5.10 \times 10^{21}$ cm^3.

(b) Minimal densities of heterotrophs--i.e., number densities of the order of 10^1-10^2 microbes per cubic centimeter are assumed to live on abiologically produced organic compounds like tholins.

(c) Maintenance carbon and energy source requirements for primitive hetrotrophs are based on data for Methylmonas, (a species of methylotrophic archaebacteria) growing anaerobically on glucose at .05 Moles glucose/gm dry wt per hour. (10) The molecular weight of glucose (C_6 $H_{12}O_6$) is 180 g/Mole; therefore the maintenance energy source required, R, is 9 gm/gm dry wt per hour.

For the microbes themselves, we assume an average diameter of 2 micrometers, and an average individual density of 1 gm/cm^{-3}. This yields a volume of each organism equal to 4.19×10^{-12} cm^3. Since the dry weight of microbes is about 10% of their net weight, this dry weight is 4.19×10^{-13} gm per organism. Therefore B, the dry biomass of a colony growing at density 10^1-10^2 cm^{-3}, is 4.19×10^{-12} to 4.19×10^{-11} cm^{-3}. In the calculations which follow we assume the lower value.

With these parameters and assumptions it is an easy matter to calculate the flux of organics required to maintain the organisms. The flux out (i.e., what they eat) must equal the flux in (by whatever mechanism). Multiplying B x R x V, we obtain a flux out of 1.04×10^{-11} gm cm^{-2} sec^{-1} per unit area on the surface of the Earth. Since the tholin compounds which are the postulated nutrient source are 46% carbon, (1), this represents a fixed carbon source of 2.5×10^{11} mol cm^{-2} sec^{-1}. We may consider this an absolute lower limit to maintain a biosphere, given the stated assumptions.

There are essentially two possible limitations to the rate at which carbon can be fixed and made available to the biosphere, (a) carbon and other reactant limitations, and (b) energy source limitations.

First, we consider possible sources of organics, which include abiotic systhesis in a terrestrial formation process and/or possible

extraterrestrial sources, such as comets and meteorites.

Considering the rate of supply of organic materials from carbonaceous chondrite meteors leads to severe difficulties in obtaining the necessary carbon from this source. Wethrill (11) indictes that the impact rate of late accretion decreased exponentially over a period of 4.5-3.9 G yrs. ago, from 50 x 10^7 gm sec^{-1} to 10^7 gm sec^{-1}. Chang (12) has estimated that volatile organic compounds constitute 0.05% of Murchison meteorite. Hayes (13) reviews the organic content of meteorites and shows that the extractable organic carbon in meteorites is at most 1.5%. Taking the highest impact rate and assuming that all the organic material in the meteorites reaches the earth intact, we get a maximum total flux of organic carbon of (5.0 x 10^8 gm sec^{-1}) x (1.5 x 10^{-2}) = 7.5 x 10^6 gm sec^{-1}, or 1.5 x 10^{-12} gm cm^{-2} sec^{-1} over the Earth's surface. This is an order of magnitude short of the requirement to sustain microbial life. Furthermore, the assumptions used to arrive at this figure are unreasonably optimistic. We therefore conclude that organic material required to sustain a primitive biosphere could not have been derived solely from the influx of carbonaceous meteorites.

Next we consider abiotic systhesis of organic carbon from a terrestrial formation process. Figure 1 shows the flux of possible carbon sources into the atmosphere. The relevant carbon sources are CH_4, CO, and CO_2. For the case of methane, the outgassing rate appears to be too low to supply fixed carbon to the biosphere. Methane is also photochemically unstable, though from the standpoint of supplying carbon to the biosphere that is not a problem, since its photochemical products are the very organics postulated to sustain the biosphere.(14) However the methane flux into the atmosphere to supply the biosphere would have to be at least F in = 2.5 x 10^{11} mol cm^{-2} sec^{-1}, or 4 order of magnitude greater than the current rate. Clearly methane could not have supplied the needed carbon, unless the methane flux into the atmosphere was much higher than at present.

Of the other possible carbon sources, CO_2 may have been quite abundant but does not appear to be very useful for the formation of organic compounds, except possibly in a hydrogen rich environment. (15)

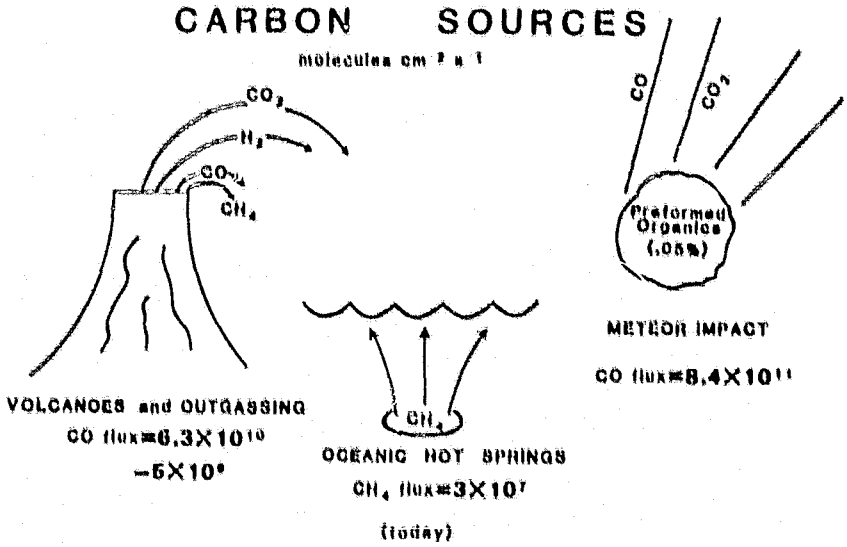

Figure 1: Estimated flux of carbon into the terrestrial atmosphere as provided by volcanic sources, oceanic hot springs and meteor impact. The volcanic source estimate is based on the assumption that the carbon at the surface of the Earth was released at a constant rate over a period of 5 x 10^8 years. The two extremes are for the cases with and without metal-silicate-volatiles equilibration between the core, surface metals and the mantle (16). Methane evolution from oceanic hot springs is reported in ref. (14). It is difficult to determine this figure from in situ measurements today because methanogenic bacteria living in the hot springs may be metabolizing a significant fraction of the evolving methane before it reaches the surface. The rate of CO flux from meteoritic impact is derived by assuming that late accreting planetesimals supplied the entire inventory of atospheric volatiles, and that carbonaceous chondritic planetesimals were vaporized on impact to yield up their carbon entirely as CO in $\sim 10^8$ years. This value represents an upper limit (16).

Boston, P. J. and C. Stoker

This leaves CO as a candidate to supply the required carbon. Relatively few organic synthesis experiments have been performed using carbon monoxide. We don't know, for example, much about energy requirements for CO reactions, nor have we established that organisms can metabolize CO-generated products. Carbon monoxide as supplied from direct impact of late accreting planetesimals could have provided a large enough carbon source, assuming somewhat optimistically that the planetesimals provided the large fraction of the Earth's complement of volatiles and that the planetesimals vaporized on impact to form CO. (16) These assumptions lead to the value quoted in Figure 1 which is the average CO flux over 500 million years. This type of source would necessarily be episodic, providing abundant atmospheric CO at some times and none at others.

Now we consider the energy efficiency of carbon fixation required to sustain the postulated biosphere. Table 1 shows the energy sources that can contribute to fixation of carbon into an organic form as well as experimental results for the production rate for the amino acid glycene in prebiotic synthesis experiments involving NH_3 and CH_4. It is important to notice that shock heating is a more efficient process for organic synthesis than short wavelength ultraviolet light by six orders of magnitude. Multiplying column 1 by column 2 in Table 1 shows that the maximum allowed production rate of glycine is $p = 2.2 \times 10^{18}$ mol cm^{-2} yr^{-1}, if every erg of energy is absorbed (19). Glycine is the most abundant amino acid produced in these experiments, with typical production of about 1% of the initial carbon in the reactants. If we assume that the total organic production is 100 times the glycine production (thus assuming the maximum possible organic production allowed), and the average molecular weight of compounds produced is 100, we get the flux of organics allowed by energy considerations as $F_{in} = 1.4 \times 10^{-9}$ gm cm^{-2} s^{-1}. Thus a lower bound to the energetic efficiency of conversion of atmospheric carbon to an organic form of approximately 1% is required to sustain the biosphere. It remains to be seen whether such a high efficiency is reasonable for realistic organic formation processes in the Earth's atmosphere.

TABLE 1: AVAILABLE ENERGY

FORM OF ENERGY	TOTAL FLUX (cal per cm^2 per year)	Estimated Production rate of Glycene (molecules/cal.)	Global Production rate (molecules cm^{-2} y^{-1})
Solar Radiation below 2000 Å	-7.75*	2.79×10^{12}	8.4×10^{13} - 2.2×10^{16}
	-7.75×10^2 (Canuto et al.)		
High-energy radiation	47.0	8.18×10^{13}	3.8×10^{15}
Heat from Volcanic Emission (rocks and lava)	0.15	3.01×10^{14}	4.5×10^{13}
Eletrical discharge	1*	1.5×10^{14}	1.5×10^{14}
Shock heating (thunder)	1*	2.0×10^{18}	2.0×10^{18}
Shock heating (meteor impact)	0.1	2.0×10^{18}	2.0×10^{17}

* = contemporary earth

Total production allowed by Energy = 2.2×10^{18} molecules/cm^2 yr (Absolute Maximum)

Table 1: Total flux of energy of various forms which could have provided an energy source for the production of organic compounds. The estimated production rate of glycene for the various energy sources represent experimental values utilizing methane and ammonia as initial reactants as reviewed by Dose (19).

In summary, our new result--that anaerobic heterotrophic microorganisms are able to metabolize tholin, apparently at low concentrations--suggests that this material could have been a viable energy source for primitive heterotrophs. Extrapolating from the assumptions of the Oparin-Haldane paradigm leads to some definite conclusions about the flux of carbon into the primitive atmosphere from the time of the origin of life until the development of autotrophy, which probably was well established by about 3.5 billion years ago. The important questions posed by these results regarding the volatiles complement of the primitive Earth are: what were the probable fluxes of carbon into the primitive atmosphere, and what was the oxidation state of that carbon during the first half billion years of Earth's history?

REFERENCES

1. Sagan, C. and Khare, B.N. 1979. Nature 277: 102-107.

2. Khare, B.N. and Sagan, C. 1981. Icarus 48: 290-297.

3. For a discussion see, Keeton, W.T. 1980. Biological Science. Third Edition. W.W. Norton and Co., New York. pp 163-176.

4. e.g. see Miller, S.L. and Orgel, L. 1974. The Origins of Life on Earth. Prentice Hall, Englewood Cliffs.

5. Oparin, A.I. 1924. The origin of life. Translated from the Russian; Haldane, J.B.S. 1929. The origin of life. Articles reprinted in J.D. Bernal, ed., 1967. The Origin of Life. World Press, Cleveland.

6. Urey, H.C. 1952. The Planets. Yale Univ. Press, New Haven, Connecticut. Miller, S.L. and Urey, H.C. 1959. Science 130: 245-251.

7. e.g. Miller, S.L. 1953. Science 117: 528-529. Sagan, C. and Khare, B.N. 1971. Science 173: 417-420. Sagan, C. and Miller, S.L. 1960. Astron. J. 65: 499. (Abstract). Ponnamperuma, C., Woeller, F., Flores, J., Romiez, M., and Allen, W. 1969. Advan. Chem. 80: 280-288.

8. Ferris, J.P. and Nicodem, D.E. 1972. Nature, Vol 238, p. 268-269.

9. Hart, M.H. 1978. Icarus 33, 23-39.

10. Stouthammer, A.H. 1977. Microbial Energetics, Society for General Microbiology, Symposium 27 for Microbiology, Cambridge University Press, B.A. Haddock, W.A. Hamilton, ed.: 285-315.

11. Wetherill, G.W. 1977. Lunar Science 8: 1005-1007. Lunar Science Institute, Houston.

12. Chang, S. 1979. in Space Missions to Comets. NASA Conference Publication 2089.

13. Hayes, J.M. 1967. Geochem. et. Cosmochim. Acta; 31: 1395-1440.

14. Kastings, J.F., Zahnle, K.J., and Walker, J.C.G., Precambrian Res., in press.

15. Miller, S.L. and Schlesinger, G. 1982, Abstracts 24 Plenary Meeting, COSPAR, Ottawa, Canada: 510.

16. Bar-Nun, A. and Chang, S. 1982, submitted to J. Geophys. Res.

17. Newman, M.J., and Rood, R.T., 1977. Science 198: 1035.

18. Canuto, V.M., Levine, J.S., Augustsson, T.R. and Imhoff, C.L., 1982. Nature 296, 816-820.

19. Table after Dose, K. 1975. Biosystems 6: 224-228.

BRINES AT LOW TEMPERATURES G. W. Brass and V. L. Thurmond, Rosentiel School of Marine and Atmospheric Science, University of Miami, 4600 Rickenbacker Causeway, Miami, FL

The freezing point of pure water is relatively high compared to temperatures prevailing on planetary bodies farther from the sun than Earth. Aqueous fluids are, however, stable at temperatures as low as 210°K if they are sufficiently salty. In fact, the presence of modest amounts of those salts with the greatest freezing point depression effects requires that aqueous brines form by reaction of salt crystals with ice.

The general rules of freezing point depression are: 1. Sulfates are less effective depressors than chlorides. 2. Alkaline Earth chlorides are more effective than alakli chlorides. 3. Sodium is more effective than potassium and calcium more effective than magnesium.

The four component system $CaCl_2$ - $MgCl_2$ - NaCl - H_2O begins to melt at 215°K (-58°C) (Linde, 1958). The effect of ferrous and ferric iron chlorides in combination with other salts is being investigated now with the differential scanning calorimeter and the results will be presented at the meeting along with a suggestion for the production of the red coloration of the martian regolith.

The ternary phase diagram for the system H_2O - $CaCl_2$ - $MgCl_2$ shows both a strong freezing point depression at the eutectic, and the stability of several highly hydrated salts at higher temperatures.

Evaporation of brine leads to the formation of these hydrated salts which may buffer the water content of planetary surfaces even in the absence of brine or ice.

Chlorine and sulfur are abundant components of the terrestrial excess volatiles. Their presence on other planetary bodies is now well established. Their effect on the behavior of water and ice at

low temperatures is profound and must be taken into consideration in models of planetary volatiles.

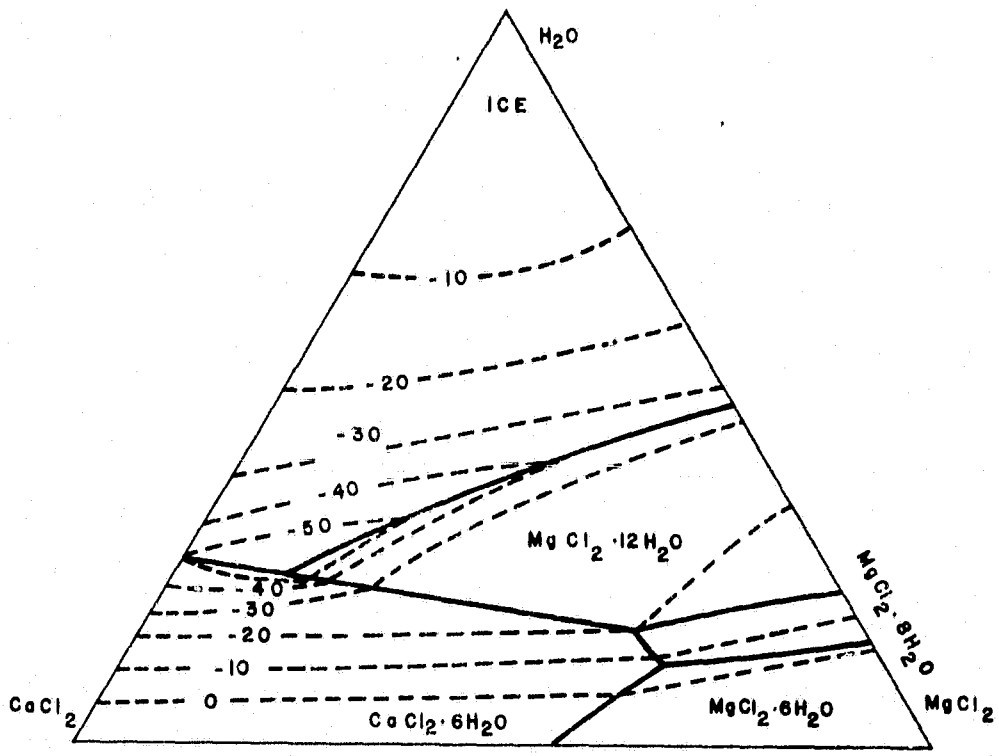

(Figure reproduced courtesy of Academic Press, Inc.)

Stability fields in the system H_2O - $CaCl_2$ - $MgCl_2$, from Brass, 1980.

REFERENCES

Brass, G.B. (1980) Icarus 42, p.20-28.

Linke, W.F. (1958) Solubilities of Inorganic and Metal-Organic Compounds (2 volumes) Van Nostrand, New York.

WAS THE EARTH'S ATMOSPHERE ANOXIC BETWEEN 3.8 and 2.0 GA AGO?

Kevin Burke, Department of Geological Sciences, State University of New York at Albany, New York, 12222 and Lunar and Planetary Institute, 3303 NASA Road 1, Houston, Texas 77058.

Attempting to assess the character of the ancient atmosphere from preserved Archean rocks is exceedingly difficult. Although a substantial proportion of the continental volume had fractionated from the mantle by 2.5 Ga ago, only about 2% of continental area exposes Archean rocks that have not been subsequently highly metamorphosed. More than half of this relatively unaltered terrane consists of plutonic rocks and volcanic rocks (mainly erupted under water) make up most of the rest. Archean sediments which constitute a relatively small volume of all Archean rocks were mostly deposited under water although some are fluviatile in origin. Diagenesis, usually under reducing conditions and low-grade metamorphism, have modified all ancient sediments. Curtis (1977) wrote "one thing is clear: it is difficult to link the mineralogy of ancient sediments with the composition of the atmosphere - only with the combined atmosphere/hydrosphere system".

Because of the prevalence of diagenetic modification some of the strongest evidence of the composition of the ancient ocean comes, somewhat paradoxically, from the occurrence of pseudomorphs. Gypsum pseudomorphs occur in the Barberton (>3.4 Ga) and Pilbara (>3.4 Ga) terranes. The implied occurrence of sulfate ions in ancient seawater seems indicative of at least slightly oxidizing conditions (but see Clemmey and Badham, 1982 and Lambert et al. 1978 for discussion of the significance of these occurrences). By the Early Proterozoic, evidence, [usually pseudomorphous], of gypsiferous evaporites is relatively common (e.g. Badham and Stanworth, 1977).

The close resemblance between the structures of Archean stromatolites and those of today which are built by photosynthesizing, oxygen-producing cyanophytes suggests that the ancient structures were produced in the same way indicating that free molecular oxygen was being released to the atmosphere-hydrosphere system by 3.5 Ga ago. Archean stromatolites are quite abundant, in spite of forming in environments in which preservation is relatively unlikely, indicating that molecular oxygen release associated with stromatolites was probably early a widespread phenomenon.

The occurrence of sediments and residual deposits which are red because of the presence of ferric iron is a strong indication of oxidizing conditions. Archean red beds, for example, in the Lake Shebandowan area of the Superior Province (Shegelski, 1980), have been interpreted as including both primary red beds (those involving the deposition of detrital hematite) and secondary red beds (involving diagenesis by oxidizing interstitial fluids). Gay and Grandstaff (1980) have described, from beneath Huronian sediments at Elliot Lake, an approximately 2.3 Ga old soil profile on granite which shows both iron-enrichment and oxidation. Subaerial residual soil profiles are likely to be among the most direct indicators of ancient atmospheric chemistry. Beneath an oxidizing atmosphere whether profiles are oxidized or reduced depends primarily on the position of the water-table; beneath a reducing atmosphere only reduced profiles form.

BURKE, K.

Ancient detrital uraninite has long been cited as evidence of a reducing atmosphere, but Simpson and Bowles (1977) showed that all the detrital grains from the Witwatersrand basin which they studied contained more than 1% Th O_2 and were similar to the thorian uraninites that survive today in the sediments of the Indus River under the modern oxidizing atmosphere.

Precambrian iron-ores have sometimes been considered related to a reducing atmosphere. Here again Curtis' (1977) comments are relevant:

> "At the present time (and through the Phanerozoic) almost all the oxidized iron entering the sedimentary column is reduced by organic matter"..... "Rather rare circumstances allow for oxidized sediment preservation: either a lack of deposition of organic matter within rapidly deposited terrestrial detritus from arid environments or its complete destruction within the uppermost oxidizing layer of extremely slowly deposited sediments. The predominance of reduced sedimentary iron minerals within the fragmentary Pre-Cambrian record therefore is not, of itself, very convincing evidence of a reducing atmosphere."

At one time there was a suggestion that most Precambrian iron-ores had formed at about the same time ~2.0 Ga ago possibly marking a transition in the oxidation state of the atmosphere. More dating has shown that some iron formations are older and many are younger than this age. There is no great concentration of iron formation of one age and even if there was it would be more likely to relate to selective preservation rather than selective formation. If there is a peculiarity of Precambrian iron ores it lies in their large numbers and the great size of individual deposits (Gole and Klein, 1981). Whether these properties indicate geochemically different conditions from today is not clear. What is clear is that we do not understand very well how Phanerozoic iron-ores were formed and that Precambrian iron-ores are themselves quite varied (Kimberley, 1978).

In conclusion it appears that evidence of an early anoxic atmosphere is less strong than was once thought and that numerous processes, but especially diagenesis, render making inferences about the oxidation state of the ancient atmosphere/hydrosphere system very difficult. Specifically isotopic compositions of such elements as sulfur and oxygen are more likely to reflect conditions at diagenesis than to reflect the composition of contemporary seawater.

REFERENCES

Badham, J.P.N. and Stanworth, C.W., 1977. Evaporites from the Lower Proterozoic of the East Arm, Great Slave Lake: Nature, v.268, p. 516-518.

Clemmy, H. and Badham, N, 1982. Oxygen in the Precambrian atmosphere: An evaluation of the geological evidence. Geology, v.10, p. 141-146.

Curtis, C., 1978. Sedimentary geochemistry; environments and processes dominated by the involvement of an aqueous phase. Roy. Soc. Lond. Phil. Trans. Ser. A,v.186, p. 353-372.

Gay, A.L. and Grandstaff, D.E., 1980. Chemistry and mineralogy of Precambrian paleosols at Elliot Lake, Ontario, Canada. Precamb. Res., v.12, p. 349-373.

Gole, M.J. and Klein, C., 1981. Banded iron-formations through much of Precambrian time. Jour. Geol. 89, p. 169-183.

Kimberley, M.M., 1978. Paleoenvironmental classification of iron formations, Econ. Geol., v.73, p.215-229.

Lambert, I.B., Donnelly, T. H., Dunlop, J.S.R., and Groves, D.I., 1980. Stable isotopic compositions of early Archean sulphate deposits of probably evaporitic and volcanogenic origins, Nature, v.276, p.808-811.

Shegelski, R.J., 1980. Archean cratonization emergence and red bed development, Lake Shebandowan area, Canada. Precamb. Res., v.12, p. 331-347.

Simpson, P.R. and Bowles, J.F.W., 1977. Uranium mineralization in the Witwatersrand and Dominion Reef Systems. Roy. Soc. Lond. Phil. Trans. Ser. A, v.186, p. 527-548.

COMPOSITIONAL CLUES TO THE HISTORY OF THE TERRESTRIAL PLANET ATMOSPHERES, A.G.W. Cameron, Harvard College Observatory, Cambridge, MA 02138.

Much has been made of the so-called "gradient" in the abundance of ^{36}Ar in going from Venus to Earth to Mars. Attempts to interpret this have led to some strange views of processes in the primitive solar nebula. However, my work on other aspects of the history of the Earth-Moon system has led me to suspect that the history of the Earth's atmosphere should have been quite unlike that of any of the other terrestrial planets. Viewed in this light, the abundances of the noble gases in the three terrestrial planet atmospheres would no longer form a "gradient".

The anthropocentric tendency is to assume that the Earth represents the normal condition, and that departures from it are anomalies which need investigation. However, in this case it appears to me more likely that Venus represents the normal condition for the abundances of the noble gases, and the Earth represents the anomaly. The reason for this has to do with the presence of the Moon, which is itself a very anomalous body, and the likelihood that the formation of the Moon involved the Earth in an energetically-violent episode.

The pattern of the noble gases in the terrestrial planet atmospheres resembles typical patterns of these trapped gas abundances in meteoritic materials. For a long time this has been very reasonably interpreted as implying that the bulk of the atmospheres were derived from solids impacting onto the planets during the accumulation process, rather than implying that the gases were some sort of remnant of a concentration of the primitive solar nebula toward these gravitating bodies. I accept this interpretation. The simplest a priori expectation is that Venus and the Earth, being of about the same mass and mostly outgassed, would have about the same initial atmospheric content of the noble gases. This is consistent with the fact that the planetary CO_2 contents of these two objects seem to be about the same. Mars has a much smaller atmospheric mass per unit mass. Unless one is prepared to assume that outgassing has been grossly inefficient, it follows that Mars has suffered the bulk loss of a major part of its atmosphere, probably from collisions of incoming planetesimals.

If one accepts the above point of view, then it follows that the Earth must also have suffered a bulk loss of a major part of its atmosphere, in order to reduce the xenon to an intermediate level between that of Venus and Mars. In the case of the Earth, one cannot suggest that this has resulted from planetesimal impacts, for similar impacts would have produced similar effects on Venus. However, there may have been a much more violent event affecting the Earth.

Bill Ward and I have suggested (1,2) that a major collision with the protoearth was responsible for the formation of the Moon. The reasoning that led to this conclusion started with a calculation of the mass of an object hitting the protoearth tangentially that would be required to give the Earth-Moon system its present angular momentum. The mass is about that of Mars, an order of magnitude larger than the Moon. We then investigated the effects of such a collision.

If planetary accumulation takes place initially rather rapidly, as I think likely, then the initially rapid rate of heating will lead to prompt planetary differentiation, so that the two colliding objects are likely to have formed cores and their mantles may have been molten. At a collision velocity which must have been 11 km/sec or higher, solid rock is vaporized and molten rock is even more easily vaporized. Hence at the site of the major collision a large mass of vapor from rock decomposition products would be formed. After a small amount of expansion, these products will recondense. However, in the meantime, nongravitational forces in the form of pressure gradients will place a small part of the vaporized mass in orbit around the Earth. Most of the impacting object will be absorbed by the protoearth after less than one complete orbit away from the site of the collision.

The collision produces an extremely hot environment for the protoearth. I have estimated that the internal release of energy will expand the protoearth by about ten percent in radius. The disk of condensed vapors tends to clump and then shear (2), producing a strong tidal interaction with the protoearth, leading to a rapid spreading out and general recession from the protoearth toward the Roche limit, where accumulation of the Moon can begin. Dissipative friction keeps this material heated near the melting point. As a result of these processes, the Moon is formed strongly depleted in siderophile elements and the more volatile elements.

The protoearth is likely to lose practically all of its early atmosphere in this event, possibly in part because of the collision, but also because of the high temperature. There is evidence for

this in the isotopic composition of atmospheric xenon. The fractionation pattern exhibited by the xenon isotopes is unique in nature but is consistent with the xenon being a remnant of a much larger reservoir that has been subject to distillation. Thus, if xenon has mostly thermally evaporated, then there would be no traces of lighter gases from the earlier protoearth atmosphere. The present atmosphere of the Earth would have been generated either from gases trapped in solid materials that accumulated onto the Earth after the major collision had taken place, or from materials that had not been outgassed from the interior before the collision. The persistence of the fractionation pattern in xenon suggests that the precollision component continues to dominate the abundance of that element.

The comparison of Earth to Venus as far as atmospheric content is concerned is subject to a compounding of possible errors of the order of factors of two or three, but nevertheless the differences are so great that a quantitative comparison is useful. In the Venus atmosphere the amount of ^{36}Ar is two orders of magnitude greater than in the terrestrial atmosphere, but there is only one-third as much ^{40}Ar (3,4). Since potassium appears not to be depleted in Venus surface rocks relative to the Earth, it appears that Venus is less outgassed than the Earth. The present ^{36}Ar is new argon, introduced since the collision. It follows that the present xenon, which is still mostly original fractionated xenon, is still more abundant than the fresh xenon by a factor of several. Most of the xenon, both new and old, must have been ingassed by the Earth in view of its small atmospheric content. It appears that the fractionation of the original xenon is just consistent with a gravitational escape fractionation process.

If it is assumed that the terrestrial planets formed entirely by accumulation of planetesimals, then the time scale for the process is of the order of 10^8 years (6). If, as I believe likely (7), the bulk of the terrestrial planets were formed as refractory precipitates in giant gaseous protoplanets which were then thermally evaporated, the subsequent accumulation of solids bearing volatile materials will still take roughly 10^8 years. It is clear that the giant collision discussed here must have taken place toward the end of this accumulation process, since so little gas was brought in afterwards. The time scale for the dissipation of the primitive solar nebula should not exceed about 10^6 years, so at the time under discussion the protoearth and the colliding object were isolated in space. Hence no additional gas can be added from the solar nebula. One possible origin for the colliding object is as a fragment of the unstable gaseous ring that led to the formation of the Earth giant gaseous protoplanet (8); smaller fragments are dynamically unstable against perturbation into eccentric orbits, and subsequently it is likely that a collision would occur with one of the terrestrial planets in a time of the order of 10^8 years. In principle, the colliding body could be a fragment of any of the unstable rings associated with the formation of protoplanets. However, the Moon will be formed almost entirely from material in the original protoearth, while the Earth will absorb most of the impacting material. Since the oxygen isotope ratios in the two bodies are the same, and since isotopic homogenization occurs rapidly around an orbit in the nebula, this is a mild argument for origin of the fragment in the same unstable ring as the protoearth.

REFERENCES

(1) Cameron, A.G.W. and Ward, W.R. (1976) Lunar Science VII. (2) Ward, W.R. and Cameron, A.G.W. (1978) Lunar Science IX. (3) Hoffman, J.H., Oyama, V.I., and von Zahn, U., (1980) J. Geophys. Res., **85**, 7871-7881. (4) Hoffman, J.H., Hodges, R.R., Donahue, T.M., and McElroy, M.B. (1980) J. Geophys. Res., **85**, 7882-7890. (5) Pepin, R.O., and Phinney, D. (1979) Preprint. (6) Wetherill, G.W. (1980) Ann. Rev. Astron. Astrophys., **18**, 77-113. (7) Cameron, A.G.W., DeCampli, W.M., and Bodenheimer, P. (1982) Icarus, in press. (8) Cameron, A.G.W. (1978) Moon and Planets, **18**, 5-40.

46 MODELS OF THE SOLAR NEBULA: WHAT DETERMINED THE THERMAL STRUCTURE?

P. M. CASSEN, NASA Ames Research Center, Moffett Field, CA 94035

The time scale for the accumulation of kilometer-sized bodies (protoplanetary-sized, in some theories) in the solar nebula has been estimated to be 10^4 years or less. The time scale for the collapse of a protostellar cloud to form the protosun and its nebula is probably in the range of 10^4-10^6 years. It therefore seems likely that the thermodynamic conditions under which volatiles become associated with the solid objects that eventually become the bodies of the solar system (planets, meteorites, comets, etc.) were those that prevailed during the formation of the nebula. The thermal structure during this stage was determined by the dissipative transport of mass and angular momentum. However, the processes by which this transport occurred would have been very different for a nebula with high angular momentum (as measured by an appropriate non-dimensional parameter) than for one with low angular momentum. In the former case, gravitational torques caused by shock-producing spiral density waves are expected; in the latter case, hydrodynamic turbulence may be the predominant mechanism of transport. The appropriate measure of angular momentum in this context is the inverse of the parameter $P \equiv \nu (GM/c_s)^3 (M/J)^4$, where M is the total mass of protosun and nebula, J is the total angular momentum, G is the gravitational constant, c_s is the sound speed in the cloud, and ν is the turbulent viscosity in the nebula. Cassen and Moosman (1981) and Cassen and Summers (1982) have shown that for $P \lesssim 1$, $M_n/M_\star = 0(1)$ (where M_n = nebula mass and $M_\star$ = protosun mass), and for $P \gg 1$, $M_n/M_\star = 0(P^{-\frac{1}{4}})$.

Based on models of hydrodynamic collapse, and assumed values of J and ν one can construct models of the formation and evolution of the solar nebula that yield surface density and photospheric temperature as functions of radius and time. Further assumptions regarding the vertical transport of energy in the direction parallel to the nebula's rotation axis enable one to calculate vertical thermal structures. Although the details of the results obtained depend on the specific assumptions adopted, some important general conclusions can be drawn which do not depend on the details. These are as follows:

All nebula models predict temperatures high enough during the formation stage to vaporize silicate material within an AU (or appreciable fraction thereof) of the protosun. All models predict low temperatures (100°K or less) beyond 5-10 AU.

The condensed material in the outer parts of a low mass nebula would be a mixture of mostly "processed" stuff - dust that has been vaporized or heated to a high temperature and subsequently cooled, and some unprocessed stuff that had never been heated. For a high mass nebula, there would be very little processed material in the outer parts.

Low mass nebulas heat up during formation and cool down after accretion from the protostellar cloud stops. High mass nebulas cool during formation, at least until they become gravitationally unstable. After that, localized shock heating might occur.

The net mass flux in a low mass nebula is generally outwards during formation, with a region of inward flux growing from the center after accretion stops. The net mass flux of a massive nebula is inwards during formation until gravitational instability occurs, after which the outer regions may experience irregular outward flux.

References

Cassen and Moosman (1981) Icarus 48, 353-376.

Cassen and Summers (1982) Icarus (submitted).

PREBIOTIC CARBON CYCLE: PHOTOCHEMICAL REDUCTION OF CO IN EARTH'S PRIMITIVE ATMOSPHERE. S. Chang, NASA Ames Research Center, Moffett Field, CA 94035, and A. Bar-Nun, Tel-Aviv University, Ramat Aviv, Israel.

Since the time of their earliest known occurrence, biological systems have been an integral part of the geochemical cycle of carbon (and other biogenic elements)involving, on the one hand, the transfer of carbon from atmosphere and hydrosphere into sediments and, on the other hand, the replenishment of the first two reservoirs as a result of the burial of sediments and the expulsion of volatiles from Earth's interior. Implicit in the view that biological systems arose by natural selection from chemical systems is the existence of an analogous prebiological carbon cycle driven by the natural fluxes of mass and energy at Earth's surface. Indeed, it may be hypothesized that a prebiotic cycle was a prequisite for the origin of life, and that the courses of planetary evolution responsible for the absence of such a cycle now on Venus and Mars are also responsible for the conditions inimical to life on those planets. In this context the origin of life on Earth and the origin of the geochemical cycle for carbon were inextricably intertwined. For these reasons, the development of models for the prebiotic carbon cycle would appear to be essential to gaining clearer understanding of the origin of life within the framework of geologic evolution. Among the data needed for development of such models are more quantitative assessments of geologically plausible pathways by which carbon in the prebiotic atmosphere may have been transferred into surface reservoirs through abiotic synthesis of organic matter.

The absence of a geological record makes a firm assessment of the atmospheric composition during Earth's first 0.8 billion years virtually impossible. Suppositions for the atmosphere range from H_2-rich, containing H_2-CH_4-NH_3-N_2-H_2O-H_2S, to H_2-depleted, containing CO-CO_2-N_2-SO_2. Although organic synthesis in hydrogen rich mixtures has been studied extensively, relatively little work has been reported on the CO-CO_2-N_2-H_2O system. Since solar radiation is the most abundant energy source in the atmosphere, photolytic investigations of the latter mixture are essential for an assessment of the full range of possibilities for the synthesis of organic matter on the primitive Earth. The photochemical experiments summarized below focused on the purely gas phase reactions of H_2O, CO, CO_2 and N_2; they were intended both to elucidate production mechanisms and to simulate reactions that could have occurred on the prebiotic Earth either above the cloud tops, at altitudes of about 10 km, where the abundance of water vapor is still considerable, or in an atmosphere containing few clouds.

Gas mixtures containing H_2O and CO with various proportions of H_2, CO_2, and N_2 were irradiated with 185 nm light or a simulated solar spectrum from which short wavelength uv was blocked by a filter cell containing O_2. The major products were H_2 and CO_2; alcohols, aldehydes, hydrocarbons, acetone and acetic acid were also formed; but no nitrogen-containing organic compounds were detectable. The initial step in the reactions involved photodissociation of H_2O molecules to yield hot H-atoms and hydroxyl radicals; the former reduced CO and recombined to H_2, while the latter oxidized CO to CO_2 and generated additional H-atoms. Changes in gas composition with irradiation time suggest that the organic products arose from a series of consecutive reactions in which CO was converted first to aldehydes and alcohols, which then were further hydrogenated to hydrocarbons. The overall apparent

quantum yield for conversion of CO to organic carbon varied between 0.23 and 0.03 as a function of CO partial pressure between 0.39 and 0.004 atm. These results indicate that, even if the primordial atmosphere contained carbon only in the form of CO or a mixture of CO and CO_2, and no molecular hydrogen, a variety of organic compounds would have been produced by gas phase photochemical processes.

Upper and lower bounds can be crudely estimated for the "average" concentration of organic carbon in a hypothetical "global" ocean resulting from rain-out of compounds produced solely by photolysis of H_2O in the presence of CO. These calculations are made in the context of existing models for formation of the atmosphere and rely on estimates of primordial uv fluxes and terrestrial H and C inventories, coupled with the apparent quantum yields for synthesis of organic carbon. For the case in which the total carbon inventory was released as CO over 10^8 years, in 10^6 years, the concentration of organic carbon could have been as high as 0.02 M in a global ocean 30 m deep. For the case in which CO was released as a minor constituent and the inventory release time was 5×10^8 years, the concentration would have been 0.0004 M in 5×10^6 years.

Gas phase photochemistry was certainly only one of the many possible prebiotic production mechanisms for organic compounds. Other processes and reactants appear to have been required to produce nitrogen-bearing organic compounds (e.g., amino acids) in atmospheres containing N_2; and entire classes of heterogeneous reactions involving liquid-solid, gas-solid, and gas-liquid interfaces and other energy sources are virtually unexplored. It is uncertain whether the types and amounts of organic compounds discussed above were necessary or sufficient for the chemical evolution of organic matter to proceed beyond the monomer stage to attain higher levels of molecular organization. It is also unclear what the fate of these compounds would have been in the water column or how they may have been incorporated in sediments and at what rates. Resolution of these uncertainties awaits more detailed reconstructions of the prebiotic environment, more thorough accounting of the sources of simple organic compounds and the pathways for their conversion to more complex systems, and a better understanding of the interactions between organic and inorganic matter in that environment.

ACCRETION OF VOLATILES. S. Chang, NASA Ames Research Center, Moffett Field, CA 94035, and J. F. Kerridge, University of California, Los Angeles, CA 90024

It seems likely that the terrestrial planets acquired their inventories of volatile elements as a late-accreting veneer of volatile-rich material [1, 2]. That hypothesis is reinforced by recent calculations which show that equilibration condensation could not have supplied the terrestrial planets with their initial endowments of C and N [3,4]. The hypothetical volatile-rich veneer is commonly identified with carbonaceous chondrite-like material [1,2]. Ages and elemental compositions of extant carbonaceous chondrites are broadly consistent with this view; we consider first the isotopic composition of C,H,N in such meteorites, as it bears upon this issue. Then, we consider the accretion of volatiles in the inner solar system within the context of nebular thermal history.

Reasonable estimates of $\delta^{13}C$, δD and $\delta^{15}N$ for the bulk earth may be made[2]; differences from these values, observed for some elements on Mars and Venus, are generally attributed to post-accretional fractionation [5,6]. Chondritic values may be found which are similar to terrestrial; for example, a mixture of CV3 chondritic material with a small proportion of CM2 material has been suggested as a suitable veneer [2].

Recent analyses of carbonaceous chondrites have revealed considerable inter- and intrameteorite variability in the isotopic composition of C,H,N [7,8,9]. For H and N this variability exceeds the fractionating capability of reasonable solar system processes. In addition, H and possibly N in meteorites and those terrestrial planets for which global estimates are available, are substantially enriched in the heavier isotope with respect to estimated protosolar values [10,11]. It seems likely that both nucleogenetic and mass-dependent processes have contributed to the observed variability. Ion-molecule reactions in interstellar clouds may account for the postulated mass-fractionation [10,12]. Apparently widespread survival of isotopic inhomogeneity in C,H,N has a number of implications for planetary accretion of these elements. It should be noted that this inhomogeneity could have been spatial, temporal or both.

First, the initial population of volatile-rich objects may have exhibited even greater isotopic variability than that currently observed in meteorites.

Second, different planets may have sampled different populations of volatile-rich objects. Assumptions of initially earth-like isotopic compositions of C,H,N for Mars and Venus may not be justified.

Third, temperatures in the inner solar system were apparently sufficiently low during the final stages of accretion to permit survival of C,H, N-bearing species. It is tempting to identify some of these with organic molecules synthesized in interstellar clouds.

Observations of interstellar clouds indicate that volatiles carried into the solar nebula would have included non-condensable gases; ices (H_2O, NH_3); organic compounds containing C,H,N,S,O; and carbonaceous grains. In accordance with the low temperature (~10 K) associated with the isothermal stage of protostellar collapse models, virtually all volatile elements, except H_2 and He, should have entered the nebula in the form of interstellar grains and interstellar atoms (including noble gases) and molecules (including CO, N_2, CH_4) accreted as mantles on grains. Apparently, on the sub-micron to micron scale of primitive dust and mantled dust grains, a variety of stellar and interstellar source regions could have been sampled, and heterogeneity in elemental, isotopic and molecular composition would have resulted. The degree

S. Chang and J. F. Kerridge

to which heterogeneity would have been preserved must have been related to the thermal histories of these grains. Their thermal histories can be characterized by three stages: pre-accretion (gas-dust), accretion (planetesimal-parent body) and post-accretion (parent body); and volatiles could have been lost or gained (or both) at each of these stages.

In the past, most discussions of volatiles in primitive bodies focused on the origin of their carriers in the pre-accretion stage as a result of hypothetical nebular condensation processes. We emphasize the view that differential vaporization of pre-solar volatile carriers at both the pre-accretion and accretion stages may be a more relevant consideration for the distribution of volatile elements in the inner solar system. Throughout the adiabatic stage of protostellar collapse, the nebular thermal gradient within 5 AU would have caused evaporative and pyrolytic fractionation of the volatiles accreted into planetesimals. Moderately refractory carbonaceous grains (including presolar carriers of noble gases) could have survived and accreted closer to the protosun than ices, and ices closer than clathrates. After the nebula began to cool it would have become possible to condense, accrete and preserve the more volatile and thermally labile substances in regions where this was prevented earlier by higher temperatures. Thus, ices, clathrates and organic compounds in grains or planetesimals probably infiltrated the inner solar system late in nebular evolution by transport of material accreted at greater radial distances, by late infall of interstellar matter, or by accumulation of local material condensed and accreted from cooling residual gas (or combinations of these). We point out, however, that in carbonaceous meteorites the evidence for condensates formed by nebular gas-dust equilibration below 400 K is weak, at best [13].

The evidence of pervasive aqueous alteration on carbonaceous chondrite parent bodies [13] is consistent with a temporal separation between the accretion of anhydrous phases and their subsequent alteration by volatile-rich fluids. It is not clear, however, whether these hydrous fluids originated elsewhere within the parent bodies as a result of melting of solid phases (ices?) previously co-accreted with anhydrous phases or whether such fluids resulted from later addition of volatiles. In either case the accretion of parent bodies of aqueously-altered carbonaceous chondrites appears to be inconsistent with models of either homogeneous accretion or simple heterogeneous accretion of equilibrium condensates. Although these considerations suggest that similar models for planetary accretion may be inadequate, they are consistent with the hypothesis that the terrestrial planets acquired volatile inventories at a late stage in their accretion.

[1] Turekian K.K. & Clark S.P., EPSL 6, 346 (1969). [2] Anders E. & Owen T., Science 198, 453 (1977). [3] Lewis J.S. et al., Icarus 37, 190 (1979). [4] Fegley M.B., Meteoritics 16, 314 (1981). [5] McElroy M.B. et al., Science 194, 70 (1976). [6] Donahue T.M. et al., Science 216, 630 (1982). [7] Chang S. et al., Lunar Planet. Sci. IX, 157 (1978). [8] Kolodny Y. et al., EPSL 46, 149 (1980). [9] Robert F. & Epstein S., Geochim. Cosmochim. Acta 46, 81 (1982). [10] Geiss J. & Reeves H., Astron. Astrophys. 93, 189 (1981). [11] Kerridge J.F., Nature 283, 183 (1980). [12] Kerridge J.F., Lunar Planet. Sci. XI, 538 (1980). [13] Bunch T.E. & Chang S., Geochim. Cosmochim. Acta 44, 1543 (1980).

MECHANISMS FOR THE VERTICAL TRANSPORT OF H_2O WITHIN THE MARTIAN REGOLITH. S. M. Clifford, Department of Physics and Astronomy, Univ. of Massachusetts, Amherst, MA. 01003.

Various lines of morphologic evidence suggest that substantial quantities of ground ice have existed in the equatorial regolith of Mars throughout its geologic history (1,2,3). However, recent calculations on the stability of ground ice in this region suggest that any ground ice, emplaced earlier than 3.5 billion years ago, may have long since been lost by evaporation to the atmosphere (4). It has been proposed that one possible explanation for the continued existence of ground ice in the equatorial regolith is that it may be replenished by subsurface sources of H_2O (5,6). For example, recent estimates of the planetary inventory of H_2O on Mars have ranged from a globally averaged layer some 10^2 - 10^3 meters deep (7,8). These estimates have led several investigators to suggest that Mars may possess subpermafrost groundwater systems of regional and possibly even global extent (1,5,6,9). The vertical transport of H_2O, from such groundwater systems, appears to be a viable mechanism for the replenishment of equatorial ground ice on Mars - even when the vertical distances separating the groundwater from the base of the ground ice layer are measured in kilometers.

In light of the photogeologic evidence for the widespread occurrence of volcanism on Mars (10), probably the most obvious mechanism for the vertical transport of H_2O is hydrothermal convection. This process has already been proposed as the possible cause of dark surface stains which appear just west of Olympus Mons (11) and has been suggested as a possible explaination for the origin of the numerous small channels which are frequently observed to eminate from the outside rims of craters in the heavily cratered terrain of Mars (5,12,13). Unfortunately, while hydrothermal convection may have been an important process for the vertical transport of H_2O on Mars - its magnitude and areal extent are, at present, impossible to quantify.

Similar difficulties arise when attempting to address the importance of shock-induced transport. Shock waves generated by earthquakes, impacts and explosive volcanic eruptions, can produce a transient compaction of water-bearing sediments which may force water up to the surface through regolith fractures and pores. During the great Alaskan earthquake of 1964, this process resulted in water and sediment ejection from the ground as far as 250 miles from the earthquake's epicenter (14). The energy released by this earthquake was approximately 2×10^{17} J (15) - or roughly equivalent to that of a 50 Megaton nuclear explosion. While the historical frequency of earthquakes of this magnitude on Mars may have been low, the martian cratering record provides abundant evidence that the planet has witnessed numerous events of a similar, and often much greater, magnitude. Indeed, the impacts that produced the larger basins such as Hellas and Argyre may alone have generated enough seismic energy to have replenished martian ground ice on a global scale. Even without these larger impacts, however, the density of craters found over much of the martian surface suggests that shock-induced transport resulting from smaller impacts may have been sufficient to replenish near surface ground ice over much of the planet.

Although far less dramatic and energetic than either of the two processes discussed above, perhaps the most important mechanism for the vertical transport of H_2O on Mars has been the process of thermal moisture movement (5). It has been known for almost 70 years that H_2O transport, in excess of that predicted by Fick's law, will occur in a porous medium under the influence of a temperature gradient - the direction of transfer being from warm to cold (16). The importance of this process on Mars is that the existence of a crustal geothermal gradient could provide the means necessary to thermally cycle H_2O between a deeply buried reservior of groundwater and the base of a near-surface layer of ground ice. Philip and deVries (17) and Taylor and Cary (18, 19) have formulated two different but widely accepted models for calculating the magnitude of this type of thermally driven moisture transfer. Despite the differences in approach, it has been shown that the final form of the flux equations for both models are identical (19,20). After Cary (21), we can describe the thermally driven vapor flux by the equation:

$$J_v = - \frac{\beta D_{AB} P_s H}{R^2 T^3} \frac{dT}{dz} \qquad (1)$$

where D_{AB} is the binary diffusion coefficient of H_2O in CO_2, P_s is the saturated vapor pressure of H_2O at a temperature T, H is latent heat of vaporization, R is the universal gas constant, and β is a dimensionless factor whose value (typically around 1.83 (20)) depends on regolith temperature, porosity, and water content. Making use of this equation we find that for a martian geothermal gradient of 45 K/km, the calculated flux of H_2O to the freezing front at the base of the ground ice layer is approximately 7×10^{-5} gm/cm^2 per martian year. At this rate, over the course of martian geologic history, the martian geothermal gradient could supply enough H_2O from a subpermafrost groundwater system to replenish a layer of ground ice nearly 1.7 km thick. Further, unlike the first two processes discussed in this abstract, this transport will occur on a continuous and global basis for as long as there exists a geothermal gradient and subsurface reservoir of H_2O.

Inspection of Equation 1 reveals that, for the higher temperatures expected at depth, the flux of H_2O leaving the groundwater surface greatly exceeds that which finally reaches the freezing front at the base of the ground ice layer. This difference is due to the decrease in saturated vapor pressure which occurs with decreasing temperature. As shown by Jackson et al. (22), once a closed system has been established (ie., the ground ice capacity of the near-surface regolith has been saturated under conditions where the ice exists in stable equilibrium with the atmosphere) a dynamic ballance of opposing fluxes is achieved. As water vapor rises from the warmer depths to the colder regolith above, it will condense - creating a circulation system of rising vapor and descending liquid condensate. In those instances where the system is not closed (eg., where ground ice is not in equilibrium with the atmosphere

H_2O TRANSPORT WITHIN THE MARTIAN REGOLITH

Clifford, S. M.

- such as near the martian equator) it is possible for H_2O transport to occur from the freezing front at the base of the ground ice to those areas undergoing depletion. Transport in this subfreezing region may occur via thin films of unfrozen water which are adsorbed on mineral surfaces (23,24). These films have been shown to exist down to very low temperatures - especially in the presence of potent freezing point depressors such as $CaCl_2$ (25). As before, this transport through the frozen regolith of Mars may be thermally driven (23,24).

A more detailed discussion of these processes and their potential importance to the distribution of equatorial ground ice on Mars is in preparation.

Acknowledgement: This research was supported under NASA Grant NSG 7405.

References: 1) Johansen, L. A. (1978) Proc. 2nd Colloq. Plan. Water and Polar Processes, 109. 2) Allen, C. C. (1979) Icarus 39, 111. 3) Rossbacher, L. A., and S. Judson (1981) Icarus 45, 39. 4) Clifford, S. M., and D. Hillel (1982) JGR (in press). 5) Clifford, S. M. (1980) Proc. 3rd Colloq. Planet. Water, 68. 6) Clifford, S. M. (1981) Proc. 3rd Int. Colloq. Mars, 44. 7) Pollack, J. B. and D. C. Black (1979) Science 205, 56. 8) Lewis, J. (1980) personal communication. 9) Carr, M. H. (1979) JGR 84, 2995. 10) Greeley, R. and P. D. Spudis (1981) Rev. Geophys. Space Phys. 19, 13. 11) Morris, E. C. (1980) NASA TM 81776, 162. 12) Pieri, D. (1979) Ph.D. Thesis, Cornell University. 13) Newsom, H. E. (1980) Icarus 44, 207. 14) Waller, R. M. (1968) The Great Alaskan Earthquake of 1964: Hydrology Part A., pp. 97-116, Pub. Nat. Acad. Sci.. 15) Stacey, F. D. (1977) Physics of the Earth, John Wiley & Sons. 16) Bouyoucos, G. J. (1915) J. Agr. Res. 5, 141. 17) Philip, J. R. and D. A. deVries (1957) Trans. A.G.U. 38, 222. 18) Cary, J. W. (1963) J. Phys. Chem. 67, 126. 19) Taylor, S. A. and J. W. Cary (1964) Soil Sci. Soc. Proc. 28, 167. 20) Jury, W. A., and J. Letey, Jr. (1979) Soil Sci. Soc. Amer. J. 43, 823. 21) Cary, J. W. (1966) Soil Sci. Soc. Amer. Proc. 30, 428. 22) Jackson, R. D., D. A. Rose and H. L. Penman (1965) Nature 205, 314. 23) Cary, J. W., R. I. Papendick, and G. S. Cambell (1979) Soil Sci. Soc. Amer. J. 43, 3. 24) Miller, R. D., J. P. G. Loch, and E. Bresler (1975) Soil Sci. Soc. Amer. Proc. 39, 1029. 25) Anderson, D. M., and A. R. Tice (1973) in: Ecological Studies. Analysis and Synthesis, Vol. 4., pp. 107-124, Springer-Verlag Berlin.

COMPARISON OF He, Sr AND Pb ISOTOPIC VARIATIONS IN THE ICELANDIC 'HOTSPOT', M. Condomines[1], K. Gronvold[2], P.J. Hooker[1], R.K. O'Nions[1] and E.R. Oxburgh[1], [1]Dept. Earth Sciences, University of Cambridge; [2]Nordic Volcanological Institute, Reykjavik, Iceland.

Basalts erupted in the neovolcanic zones of Iceland and Reykjanes Ridge exhibit a broad correlation between $^{87}Sr/^{86}Sr$ and $^{206}Pb/^{204}Pb$ ratios (1,2,3,4) indicating a coherence between Rb/Sr and U/Pb in the reservoirs that have contributed to the source of Icelandic magmas. These observations are commonly reconciled by models involving interactions between a depleted reservoir in the upper mantle and a relatively undepleted reservoir (generally the lower mantle). In the most simple models it would be anticipated that ^{3}He and other primordial rare gases should be principally stored in the less depleted reservoir and that $^{3}He/^{4}He$ should exhibit a coherent relationship with $^{87}Sr/^{86}Sr$ for example in erupted volcanics.

This possibility has been investigated in detail through the analysis of samples from the actively rifting neovolcanic zone of Iceland. Glassy samples appear to be the most appropriate for analysis of $^{3}He/^{4}He$ and the present suite includes basaltic pillow margins and hyaloclastites and glassy intermediate and acid lavas. He concentrations in these rocks are typically ca 10^{-8} cc g^{-}, some two orders of magnitude lower than most oceanic ridge glasses. He has been separated by total fusion with a typical blank of $< 2 \times 10^{-9}$ cc STP; which results in negligible blank corrections in most cases.

$^{3}He/^{4}He$ ratios are variable along the active rift zones and R/Ra ($(^{3}He/^{4}He)_{rock}/(^{3}He/^{4}He)_{atmosphere}$) $\geq 5 \leq 24$ for basaltic rocks, and R/Ra $\simeq 1$ for intermediate and acid rocks. $^{87}Sr/^{86}Sr$ ratios measured on the same samples show no clear correlation with $^{3}He/^{4}He$, as might be expected from a simple 'hotspot' model. A crucial question however is whether the measured ratios in the erupted basalts are equal to the mantle values. There are two processes which may lead to their modification: isotope fractionation either during magma generation or in a shallow crustal reservoir, or during post-eruptive cooling of the lava. The comparatively low He concentrations in Icelandic basalts may be ascribed to the low pressure at magma eruption compared to ocean ridge basalts. As a consequence the trapped He is residual and may be isotopically fractionated relative to the He in the primitive parental magam. This may be the explanation for the difference between the ratios in gas samples (R/Ra $\simeq$ 8.5) and lavas (R/Ra $\simeq$ 5) in the presently active Krafla region of N. Iceland. Contamination of magmatic He by crustal He (with lower $^{3}He/^{4}He$ ratio) may occur either during transfer of magma through the crust or its residence in a magma chamber. In this respect it is noteworthy that the highest $^{3}He/^{4}He$ ratios are found in fissure basalts from the Reykjanes peninsula, and the lowest for central volcanoes in the centre of Iceland (Askja and Krafla) in parallel with the $\delta^{18}O$ and ($^{230}Th/^{232}Th$) variations (5,6). The origin of low $^{3}He/^{4}He \simeq 1$ in intermediate and acid rocks remains unclear. Post-eruptive equilibration with atmospheric He or formation of the magmas by melting or assimilation of hydrothermally altered crustal rocks with R/Ra $\simeq$ 1 remain possible explanations at this stage.

Overall the results obtained from the classic Icelandic hotspot are not readily reconcilable with simple hotspot models. Hign-level processes operative within the crust leading to the modification of $^{3}He/^{4}He$ ratios must be better understood before all observed variations of $^{3}He/^{4}He$ can be ascribed to variability existing within mantle reservoirs.

REFERENCES

(1) Hart, S.R., Schilling, J.G., Powell, J.L. (1973) Nature Phys. Science, 246, 104. (2) Sun, S.-S., and Jahn, B.M. (1975) Nature 255, 527. (3) Sun, S.-S., Tatsumoto, M. and Schilling, J.G. (1975) Science, 190, 143. (4) Cohen, R.S. and O'Nions, R.K. (1982), J. Petrol. (in press). (5) Muehlenbachs, K., Anderson, A.T., Sigvaldason, G.E. (1974) Geochim. Cosmochim. Acta, 38, 577. (6) Condomines, M., Morand, P., Allegre, C.J. and Sigvaldason, G. (1981) Earth Planet. Sci. Lett. 55, 393-406.

STABLE CARBON ISOTOPES IN MIDOCEANIC BASALTIC GLASSES

David J. Des Marais, Ames Research Center, NASA, Moffett Field, CA 94035
H. Sakai, Okayama University, Misasa, Tottori-ken, 682-02 Japan, and
J. G. Moore, U. S. Geological Survey, Menlo Park, CA 94025

Studies of the earth's carbon cycle and its history require that we know the average stable isotopic composition of carbon in the crust and upper mantle. Early estimates (1,2) of this value ($\delta^{13}C_{PDB}$ = -6 to -7) were obtained by mass balance estimates of the sedimentary carbon reservoir. This approach, though very useful, suffers both from inaccurate estimates of reduced sedimentary carbon inventories and from the possibility that the average carbon isotopic composition of the sedimentary reservoir has varied over geologic time, due to isotopically selective carbon losses to the lower crust. Igneous rocks offer another opportunity to measure the average crustal carbon isotopic composition, provided that any isotope effects associated with petrogenesis are understood. Midoceanic basaltic glasses were selected for this work because they constitute our best opportunity to analyze rocks which are free of sedimentary contamination. Previous work (3,4,5) has suggested that igneous rocks contain carbon whose isotopic composition is substantially depleted in ^{13}C, relative to the overall average composition reported for sediments. The present work indicates that, at least for midoceanic basaltic glasses, the carbon which is depleted in ^{13}C is not indigenous to the glasses.

Each of six midoceanic basaltic glasses was combusted sequentially at three temperatures (Table 1) using the method employed previously for lunar rocks (6). The lower combustion temperatures are intended to remove surficial carbon contamination while causing minimal losses of the indigenous carbon. That minimal indigenous carbon is lost is consistent with the very small losses at temperatures below 750°C of sulfur, which is presumed to be indigenous. Carbon released below 750°C is depleted in ^{13}C and probably represents surficial organic contamination.

The pattern of carbon abundances measured when the glasses melt support other observations (7,8) that carbon content is proportional to the depth of eruption. Note that the Hawaiian basalt #71-AP3 was erupted subaerially and apparently lost essentially all of its indigenous carbon. The ^{13}C-depleted trace of carbon that remains is likely either contamination or else a residuum which is highly fractionated isotopically. The carbon released from these glasses which erupted beneath the ocean has a remarkably constant carbon isotopic composition ($\delta^{13}C_{PDB}$ ranges from -5.8 to -6.4). Very recent $\delta^{13}C_{PDB}$ measurements of basaltic glasses from these localities (Des Marais and Moore, submitted to Earth and Planet. Sci. Lett.) range from -4.7 to -8.8. Apparently some isotopic fractionation accompanies the loss of carbon gases from these magmas as they ascend to the ocean floor. This notion is supported by the work of Javoy et al. (9), who observed experimentally that gaseous carbon dioxide in equilibrium with carbon dissolved in a 1200°C tholeiitic melt is enriched in ^{13}C by about -4 to -4.6 permil.

The range of carbon isotopic compositions observed in the glasses is the same as that observed for carbon which emanates from deep sea hydrothermal vents (10) and which is trapped in vesicles in midoceanic basaltic glasses (5). This isotopic composition is also remarkably similar to estimates obtained for the total sedimentary carbon reservoir. If these new isotope values from the midoceanic basalts and hydrothermal vents indeed represent the isotopic

composition of juvenile carbon, then the average carbon isotopic composition of crustal sediments has been remarkably constant over geologic time.

Table 1. Carbon and sulfur data from the basaltic glasses.

Sample and Eruption Depth, m.	Temperature, °C	Carbon Abundance, μg/g	$\delta^{13}C_{PDB}$	Sulfur Abundance, μg/g
Cayman Trough	450	18	-24.8±0.2	2
(18°39'N,81°46'W)	710	20	- 9.3±0.2	1
6000m	1220	164	- 6.3±0.2	990
FAMOUS	488	34	-24.8±0.1	2
(~36°N,33°W)	730	17	- 6.7±0.2	2
#519-4, 2690m	1230	136	- 6.2±0.1	810
Galapagos Ridge	450	5.6	-21.6±0.2	0.1
(0°50'N,86°W)	750	0.5	-15.8±0.4	0.5
#717-3;~2500m	1200	68	- 6.4±0.2	1310
Galapagos Ridge	450	3.6	-26.2±0.3	2
(as above), #714-1-A	1200	99	- 5.8±0.1	1360
Island of Hawaii	460	14	-22.1±0.1	0.5
#71 AP3: 0m (land)	740	4	-20.9±0.1	0.7
	1230	1.9	-23.7±0.3	38
Kilauea East Rift	440	19	-24.4±0.3	1
(19°40'N,154°30'W)	700	3	-20.2±0.2	2
#JM-1742; 1400m	1220	22	- 6.1±0.3	904

References

(1) Wickman F. E. (1956) Geochim. Cosmochim. Acta 9, 136-153.

(2) Craig H. (1953) Geochim. Cosmochim. Acta 3, 53-92.

(3) Hoefs J. (1973) Contr. Mineral. and Petrol. 41, 277-300.

(4) Fuex A. N. and Baker D. R. (1973) Geochim. Cosmochim. Acta 37, 2509-2521.

(5) Pineau F., Javoy M. and Bottinga Y. (1976) Earth Planet. Sci. Lett. 29, 413-421.

(6) Des Marais D. J. (1978) Proc. Lunar Planet. Sci. Conf. 9th, 2451-2467.

(7) Anderson A. T. (1975) Reviews Geophys. Space Sci. 13, 37-55.

(8) Moore J. G. (1979) Nature 282, 250-253.

(9) Javoy M., Pineau F. and Iiyama I. (1978) Contr. Mineral. Petrol. 67, 35-39.

(10) Craig H., Welhan J. A., Kim K., Poreda R. and Lupton J. E. (1980) EOS 61(46), 992.

HIGH ELECTRICAL CONDUCTIVITY IN CARBON-BEARING ROCKS AND METEORITES: IMPLICATIONS FOR PLANETARY INTERIORS AND ASTEROIDS

A. G. Duba, University of California, Lawrence Livermore National Laboratory, P.O. Box 808, Livermore, California 94550
T. J. Shankland, Los Alamos National Laboratory, University of California, Los Alamos, NM 87545

The electrical conductivity of the carbonaceous chondrite Allende has been measured to 950°C under controlled oxygen fugacity. The conductivity measured at a given temperature is a strong function of heating rate, similar to results reported for oil shale (Duba, 1982). Unlike oil shale with similar carbon content, the electrical conductivity of Allende remains high during dehydration (around 10^{-5} S/m) an indication that there is initial free carbon present at grain boundaries in this meteorite, as suggested by Duba and Shankland (1982) in their discussion of the high conductivity at 25°C observed by Brecher et al (1975) for carbonaceous chondrites. As the hydrocarbons which comprise Allende are pyrolyzed in flowing CO/CO_2 mixtures, the conductivity increases with time at constant temperature, again similar to behavior observed for oil shale. Such behavior is not observed for other rocks or for minerals at similar conditions. By 400°C, conductivity as high as 0.01 S/m is observed, depending on heating rate. The conductivity remains high and approaches 0.1 S/m until about 900°C, where it begins to decrease as a function of both time and temperature, apparently the result of volatilization of carbon in the unconfined sample.

Because graphite and amorphous carbon have conductivities of 10^4 to 10^5 S/m while dry rocks and minerals have values from 10^{-12} to 10^{-1}, it is not surprising that a small amount of carbon has such a large effect. These observations for oil shale and Allende allow us to speculate on the implications for planetary interiors if carbon is present as a grain boundary phase.

Examination of literature conductivity data for olivine and MgO indicates that small amounts of carbon at grain boundaries can strongly influence conductivity. Even at 1000°C where mantle minerals may have conductivities as high as $10^{-2.5}$ S/m, calculations indicate that about 100 ppm of carbon contamination at grain boundaries would cause conductivities as high as 1 S/m. Such concentrations of carbon are consistent with carbon petrology in mantle rocks. An interconnected amorphous or graphitic carbon phase on grain boundaries could provide sufficiently high conductivities to explain high conductivity layers in the mantle at subsolidus temperatures. Presumably a zone of carbon-enhanced conductivity is a less sensitive temperature probe than a partial melt zone would be.

If the early solar system experienced a T Tauri phase of the sun with high interplanetary electric and magnetic fields postulated by Sonett et al (1970), it is likely that a portion of the carbonaceous chondritic material present would have been subjected to considerable inductive heating because of its high electrical conductivity. With the reducing conditions implicit in the heating of a carbon-rich body in a vacuum, asteroid differentiation could have proceeded at a later time after condensation than that required by heating due to short-lived radionuclides.

REFERENCES

Brecher, A., Briggs, P. L., and G. Simmons, The Low-Temperature Electrical Properties of Carbonaceous Meteorites, E.P.S.L. 28, 37-45, 1975.

Duba, A. G., The Electrical Conductivity of Oil Shale to 900°C, submitted to Fuel, 1982.

Duba, A. G. and Shankland, T. J., Free Carbon and Electrical Conductivity in the Earth's Mantle, Geophys. Res. Letts., in press, 1982.

Sonett, C. P., Colburn, D. S., Schwatz, K., and Keil, K., The Melting of Asteroidal Sized Bodies by Unipolar Dynamo Induction from a Primodial T Tauri Sun, Astrophys. Space Sci., 7, 446-488, 1970.

Work performed under the auspices of the Office of Basic Energy Sciences of the U.S. Department of Energy by the Lawrence Livermore National Laboratory under contract number W-7405-ENG-48 and by Los Alamos National Laboratory under contract number W-7405-ENG-36.

CONSTRAINTS ON ARCHAEAN GEOTHERMAL REGIMES AND THEIR IMPLICATIONS FOR EARTH THERMAL HISTORY MODELS; Philip England, Department of Geological Sciences, Hoffman Laboratory, Harvard University, Cambridge, MA 02138 and Michael Bickle, Department of Geology, University of Western Australia, Nedlands, Western Australia 6009.

Irrespective of the detailed mechanisms involved, many models of the loss of volatiles from the solid earth assume a dependence of the rate of transport of volatiles on the global heat flow. The present rate of heat loss from the Earth is approximately 4.2×10^{13} W [1], while recent estimates of the internal radiogenic heat production [e.g., 2, 3, 4] range between 1.4 and 2.5×10^{13} W, and in general geochemical estimates account for around one half of the observed surface heat loss. As these observations clearly do not represent a simple steady-state balance between heat production and heat loss, it is important to determine what is responsible for the discrepancy before we can make assertions about the heat flux out of the earth during its history as a solid planet.

One possibility is that the geochemical estimates of the internal heat generation are incorrect by a factor of two.

The alternative involves considering models for the thermal history of the earth. It appears that the least uncertain factors in this subject are the decay times of the principal contributors to the radiogenic heat production in the earth and, less certainly, their relative abundances. These figures lead to the conclusion that the

earth's internal heat production was approximately twice the present rate at the end of the Archaean (2.5×10^9 years ago) and was around four times as great (4×10^9 years ago). For the purposes of this discussion, the problem lies in determining how the ratio between the earth's heat loss and its internal heat generation has changed with time.

There are many published models for the thermal history of the earth [e.g., 5, 6, 7, 8, 9] and they produce estimates for the ratio of surface heat flow to internal heat production that vary from around unity to more than two. In order to constrain models of the thermal history of the earth, it is desirable to have an estimate of the surface heat flux at some time during the past when the internal heat generation was significantly different from the present. As the oldest oceanic rocks are no more than 200 Myr old, such an estimate must come from continental material; this is unfortunate, as much of our knowledge of the present thermal state of the earth comes from observations in the oceans. However, it appears that we may at least draw inferences about the heat flow through the continents during the Archaean which bear directly on current thermal history calculations.

Pressures estimated from mineral assemblages in Archaean high grade terrains [10, and data summarized by 11] may be used to estimate geothermal regimes in the Archaean continental crust in two ways. First, they may be combined with temperature estimates to yield bounds on the geothermal gradient during the thickening event which produced the metamorphism; this yields a maximum estimate for the geothermal gradient which is not significantly higher than analogous estimates

from Phanerozoic terrains. Secondly, the pressures alone may be used to infer the height of Archaean mountains; these mountains appear to have had elevations comparable to present day mountain belts. It seems probable that the elevation of present day belts is limited by the creep strength of the lithosphere and, in view of the strong temperature dependence of creep in earth materials, this second observation also implies Archaean continental thermal regimes were similar to present day ones [12].

One way in which continental thermal regimes similar to today's could be reconciled with a significantly increased total internal heat generation would be to permit a greater proportion of the total surface heat flux to be carried by the creation and subduction of oceanic plates [11, 13]. However, none of the published models of earth thermal history predicts any change in this proportionation.

A second way of effecting this reconciliation is by assuming that the global surface heat flux in the Archaean was approximately the same as the present one; such an assumption would be supported by thermal history models in which the time that the convecting system takes to respond to changes in heat supply is comparable to the timescale for the decay of the principal radiogenic elements in the system. The presence of a double thermal boundary layer at the interface in a two-layered mantle would be one way to obtain such a timescale [9].

The occurrence of komatiitic vulcanism in Archaean terrains implies that conditions existed within the Archaean mantle that were conducive to melting at appreciably higher temperatures than present day magmas require (around 1650°C as opposed to 1200-1400°C for present

magmas [14, 15]); this observation is often taken to imply that mantle temperatures in general were comparably higher. If the implication is correct, it is hard to see how the mantle could have been considerably hotter in the past without there also being a considerably enhanced global surface heat flux.

Thus the only geological evidence about Archaean geothermal regimes appears to be contradictory to the present models of earth thermal history. This contradiction may be resolved by a refinement in our understanding of the convective behaviour of the strongly temperature-dependent fluid that makes up the mantle, or perhaps by an improved understanding of the tectonic setting of komatiites. It may be that this resolution will require only minor emendment of the current models of earth thermal history, but until this is known it is as well to be cautious in our inferences about global heat flux throughout geological time.

REFERENCES

[1] Sclater, J. G., C. Jaupart and D. Galson, heat flow through oceanic and continental crust and the heat loss of the earth, Rev. Geophys. Space Phys. 18, 269-311, 1980.

[2] O'Nions, R. K., N. M. Evensen and P. J. Hamilton, Geochemical modelling of mantle differentiation and crustal growth, J. Geophys. Res. 84, 6091, 1979.

[3] Taylor, S. R., Lunar and terrestrial potassium and uranium abundances: implications for the fission hypothesis, Proc. Lunar Sci. Conf. 10th, 2017, 1979.

[4] Jacobsen, S. B. and G. J. Wasserburg, The mean age of mantle and crustal reservoirs, J. Geophys. Res. 84, 7411, 1979.

[5] Sharpe, H. N. and W. R. Peltier, A thermal history model for the earth with parameterized convection, Geophys. J. Roy. Astron. Soc. 59, 171, 1979.

[6] Schubert, G., D. Stevenson and P. Cassen, Whole planet cooling and the radiogenic heat source contents of the earth and the moon, J. Geophys. Res. 85, 2531, 1980.

[7] Turcotte, D. L., On the thermal evolution of the earth, Earth Planet. Sci. Lett. 48, 53, 1980.

[8] Davies, G. F., Thermal histories of convective earth models and constraints on radiogenic heat production in the earth, J. Geophys. Res. 85, 2517, 1980.

[9] McKenzie, D. P. and F. M. Richter, Parameterized thermal convection in a layered region and thermal history of the earth, J. Geophys. Res. 86, 11, 667, 1981.

[10] Perkins, D. and R. C. Newton, Charnockite geobarometers based on coexisting garnet-pyroxene-plagioclase-quartz, Nature 292, 144, 1981.

[11] Bickle, M. J., Heat loss from the earth: A constraint on Archaean tectonics from the relation between geothermal gradients and the rate of plate production, Earth Planet. Sci. Lett. 40, 301, 1978.

[12] England, P. C. and M. J. Bickle, Constraints on Archaean thermal and tectonic regimes from metamorphic mineral assemblages, submitted to Tectonics.

[13] Burke, K. and Kidd, W. S. F., Were Archaean continental geothermal gradients much steeper than those of today?, Nature 272, 240, 1978.

[14] Green, D. H., I. A. Nicholls, M. Viljoen and R. Viljoen, Experimental demonstration of the existence of peridotitic liquids in earliest Archaean magmatism, Geology 3, 11, 1975.

[15] Bickle, M. J., C. E. Ford and E. G. Nisbet, The petrogenesis of peridotitic komatiites: Evidence from high pressure melting experiments, Earth Planet. Sci. Lett. 40, 301, 1977.

ICE-POOR REGOLITH DEVELOPMENT AND DESTRUCTION ON SMALL ICY-DUSTY OR ICY-ROCKY OBJECTS, F.P. Fanale and J.R. Salvail, Planetary Geosciences Division, Hawaii Institute of Geophysics, University of Hawaii at Manoa.

Development of ice-poor/silicate-rich "mantles" on cometary objects has been described by several investigators and has been the subject of at least one detailed quantitative model (Brin & Mendis, 1979; Brin, 1980). Ice sublimation is the creator, the "boiler"/disrupter, and the launcher of ice-poor regoliths. In our model, the major physical processes which are quantitatively described are: 1) Modification of the periodic orbital thermal "wave" that reaches buried condensed volatiles, by the finite thermal conductivity of any overlying ice-poor regolith, 2) Modification of the vapor outflux by the finite and changing vapor diffusivity of the incipient regolith, 3) The effect of volatile flux and preferential launching of smaller grains on the thickness and grain size distribution of the regolith, 4) Continuous feedback of developing regolith properties into the thermal and vapor transport described in "1." and "2." 5) The compound effects of multiple passes.

The model includes latent heat effects, H_2O and CO_2 properties, obscuration by streaming dust, and possible transitions from one dominant volatile loss mechanism to another (see below). In its preliminary form, it does not currently include scattering effects of ice halos or global effects such as systematic launching of grains from one region on a comet accompanied by their systematic accretion on another. Also, because of the complexity of the mantle development model, we have not yet coupled it with sophisticated insolation histories for comets with appropriate rotation rates, orbits and obliquities. Rather we have so far considered only two latitudes on comets with archtypical orbits and an obliquity of 90 degrees. We hope to consider more interesting and realistic orbits, obliquities and rotation rates.

Despite the preliminary stage of the investigation, our results suggest some general inferences: An object in an "archtypical" short period cometary orbit can undergo at least three distinct phases of regolith development including 1) A molecular diffusion phase, when the gas:silicate ratio of the outflux is high but the gas flux is very low. This phase is most effective ~ 3-5 AU and a comet in near circular at this heliocentric distance would probably first develop a water ice and dust regolith poor in other volatiles and then, ultimately, a permanent silicate-rich regolith. In this phase, the regolith inhibits vapor flux and thermal flux via its porosity and absorptive properties which, in turn, are determined by grain size distribution and prior history. 2) A phase (onset ~3AU) in which the thermally controlled volatile flux can in turn control the regolith geometry by regolith-disrupting processes, commencing when gas pressure exceeds lithostatic pressure. The transition from molecular diffusion through a fixed regolith matrix to volatile flux control of the matrix geometry might be analogous in some ways to the transition from still evaporative processes to boiling. During the molecular diffusion phase launching of even small grains by H_2O sublimation alone (without participation of other ices) is extremely ineffective. However, during the disruption/boiling phase, H_2O sublimation rates approach free sublimation of dusty H_2O ice, and can generally launch a substantial dust flux, albeit still strongly weighted to finer grains. 3) At small heliocentric distances (~1AU) launching of grains can become indiscriminate and at very small distances (~.3AU) even H_2O sublimation can launch large boulders. However the dependence of launch ability on heliocentric distance and ice composition is greatly moderated by latent heat effects. Table I gives a rough idea of these dependencies. However it should be borne in mind that the values in this table are for idealized thermal histories - a fixed subsolar point or a fixed 60 degrees incidence angle - and may not be generally applicable to comets. During the indiscriminate launch phase, ejectae have the same H_2O: rock flux as the comet mass, and severe erosion occurs in steady state and is not accompanied by any ice poor-regolith retention.

An ice poor regolith is "self-protecting" and mantle growth is "self-aggraveting" because a mantle modulates the thermal shock experienced at the buried ice interface near perihelion. Even with thermal transfer in radiative, conductive and convective modes, a static mantle of sufficient thickness and fineness can protect and enlarge itself because of its insulating properties and further suppress the volatile flux diffusing up through it for any given thermal history. Also, the thicker the existing regolith the less vulnerable it is to physical disruption by an excess of vapor pressure over its lithostatic pressure. Hence whether a particular comet undergoes the above transitions depends on whether incipient regolith growth achieved since the last perihelion is sufficient to protect the mantle against the next perihelion. If it is, then the mantle will

Fanale, F. P. and Salvail, J. R.

irreversibly evolve to permanence. If not, the comet will cycle reversibly through the preceding stages until it is globally dissipated. It would appear that any virginal icy rocky object placed in an orbit with perihelion <1AU would have little chance of developing a permanent regolith (except for "global" effects mentioned above which are not considered here). Hence it would disappear after, say, hundreds of passes. On the other hand, any postulated existing initial mantle of ~4cm or more could protect itself even at a perihelion distance of ~1.7AU if only H_2O ice were present. A much greater initial thickness of ice poor mantle would be required if the comet expected to survive a typical Apollo perihelion passage at 0.7AU without beginning to cycle. If an ice-poor regolith did survive initial passage intact, it would stay in the molecular diffusion stage and would grow asymptotically with time to a thickness of perhaps several tens to hundreds of meters - depending on exact vapor diffusivity and heliocentric distances. Whether the "cometary" core of such an object would be detectable by remote sensing techniques in lieu of density measurements is a fascinating question, and the water flux itself is probably the most telling clue to such an object. The greater the sensitivity of gas flux measurements, and the greater the range of heliocentric distances at which these can be made on objects in eccentric orbits, the more chance of evaluating the actual nature of cometary regolith evolution by observing phenomena such as the sharp hypothesized transition between increasing molecular diffusion and the boiling/disruption phase or predicted strong variations in the H_2O: dust ratio.

In general, the main difference between our model results and those of others is that, where appropriate, we allow Knudsen flow (where mantle properties control the flux) and not continuum flow be the rate limiting mode of vapor transport. As a consequence, the inhibiting effect of any incipient regolith which develops toward aphelion is a very effective barrier to development of what would otherwise be a multicentimeter ice poor regolith.

Table I. Minimum* Requirements for Launching Silicates From a Comet With Albedo = 0.1, Radius = 2 km

Maximum Launchable (Radius, cm)	Required H_2O [CO_2] Flux, g/cm^2sec	Required T for Flux, °K	Required Insolation erg/cm^2sec	Required AU if Subsolar Point	Required AU 60° Latitude
1×10^{-4} (dust)	1.2×10^{-9} [2.3×10^{-9}]	151 [97]	2.6×10^{4} [4.5×10^{3}]	6.9 [16.8]	4.9 [11.9]
1×10^{-2} (sand)	1.1×10^{-7} [2.2×10^{-7}]	170 [113]	4.6×10^{4} [9.4×10^{3}]	5.2 [11.5]	3.7 [8.2]
1×10^{0} (pebbles)	1.1×10^{-5} [2.0×10^{-5}]	195 [135]	3.7×10^{5} [1.4×10^{5}]	1.8 [3.0]	1.3 [2.2]
1×10^{2} (boulders)	9.7×10^{-4} [1.7×10^{-3}]	229 [168]	2.8×10^{7} [1.1×10^{7}]	0.21 [0.34]	0.47 [0.76]
1×10^{3} (large boulders)	9.3×10^{-3} [1.7×10^{-2}]	250 [191]	2.6×10^{8} [1.0×10^{6}]	0.07 [0.11]	0.05 [0.08]

* assume launch accomplished with diurnal maximum flux

References: Brin, G.D. and Mendis D.A., Dust Release and Mantle Development in Comets, The Astrophysical Journal, 229, 402-408, 1979. Brin, G.D., Three Models of Dust Layers on Comet Nuclei, The Astrophysical Journal, 237, 265-279, 1980.

A CONDENSATION-ACCRETION MODEL FOR VOLATILE ELEMENT RETENTION.

B. Fegley, MIT, Cambridge, MA 02139.

Chemical equilibrium calculations are widely used to discuss elemental fractionations among chondrites and planets. These calculations are now being applied to models of volatile element retention by the terrestrial planets. Recent work (1-4) suggests that equilibrium mechanisms can supply the planetary inventories of halogens, alkalis, and phosphorus. This same body of work also strongly suggests that, at least at high temperatures, equilibrium mechanisms cannot supply the planetary inventories of C, H, and N. These results, plus the earlier work of Anders and Owen (5) and Sill and Wilkening (6), indicate that accretion of meteoritic material and low temperature volatile-rich phases may supply the planetary inventories of C, H, N, and the noble gases. The present work attempts to quantify a condensation-accretion model for retention of these elements. This work deals with elemental abundances and does not address the question of isotopic fractionations.

Figure 1 illustrates the composition of low temperature equilibrium condensate as a function of T, P, and distance for an adiabatic model of the solar nebula (1-4). The calculations for this figure were done assuming incomplete conversion of CO to CH_4 and N_2 to NH_3 (4). The condensation temperatures for pure phases are: H_2O(s) 160 K, NH_4HCO_3(s) 155 K, CO_2(s) 71 K, $Xe \cdot 6H_2O$(s) 59 K, $CO \cdot 7H_2O$(s) 50 K, $CH_4 \cdot 7H_2O$(s) 48 K, $N_2 \cdot 7H_2O$(s) 46 K, $Kr \cdot 6H_2O$(s) 42 K, $Ar \cdot 6H_2O$(s) 38 K. If NH_4HCO_3(s) does not form, then $NH_4CO_2NH_2$(s) condenses at 142 K. If CO_2(s) does not form, then $CO_2 \cdot 6H_2O$(s) condenses at 68 K. Unclathrated CO and N_2 condense in the vicinity of 20 K.

Previous workers (6) pointed out that the clathrate which forms is actually a solid solution whose composition is temperature dependent. This effect has been considered in this work and the composition of the clathrate in Fig. 1 has been calculated as a function of temperature. In this case the initial clathrate is practically pure $Xe \cdot 6H_2O$(s). Once the temperature is below the condensation point of pure CO clathrate, however, the clathrate composition is dominated by CO and N_2. Further decreases in temperature lead to a progressively N_2-rich clathrate. The amounts of different noble gases in the clathrate are also temperature dependent. Xe is quantitatively retained in the clathrate below 59 K. Kr is completely condensed below 50 K and Ar is completely retained below 40 K.

Sill and Wilkening (6) also considered clathrate condensation in the solar nebula. Several important differences exist between this work and their results. They considered formation of CH_4 clathrate which is only a very minor component in this work. This is due to kinetic inhibition of the CO to CH_4 conversion (4). Second, they did not consider clathrates of any other carbon and any nitrogen compounds. Third, they concluded that clathration discriminates against the lighter noble gases at progressively lower temperatures. The present work shows that as the temperature decreases the amounts of Kr and Ar included in the clathrate increase.

Can accretion of low temperature equilibrium condensate supply the volatile inventories of the terrestrial planets? Table 1 displays H/C, H/N, and C/N ratios (gram/gram) for terrestrial surface reservoirs (atmosphere, crust, and oceans) from Barsukov et al (7), for three bulk earth models from Smith (8), for low temperature equilibrium condensate at 3 T points, for a special case called no clathrate, and for carbonaceous chondrites (5).

Table 1 and Figure 1 illustrate several important points. First, accretion of low temperature equilibrium condensate cannot match the terrestrial H/C, H/N, and C/N ratios for surface reservoirs or for bulk earth models. Linear combinations of any mixture of low temperature equilibrium condensate fail to match all three ratios, although the surface H/C ratio can be matched. Slow diffusion of gaseous molecules into H_2O ice may prevent clathrate formation. In this case (no clathrate) the condensate composition is frozen in at 70 K until $\sim$ 20 K where CO and N_2 condense. (These low temperatures were probably not reached in the solar nebula. In any case the match between terrestrial volatile ratios and low temperature equilibrium condensate then becomes worse). The no clathrate case is also unable to match the terrestrial volatile ratios.

Anders and Owen (5) suggested that accretion of small amounts of C3V-like material could supply terrestrial volatiles. However, the data in Table 1 show large differences between the terrestrial and meteoritic volatile ratios for all potential meteoritic volatile carriers. What about mixtures of low temperature equilibrium condensate and known meteorite classes? Again, linear combinations of these materials cannot match the terrestrial volatile ratios.

Volatile Accretion Model

Fegley, B.

The concept that accretion of low temperature condensate and meteoritic material provided the volatile inventories of the terrestrial planets is very attractive. These preliminary results illustrate that the concept is difficult to quantify using known meteorite classes and condensate compositions from equilibrium calculations. Two approaches to this problem are now being pursued. First, using either the low temperature equilibrium condensate or different carbonaceous chondrites as one component, what are the compositions of additional components? Second, can the additional components be identified with materials such as comets, Brownlee particles, volatile-rich carriers in meteorites? Results illustrating compositions required to match the volatile inventories of the terrestrial planets will be given and discussed in terms of a condensation-accretion model.

References: (1) Barshay, S.S. (1981) Ph.D. thesis, MIT; (2) Fegley, B. (1982) Proc. 13th LPSC, in press, (1981) Meteoritics **16**, 314, Fegley, B. and Lewis, J.S. (1980) Icarus **41**, 439-455; (3) Lewis, J.S. et al (1979) Icarus **37**, 190-206; (4) Lewis, J.S. and Prinn, R.G. (1980) Astrophys. J. **238**, 357-364; (5) Anders, E. and Owen, T. (1977) Science **198**, 453-465; (6) Sill, G.T. and Wilkening, L.L. (1978) Icarus **33**, 13-22; (7) Barsukov et al. (1980) Proc. 11th LPSC, 765-773; (8) Smith, J.V. Proc. 8th LPSC, 333-369.

Acknowledgments: I thank A.G.W. Cameron and J.S. Lewis for supporting this research under NASA Grant NGR-22-007-269 and NGL-22-009-521, respectively.

Table 1
Elemental Ratios (g/g)

Material	H/C	H/N	C/N
Earth:			
Barsukov	2.3	67	29
Smith SI	0.05	3	50
SII	0.41	3.7	8.9
SIII	1.0	3.1	3.1
Condensate:			
150 K	22	19	0.9
70 K	9.5	19	2.0
50 K	0.9	2.6	2.8
No clathrate	9.5	19	2.0
Chondrites:			
CI	0.22	2.8	13
CM2	0.39	5.9	15
C3V	0.07	8.2	110
C3O	0.21	17	78

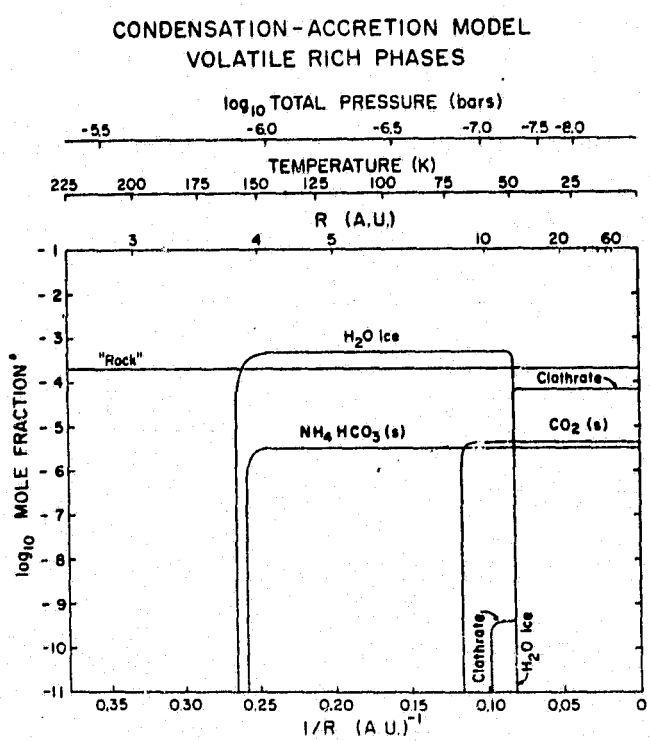

HOMOGENEITY OF ARGON AND THE $^{40}Ar/^{36}Ar$ RATIO WITHIN THE SOLID EARTH, David E. Fisher, Rosenstiel School Of Marine And Atmospheric Science, University of Miami, Miami, Fl 33149

Argon fills a unique niche in the spectrum of volatile tracer elements, being: (1) a pure volatile, i.e., forming no solid compounds; (2) composed of two isotopes which have always been gases and one (^{40}Ar) which has spent most of its terrestrial life as a solid-state element, so that the ratio $^{40}Ar/^{36}Ar$ in the various terrestrial reservoirs will reflect the degassing history of those reservoirs; and (3) being heavy enough to have been quantitatively retained in the earth's atmosphere throughout geologic time. All three of these factors are shared by only one other element, xenon, in which the radiogenic component is so small as to be difficult or impossible to measure in many samples of geologic interest.

Ozima (1) first recognized that since today's atmospheric $^{40}Ar/^{36}Ar$ value is fixed at 295.5, determination of the value of this ratio within the solid earth would define the degassing history of the earth. The fact that oceanic basalts quantitatively trap magmatic argon has been coupled with Ozima's suggestion to suggest and investigate several models of earth degassing (2-6). But recent measurements both on basalts from various tectonic regimes and on ultramafic nodules which have been shown to trap interior-earth rare gases have raised the question of whether there exists in fact a unique $^{40}Ar/^{36}Ar$ ratio which can be described as characterizing the interior of the earth (7-14). Most tectonic earth models would predict a heterogeneous argon isotopic distribution: an upper depleted mantle will have lost nearly all its primordial Ar, and therefore will be low in total ^{36}Ar yet high in $^{40}Ar/^{36}Ar$ due to 40K-decay into the depleted system; an undepleted lower mantle will have more radiogenic ^{40}Ar but lower $^{40}Ar/^{36}Ar$ due to retention of much of its primordial ^{36}Ar.

In order to investigate these possibilities one must first disentangle the components of measured Ar values. In this paper I address the question of how to identify pristine trapped deep-earth gases, and to what extent the measured data reflect such values rather than values modified by exchange with atmospheric gases.

Oceanic basaltic glasses in general show high ($\sim 10^4$) but not identical $^{40}Ar/^{36}Ar$ values. I present new data here on many glass, interior rock, and altered rock samples to show clearly the effect of sea water alteration: lower ratios and higher total ^{36}Ar contents. Plots of $^{40}Ar/^{36}Ar$ vs. $(^{36}Ar)^{-1}$ for several samples from specific locations demonstrate that the glasses have quantitatively trapped and retained magmatic Ar. The values obtained from all samples for which sufficient data are available are remarkably similar, considering that they embrace the Atlantic, Pacific, and Caribbean; they show $^{40}Ar = 60\text{-}175 \times 10^{-8}$ cc/gm, $^{40}Ar/^{36}Ar \geq 7500$, and $^{36}Ar \leq 1.5 \times 10^{-10}$ cc/gm. Lower values of the ratio and higher values of ^{36}Ar are in all cases due to sea water alteration and/or atmospheric contamination. Data are also presented for an African non-tholeiitic basalt which has trapped magmatic argon and retained it quantitatively: $^{40}Ar = 400 \times 10^{-8}$ cc/gm, $^{40}Ar/^{36}Ar \geq 8000$, $^{36}Ar \leq 2 \times 10^{-10}$ cc/gm. This indicates a somewhat less depleted magmatic source.

Previous data in ultramafic nodules from Africa and Hawaii have shown $^{40}Ar/^{36}Ar$ similar to the atmospheric ratio, and models of mantle degassing and earth accumulation have been built on the postulate that these ratios represent the deep, undepleted mantle (5, 15). I present here data on two Hawaiian nodules that show clearly the presence of atmospheric (non-mantle)

Ar; when this is accounted for the Ar isotopic ratios and absolute values are similar but not identical to the basaltic data quoted above.

In summary, for all samples in which it has been possible to clearly identify the trapped magmatic component there is a measureable difference in total Ar content and isotopic ratio in the samples from different tectonic regimes, but the difference is surprisingly small. Near-atmospheric ratios seem to disappear when atmospheric contamination is properly monitored.

References

1. Ozima, M., 1937. Geochim. Cosmochim. Acta, 39: 1127-1134.
2. Schwartzman, D.W., 1973b. Geochim. Cosmochim. Acta, 37: 2479-2495.
3. Hamano, Y. and Ozima, M., 1978. In: E.C. Alexander, Jr. and M. Ozima (Eitors), Terrestrial Rare Gases. Center for Academic Publications, Tokyo, pp. 155-172.
4. Fisher, D.E., 1978. In: E.C. Alexander, Jr. and M. Ozima (Editors), Terrestrial Rare Gases. Center for Academic Publications, (Tokyo), pp. 173-183.
5. Hart, R., Dymond, J. and Hogan, L., 1979. Nature (London), 278: 156-159.
6. Tolstikhin, I.N., Drubetskoy, Ye.R. and Sharas'kin, A.Ya., 1978. Geokhimiya, 4: 514-520.
7. Dymond, J. and Hogan, L., 1973. Earth Planet. Sco. Lett., 20: 131.
8. Dymond, J. and Hogan, L., 1978. Earth Planet. Sci. Lett., 38: 117-128.
9. Fisher, D.E., 1971. Earth and Planet. Sci. Lett., 12: 321-324.
10. Fisher, D.E., 1981a. Nature (London), 290: 42-44.
11. Kaneoka, I. and Takaoka, N., 1978. Earth Planet. Sci. Lett., 39: 382.
12. Kaneoka, I., Takaoka, N. and K., Aoki, 1978. In: E.C. Alexander, Jr. and M. Ozima (Editors), Terrestrial Rare Gases. Center for Academic Publications, pp. 71-83, Tokyo.
13. Saito, K., Basu, A.R., and Alexander, E.C., Jr., 1978. Earth Planet. Sci. Lett., 39: 274-280.
14. Takaoka, N. and Nago, 1978. Nature (London), 276: 491-492.
15. Manuel, O.K., 1979. In: E.C. Alexander Jr. and M. Ozima (Editors), Terrestrial Rare Gases. Center for Academic Publications, Tokyo, pp. 85-92.

ESCAPE OF NITROGEN FROM THE MARTIAN ATMOSPHERE, J.L. Fox, Center for Astrophysics, Cambridge, Mass. 02138

The notion that substantial quantities of nitrogen have escaped from Mars was introduced by Brinkman[1] who considered the role of photodissociation in producing nitrogen atoms with energies exceeding the escape energy, about 1.72 eV for ^{14}N. Support for this idea was provided by the Viking mass spectrometers, which recorded an anomalous $^{15}N/^{14}N$ ratio, 1.62 $\pm$ .16 times the terrestrial value[2]. Subsequent models have considered other methods for producing energetic nitrogen including dissociative recombination of N_2^+ [3] photoelectron impact dissociation[4,5] and chemical reactions[6]. The computed rates for dissociative recombination of N_2^+ and of the reaction, $N_2^+ + O \rightarrow NO^+ + N$, depend on model N_2^+ densities which were not measured by Viking. We have refined our model to include better estimates of the N_2^+ densities from models which reflect the improved understanding of ion chemistry in CO_2 atmospheres obtained from Pioneer Venus[7,8]. In particular, the reaction $O^+(^2D) + N_2 \rightarrow O + N_2^+$ has been measured recently[9,10] and we have found it to be a major source of N_2^+ above the exobase on Mars.

Dissociative recombination produces an escape flux of 3×10^5 cm^{-2} s^{-1} and is the major source of escaping ^{14}N atoms. The escape rates for ^{15}N and ^{14}N in dissociative recombination differ substantially for ground state N_2^+ [11]. This effect will be mitigated for ions in excited vibrational levels. We have modeled the vibrational distribution of N_2^+ at the Martian exobase in order to determine the ^{15}N-^{14}N fractionation due to dissociative recombination. At 200 km, 40% of the N_2^+ ions are found to be vibrationally excited.

Photodissociation of N_2 contributes an escape flux of about 1×10^5 cm^{-2} s^{-1}. Other processes bring the total escape flux to about 5.6×10^5 cm^{-2} s^{-1}.

Fanale et al.[12] have constructed a model of the regolith-atmosphere-polar cap system in which oscillations in the obliquity of the planet, and therefore in the insolation produce periodic changes in the CO_2 pressure of the atmosphere. Pressure variations will affect the escape flux of nitrogen since the pressure determines the altitude of the exobase and the fraction of N_2 found there. We have incorporated these effects into our model and have found that the net escape rate is reduced compared to the average pressure model. For the basalt regolith, we obtain an initial $^{15}N/^{14}N$ ratio of 2.74 and an initial column density of 9.7×10^{22} cm^{-2}. For the nontronite regolith, the isotope ratio is 1.54 and the initial reservoir is 4.0×10^{22} cm^{-2}. Our model shows that a regolith material with adsorptive properties intermediate between basalt and nontronite will yield an appropriate $^{15}N/^{14}N$ ratio and total C/N ratio.

1. Brinkman R.T. (1971) Science 174, p. 944.
2. Nier A.O. and McElroy M.B. (1977), J. Geophys. Res. 82, p. 4341.
3. Yung V.L., Strobel D.F., Kong T.Y. and McElroy M.B. (1977) Icarus 30, p. 26.
4. Nier A.O., McElroy M.B. and Yung Y.L. (1976) Science 194, p. 68.
5. McElroy M.B., Kong T.Y. and Yung Y.L. (1977) J. Geophys. Res. 82, p. 4379.
6. Fox J.L. and Dalgarno A. (1980) Planet. Space Sci. 28, p. 41.
7. Nagy A.F., Cravens T.E., Smith S.G., Taylor H.A. and Brinton, H.C. (1980) J. Geophys. Res. 85, p. 7795.
8. Fox J.L. (1982), Icarus (in press).
9. Rowe B.R., Fahey, D.W., Fehsenfeld F.C. and Albritton D.L. (1980) J. Chem. Phys. 73, p. 194.

10. Johnsen R. and Biondi M.A. (1980) Geophys. Res. Lett. 7, p. 401.
11. Wallis M.K. (1978) Planet Space Sci. 26, p. 949.
12. Fanale F.P., Salvail J.R., Banert W.B. and Saunders R.S. (1982) Icarus (in press).

A REVIEW OF DISTRIBUTIONS OF SULFUR IN SOLAR SYSTEM OBJECTS

Everett K. Gibson, SN7, Geochemistry Branch, NASA-JSC, Houston, TX 77058

This contribution will review the abundances and distributions of sulfur as a volatile phase in planetary materials. Exploration of the solar system during the last decade has shown the element sulfur to be ubiquitous. It plays a very active role in the chemical processes operating beneath the surface, on the surface and in the atmosphere, and is essential to all life forms that we know. The geochemical versatility of sulfur may be attributed to its ability to exhibit a variety of valence states (-2, 0, +2, +4, +6) and to combine with both metals and non-metals via either covalent or ionic bonds. At the present time, sulfur abundances have been measured in situ on five planetary materials: earth, moon, meteorites, Mars and Venus. Remote measurements of sulfur abundances have been obtained for Jupiter, Io, the rings of Saturn, the sun, and at least one comet. Sulfur compounds have been observed in the interstellar dust clouds.

A summary of sulfur abundances for the five types of planetary objects sampled is shown in Fig. 1. As a group, meteorites contain the greatest sulfur abundances. Chondritic meteorites have sulfur contents up to 6% for CI carbonaceous chondrites. Within this class of meteorites sulfur is present in the reduced sulfide form, elemental sulfur, and oxidized sulfate. Distributions of these components reflect the past history of the primitive objects. Within the H, L, and LL chondrites the total sulfur abundances is very constant (2.2±0.8%). Enstatite chondrites contain abundances approaching those of CI chondrites but all of the sulfur is present as sulfide. Achondrites typically have sulfur abundances ranging from 200 to 11,400 μgS/g (1). Eucrites typically range from 1000 to 1500 μgS/g whereas howardites have somewhat higher concentrations (1, 2, 3). It has been noted that sulfur abundances of shergottites are similar to terrestrial dolerites (2).

Average sulfur content of the earth crust has been given as 260 μgS/g (4). Despite the apparent low sulfur abundance for the earth's crust, sulfur has played a major role in the earth's history. The core of the earth is believed to be mostly iron with minor amounts of alloyed nickel with upwards of 10 to 20% sulfur, and Brett (5) has suggested that sulfur played an active role during core formation. The extraction of sulfur from the earth's crust and mantle during core formation has left the crust with abundances which are low when compared to other values shown in Fig. 1. Sulfur species observed in volcanic gases and emanations are H_2S, S_2, SO_2, and SO_3, with SO_2 dominating at magmatic temperatures (>1200°C) and with H_2S the major component at lower temperatures. Sulfur has recently been observed to be the major component outgassing from the active hydrothermal submarine vents. Presence of H_2S and CO_2 in the water surrounding the vents, along with sulfur-oxidizing bacteria, shows that sulfur plays an important role in the ecosystems and life related processes of primitive organisms. Basalts from the terrestrial ocean floors (MORB) range between 60 and 800 μgS/g (6), whereas subaerially extruded basalts contain 50 to 2000 μgS/g. It has been shown that sulfur contents decrease with degassing. Naldrett et al. (7) noted that Archean basalts had a wide range of sulfur abundances (0 to 8000 μgS/g) but an average of 1000 μgS/g was observed for most samples. High sulfur content of Archean basalts relative to recent basalts (mean of 200-400 μgS/g) suggest retention of sulfur as a result of the rapid accumulation of Archean volcanic rocks and their limited interaction with seawater.

Lunar basalts were found (8) to range from approximately 400 μgS/g for the Apollo 12 and 15 basalts to 2600 μgS/g for the Apollo 11 and 17 basalts. High sulfur contents are correlated with the high FeO and Ti contents of the basalts.

Apollo 11 and 17 mare basalts were saturated with respect to sulfur, whereas those from Apollo 12 and 15 were undersaturated (8). Lunar anorthosites typically contain less than 60 μgS/g. The low sulfur contents of the crustal materials is probably a consequence of the fact that plagiclase cannot dissolve sulfur. The high sulfur contents of lunar basalts implies that the lunar mantle is enriched in sulfur. Sulfur abundances of lunar soils can be accounted for by mixing of various components present in the regolith.

The surface of Mars has been analyzed in two sites by the Viking landers. Data returned from the XRF instruments showed a regolith enriched in sulfur (2.0 to 3.5% S) (9). Samples of the upper crust (duricrust) were found to contain the greatest sulfur concentrations. Since the sampling sites appear to be areas where evaporation or sublimation processes have operated, the analysis may represent analysis of salts deposited within the regolith and are not representative of the planet as a whole. Similar sulfur enrichments have been noted from cold desert regions on earth (10).

Clark (11) has examined the Venera 13 and 14 XRF data of Surkov et al.(12) and found that the V-14 site contained about 0.1 to 0.5% sulfur. Data from Venera 13 could not be deconvoluted in a satisfactory manner. Data for the basalt-like sample at V-14 is similar in sulfur abundances to those found for lunar basalts, achondrites and terrestrial basalts. The atmosphere of Venus has been shown to contain sulfur species--especially sulfuric acid--within selected cloud regions. Formation of sulfuric acid appears to be the result of a series of photochemical reactions culminating in the formation of SO_2 and SO_3.

It can be seen from the data given in Fig. 1 that sulfur's abundances range from a major element in selected meteorites to a trace element in some basalts. Distribution of sulfur reflects the oxidation-reduction conditions and processes which operate on the particular solar system object. Sulfur is indeed an important planetary volatile whose abundances and distributions reflect major solar system processes and formational conditions.

References: 1. Moore C.B. (1981) per. comm.; 2. Gibson E.K. (1982) unpublished data; 3. Moore C.B. (1971) Handbook of Elemental Abundances in Meteorites (B. Mason, ed.); 4. Fairbridge R.W. (1972) Encyclopedia of Geochemistry and Environmental Sciences; 5. Brett P.R. (1973) Geochim. Cosmo. Acta 37, 165-170; 6. Moore J.G. and Fabbi B.P. (1971) Contrib. Min. Petrol. 33, 118-127; 7. Naldrett A.J. et al. (1978) Can. J. Earth Sci. 15, 715-728; 8. Gibson E.K. et al. (1977) Proc. Lunar Sci. Conf. 8th, 1417-1428; 9. Clark B. et al. (1982) J. Geophys. Res. (in press); 10. Gibson E.K. et al. (1982) J. Geophys. Res. (in press); 11. Clark B. (1982) per. comm.; 12. Surkov Y.A. et al. (1982) Anal. Chem. 54, 957A-966A.

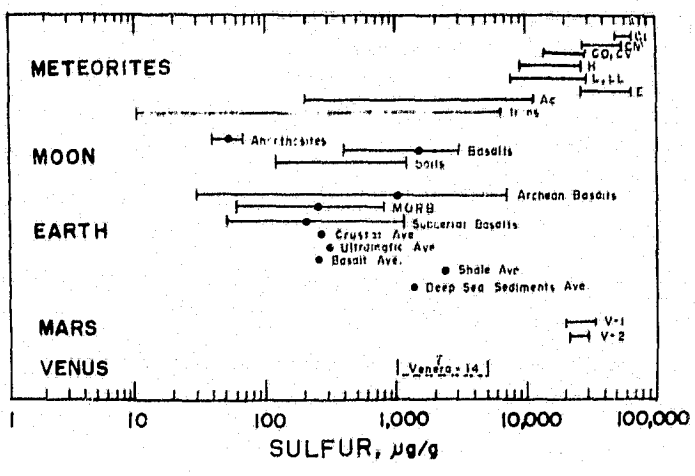

Figure 1. Sulfur abundances for five types of solar system objects which have had sulfur measurements carried out *in situ*.

SPUTTERING OF VOLATILE RESERVOIRS

P. K. Haff, W.K. Kellogg Radiation Laboratory, Caltech, Pasadena, California 91125.

The term "sputtering" refers to the ejection from a "target" of atoms or molecules following the impact of an energetic atom or ion. Values of the sputtering yield can range from much less than unity to upwards of 1000. At low energies, below a few keV/amu, billiard ball-like collisions lead to ejection of surface molecules. At higher energies, energy deposited in electron excitation along the path of the incident particle is ultimately converted to kinetic energy of atomic motion, again with the subsequent ejection of target particles. High energy sputtering yields are often orders of magnitude greater than low energy yields. By combining theoretical models with laboratory experiments, we can gain some idea of the role which sputtering plays in the transport of volatile materials on planetary bodies.

There are two principal sources of energetic ions occuring naturally in the solar system: the solar wind and planetary magnetospheres. The solar wind may interact directly with planets and satellites not protected by a magnetic field, such as Venus, Mars, and the Moon. Planetary magnetospheres contain energetic particles which can impinge upon satellites and upon the planet itself. Thus, the Galilean satellites, the icy satellites of Saturn, and the Earth itself are all subjected to magnetospheric particle impact. Sputtering of airless bodies can lead to loss of matter to space, to redistribution of matter across a planetary body, and to generation of a thin sputter induced coronal atmosphere. Sputtering of a body already having an atmosphere can lead to depletion of this atmosphere, and to preferential loss of the lighter constituent molecules.

Examples of volatile transport mediated by sputtering are

(1)Direct solar wind impact into the upper atmospheres of Venus and Mars is retarded by shock-wave formation, but to the extent that the impinging particles can interact directly, otherwise gravitationally bound gases can be lost to space. Thus, on Venus He is lost by collision with solar protons at a rate which may be as large as 10^5 cm-2 s-1. This is about 10% of the assumed He outgassing rate.

(2)Likewise, to the extent that solar particles impinge the Martian atmosphere, CO_2 may be lost. While photochemical loss mechnisms predominate for O, sputtering is an efficient way in which C and N can be removed from Mars. Sputtering of the Martian atmosphere over geological times is calculated to have been capable of removing nearly 97% of the mass of the initial Martian N component and about 33% of the initial CO_2. Thus, N is removed preferentially with respect to CO_2, and lighter isotopes of C, N, and O are removed preferentially with respect to their heavier isotopes. Thus the present N poor atmosphere and the observed fractionation of the C and N isotopes can be attributed at least partly to sputtering.

(3)The atmosphere of the Earth itself is subjected to sputtering by precipitated magnetospheric particle fluxes. Using a hard-sphere model of low energy O-O collisions, Torr et al. [1974] calculated that earth satellite data on O precipitation meant that O escape fluxes as large as $\sim 10^9$ cm-2 s-1 could be attained locally. Averaging over the area of the earth and over time implies an escape flux of $3X10^7$ cm-2 s-1.This is comparable to the escape flux of H. Unpublished calculations by Haff which account for the O-O interaction in a more realistic way suggest that the loss of O by atmospheric sputtering is perhaps only 10^6 cm-2 s-1. This smaller result is only about 1% of the H escape flux, but nevertheless represents an interesting and possibly important escape route for O atoms.

SPUTTERING OF VOLATILE RESERVOIRS

Haff P. K.

(4)Arnold [1979] and Lanzerotti et al [1981] have considered the question of whether solar wind impact could erode patches of ice on the Moon which might otherwise build up in permanently shadowed coldtraps in the lunar polar regions. The enhanced sputtering yields associated with energetic ion impact on H_2O ice [Brown et al, 1978; Cooper, 1982] have led to the conclusion [Lanzerotti et al, 1981] that ion erosion could be an effective mechanism for limiting the occurence of such ice pockets.

(5)In the Jovian system, possible SO_2 frost on Io, an Io SO_2 atmosphere, and the frozen H_2O surfaces of Europa, Ganymede and Callisto are all candidates for magnetospheric sputter erosion. As originally pointed out by Matson et al [1974], charged particle sputtering offers one mechanism which is energetic enough to inject heavy atoms like S, O, Na, and K into the Jovian magnetosphere. Haff et al [1981] calculated that sputtering of an unprotected Ionian surface by corotating S ions might be able to sustain the observed Na and K clouds, but would be unable to provide a sufficiently high escape flux to maintain the S torus. Sputtering of an SO_2 atmosphere would be able to supply the S torus only if the atmosphere were hot enough that the exobase lay at an altitude of $\sim 2\ R_{Io}$.

(6)Sieveka and Johnson [1982] have studied the global transport of H_2O molecules on the icy Galilean satellites due to both low energy and high energy sputtering. Depending on the local surface temperature, sputtering can compete with sublimation as the most effective mechanism for volatile transport. Thus, especially in the polar regions, sputtering is the primary determinant of water mobility.

(7)Lanzerotti et al [1978] suggested that sputtering could lead to the formation of a thin atmosphere on otherwise airless satellites. Watson [1981] developed this idea in some detail, predicting an exospheric corona with a column density on the order of $5X10^{12}$ cm-2 on Europa.

(8)In the Saturnian system, sputtering plays a similar role. Morfill et al [1982], Cheng et al [1982], and Haff et al [1982] have discussed the role of ice sputtering near Saturn. They find that sputtering is unable to account for the H ring atmosphere, but that the lifetime of E-ring ice motes (~135y) is influenced strongly by low energy sputtering by co-rotating O ions. Atmospheric coronae are ill-developed,because the icy satellites are small compared to the Galilean satellites, but sputtering is a prime candidate for the source of heavy ions, presumably O, which have been detected inward from Tethys.

REFERENCES:Arnold, J. Geophys. Res. 84 ,5659, 1979; Brown et al, PRL 40, 1027, 1978; Cheng et al, JGR 87, 4567, 1982 Cooper, PhD Thesis, Caltech, 1982; Haff et al, sub. to Icarus, 1982; Haff et al, J. Geophys. Res. 86, 6933, 1981; Lanzerotti et al, Geophys. Res. Letters 5, 155, 1978; Lanzerotti et al, J. Geophys. Res. 86, 3949, 1981; Matson et al, Ap.J. 192, L43, 1974; Morfill et al, J. Geophys. Res., in press, 1982; Sieveka and Johnson, Icarus, in press, 1982; Torr et al, J. Geophys. Res. 79 ,5267 ,1974; Watson et al, Proc. Lun. Plan. Sci. Conf. 11, 2479,1980; Watson, Proc. Lun. Planet. Sci Conf. 12, 1569, 1981.

Work supported in part by NASA [NAGW-202 and -148] and by NSF [PHY79-23638].

METAL-SILICATE REDOX REACTIONS: IMPLICATIONS FOR CORE-MANTLE EQUILIBRIUM AND THE OXIDATION STATE OF THE UPPER MANTLE. R.D. Holmes and R.J. Arculus, Research School of Earth Sciences, Australian National University, P.O. Box 4, Canberra, A.C.T. 2600, Australia.

It is generally accepted that the core was formed early in the history of the Earth by the separation of a denser, Fe-rich metallic phase from a lighter silicate residue. However, the details of this process are still widely disputed, including such fundamental parameters[1] as the composition of the metallic phase, its original distribution within the proto-Earth, and its possible equilibrium or disequilibrium with the primitive mantle.

Recent measurements[2,3] of the intrinsic oxygen fugacity (fO_2) of mantle-derived peridotite nodules have suggested that the current redox state for the bulk of the upper mantle is close to or slightly below that defined by the iron-wustite (IW) buffer. One such investigation[4] concluded that these oxidation states were only about two log10 fO_2 units more oxidized than that required for saturation with an Fe-Ni metal, and suggested that redox conditions during core separation would be controlled by the Fe-analogue of the Metal-Olivine-Orthopyroxene ("MOO") oxygen buffer: $2M + O_2 + M_2Si_2O_6 = 2M_2SiO_4$. Although iron is the most abundant aliovalent element in both the core and mantle systems, similar MOO-type reactions can be written for other transition metals and, if the present oxidation state of the mantle was established by metal(s.l.)-silicate equilibrium, thermodynamic analysis of the MOO reactions for different transition elements (e.g. Fe, Ni and Co) combined with the concentrations of these elements in peridotite samples should yield a single concordant estimate of fO_2.

Using oxygen-specific zirconia solid electrolyte cells, we have obtained new data on the standard free energies of the Fe, Ni and Co Quartz-Metal-Olivine ("QMO") buffers: $SiO_2 + 2M + O_2 = M_2SiO_4$. These results are summarized in Fig. 1 for a total pressure of 1 bar. Increasing the total pressure to 30 kbar raises the equilibrium fO_2 of each buffer by about 1 log unit, but does not significantly affect their relative positions. Therefore, in order to facilitate comparisons with intrinsic fO_2 measurements carried out at ambient pressure, the calculations reported below have been made for a total pressure of 1 bar. Using estimates of SiO_2 activity derived from the Quartz-Olivine-Orthopyroxene ("QOO") reactions ($SiO_2 + M_2SiO_4 = M_2Si_2O_6$) for Mg and Fe[5,6], the QMO data can be used to calculate equilibrium fO_2's exactly equivalent to those implied by the corresponding MOO reactions (MOO = QMO-QOO).

In order to evaluate the conditions under which mantle-derived peridotites might have been in equilibrium with a core-forming metallic phase, these thermodynamic data have been applied to the analysis of two spinel lherzolites (#'s 270 & 271) previously used for intrinsic oxygen fugacity measurements in our laboratory[2]. Fig. 2 shows the results of QMO equilibrium calcuations made assuming the composition of the metallic phase to be similar to that found in iron meteorites (i.e. X(Fe)=0.9, X(Ni)=0.1, and X(Co)=0.005). The large intrasample discordancies (~4 log10 fO_2 units) between the different QMO buffers provide strong evidence that these peridotites have never been equilibrated with an Fe-rich metallic phase. Even large changes in pressure and temperature have no significant effect on this conclusion. Equilibrium with an Fe-rich metal could only be obtained by reducing the concentrations of Ni and Co in the silicates by factors of about 90 and 15, respectively. If the mineralogy of the silicate residue includes olivine and orthopyroxene, there is no geochemically plausible set of P-T-X conditions (including simple dilution of the metal with O or S) under which equilibration with an Fe-rich metallic phase can produce the

relative abundances of Fe, Ni and Co observed in these spinel lherzolites. This implies that either: (1) core separation was a disequilibrium process, or (2) the chemical equilibria involved phases other than just the silicates and metal considered here (e.g. sulfides[7]), or (3) if core separation was an equilibrium event, the silicate phases involved in this process were of a fundamentally different nature to those of the present-day upper mantle (i.e. the perovskite-structured minerals of the deep mantle). Fig. 3 generalizes the QMO calculations to show the oxygen fugacties required for these peridotites to be in equilibrium with a metallic phase consisting of either pure Fe, pure Ni or pure Co. These values represent the most reducing conditions under which these silicate phases could retain their present abundances of Fe, Ni and Co. They show that the present relative abundances of Fe, Ni and Co in these silicates can coexist with a metallic phase, but only if the metal is dominated by Ni (i.e. Ni:Fe:Co of about 4:1:1/20) and only at an fO_2 approximately equal to IW. The observation that these peridotites do not presently contain a metallic phase of any composition requires their redox state to be more oxidized than the Ni-QMO "baseline" (Fig. 3) and provides a strong constraint on the lower boundary for estimates of mantle fO_2 (i.e. somewhat higher than IW). Assessed by this criterion, the intrinsic fO_2 for peridotite #271 reported by (2) is anomalously reduced, suggesting either that the measurement is inaccurate or that the redox state of the spinel separate is somehow unrepresentative of the coexisting silicate phases. It is noteworthy that the intersample differences for the QMO buffers are quite small (<0.3 log units). This suggests that the redox state of the upper mantle, as represented by abundant spinel lherzolite nodules, is relatively uniform on a worldwide basis.

Similar metal-silicate equilibrium calculations have been carried out for the pallasitic meteorites (Fig. 4). The excellent agreement between the independently determined Fe- and Ni-QMO buffers is in striking contrast to the discordant results obtained for the mantle-derived peridotites (Fig. 2) and reflects the much lower concentrations of Ni and Co in pallasitic olivine (i.e. 50 & 7 ppm, respectively, vs. 3000 & 200 ppm)[8]. In contrast to the mantle-derived peridotites, this suggests that metal-silicate equilibrium controls the redox state of the pallasites. This thermodynamically-inferred conclusion of metal-silicate equilibrium is in good agreement with the slow cooling rates estimated for the pallasitic metal (~1K/m.y.) and with the observed lack of compositional zoning in pallasitic olivine[9]. The discrepancy between the calculated fO_2 of the Co-QMO and that of the Fe- and Ni-QMO's is probably due to the assumption of ideal mixing for the Co-olivine. By assuming that the pallasites represent a natural equilibrium assemblage, we may estimate that $\gamma(Co_2SiO_4) \simeq 2$.

Orthopyroxene does not generally coexist with olivine in the pallasites[10] and, for this reason, the QMO buffer lines shown in Fig. 4 were calculated with the assumption that $\log a(SiO_2)=0$ (i.e. $a(SiO_2)=1$). Hence the QMO buffer lines shown in Fig. 4 represent the minimum fO_2 values prevailing in the pallasites. It has been suggested by (11) that the minimum fO_2 of the pallasites is constrained by the stability of the phosphate-phosphide-metal assemblage and that their maximum fO_2 must lie below the IW buffer. By combining the calculated metal-silicate equilibria with this independent estimate of pallasite fO_2, the QMO calculation can then be inverted to obtain an estimate of $\log a(SiO_2) = -1.0$ to -1.5 in the pallasitic mineral assemblage (cf. Fig. 2.3 of (12)). The conclusion that the pallasites are significantly silica-undersaturated is supported by the observation that pyroxenes are absent from the equilibrated metal-silicate

assemblage of the pallasites. It is noteworthy that the equilibrium fO_2's calculated for the pallasites are not exceptionally reduced; their most probable fO_2 range is only about 0.5-1.0 log units below IW. Fig. 4 also shows the preliminary results of intrinsic fO_2 measurements carried out in our lab for an olivine separate from the Brenham pallasite; this measurement falls within the fO_2 range estimated from the phosphate-phosphide equilibrium. Inasmuch as it lies below the phosphate-phosphide stability boundary for $T<1550^{\circ}$ C and below the QMO buffer lines ($a(SiO_2)=1$) for $T<\sim1000^{\circ}$ C (Fig. 4), the intrinsic fO_2 measurement for the Salta pallasite reported by (13) appears to be anomalously reduced. In conclusion, the pallasites represent a strongly silica-undersaturated metal-silicate assemblage which probably equilibrated at redox conditions only slightly more reducing than that represented by the IW buffer.

References

(1) Ringwood AE (1979) Origin of the Earth and Moon. Springer-Verlag, 295pp
(2) Arculus RJ, Delano JW (1981) Geochim Cosmochim Acta 45:899-913
(3) Arculus RJ, Gust DA, Holmes RD (1982) This volume
(4) Arculus RJ, Delano JW (1980) Nature 288:72-74
(5) Robie RA, Hemingway BS, Fisher JR (1978) U.S.G.S. Bull 1452, 456pp
(6) Bohlen SR, Essene EJ, Boettcher AL (1980) Earth Planet Sci Lett 47:1-10
(7) Arculus RJ, Delano JW (1981) Geochim Cosmochim Acta 45:1331-1343
(8) Davis AM (1977) PhD Thesis, Yale Univ.
(9) Buseck PR, Goldstein JI (1969) Geol Soc Am Bull 80:2141-2158
(10) Buseck PR (1977) Geochim Cosmochim Acta 41:711-740
(11) Buseck PR, Holdsworth E (1977) Mineral Mag 41:91-102
(12) Carmichael ISE, Turner FJ, Verhoogen J (1974) Igneous Petrology. McGraw-Hill, 739 pp
(13) Brett RJ, Sato M (1976) Meteoritics 11:258-259
(14) Rammensee W, Fraser DG (1981) Ber Bunsenges Phys Chem 85:588-592
(15) Conard BR, McAneney TB, Sridhar R (1978) Metallurgical Trans 9B:463-468
(16) Wood BJ, Kleppa OJ (1981) Geochim Cosmochim Acta 45:529-534
(17) Campbell FE, Roeder P (1968) Am Mineral 53:257-268

Figures

Fig. 1. Standard free energies of the Metal-Oxide ("MO") ($2M + O_2 = 2MO$) and QMO oxygen buffers of Fe, Ni and Co ($\log fO_2 = \Delta G^{\circ}/2.303RT$). The difference between the QMO buffers and their corresponding MO buffers is equal to the free energy of formation of the olivine from its constituent oxides, which becomes increasingly negative in the order Ni-Co-Fe.

Fig. 2. QMO equilibrium calculations for peridotites #270(top) and #271(bottom) assuming the metal to have a composition of X(Fe)=0.9, X(Ni)=0.1, and X(Co)=0.005. γ(Fe), γ(Ni), and γ(Co) after (14) & (15); γ(Fo) and γ(Fa) after (16); $\gamma(Ni_2SiO_4)=1$ (cf.(17) & Fig. 4); $\gamma(Co_2SiO_4)=2$ (Fig. 4).

Fig. 3. QMO "baseline" calculations for peridotites #270(top) and #271(bottom), based on the observed concentrations of Fe, Ni and Co in olivine and assuming X(Fe)=1, X(Ni)=1, and X(Co)=1, respectively (γ(metal)=1). Diluting the pure metal can only raise the indicated fO_2 for each buffer. Subject to the constraint that X(Fe)+X(Ni)+X(Co)=1, the only metal which can coexist with these olivines has a composition of X(Ni)=0.80, X(Fe)=0.19, & X(Co)=0.009 [γ(Ni)=0.92, γ(Fe)=0.55; other γ's as in Fig. 2].

Fig. 4. QMO equilibrium calculations for the main group pallasitic meteorites. Activity coefficients as in Fig. 2, except that $\gamma(Co_2SiO_4)=1$. The upper and lower limits of pallasite fO_2 estimated by (15) are shown by "IW" [X(Fe)=0.9] and by "FSM" (Farringtonite-Schreibersite-Metal), respectively. Also shown are intrinsic fO_2 measurements for an olivine separate from Brenham (ANU) and for a sample of the Salta pallasite[13].

Fig.1. MO & QMO Buffers

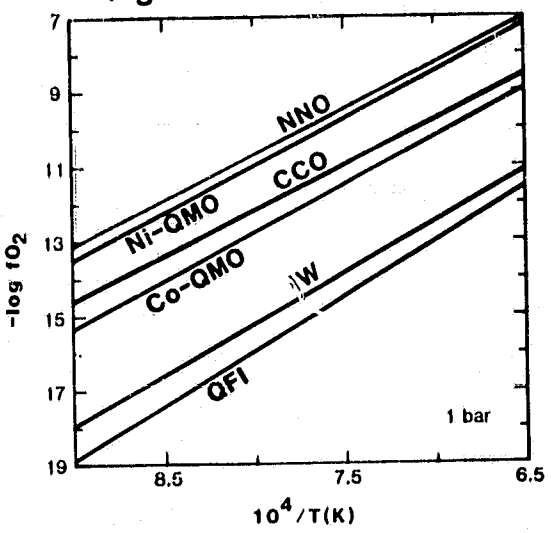

Fig.2. QMO Equilibria

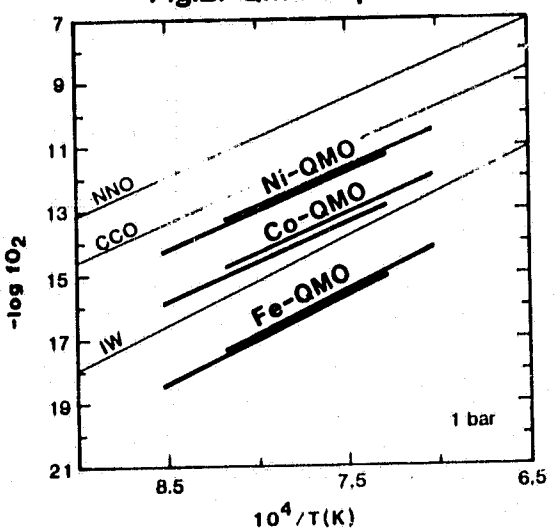

Fig.3. QMO Baselines

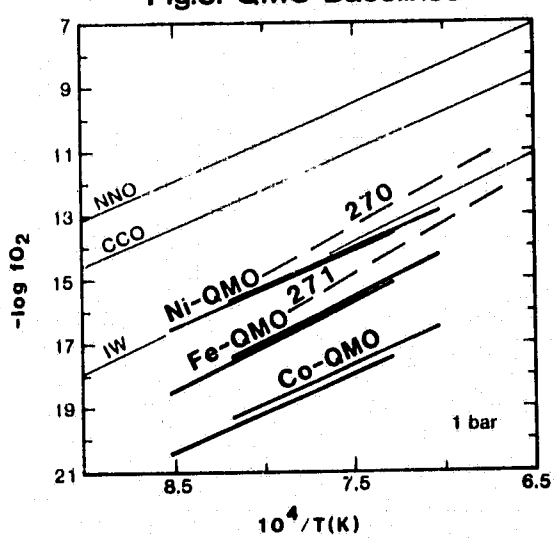

Fig.4. Pallasites

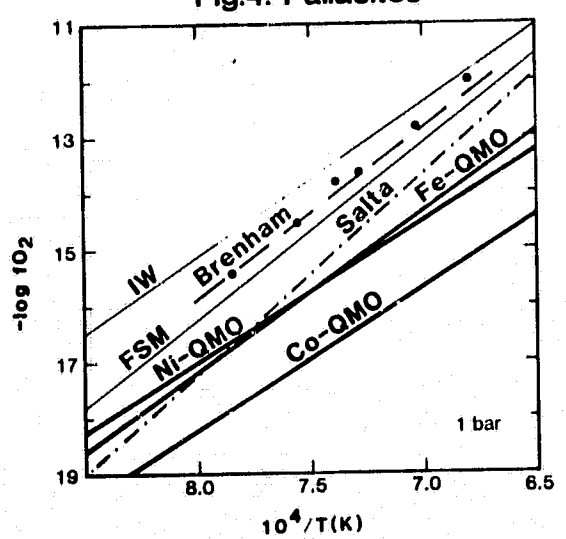

BOUNDARY CONDITIONS ON THE PALEOENVIRONMENT: THE CHEMICAL COMPOSITIONS OF PRE-SOLAR NEBULAE.

Dr. W. M. Irvine, Dept. of Physics and Astronomy, University of Massachusetts, Amherst, MA 01003

Accumulating evidence suggests that at least some interstellar volatile and particulate matter survived the formation of the solar system: anomalous noble gas isotope ratios in meteoritic carbonaceous host phases, the possible presence of carbynes in both interstellar clouds and carbonaceous chondrites, and models of cometary composition which best match the spectra of radicals and ions in the coma (e.g., (1), (2), (3)). The chemical composition of the condensing molecular cloud which formed the solar system (the "pre-solar nebula") thus provides basic initial conditions for the study of planetary volatiles, and is probably quite directly related to the present composition of cometary nuclei.

Direct analysis of this pre-solar nebula is unfortunately not possible, since it no longer exists. Solar-type stars are, however, being formed even today. If we could determine the type of region in which the sun formed, detailed studies might then specify the physical, chemical, and dynamical state of the proto-solar system. Although it has been apparent for some years that star formation occurs in dense interstellar clouds of gas and "dust" (particulate matter), only recently is it becoming clear that such regions exhibit striking differences in chemical composition (4).

The so-called giant molecular clouds, of which that in Orion is the nearest example, are clearly the sites of on-going formation of stars considerably more massive than the sun. Whether the sun itself was formed in such a cloud is unclear, however, since low mass stars may also be born in the colder, more quiescent, lower mass regions known as "dark" clouds.

We have recently compiled the first systematic, continuous spectrum of the Orion molecular cloud in the region 72-91 GHz (5). Several molecular species and isotopic variants were identified which had not previously been detected in Orion, including methyl formate, isocyanic acid, acrylonitrile, ketene, and cyanobutadiyne. For heavier polyatomic species several rotational transitions were typically observed, making possible an accurate analysis of excitation and hence abundance.

The region called Taurus Molecular Cloud One (TMC 1) is an example of a dark cloud. It contains fragments with masses approximately equal to those postulated by Cameron (6) for the solar nebula and is cold (kinetic temperature ~ 10K) and quiescent. Such clouds had been believed to be chemically simpler than the giant clouds, but recently a number of molecular species have been found in TMC 1 which are not present in Orion or in the Galactic center cloud Sgr B2 (7, 8, 9). We have now succeeded in making the first detection of interstellar methylcyanoacetylene in this source (10).

PRE-SOLAR NEBULAE

82

Irvine W. M.

Fractional abundances for known constituents of the Orion molecular cloud and for TMC 1 will be tabulated and compared. Particular attention will be given to the degree of saturation of simple nitriles in the two environments, and how this may relate to modes of molecular formation.

REFERENCES

(1) Hayatsu, R. and Anders, E. (1981). Topics Current Chemistry 99, 1.
(2) Huebner, W.F., Giguere, P.T., and Slattery, W.L. (1982). In Comets, ed. L. Wilkening (Tucson: U. Arizona Press), p. 496.
(3) Greenberg, J.M. (1982). In Comets, op. cit., p. 131.
(4) Irvine, W.M. and Hjalmarson, Å. (1982). In Cosmochemistry and the Origin of Life, ed. C. Ponnamperuma (Dordrecht: D. Reidel), in press.
(5) Johansson, L.E.B., Irvine, W.M., et al., in preparation.
(6) Cameron, A.G.W. (1978). In Protostars and Planets, ed. T. Gehrels (Tucson: U. Arizona Press), p. 453.
(7) Friberg, P., Hjalmarson, Å., Irvine, W.M., and Guelin, M. (1980). Ap. J. (Lett.) 241, L99.
(8) Irvine, W.M., Hoglund, B., Friberg, P., Askne, J., and Elldér, J. (1981). Ap. J. (Lett.) 248, L113.
(9) Avery, L.W. (1980). In Interstellar Molecules, ed. B.H. Andrew (Dordrecht: D. Reidel), p. 47.
(10) Avery, L.W., Irvine, W.M., et al., in preparation.

SOURCES OF VOLATILES IN SUBDUCTION ZONE MAGMAS: POSSIBLE GEOLOGIC CYCLING OF CHLORINE AND WATER.

E. Ito, Dept. Geology and Geophysics, University of Minnesota, Minneapolis, MN 55455; A.T. Anderson, Jr., Dept. Geophysical Sciences, University of Chicago, Chicago, IL 60637

Volatiles such as H_2O, HCl, CO_2, and S in subduction zone magmas may originate from surficial or deep sources. Surficial sources include aquifers and sedimentary rocks. Deep sources include lower crustal rocks, unmodified mantle, and subducted rocks. We investigate the possibility that H_2O and Cl in subduction zone magmas originate from subducted rocks, and if so how material balance works out for the two. It appears that for a reasonable range of estimates, about 10% of Cl and 50% of H_2O in subduction zone magmas could come from subducted amphibole minerals. Equivalent of about 50% of Cl but about 1,000% of H_2O in subduction zone magmas are contained in subducted rocks (Fig. 1).

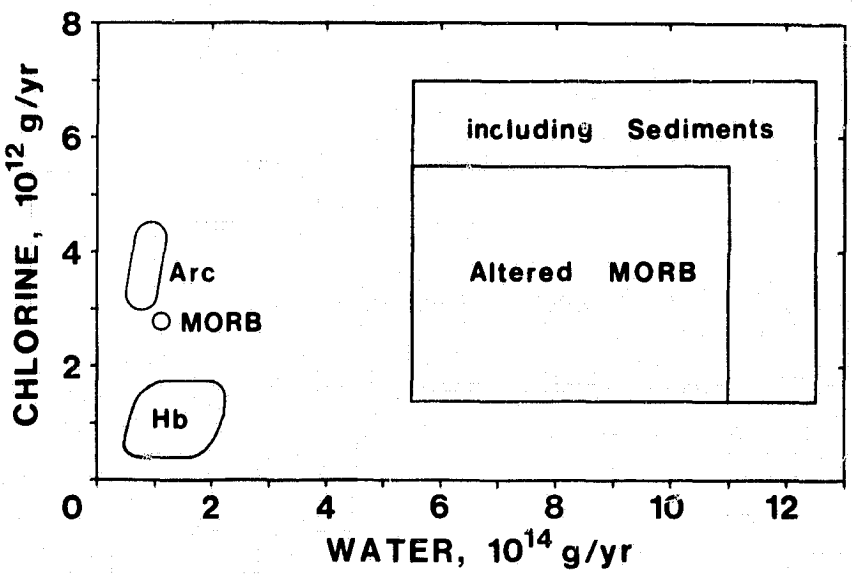

Figure 1. H_2O and Cl balance between subduction zone magmas and subducted oceanic crust. The ranges shown for total H_2O and Cl contained in fresh oceanic crust, altered oceanic crust ± sediments, amphibole in altered oceanic crust, and subduction zone magmas (on per year basis) are based on the estimates given in Table 1.

SOURCES OF VOLATILES IN SUBDUCTION ZONE MAGMAS

Ito E. and Anderson A. T., Jr.

Assessment of production rate of volatiles by subduction zone magmatism requires that a) the volatiles from shallow and deep sources can be discriminated, and b) the magma production rate and average concentrations of volatiles in parental magmas can be estimated. Similarly, we need to estimate the average concentrations of volatiles in material subducted at trenches as well as the rate of subduction. Our estimates are summarized in Table 1, and what we consider to be important sources of uncertainties in our estimates are shown in Table 2.

The ratio of Cl/K_2O in arc magmas may be useful in identifying the source of volatiles. The ratio is highly variable in the upper crustal material, whereas it may be relatively uniform in the lower crustal and mantle material. Such difference in Cl/K_2O may arise from the sedimentary separation of Cl and K. Cl goes into solution, i.e., into seawater. K goes into K-rich clays which after diagenesis/metamorphism resides in K-feldspar and micas, i.e., into crust. Hence Cl/K_2O of arc magmas contaminated by crustal material may be highly variable. Another factor controlling the Cl/K_2O of arc magmas is crystallization-differentiation process. As outlined by Anderson (1), Cl/K_2O decreases when a magma becomes gas saturated and some Cl is carried away in a fractional process with H_2O. The changes in Cl/K_2O with differentiation can then be used to identify the parental liquid. The compositional range of parental magmas identified from Cl/K_2O ratios of trapped melt in phenocrysts indicate that high-alumina basaltic liquids are parental to new crust and have similar Cl/K_2O of about 0.08 (Fig. 2). Parental liquids from some volcanoes, however, show large and variable Cl/K_2O ratios. This may be due to crustal contamination: (a) at the Shasta region, the high Cl (and H_2O) probably comes from the nearby hydrous Trinity ultramafic body which are found as dehydrated xenoliths in Shasta rocks; and (b) at Asama, there is evidence of a separate body of silicic magma lying above the

basaltic one. The average concentrations of Cl and H_2O found in parental magmas with $Cl/K_2O \sim 0.08$ are 0.09% and 2%, respectively.

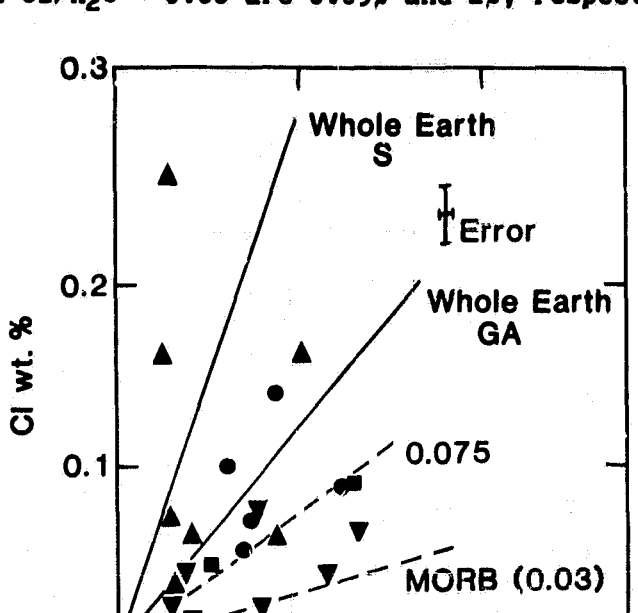

Figure 2. Concentrations of Cl and K_2O in some subduction zone parental magmas are shown.

● = Hypersthenic magmas

■ = Pigeonitic magmas

▲ = Shasta, California

▼ = Modoc, California

Adapted from reference (1).

Material subducted at trenches include igneous crust which has been subjected to some submarine alteration, and overlying sediment of variable composition and thickness. Average fresh MORB (glass) contains about 0.005% Cl and 0.2% H_2O (e.g, 2,3). In fresh crystalline MOR basalt and gabbros, some Cl resides in apatite, but Cl may also be present along intergranular surface and be quite labile. Water in fresh crystalline rocks may be present in

some deuteric amphibole, and also along intergranular surface. With alteration, main residence of Cl becomes hornblende (4), while that of H_2O becomes various hydrous minerals that are formed (Figs. 3,4). The result of submarine alteration is 10x increase in H_2O concentration, and probably little change ($\frac{1}{2}$ to 2x original conc.?) in Cl concentration.

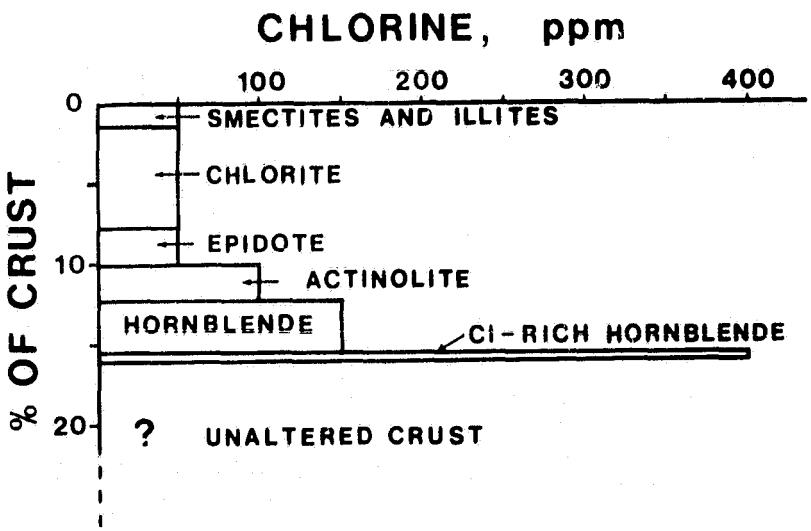

Figure 3. Amount of various hydrous minerals in altered oceanic crust and average concentration of H_2O in each mineral. After reference (4).

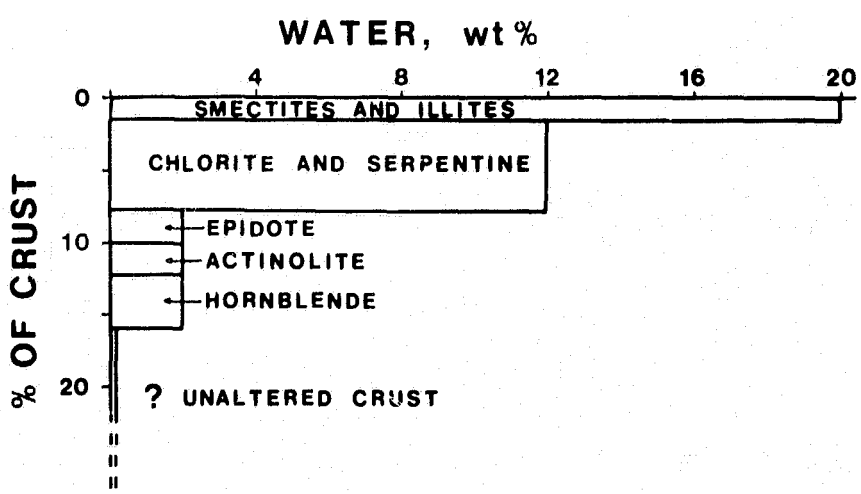

Figure 4. Amount of various hydrous minerals in altered oceanic crust and average concentration of Cl in each mineral. After reference (4).

SOURCES OF VOLATILES IN SUBDUCTION ZONE MAGMAS

Ito E. and Anderson A. T., Jr.

How deeply the volatiles are subducted depends on (a) the stability of host minerals in the P-T regime; (b) whether the host minerals simply dehydrate or melt, or whether prograde metamorphism, for example, of greenstone to amphibolite takes place; (c) the expulsion rate of sedimentary pore-waters; and (d) the depth to which sediment is subducted. Some arc rocks show isotopic evidence of subducted sediment (e.g., 5,6), but others do not (e.g., 7). Chlorite and clays breakdown at less than 50 km depth, whereas hornblende (and epidote), which is the major reservoir of Cl, persists to about 80 km where it either melts or dehydrates (8). Released H_2O, probably rich in incompatible and volatile elements, or partial melt probably rises to overlying mantle where it takes part in generation of subduction zone magmas.

Assuming that subducted sediment does not participate in the genesis of arc magmas, 25% to 100% of Cl and 500% to 1,000% of H_2O in arc magmas can be supplied by subducted oceanic crust if all of Cl and H_2O are expelled in the region of magma generation. If only Cl and H_2O contained in hydrous minerals that are stable to 80 km or deeper (e.g., amphibole) participate in magma genesis, 5% to 20% of Cl and 25% to 100% of H_2O in arc magmas can be accounted for. Taking a simple black-box approach, if the main source of subduction zone magmas were mantle, then some or most of the volatiles can come from the subducted oceanic crust. This is further supported by the observation that Cl and H_2O concentrations in arc magmas are higher than those in MORB or hotspot magmas. The real problem, however, seems to be that not enough H_2O is being expelled by arc magmas compared to the amount subducted with oceanic crust.

(1) Anderson A.T. (1982) J. Geophys. Res. 87, 7047-7060.

(2) Moore J.G. (1970) Contrib. Mineral. Petrol. 28, 272-279.

(3) Schilling J.-G., Unni C.K. and Bender M.L. (1978) Nature 273, 631-636.

(4) Ito E. and Anderson A.T., Jr. submitted to Geochim. Cosmochim. Acta.

(5) Magaritz M., Whitford D.J. and James D.E. (1978) Earth Planet. Sci. Lett. 40, 220-230.

(6) Hawkesworth C.J., O'Nions R.K. and Arculus R.J. (1979) Earth Planet. Sci. Lett. 45, 237-248.

(7) Ito E. and Stern R.J. (1981) Carnegie Inst. Wash. Yrbk. 80, 449-454.

(8) Wyllie P.J. (1982) Geol. Soc. Am. 93, 468-476.

(9) Parsons B. (1981) Geophys. J. Roy. Astr. Soc., 67, 437-448.

(10) Brown G.C. (1973) Nature Phys. Sci. 24, 26-27.

Anderson A.T., Jr. (1975) Rev. Geophys. Space Phys. 13, 37-55.

(11) Edmond J.M. et al. (1979) Earth Planet. Sci. Lett., 46, 1-18.

Edmond J.M. et al. (1982) Nature, 297, 187-191.

Seyfried W.E. (1982) Personal communication.

(12) Ito E., Anderson A.T., Jr. and Harris D.M., submitted to Geochim. Cosmochim. Acta.

Table 1. Estimates* used in Figure 1.

	Fresh MORB	Altered MORB	Amphibole in alt. MORB	Arc	Sediments
rock ($\times 10^{15}$ g/yr)	60 (9)	60 (9)	0.7 to 3 (4)	3 to 5 (10)	3 (7)
H_2O (wt %)	0.2 (2)	1 to 2 (11)	2 (4)	2 (1)	3.5 to 20 (12)
Cl (ppm)	50 (3)	25 to 100 (4)	150 (4)	900 (1)	430 to 2500 (12)

* sources of the estimates are given in parentheses.

Ito E. and Anderson A. T., Jr.

Table 2. Sources of uncertainties in the estimates given in Table 1.

	Uncertainties
Fresh MORB	Difference in concentrations between glassy and crystalline rocks. Reliability of average concentrations.
Altered MORB	Bulk concentrations of Cl and H_2O, i.e., average mineralogy of altered oceanic crust, average Cl and H_2O concentrations in hydrous minerals, and amount of intergranular Cl and H_2O.
Amphibole in altered MORB	Abundance. Average concentration of Cl (analyzed range 100 ppm to 1%)
Arc	Magma production rate Composition(s) of parental magma
Sediments	Composition and thickness Porosity Dewatering behavior in the trench environment

EXCHANGE OF WATER BETWEEN THE REGOLITH, ATMOSPHERE, AND POLAR CAPS OF MARS. Bruce M. Jakosky*, Division of Geological and Planetary Sciences, Caltech, Pasadena, CA 91125.

Understanding the evolution of volatiles on Mars requires understanding the processes which are currently acting to cause exchange between the various reservoirs on annual and longer timescales. On the seasonal timescale, exchange of water can occur between the atmosphere and reservoirs of ice in the polar caps and of adsorbed water in the near-surface regolith covering the remainder of the planet. This exchange is driven by the seasonally-varying insolation and its consequent effects on the surface and subsurface temperatures and on the seasonal advance and retreat of the predominantly-CO_2 polar caps. On the longer timescale, exchange can occur between these same reservoirs, and is driven by the changing annual insolation patterns which result from the 10^5-year timescale variations in Mars' orbital elements (predominantly the orbital obliquity).

Observations of the seasonal water cycle and its variations from year to year from the Viking spacecraft and from Earth provide clues as to the importance of the various reservoirs on the seasonal cycle and provide boundary conditions against which models of the various processes can be compared. The results of the investigation of the seasonal behavior also have implications for the longer-timescale exchange of water between the reservoirs.

The water vapor content of the Mars atmosphere was measured from the Viking Orbiter Mars Atmospheric Water Detectors (MAWD) for a period of more than one Martian year, from June, 1976, through April, 1979. Column abundances vary between zero and about 100 precipitable microns (pr μm), depending on location and season, while the entire global abundance varies seasonally between an equivalent of about 1 and 2 km^3 of ice. The first appearance of vapor at non-polar latitudes as northern summer approaches, and the drop in abundance at mid-latitudes as summer ends, both strongly imply the existence of a seasonal reservoir for water within the regolith. There appear to be no net annual sources away from the poles that contribute significant amounts of water.

The strong annual gradient of vapor from north to south implies a net annual flow of vapor toward the south; this southward flow may be balanced in part by a northward flow during the global dust storms, by transport in the form of clouds or adsorbed onto dust grains, or during other years. The perennially-cold nature of the south-polar residual cap, along with the relatively large summertime vapor abundances over the cap, implies a net annual condensation of water onto the south cap. Estimates of the amount of water transported south each year are consistent with the movement of ice being important in the formation and evolution of the polar layered terrain, and with the formation of the individual layers at the rate of one per obliquity cycle (10^5 years).

Earth-based observations of the water vapor column abundance made over the last twenty years show that the seasonal cycle has a remarkable repeatability, except during 1969 when large vapor abundances were present during southern summer. This difference can be explained if all of the CO_2 had sublimed off of the south residual cap that year, exposing the underlying water cap. The ice would subsequently sublime and produce large amounts of atmospheric vapor at that season. The rate and amount of CO_2 sublimation may depend on the degree of dust storm activity each year and hence on the

different thermal loads placed on the cap. The net effect of this different behavior is to remove the latitudinal gradient of water vapor and to mitigate the net southward transport of water that year.

The possible processes for producing seasonal changes in the atmospheric vapor abundances have been modeled in order to infer the relative importance of each process in the seasonal cycle. The equilibrium between water vapor and water adsorbed onto the regolith grains is sufficiently temperature-dependent that seasonal subsurface temperature variations are capable of driving a large exchange of water between the atmosphere and subsurface. For the likely range of regolith properties, this exchange can be from 10-150% of the observed seasonal change in atmospheric abundance; the differences between this exchange and the observed vapor abundances result from the effects of transport of vapor due to the atmospheric circulation. Due to the latitudinal gradient of atmospheric vapor, there will also be a gradient of subsurface adsorbed water, with the south regolith containing much less water than that in the north; this gradient in the regolith will result independent of the regolith vapor diffusivity, as the near-surface water will be able to equilibrate on some timescale.

Models have been constructed which include regolith exchange, polar cap formation, and atmospheric transport coupled together. Comparison of the model results with the vapor observations and with other data regarding the physical nature of the surface allows constraints to be placed on the relative importance of each process. The models are capable of satisfactorily explaining the gross features of the observed vapor behavior using plausible values for the regolith and atmospheric mixing terms. In the region between the polar caps, the regolith contributes as much water to the seasonal cycle of vapor as does transport in from the more-poleward regions, to within a factor of two. Globally, 10-50% of the seasonal cycle of vapor results from exchange of water with the regolith, about 40% results from the behavior of the residual caps, and the remainder is due to exchange of water with the seasonal caps. It is difficult to determine the relative importance of the processes more precisely because both regolith and polar cap exchange of water act in the same direction, producing the largest vapor abundances during the local summer.

The system is ultimately regulated on the seasonal timescale by the polar caps, as the time to reach equilibrium for exchange of water between the atmosphere and regolith or between the polar atmosphere and the global atmosphere is much longer than the time for the polar caps to equilibrate with water vapor in the local atmosphere. This same behavior will hold for longer timescales, with the polar caps being in thermal equilibrium with the insolation as it changes on the obliquity timescale (10^5 years), and the water vapor in the atmosphere and regolith following along. This long timescale exchange of water has implications for the Mars climate and for evolution of the polar layered terrain during the past billion years.

* Now at Laboratory for Atmospheric and Space Physics, Campus Box 392, University of Colorado, Boulder, CO 80309.

Jakosky, B.M.

RELATED REFERENCES:

Jakosky, B.M. and C.B. Farmer, The seasonal and global behavior of water vapor in the Mars atmosphere: Complete global results of the Viking atmospheric water detector experiment, J. Geophys. Res. 87, 2999-3019, 1982.

Farmer, C.B. and P.E. Doms, Global seasonal variation of water vapor on Mars and implications for permafrost, J. Geophys. Res. 84, 2881-2888, 1979.

Barker, E.S., Martian atmospheric water vapor observations: 1972-74 apparations, Icarus 28, 247-268, 1976.

Jakosky, B.M., The seasonal behavior of water vapor in the Mars atmosphere, Ph.D. Thesis, California Institute of Technology, Pasadena, 1982.

Fanale, F.P. and W.A. Cannon, Exchange of adsorbed H_2O and CO_2 between the regolith and atmosphere of Mars caused by changes in surface insolation, J. Geophys. Res. 79, 3397-3402, 1974.

Jakosky, B.M., The role of seasonal resrvoirs in the Mars water cycle. I. seasonal exchange of water with the regolith, submitted tc Icarus, 1982.

Jakosky, B.M., The role of seasonal reservoirs in the Mars water cycle. II. Coupled models of the regolith, the polar caps, and atmospheric transport, submitted to Icarus, 1982.

Pollack, J.B. and O.B. Toon, Quasi-periodic climate changes on Mars: A review, Icarus 50, 259-287, 1982.

TERRESTRIAL HELIUM ISOTOPIC SYSTEMATICS

Dr. W. J. Jenkins, Woods Hole Oceanographic Institution, Woods Hole, MA 02543

A study of terrestrial helium isotopic systematics is of interest for two reasons: (1) Because of their short atmospheric residence times, fluxes of these isotopes from the solid earth are "visible" and hence, in principle, measurable.

(2) Each of the two isotopes are dominated by different "source terms". ^{4}He is primarily radiogenic, being produced by U and Th decay. ^{3}He is primarily primoridal (inherited), although there is a small radiogenic contribution.

We see a bimodal distribution of isotopic (^{3}He/^{4}He) ratios in terrestrial systems. "Primitive" or deep, undepleted mantle is characterized by high ^{3}He/^{4}He ratios, typically in the range of 10^{-5} to 10^{-4}. Mid-ocean ridge basalts, the most prolific of mantle produced rocks, cluster near 10^{-5} whereas "plume basalts" are higher in ^{3}He/^{4}He. Continentally derived helium is characterized by a low ^{3}He/^{4}He, typically 10^{-8} to 10^{-7}, as would be expected from a U, Th rich, initially degassed source region.

Detailed studies of the distribution of He isotopes in rocks, gas wells and hydrothermal systems is revealing much about mantle structure, mantle-crust interaction and the large scale tectonic structure of the continental crust. What is also of value is the fact that we are able to measure the fluxes of these isotopes and thus place real constraints on not only the present day degassing rate of the earth but also, through isotopic ratio of the deep earth, the long term degassing history.

The study of the oceanic flux of ^{3}He by Craig and Clark (1) led to an estimate of the oceanic ^{3}He flux of 4 atoms $cm^{-2}s^{-1}$, a value which later, more detailed work has verified. Preliminary work at this laboratory on hot springs in the western U. S. show a ^{4}He/heat ratio of $(1.2\pm0.3)\times10^{-7}$cc(STP)/cal, or about 3.2×10^6 atoms ^{4}He/cm^2/s/H.F.U. This ratio is within the uncertainty of the calculated present day source ratio for the continents. Using the "shallow" (non-mantle) heat flow distribution to estimate a ^{4}He flux, we thus obtain a continental contribution of $\approx1.7\times10^{24}$ atoms ^{4}He s^{-1}, or a contribution roughly equivalent to the oceanic "mantle" contribution. The equivalent continental radiogenic ^{3}He contribution from Li $(n,\alpha)^3H \rightarrow {}^3$He is entirely negligible compared to the mantle flux.

A simple bulk-earth coherent degassing model calculation using U, Th, K, He and Ar indicates that the terrestrial degassing rate was substantially greater in the past, and suggests that the earth had perhaps 1% of the ^{3}He abundance of chondritic material. This calculation also points to a deep earth ^{40}Ar/^{36}Ar of the order of 200-400.

(1) Craig, H., and Clarke, W. B. (1980) Earth Planet. Sci. Lett., 9, 45-48.

TRAPPING OF GASES AND LOW TEMPERATURE VOLATILES IN LUNAR SAMPLES. S. Jovanovic and G. W. Reed, Jr., Chemistry Division, Argonne National Laboratory, 9700 South Cass Avenue, Argonne, Illinois 60439

Trapping of volatiles on the moon may be viewed from two perspectives. One is the condensation of gases and volatiles at very low (<100 K) temperatures. The other involves fixing of gases and volatiles at much higher (up to subsolar) temperatures. The status of cold trapping is summarized in Section I. A brief discussion of Cl in lunar samples and the implications with regard to H_2O is included in this section. We will concentrate, in this presentation, on higher temperature adsorption and propose trapping mechanisms, Section II and Conclusions.

I. Pre-Apollo, the lack of an atmosphere on the moon did not deter Watson, Murray and Brown (1961) from addressing the question of the presence, location and quantity of H_2O that might be at the surface of the moon. Their treatment of this problem has been up-dated by Arnold (1979); see also Hodges (1980). The picture that emerges is that volatiles released to the lunar exosphere will eventually encounter a cold trap in permanently shadowed regions near the lunar poles, if they do not escape from the moon. Temperatures of <100°K are expected. Water should be the major trapped volatile and be present in quantities up to 10^{17} gm. The sources of H_2O proposed are solar wind H on Fe-oxides, H_2O bearing meteoroids, cometary impact and possibly degassing of the interior.

The lunar sample data have not contributed further insights. Except in rare cases, there is no evidence for H_2O in the sampled lunar surface.

A case for volatiles in the moon must be made on bases other than H_2O. One which should be considered is the presence of Cl in lunar samples. Lunar rocks and soils contain from a few to 300 ppm Cl; this is comparable to that in meteorites and terrestrial rocks. The Cl is present in at least two phases - one is water soluble, the other is stoichiometrically related to phosphorus, i.e. apatites. Since in terrestrial magmatic processes both Cl and H_2O play important roles, the presence of Cl but lack of evidence for H_2O on the moon needs to be understood. If Cl was a volatile in the solar nebula and was accreted by the earth, then it appears that H_2O should have been accreted by the moon. Perhaps all lunar magmas lost H_2O at the surface.

IIA. Four volatiles that have been identified in lunar samples are the gases Ar and Xe and the elements Hg and Br or their compounds. These all appear to be indigenous volatiles in that they exhibit surface correlated behavior both on the moon and in returned samples and they are not produced in the material in which they are found or in related material such as local soils and rocks.

Jovanovic S. and Reed G. W., Jr.

The persistence of the gases, parentless ^{40}Ar and excess fissiogenic Xe, and of low temperature volatile non-gaseous Hg and Br in lunar surface material and, in the case of Ar, also in the atmosphere has posed a number of problems of fundamental importance in understanding the moon. These include the volatile or gaseous sources or reservoirs; how these elements are associated with substrate material, i.e. why they have not been totally depleted; their behavior in the regolith and in the lunar atmosphere; and as a result of their mobility, possible ponding in permanently shadowed cold traps.

Heymann and Yaniv (1970) and Manka and Michel (1970) first addressed the problem of parentless ^{40}Ar in lunar samples. Reed et al. (1971) discussed the presence of Hg and the fraction found to be volatile in subsolar temperature. Hodges and Hoffman (1975) reported on Ar in the lunar atmosphere. The Washington University team of Podosek, Hohenberg and others (Crozaz et al., 1972, Drozd et al., 1972 and Beratowicz et al., 1979 included references) identified unsupported fissiogenic Xe in solar and gas-rich breccias. Since any lunar atmospheric component will be electromagnetically accelerated and lost, all of these authors (see also Hodges, 1982) attempted to explain why the various atmophile elements have persisted.

Activation energies for sorption or diffusion have been determined for Ar, Xe and Hg. Ar (Hodges, 1982) and Hg (Reed and Jovanovic, 1979) estimates were based on essentially in-situ lunar measurements; Xe was measured in the laboratory (Podosek et al., 1981; Bernatowicz et al., 1982). The Hg measurement was based on concentration gradients of Hg (and Br) in lunar soil in response to the subsolar heating; it is model dependent. The Ar measurement was based on mass spectrometric detection of pre-sunrise increases in Ar in the lunar atmosphere. Xe sorption measurements were made on pulverized terrestrial and on lunar soil samples after pumping and heating to generate clean surfaces.

Element	E* (Kcal/mole)
Ar	6-7
Xe	5-7
Hg	8

These activation energies are higher than have been reported for Ar and Xe on graphitized carbon black (2.20 and 3.69 kcal/mol) and also higher than the 3.78 kcal/mol for Ar on heterogeneous surfaces (Hobson, 1973-74). From his data, Xe would have ~6.3 Kcal/mol adsorption energy on such surfaces; this is about the same as that noted above.

Such low E* should not permit surface adsorbed fractions to persist at the lunar surface. Hence, some other trapping mechanism appears to be required since returned samples contain these volatiles. Implantation by solar wind or acceleration back to the surface from the lunar atmosphere can be ruled out

since Xe is found inside non-regolith rocks such as troctolite 76535 (Caffee et al., 1981). We have established that Hg is enriched on the underside of rocks relative to the interior or exposed surfaces, it is enriched in permanently shadowed areas under rock overhangs (see also Wegmüller et al., 1982) and at depth (5-8 cm) in drill cores. It should be noted that the excess Xe containing breccias range from extremely friable 14082 to tough 15455. The open (friable) rock has not lost Xe. In addition, during storage on earth mobile fractions of Hg and Br have not migrated to uniformly coat surfaces in cores.

Another observation relevant to the fixation of Hg on surfaces is from comparing vacuum sealed SRC (Apollo 16 and 17 sample return containers) with N_2-filled core tubes from Apollo 12 and 17. Surfaces were apparently not altered in the latter in a way that would cause desorption of Hg. A similar conclusion for Xe has been arrived at by Bernatowicz et al. (1982). Storage time does not appear to be a factor either, since the Apollo 12 core was stored ten years. We have not measured 12027 dissected core samples but room temperature volatile Hg from whole core pumpings is the same in the Apollo 12 core and the two SRC's (Jovanovic et al., 1981). Hg volatilized at room temperature from the 70002 core was lower than that from the Apollo 17 core.

IIB. We have acquired other data on Hg that is relevant to the trapping problem. In an experiment to determine Hg released at various temperatures by an atomic absorption method using a cold cathode, the initial [Hg] released below 130°C was lower than that previously determined by neutron activation analysis on an aliquant of the samples. When the samples were recycled between room temperature and 130°C, the two concentration measurements agreed. Thus, a fraction or all of the Hg was present originally as a compound which decomposed to Hg atoms (Reed et al., 1971).

Stepwise heating experiments almost always exhibit a significant Hg and Br release at $\leq$130°C. This is what we identify as the surface related fraction. Two sets of stepwise heating data are available. One is based on concentration gradients in cores resulting from the thermal gradient at the lunar surface, e.g. heating to a maximum of 130°C (Reed and Jovanovic, 1979). The other is based on stepwise heating of a basalt at temperatures up to 1200°C in the laboratory. Log D/a^2 vs. $1/T$ plots were made for both sets of data. The curves were straight lines after the lower temperature fractions were subtracted in both cases. The data points in the upper half of Figure 1 are the high temperature data, those in the lower half are the lunar surface data. The scale for log D/a^2 for the latter was arbitrary and was adjusted to attain the colinearity plotted. Note that regardless of this adjustment the slopes of the low and higher temperature curves are the same, i.e. the E^* is the same. Thus a common factor is determining the mobility

of Hg and the low and high temperature sites are of the same type.

Conclusions

Hg released at temperatures >450°C; rare gases released above 500°C; Hg, Br, Ar and Xe released at <130°C must be present on similar types of surfaces. Their adsorption is a property of the adsorbent. This property is physical, not compositional and is independent of the state of the material (i.e. soil or igneous rock). Hg is immobilized at low temperature probably as a compound which decomposes between 23°C and 130°C.

Microcracking is common to all regolith material and could provide the surfaces and closure needed to trap volatiles. Heymann and Yaniv (1971) reported up to 50% release of trapped gases on crushing. Open microcracks could account for the lunar surface release of Ar and migration of Hg at the lunar surface and at low temperatures in the laboratory. Opening of closed microcracks could account for rare gas and Hg release at temperatures >500°C. Batzle and Simmons (1979) measured changes in fracture porosity in rock previously fractured at 700°C. On cycling between 30°C and 230°C (to match the lunar diurnal temperature excursions) the fracture porosity of granite increased but that of diabase, a closer analog to lunar basalt, decreased. In an Abstract in this volume, S. Ramadurai (1982) suggests adsorption on micropores to account for rare gases in meteorites.

Work supported by the National Aeronautics and Space Agency.

References

Arnold J. R. (1979) J. Geophys. Res. 84, 5659-5668.

Batzle M. L. and Simmons G. (1979) Lunar and Planet. Sci. X, pp.78-79.

Bernatowicz T. J., (1979) Proc. Lunar Planet. Sci. Conf. 10th, pp. 1587-1616.

Bernatowicz T., et al. (1982) Lunar Planet. Sci. XIII, pp. 39-40.

Caffee M., et al., (1982) Proc Lunar Planet. Sci. 12th, pp.99-115.

Crozaz G., et al., (1972) Proc. Lunar Sci. Conf. 3rd, pp. 1623-1636.

Drozd R. J., et al., (1972) Earth Planet. Sci. Lett. 15, pp. 338-346.

Heymann D. and Yaniv A. (1970) Proc. Apollo 11 Lunar Sci. Conf., pp. 1261-1267.

Heymann D. and Yaniv A. (1971) Proc. Lunar Sci. Conf. 2nd, pp. 1681-1692.

Hobson J. P. (1973/74) Critical Reviews in Solid State Sciences 4, 221-245.

Hodges, Jr. R. R., and Hoffman J. H., (1975) Proc. Lunar Sci. Conf. 6th, pp. 3039-3047.
Hodges, Jr. R. R. (1980) Proc. Lunar Planet. Conf. 11th, 2463-2477.
Hodges, Jr. R. R. (1982) Lunar and Planet. Sci. XIII, 329-330.
Jovanovic S. and Reed Jr. G. W. (1968) Geochim. Cosmochim. Acta 32, pp. 341-346.
Jovanovic S. et al. (1981) Lunar Planet Sci. XII, pp. 522-524.
Marńka R. H. and Michel F. C. (1970) Science 169, pp. 278-280.
Oliver L. L. and Manuel O. K. (1981) Lunar Planet. Sci. XII, pp. 788-???.
Podosek F. A., et al., (1981) Proc. Lunar Planet. Sci. 12th, pp. 891-901.
Ramadurai S. (1982) This volume.
Reed G. W., et al., (1971) Science 172, 258-261.
Reed Jr. G. W. and Jovanovic S. (1979) Proc. Lunar Planet. Sci. Conf. 10th, pp. 1637-1647.
Watson K., Murray B. C. and Brown H (1961) J. Geophys. Res. 66, 3033-3045.
Wegmüller F., et al. (1982) Lunar Planet. Sci. XIII, pp. 847-848.

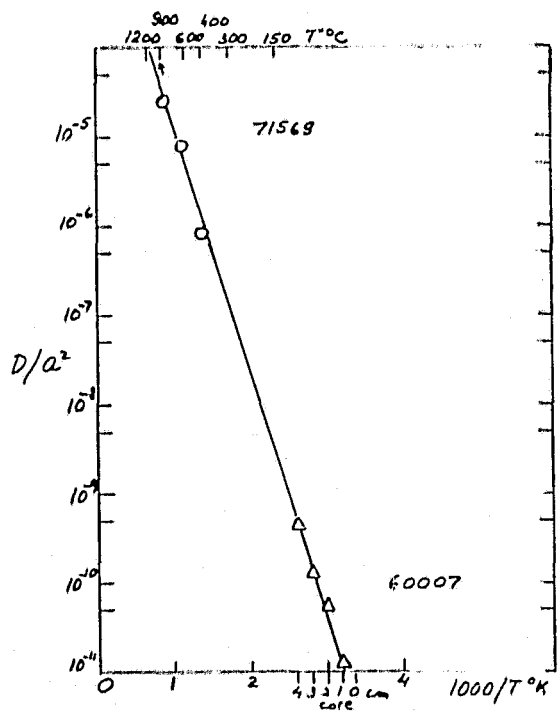

Figure 1. D/a^2 vs. 1/T plot for Hg migration in lunar material. (Δ) 60007 diffusivity data based on concentration gradients in cores related to the thermal gradient induced by subsolar heating. For model see Reed and Jovanovic (1980). (o) Diffusivity data for Hg release during stepwise heating of basalt 71568.

LOSS OF A MASSIVE EARLY OCEAN FROM VENUS, J.F. Kasting and J.B. Pollack, NASA Ames Research Center, Moffett Field, CA 94035

The recent discovery of a 100-fold enrichment in deuterium on Venus[1] strongly suggests that Venus was originally endowed with much more water than is now present in its atmosphere. If Venus and Earth had similar initial D/H ratios, the initial H_2O abundance on Venus must have been at least .14 percent that of Earth and may have been considerably higher if some deuterium has escaped or if juvenile water has continued to be degassed during the planet's history. The loss of water from the present Venus atmosphere occurs by nonthermal escape of hydrogen and oxygen to space[2,3]. The degree of deuterium fractionation depends upon which of several possible mechanisms is primarily responsible for hydrogen escape. In a primitive Venus atmosphere in which H_2O was much more abundant, these nonthermal escape mechanisms would have been superceded by rapid hydrodynamic outflow of hydrogen and loss of oxygen to the planet's crust[4,5]. Deuterium could have been lost effectively if the escape flux exceeded a certain critical value, so that a large D/H enrichment need not have occurred at this time[4]. The magnitude of the hydrodynamic escape flux depends upon the abundance of hydrogen in the Venus upper atmosphere, along with the rate of heating by absorption of solar EUV radiation. Watson et al.[4] estimated an upper bound of 1.1×10^{12} H_2 molecules $cm^{-2}s^{-1}$ for a pure molecular hydrogen thermosphere and an EUV heating efficiency of 30 percent, but did not show how closely the actual escape flux would have approached this limiting value.

We have repeated the hydrodynamic escape calculation using a coupled chemical-dynamical model of the Venus upper atmosphere. The escape flux is calculated as a function of the H_2O mass mixing ratio at the atmospheric cold trap, near 90 km for the present Venus atmosphere. The cold trap mixing ratio is then related in an approximate fashion to the H_2O concentration in the lower atmosphere, following the procedure formulated by Ingersoll[6]. Combination of these two calculations yields the variation of H escape flux versus H_2O mixing ratio in the lower atmosphere (Fig. 1). The solid portion of the curve was derived by solving the hydrodynamic equations from the cold trap out to infinity using $\lambda = 1/r$ as the vertical coordinate. The dashed portion of the curve represents classical Jeans escape of hydrogen. The transition from Jeans to hydrodynamic escape occurs at a lower atmosphere H_2O mass mixing ratio C_ℓ (H_2O) - 0.1, which corresponds to ~4 percent of a terrestrial ocean if the partial pressures of CO_2 and N_2 were the same as today. All water is presumed to have been in the vapor state due to an extremely high (> 750K) surface temperature. A full terrestrial ocean of water would yield C_ℓ (H_2O) = 0.74.

The escape fluxes calculated in our model depend upon several poorly known parameters, including the rate of heating by solar EUV radiation and the oxidation state of the lower atmosphere. The escape rates shown in Fig. 1 are for solar minimum EUV fluxes, a heating efficiency of 15 percent, and a neutral or mildly oxidizing lower atmosphere. The escaping gas is predominantly H, rather than H_2, and the maximum escape flux of 2.7×10^{11} H atoms $cm^{-2}s^{-1}$ is a factor of 5 smaller than the critical flux required to carry off significant amounts of deuterium. The escape flux rises roughly linearly with increasing EUV heating rate, so deuterium may have been lost if the heating efficiency or solar ultraviolet flux was higher than we have assumed. Accumulation of O_2 during the hydrodynamic escape phase would

have enhanced the hydrogen escape rate by increasing the absorption of ultraviolet radiation in the lower thermosphere. Escape rates would also have been higher if the lower atmosphere were reducing, as suggested by Watson et al[5], since escape of H_2 would supplement the loss of H.

Helium could have been swept away during the hydrodynamic escape process if the escape flux exceeded 7×10^{12} H atoms $cm^{-2}s^{-1}$. This mechanism might account for the low abundance of ^4He in Venus' present atmosphere compared to the amount expected from primordial and radiogenic sources[7].

References

1. Donahue, T.M., Hoffman, J.H., Hodges, R.R., and Watson, A.J. (1982), Science, 216, p. 630-633.

2. McElroy, M.B., Prather, M.J., and Rodriguez, J.M. (1982a), Science, 215, p. 1614-1615.

3. McElroy, M.B., Prather, M.J., and Rodriguez, J.M. (1982b), Geophys. Res. Lett., 9, p. 649-651.

4. Watson, A.J., Donahue, T.M., and Walker, J.C.G. (1981), Icarus, 48, p. 150-166.

5. Watson, A.J., Donahue, T.M., Kuhn, W.R., and Walker, J.C.G. (1982), Icarus, submitted.

6. Ingersoll, A.P. (1969), J. Atmos. Sci., 26, p. 1191-1198.

7. Pollack, J.B. and Black, D.C. (1982), Icarus, submitted.

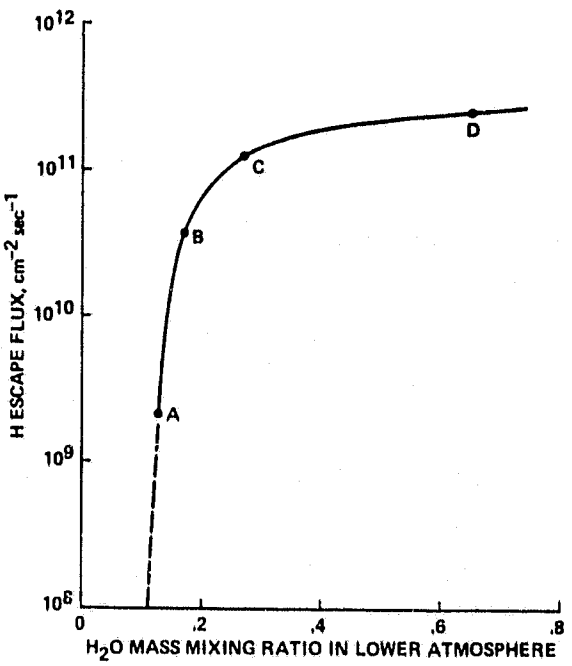

Figure 1

NONTHERMAL ESCAPE OF HYDROGEN AND DEUTERIUM FROM VENUS AND IMPLICATIONS FOR LOSS OF WATER, S. Kumar, USC Center for Space Sciences, Tucson, AZ, 85713, D.M. Hunten, Lunar and Planetary Lab., University of Arizona, Tucson, AZ, 85721, J.B. Pollack, Space Science Division, NASA-Ames Research Center, Moffett Field, CA, 94305

Venus is known to be severely deficient in water compared to Earth. From Venera 11-12 entry probe data, Moroz et al. (1981) have derived an H_2O mixing ratio of 20 ppm at the surface which corresponds to 1.0×10^{-5} gm per gm of Venus mass; the corresponding water inventory on Earth is 1.6×10^{-4} gm per gm. The scenario that Venus has lost a substantial quantity of water is almost required by recent reports on D/H ratio of 1% deduced by McElroy et al. (1982) and a value of 1.6% obtained by Donahue et al. (1982). The one-hundredfold enhancement relative to the Earth value (1.6×10^{-4}) requires at a minimum the loss of 99% of the H, and much more if some of the D has been lost too.

If Venus did indeed start out with earth equivalent ocean of water in its atmosphere, H abundance in the exosphere would be so large that H could no longer be gravitationally bound and a controlled outflow would result (Watson et al. 1981). Such hydrodynamic escape of H would cease when H_2O mixing ratio at the cold trap drops to $\sim 10^{-3}$ which corresponds to a water mixing ratio of ~0.2 at the surface (Kasting and Pollack 1982). Jeans escape (or thermal evaporation) would also be utterly negligible; the estimated escape flux for present atmosphere is only 5×10^4 cm^{-2} s^{-1} for exospheric temperature of 300 K. We must therefore look to various nonthermal processes for further loss of H to account for the severe deficiency of H in the present atmosphere.

(1) Plasmaspheric Charge Exchange: Charge exchange between cold H and O atoms in the exosphere and high temperature H^+ ions in Venus' plasmasphere leads to production of nonthermal or hot H atoms a fraction of which escape to space. Since the nightside shows a remarkable bulge in H^+ in the predawn sector which corresponds to a 400:1 bulge in neutral H density in the exosphere (Brinton et al., 1980), the escape flux at present occurs from the night side. Using Pioneer Venus ion temperature data of Miller et al. (1980), we estimate a globally averaged escape rate of 2×10^7 cm^{-2} s^{-1}. In the past atmospheres when the H density would be higher, this source would be even more significant because the hot H production rate increases approximately as the square of the H density. If the source of ionization on the nightside is kept the same as what it is at present we estimate a maximum escape of flux of $\sim 2 \times 10^9$ cm^{-2} s^{-1} from this process in the past. The energy limited saturation would occur at an H abundance roughly 10 times the present value.

Although the escape of H from the charge exchange on the dayside is small at present, it would saturate at a flux much higher than nightside value for high H abundance since the ionization source is stronger on the dayside. We find that the dayside source would saturate at a maximum H escape flux of $\sim 10^{10}$ cm^{-2} s^{-1} which would occur at ~1000 times the present H abundance in the exosphere. Thus charge exchange can maintain the H escape flux close to the diffusion limit and provide the necessary escape mechanism once the hydrodynamic escape terminates.

(2) Hot O Impact Hot O atoms are produced by the recombination of O_2^+, and the subsequent impact of these hot O atoms on the exospheric hydrogen produces nonthermal H atoms some of which are energetic enough to escape giving a hydrogen escape rate of 8×10^6 cm^{-2} s^{-1} for the present atmosphere (McElroy, et al., 1982). This source works well at night and is significant for the

escape of H at present because the O_2^+ ionosphere peak is observed at 145 km (Taylor et al., 1980) just below the exobase which is at ~152 km, making the hot O atoms available to the exospheric hydrogen. In the present atmosphere, the exobase level is determined by the atomic oxygen density, but in the past atmospheres when the H column density could be higher, it is the hydrogen gas that would determine the exobase level. Once the exobase level is above 260 km, approximately one scale height of H above the O^+ peak, this mechanism would operate very inefficiently as hot O and H atoms would collide with the cold H atoms and thermalize before they reach the exobase and contribute to H escape. We expect this source to saturate at an exospheric H abundance only a few times the present value giving a maximum escape flux of ~3 x 10^7 cm^{-2} s^{-1}. Hence this mechanism would be insignificant in the past compared to the charge exchange process described above.

(3) Ion-Molecule Reactions The important ion-molecule reaction for the production of nonthermal H atoms is the reaction of O^+ with H_2 and subsequent recombination of OH^+. The escape flux due to this mechanism clearly depends upon the H_2 mixing ratio, which is highly uncertain even for the present atmosphere. If the mass 2 ion observed by the PV-OIMS experiment is H_2^+, the implied H_2 abundance is about 10 ppm and the hydrogen escape rate on the day side is ~10^8 cm^{-2} s^{-1} (Kumar et al., 1981). This source has comparable strength on the nightside due to the presence of predawn density bulge in mass 2 ion. The mass 2 ion may, on the other hand, be D^+ (McElroy et al., 1982), in which case the H_2 mixing ratio could be quite low and the corresponding escape flux negligible. In past atmospheres, H_2 could have been more abundant due to higher outgassing rates or reactions of atmospheric H_2O with reduced minerals in the crust. But an H_2 abundance higher than 10 ppm would not lead to higher escape rate from the O^+-H_2 source because increasing H_2 density implies an increase in H density which in turn results in a drop in O^+ density. For past atmospheres the mechanism saturates at a flux of ~3 x 10^8 cm^{-2} s^{-1}. Even if this mechanism is important at present it is overtaken by charge exchange rapidly at higher H abundance.

Thus charge exchange is the major nonthermal escape mechanism for hydrogen. It is also the most important mechanism for escape of deuterium. At an ion temperature of 5000 K, the maximum measured at night, deuterium escapes with 44% the efficiency of hydrogen escape. At 2300 K, the ion temperature on the dayside, the relative efficiency drops to 11%. If the mixing ratios of H_2O in the lower atmosphere are 2 x 10^{-4} at present and 0.1 initially (onset of hydrodynamic flow), we calculate a D/H enrichment during nonthermal escape ranging from a factor of 3600 at T_i = 2300 K to 173 at T_i = 5000 K. The loss of a full terrestrial ocean of water is consistent with the observed D/H ratio if outgassing of juvenile H_2O has continued during the planet's history.

References

Brinton, H.C. et al. (1980) Geophys. Res. Lett., 7, 865.
Donahue, T.M. et al. (1982) Science, submitted.
Kasting, J.F. and Pollack J.B. (1982) Icarus, submitted.
Kumar, S. et al. (1981) Geophys. Res. Lett., 8, 237.
McElroy, M.B. et al. (1982) Science, 215, 1614.
Miller, K.L. et al. (1980) J. Geophys. Res., 85, 7759.
Moroz, I.V. et al. (1980) Nature, 284, 243.
Taylor, H.A., Jr. et al. (1980) J. Geophys. Res., 85, 7765.
Watson, A.J. et al. (1981) Icarus, 48, 150.

CONSTRAINTS ON THE EVOLUTION OF THE MANTLE FROM NOBLE GAS ISOTOPE RATIOS.

M.D. Kurz and C.J. Allègre, Laboratoire de Géochimie, Institut de Physique du Globe, 4 Place Jussieu - 75230 Paris cedex 05-France

Numerous studies of Sr, Nd and Pb isotopic variations in basaltic rocks have shown that the terrestrial mantle is heterogeneous. Recent studies of the noble gases, particularly He, Ar, and Xe, provide important constraints on the origin and evolution of the heterogeneities. Measurements of the $^{3}He/^{4}He$ and $^{87}Sr/^{86}Sr$ ratios in oceanic basalts yield clear regional correlations (1),which shows that the two isotope systems (U-He, Rb-Sr) are not decoupled. The highest $^{3}He/^{4}He$ ratios allow identification of the source regions for Hawaii, Iceland, and Reunion as relatively undepleted, a result which is at odds with criteria for selecting "primitive" mantle based on the Sr-Nd correlation. The overall helium and strontium variations require the existence of at least three mantle reservoirs (1,2). A simple model to explain the variations includes undepleted, depleted and recycled mantle reservoirs. Although available measurements do not allow unambiguous identification of the corresponding argon and xenon isotopic composition for the reservoirs (partly because of contamination effects), recent measurements on MORB glass yield important information on the depleted mantle. The mean age of $>4x10^{9}$ years, calculated from Ar and Xe measurements (3, 4), not only suggests early outgassing, but also place limits on the extent of recycling. Consideration of the global ^{3}He flux, $^{3}He/^{36}Ar$ measurements, and atmospheric ^{36}Ar inventory shows that present day degassing rates are insufficient to generate atmospheric argon, which is consistent with early outgassing. ^{3}He concentrations for the different mantle reservoirs can be inferred from the measurements, and suggest that the present day ^{3}He flux, and the ^{3}He in MORB, is ultimately derived from the lower mantle.

1) Kurz M.D., W.J. Jenkins, J.G. Schilling and S.R. Hart, Earth Planet. Sci. Lett. 58, 1-14, (1982)
2) Kurz, M.D., W.J. Jenkins and S.R. Hart, Nature 297, 43-47, (1982)
3) Staudacher, Th., and C.J. Allègre, Earth Planet. Sci. Lett. (in press).
4) Sarda, Ph., Th. Staudacher, and C.J. Allègre, EOS 63, 458.

PROCESSES OF SHOCK DEHYDRATION ON ACCRETING PLANETS.

P. Lambert, SN6/NASA JSC, Houston, TX 77058 and M. A. Lange, Seismological Laboratory, CALTECH 252-21, Pasadena, CA 91125

INTRODUCTION: Serpentine and serpentine-like layer silicates are the major water-bearing phases in carbonaceous chondrites (1,2). It appears that these minerals, and a poorly defined cometary contribution, were the most likely water-bearing phases in accreting planetesimals which led to the formation of the terrestrial planets (3,4). In several models (3,5,6) formation of a planetary atmosphere/hydrosphere is envisioned as a primary process, taking place during accretion. Water and other volatiles in minerals of the infalling planetesimals is released when these bodies hit the accreting planets, and is continually added to a growing proto-atmosphere. The aim of this study was to constrain the processes by which impact on accreting planet contributes to the evolution of the planetary volatiles. Two approaches were envisioned; (a) study of experimentally shocked minerals analog to the probable primordial water-bearing phases in accreting planet; (b) comparative study of carbonaceous chondrites.

MATERIALS/METHODS: Experimentally shocked material comprises brucite and antigorite (4,7), biotite and muscovite (8,9), talc and amphiboles (10). Experiments have been carried out with a 20 mm flat plate accelerator using impedance match technique and multiple shock reverberations. In brucite and serpentine experiments, vented and sealed target assemblies have been used to constrain vapor escape (4). Investigated pressure ranges from about 10 to 80 GPa (1 GPa $\simeq 10^4$ atm). The studied chondrites are C2 carbonaceous chondrites: Murchison, Murray, ALHA 77306 and ALHA 76261. The analytical techniques includes microprobe, SEM, IR spectroscopy, thermogravimetry and optical microscopy.

RESULTS: Shock induced dehydration of antigorite starts at P> 20 GPa and is complete at P> 60 GPa (Fig. 1). Shock dehydration of brucite and micas occur at lower pressures. Shock dehydration is more efficient in porous material (Fig. 1). Confinement favors readsorption of a portion of the shock released structural water by the shocked mineral. Dehydration intervals and activation energy for dehydration of shocked samples is less than that of the unshocked equivalent. Dehydration interval and activation energy for dehydration of a shocked mineral decreases with increasing shock pressure. Evidence of melting in experimentally shocked antigorite and micas is revealed by the highly vesicular and apparently homogeneous glasses. Shock induced melting in talc and amphiboles result in decomposition of the mineral and formation of an assemblage of vesicular glass and crystalline phases. Significant melting (affecting 10% or more of the initial phase) is detected at P> 30 GPa in micas and P> GPa in antigorite, talc and amphiboles. Compared to "dry" silicates, antigorite talc and amphibole shocked in the range 0- 50 GPa show remarkably very little deformation features.

Investigated C2 chondrites display a breccia texture characterized by an abundant matrix (50-80% of the meteorite). There is a hiatus in grain size between the matrix and the clast. The degree of "serpentinization" of clasts varies from one clast to another. Locally an oriented texture is observed in Murchison and in ALHA 77306. Preferred orientation is related to variations in the nature and/or texture of the matrix minerals and to deformation and elongation of the clasts. We have not observed vesicular phases similar to that described in the shocked serpentine (P>45 GPa) or shocked micas (P>30 GPa), in the matrix of studied C2 chondrites. There are fractures of local extension cutting through the matrix. These fractures are also filled by hydrated silicates. Shock in C2 is revealed by strong fracturing and by mosaicism in some of the clast minerals, preferentially in pyroxenes. Most remarkable is a strongly fractured enstatite fragment in Murchison which displays decorated planar elements resembling those commonly encountered in shocked tectosilicates from old and deeply eroded terrestrial impact structures (12-14). Terrestrial DPE are interpreted as result of post shock healing-dissolution processes in the mineral related to fluid interactions along shock produced planar discontinuities (15-16). Other type of healing features are also observed in olivine and pyroxenes of C2 in the form of planes of inclusions (see also (17)). Probable annealing features are observed in olivine and possibly in some pyroxenes.

IMPLICATIONS/CONCLUSION: Experimental shock does release H_2O in material analog to that considered to represent the primordial H_2O bearing phases of accreting planet. The major path for circulating H_2O vapor is represented by the presence of vesicles, their morphology and their location. Complete dehydration of serpentine is achieved by a single shock $\geq$ 60 GPa. This value can be considered as an upper limit. Successive shock and/or porosity will yield to a lower value of P for total water release by shock. Because of the lack of petrographic indicator for shock under 45-60 GPa in experimentally shocked antigorite, it cannot be decided from the present observations of C2 chondrites whether the matrix phases of C2 have been shocked or not. It can only be concluded (1) the minerals constituting the matrix have not experienced shock pressure in excess of 45-60 GPa because phyllosilicate glasses are not observed; (2) shock could be responsible for the localized fractures cutting through the matrix. Study of "veins" in C1 suggests superposed deformation events in the matrix (11). The difference of activation energy for dehydration of shocked and unshocked serpentine is considered as the most promising indicator for relatively weak shock in the matrix of C1-C2. Feasibility of the use of beam damaging under TEM to characterize this difference is currently being tested; (3) at least part of the clast population of C2 chondrites has been shocked. Healing features in clasts are significant of a thermal and possibly hydrothermal event(s). The same event(s) could be responsible for the alteration processes reported in the matrix of C chondrites (11, 17, 18). Some and possibly all

the clasts of investigated C2 chondrites could have experienced a strong reheating event after shock deformation resulting in essentially complete annealing of all olivines and partial recovery of pyroxenes.

Highly vesicular glasses in the recovery experiments are significant of a congruent melting (with exception for H_2O) of serpentine and micas. Such glasses have not been reported in natural material nor in experimental petrology experiments. These glasses are supposedly metastable and are very likely to be strongly vulnerable to alteration and recrystallization processes. It is proposed as a working hypothesis that some (perhaps PCP and glass) if not most of the matrix of C1 and C2 is related to phyllosilicates melts and/or their alteration. The similarities between C2 chondrites and hydrothermally altered terrestrial impact melts are noteworthy: texture, matrix to clast ratio, hiatus of grain size between clast and matrix, variable degree of alteration of the clast (related to shock conditions in each clast), flow like and/or lamination texture, shock and annealing features in the clast. Finally, the constituents of C2 chondrites are probably not primordial material of an accreting planet but already represent material reprocessed since crystallization via shock, thermal and hydrothermal processes. These processes are possibly all related to impact(s).

REFERENCES: (1) Wilkening, L. L., Die Naturwissenschaften 65, p. 73-79, 1978. (2) Barber, D. J., Geochim. Cosmochim. Acta 45, p. 945-970, 1981. (3) Arrhenius G., De B. R., Alven, H., in "The Sea," Goldberg E. D., Ed., Wiley, New York, p. 839-861, 1974. (4) Lange, M. A., Ahrens, T. J., in "Proc. Lunar Planet. Sci. 13," 1982, in press. (5) Benlow, A., Meadow, A. J., Astrophysics and Space Science 46, p. 293-300, 1977. (6) Lange, M. A., Ahrens, T. J., (Abs), Lunar and Planetary Sci. XI, p. 596-598, 1980. (7) Lange, M. A., Ahrens, T. J., Meteoritics, Abstract 45th Ann. Met. Society Meeting, 1982. (8) Lambert, P., Ph.D. Univ. Paris-Orsay, 515 pp, 1977. (9) Lambert, P., Meteoritics 14, p. 466-469, 1979. (10) Lambert, P., Meteoritics, Abstract 45th Ann Met. Society Meeting, 1982. (11) Richardson, S. M., Meteoritics 13, p. 141-159, 1978. (12) Robertson, P. B., Dence, M. R., Vos, M. A., in "Shock Metamorphism of Natural Materials" Ed. by French, B. M., Short, N., p. 433-452, 1968. (13) Engelhardt, W. V., Bertsch, W., Contrib. Mineral Petrol. 20, p. 203-234, 1969. (14) Stöffler, D., Fortschr. Miner. 49, p. 40-113, 1972. (15) Pagel, M., Poty, B., Fortschr. Miner. 52, p. 497-489, 1975. (16) Lambert, P., Contrib. Mineral Petrol. in press, 1982. (17) Bunch, T. E., Chang, S., Geochim. Cosmochim Acta 44, p. 1543-1577, 1980. (18) Mackinnon, I. D. R., Baker, M. B., King, T. V. V., Meteoritics 16, p. 352-353, 1981.

FIGURE 1: Shock-induced water loss in antigorite (A) and brucite (B) as a function of shock pressure in experiments. Numbers on open symbols indicate initial porosities of shocked samples.

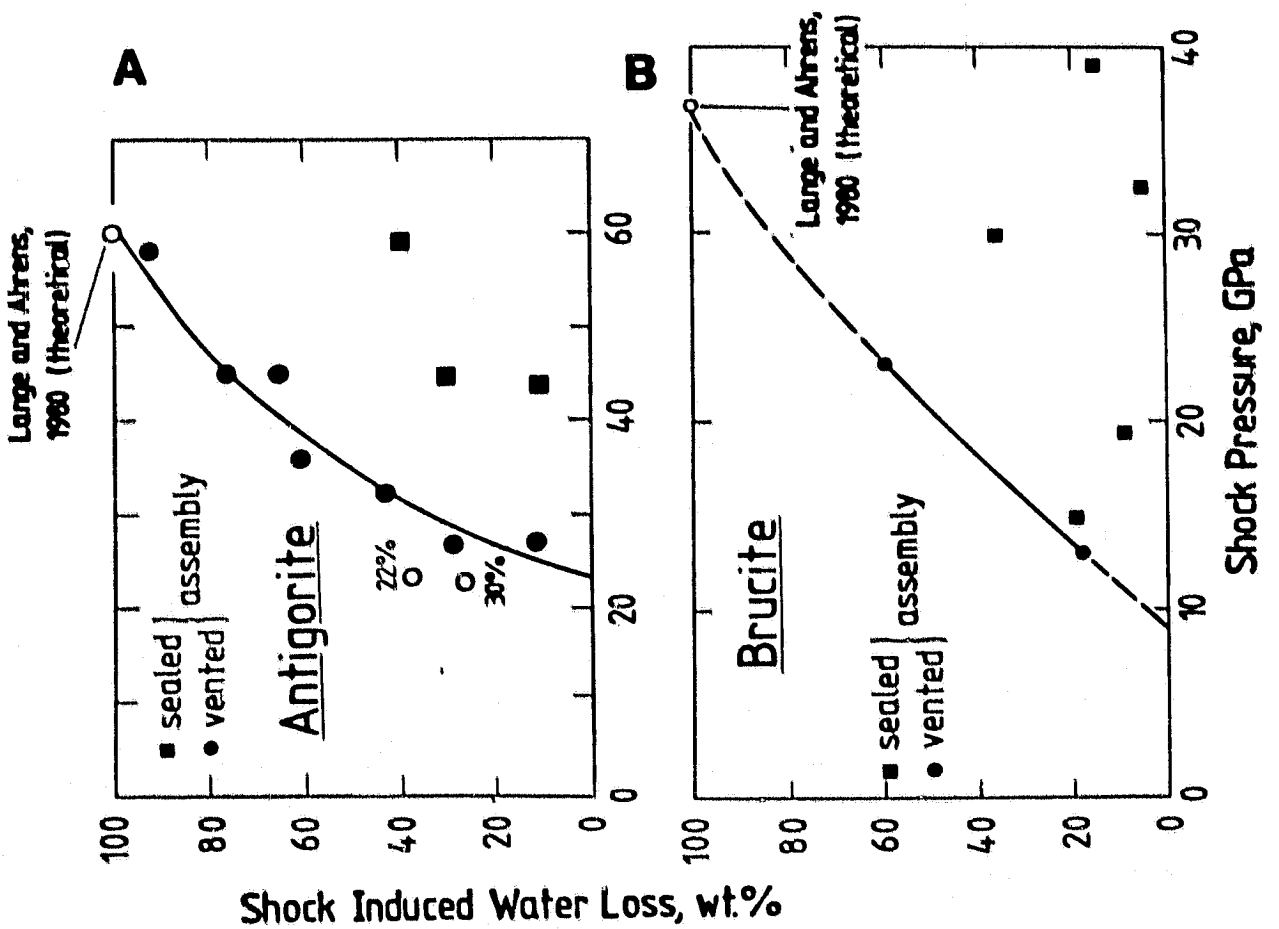

ACCRETION OF WATER BY THE TERRESTRIAL PLANETS

by M. A. Lange and T. J. Ahrens, Seismological Laboratory, 252-21, California Institute of Technology, Pasadena, CA 91125

Introduction

A primary atmosphere probably formed on the terrestrial planets due to the impact-induced release of volatiles in infalling planetesimals during accretion (1, 2, 3). We have previously (3, 4) examined constraints on the production of an impact-generated terrestrial atmosphere by examining the following processes: (i) the supply of volatiles by infalling planetesimals during accretion; (ii) the hydration of non-hydrous silicate minerals (forsterite and enstatite), which will take water from the existing proto-atmosphere; and (iii) the growth of a proto-atmosphere as a result of impact-induced devolatilization of hydrated surface layers of the growing planet. Model calculations led to a number of constraints on the conditions required to generate a primary impact-induced atmosphere. These conditions were met by the accretional environment of Earth and Venus. However, the models are limited by two assumptions. The release of volatiles as a result of shock loading was treated theoretically since data on this process were lacking and we did not model the interaction of metallic iron with water. Ringwood (5) has suggested that this interaction is a primary process by which atmospheric water is dissociated and subsequently lost.

We present new data on the shock-induced dehydration of two hydrous minerals, serpentine ($Mg_3 Si_2 O_5 (OH)_2$) and brucite ($Mg(OH)_2$), which define the amount of dehydration as a function of shock pressure and thus restrain more thoroughly the processes (i) and (iii) of our model calculations. In the present study we also consider reactions between iron and water, which bound the extent of the iron-water interactions during accretion of Earth and Venus.

Shock-Induced Dehydration of Serpentine and Brucite

We carried out shock-recovery experiments on antigorite-serpentine and brucite aimed to determine the amount of shock-induced water loss as a function of shock pressure (6). Thermo-gravimetric analysis of the shocked sample allows determination of its post-shock water content and, by comparison with the initially present water, yields the amount of shock-induced water loss. Figure 1 gives the results of these experiments, which define a single relation between water loss and shock pressure for each mineral. The experimental data agree well with the theoretical predictions for complete water loss (3) and justify the use of these predictions in previous models (3, 4). Shock pressures in serpentine, a likely water bearing phase in terrestrial planetesimals, can be related to impact velocities needed to reach these pressures. Assuming that infall velocities of planetesimals equal the increasing escape velocities of a growing planet, we can relate relative size r/R and relative mass m/M (R, M are final radius and mass of a planet, respectively)to shock pressures in antigorite-serpentine. Given the relations between shock-induced water loss and shock pressure (Fig. 1), we can determine the amount of impact-dehydration in the course of accretion of the terrestrial planets (Fig. 2). Complete water loss in serpentine occurs when Earth and Venus have grown to ~half their radius and have reached ~ 0.1 of their mass. On Mars, complete water loss in serpentine is never achieved during accretion. Thus, generation of an impact-induced atmosphere appears to be possible on Earth and Venus and less likely on Mars.

Lange, M. A. and Ahrens, T. J.

Interaction of Iron and Water During Accretion

Ringwood (5) has proposed that the reaction of iron and enstatite with water upon accretion of chondritic planetesimals provides a dominant sink for atmospheric water. Assuming homogeneous accretion, a nearly chondritic composition may be approximated by the assemblage of 7.7 wt.% anorthite, 22.5 wt.% enstatite, 34.5 wt.% forsterite, 34.4 wt.% iron and ~3 wt.% water throughout accretion. Ringwood implies that reactions between iron and water on the surface of the growing Earth proceeds rapidly such that essentially all the water present is dissociated and the resulting H_2 subsequently escapes. This process would lead to a lack of a sizable terrestrial water reservoir and to the alteration of ~1/3 of the total iron due to the reactions with water. This would result in a post-accretional FeO content of the Earth of ~17 wt.%, if FeO is not a constituent of the Earth's core (7), i.e., well above current estimates for the iron content of the Earth's mantle of ~8 wt.% (8).

We have taken the present FeO content of the mantle as a constraint to the maximum amount of iron which could have participated in a reaction of the type which causes the mantle to become more olivine rich than chondrites:

$$MgSiO_3 + Fe + H_2O \rightarrow 1/2\ Fe_2SiO_4 + 1/2\ Mg_2SiO_4 + H_2\uparrow$$

In order for the Earth to retain its water complement, we conclude that either a sufficient amount of hydrous phases were accreted before the Earth had grown to ~10% of its final mass or that the Earth's water was accreted late in its formation as proposed by Smith (9).

References: (1) Arrhenius G., De B. R., and Alven H. (1974) In The Sea, 839-861, Wiley, N.Y. (2) Benlow A. and Meadows A. (1977) Astrophys. Space Science 46, 293-300. (3) Lange M. A. and Ahrens T. J. (1980) In Lunar and Planetary Science XI, 596-598, Lunar and Planetary Institute, Houston, TX. (4) Lange M. A. and Ahrens T. J. (1982a) Icarus, in press. (5) Ringwood A. E. (1979) Origin of the Earth and Moon, 295 pp., Springer, N.Y. (6) Lange M. A. and Ahrens T. J. (1982b) J. Geophys. Res., in press. (7) Watt J. P. and Ahrens T. J. (1982) J. Geophys. Res. 87, 5631-5644. (8) Wiley P. J. (1971) The Dynamic Earth: Textbook in Geosciences, 416 pp., Wiley, N. Y. (9) Smith J. V. (1977) Proc. Lunar Sci. Conf. 8th, 333-369.

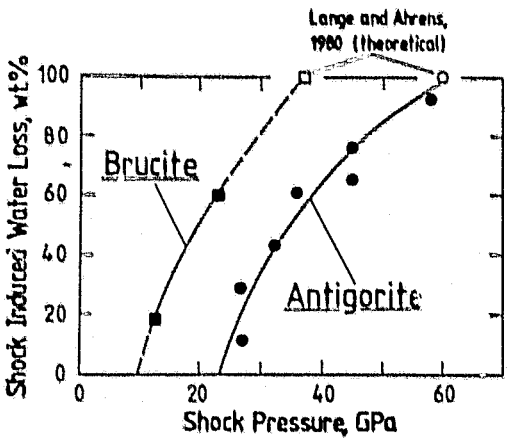

Figure 1: Shock-induced water loss in antigorite and brucite as a function of shock pressure in present experiments.

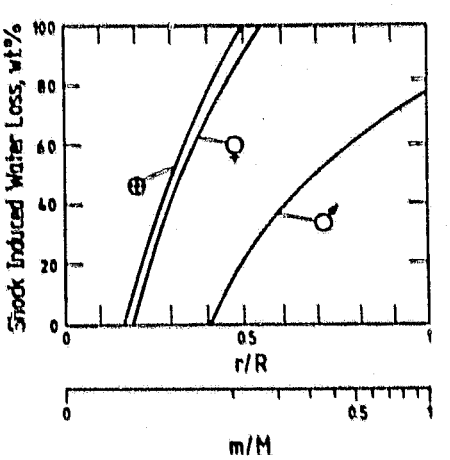

Fig. 2: Shock-induced water loss in antigorite (in wt. % of the total amount of structural water in antigorite) as a function of relative size (r/R) and relative mass (m/M) of the accreting terrestrial planets. Dehydration of antigorite in infalling planetesimals and proto-crusts of growing planets takes place when the threshold pressures as given in Figure 1 are exceeded. This takes place at different stages in the accretional sequence for each planet, the position of which depends on the mean density and the final size of the planetary body as given by the curves for Earth (⊕), Venus (♀), and Mars (♂). Further details, see text.

THE NOBLE GAS RECORD OF THE PRIMITIVE NEBULA AND THE EARTH

O. K. Manuel, Department of Chemistry, University of Missouri-Rolla
Rolla, MO 65401
D. D. Sabu, Box 552, Shreveport, LA 71162

Elemental and isotopic ratios of the noble gases in terrestrial, lunar and meteoritic solids and in planetary atmospheres provide the following information on the initial distribution and evolution of these elements in the solar system:

(i) The primitive nebula contained basically two types of noble gases, type-X and type-Y. The central region contained type-Y noble gases, consisting of isotopically "normal" Ar, Kr and Xe but no He or Ne. The outer region contained type-X noble gases, a mixture of He, Ne and isotopically "strange" Ar, Kr and Xe.

(ii) Type-Y noble gases account for the bulk of Ar, Kr and Xe in chondrites, ureilites, iron meteorites and in the four inner planets. Type-X gases are probably dominant in the outer planets. A carbon-rich phase of chondrites also contains type-X noble gases and this accounts for all of the "planetary" He and Ne in chondrites. Most of the He and Ne in the other types of meteorites and in the four inner planets were implanted on grain surfaces by an early solar wind.

(iii) Differences between the isotopic composition of Xe-X and Xe-Y are large, up to a factor of 2. Smaller differences exist between the isotopic composition of terrestrial and bulk chondritic Xe. However, troilite (FeS) separates of iron and chondritic meteorites contain terrestrial-type Xe.

(iv) The atmospheres of the terrestrial planets were produced by an early exhaustive degassing of specific regions. For Mars, Earth and Venus the degassed portions are about 1-2%, 17% and 100%, respectively. High values of $^{129}Xe/^{132}Xe$ and $^{40}Ar/^{36}Ar$ characterize the early degassed portions of the Earth.

(v) Exhaustive degassing of the upper mantle-plus-crust system produced the Earth's atmosphere during the first 2×10^8 years. The lower mantle has retained most of its initial inventory of Ar, Kr and Xe, and leakage of ^3He from the lower mantle accounts for the frequent occurrence of $^3He/^4He$ ratios that are higher than in air.

(vi) Most of the ^{40}Ar in air was produced in the crust prior to solidification about 2×10^9 years ago. Subduction of sedimentary material into the upper mantle is responsible for observations of atmospheric-like values of $^{40}Ar/^{36}Ar$ and $^{129}Xe/^{132}Xe$ in some samples from the upper mantle.

THE NOBLE GAS RECORD OF THE PRIMITIVE NEBULA AND THE EARTH

O. K. Manuel and D. D. Sabu

Differences in the elemental and isotopic compositions of primitive noble gases (item i) were the basis for our suggestion [1,2] that type-X gases came from the outer part of a supernova where light elements are abundant and that type-Y gases came from the star's interior where fusion reactions had consumed all light elements. The sole occurrence of He and Ne with specific isotopes of Xe is now well established [3,4], and this observation is finally receiving some attention from the astrophysics community [5,6].

The apportionment of type-X and type-Y noble gases (item ii) and the distribution of major elements in the planetary system led us to suggest [2,7] that the Solar System formed from the debris of a single supernova (SN) and that the sun formed by accumulating material back onto the SN core. According to this view, the giant Jovian planets are composed of elements from the outer part of the SN, the cores of the inner planets formed in the central Fe-rich region of the SN debris, and these were veneered with minerals of lighter elements as condensate from other regions fell toward the protosun. There is a growing body of evidence for condensation from chemically and isotopically distinct regions (e.g., ref. 6-10).

The occurrence [11] of terrestrial-type Xe in meteoritic troilite (item iii) provides further evidence that the primitive nebula was chemically and isotopically zoned. The injection of isotopically anomalous elements from a nearby supernova [12] or via refractory grains of interstellar dust [13] fails to explain the absence of He and Ne in type-Y noble gases or the occurrence of terrestrial-type Xe in meteoritic troilite.

Presently available data on noble gases for the terrestrial planets [14] provide additional evidence (item iv) for an undepleted lower mantle [15]. The presence of an iron core within an undepleted mantle [14,15] is compatible with the suggestion that the core was produced by heterogeneous accretion rather than by differentiation of an initially homogeneous planet.

The presence of excess ^{129}Xe in the upper mantle [14] requires an early but short period of degassing (item v). Excess ^{129}Xe occurs in the upper mantle, but primitive ^{3}He leaks from the lower mantle. The isotopic composition of terrestrial He and Ne suggest that these were implanted from the solar wind [14]. Degassing of crustal potassium can account for the bulk of the ^{40}Ar in air (item vi) and the amount of ^{40}Ar corresponds to an average age of 2 Gy for crustal rocks [14].

Our most recent review of noble gas data [16] reaffirms our conclusion that the Solar System condensed from the chemically and isotopically heterogeneous debris of a single supernova.

THE NOBLE GAS RECORD OF THE PRIMITIVE NEBULA AND THE EARTH

O. K. Manuel and D. D. Sabu

REFERENCES

[1] O. K. Manuel, E. W. Hennecke and D. D. Sabu, Nature 240, 99-101 (1972).

[2] O. K. Manuel and D. D. Sabu, Trans. Missouri Acad. Sci. 9, 104-122 (1975).

[3] O. K. Manuel, J. Geophys. Res. 84, 5683-5684 (1979).

[4] O. K. Manuel, Icarus 41, 312-315 (1980).

[5] D. D. Clayton, Proc. Lunar Planet. Sci. Conf. 12, 1781-1802 (1981).

[6] T. Gold, "On the origin of the solar system", George Darwin Lecture of the Royal Astronomical Society, 22 pp (1982).

[7] O. K. Manuel and D. D. Sabu, Science 195, 208-209 (1977).

[8] L. Grossman, Ann. Rev. Earth Planet. Sci. 8, 559-608 (1980).

[9] W. V. Boynton, Meteoritics 14, 347-358 (1979).

[10] F. Begemann, Rep. Prog. Phys. 43, 1309-1356 (1980).

[11] G. Hwaung and O. K. Manuel, Nature 299, 807-810 (1982).

[12] A. G. W. Cameron and J. W. Truran, Icarus 30, 447-461 (1977).

[13] D. D. Clayton, Earth Planet. Sci. Lett. 35, 398-410 (1977).

[14] O. K. Manuel and D. D. Sabu, Geochem. J. 15, 245-267 (1981).

[15] A. R. Basu and M. Tatsumoto, Science 205, 398-401 (1979).

[16] D. D. Sabu and O. K. Manuel, Meteoritics 15, 117-138 (1980).

CARBON IN ROCKS FROM THE EARTH'S MANTLE. E. A. Mathez[1], V. J. Dietrich[2], and A. J. Irving[1] ([1]Dept. of Geological Sciences, Univ. of Washington, Seattle, Wa., 98195; [2]Inst. Krist. und Petrog., ETH-Zürich, CH-8092 Zürich, Switzerland)

The absolute abundances of C and relative amounts of vapor phase C (mainly CO_2) + condensed C and carbonate have been determined in a representative suite of mantle-derived peridotite xenoliths from alkali basalts and kimberlites. Analyses were made of the interior portions of xenoliths least likely to have experienced chemical exchange with host lava. Samples were crushed to coarse (< 1.4 mm) fragments, washed either in H_2O or in cold 1N HCL, and fused with a flux in oxygen. All C was thus liberated as CO_2, which was then determined by titration.

A significant proportion of the C in nearly all samples is removed by acid-washing (fig. 1). This soluble fraction must consist almost entirely of carbonate present on grain boundaries and in through-going microfractures. This material probably originated from a source external to the xenolith, judging from the petrographic relations and the fact that C abundances in the unwashed samples are highly variable compared to those in the acid-washed ones. In some samples, such as those from Kilbourne Hole (KH), contamination by meteoric carbonate is suspected. In samples from areas in which obvious meteoric sources are lacking, the xenolith carbonate probably originated by post-eruption redistribution of C derived originally from the host lava. Garnet lherzolite and eclogite xenoliths from kimberlites are typically carbonate-rich (90 to 1100 ppm carbonate C). In all of these rocks, truly "indigenous" carbonate is probably restricted to the dolomite and magnesite found in polymineralic inclusions in silicates (1,2) or as daughter products in CO_2-rich fluid inclusions (fig. 2) (3). Carbonates in these occurrences are extremely rare, however.

Typical acid-washed Cr-diopside and spinel-bearing (Group 1) lherzolites contain 10-40 ppm total C (fig. 3). Although Group I xenoliths are generally believed to be residues from which a partial melt was extracted (4), some of those from KH possess REE and isotopic characteristics that would permit mid-ocean ridge tholeiites (MORBS) to be generated from them (5, 6). If the mantle below KH is indeed representative of that underlying the ocean basins, then source regions of MORBS contain approximately 20-25 ppm C.

The chemically more evolved Al-augite (Group II) pyroxenites have C abundances that are on average only slightly higher than those in the Group I rocks. This is in particular true for some composite KH xenoliths consisting of deformed lherzolites intruded by pyroxenite dikes (5,7). The close similarity of C abundances in the two rock types of the composite samples is not an expected consequence of the postulated formation of the pyroxenites as crystallization products of alkali basaltic magma. Possibly, the C signature of all KH rocks was imposed later than the initial fabric-forming deformation of the lherzolite and the subsequent igneous activity which produced the pyroxenites.

Within the spinel lherzolite suite, C abundances appear to be related to the degree of LREE enrichment (fig. 4). This is consistent with the generally accepted hypothesis that the incompatible trace element characteristics of these rocks are determined by metasomatic CO_2 or CO_2-H_2O-rich fluids (8). The behavior of C appears to be similar to that of the incompatible trace elements rather than being related to the overall degree of chemical evolution of mantle rocks (as expressed, for example, in their major elements or in absolute REE abundances).

Mathez, E. A., et al.

Many of the Hualalai xenoliths, which probably originated as cumulates in the lower crust or upper mantle (9), contain abundant fluid inclusions and are thus relatively C-rich. In contrast to the typical Groups I and II rocks, their C abundances are related to their modal clinopyroxene contents. This is because fluid inclusions and C-bearing microfractures are much more abundant in pyroxene crystals than in adjacent olivines. This may result from differences in the manner in which the two minerals deform under non-hydrostatic conditions.

Elemental C, possibly mixed with small amounts of organic matter, is observed on grain boundaries, on crack surfaces, and on the walls of fluid inclusions formed by annealing of microcracks (fig. 5) (10). The condensed C is thought to have precipitated by disproportionation of CO according to the reaction $2CO \rightarrow C+CO_2$ at moderate to low pressures ($\lesssim$ 5 kb), possibly during post-eruptive cooling of the xenolith.

Refs: (1) McGetchin, T.R., and Besancon, J.R., 1973, Earth Planet. Sci. Lett., 18, 408-410. (2) Hervig, R.L., and Smith, J.V., 1981, Am. Mineral., 66, 346-349. (3) Rovetta, M.R., and Mathez, E.A., 1982, Abs, 3d Internat. Kimberlite Conf. (4) Frey, F.A., and Green, D.H., 1974, Geochim. Cosmochim. Acta, 38, 1023-1059. (5) Irving, A.J., 1980, Am. J. Sci, 280-A, 389-426. (6) Jagoutz, E., et al., 1980, Nature, 286, 708-710. (7) Bussod, G.Y., 1981, M.S. Thesis, Univ. Washington, Seattle. (8) Wendlandt, R.F., and Harrison, W.J., 1979, Contr. Mineral. Petrol., 69, 409-419. (9) Jackson, E.D., et al., 1981, U.S.G.S. Open File Rept. 81-1031. (10) Mathez, E.A., and Delaney, J.R., 1981, Earth Planet. Sci. Lett., 56, 217-232. (11) Basaltic Volcanism Study Project, 1981, Ch. 1.2.11.

Mathez, E. A., et al.

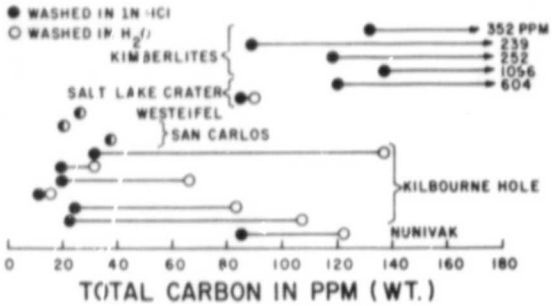

Fig. 1. Comparison of C abundances in water and acid-washed splits of selected xenoliths.

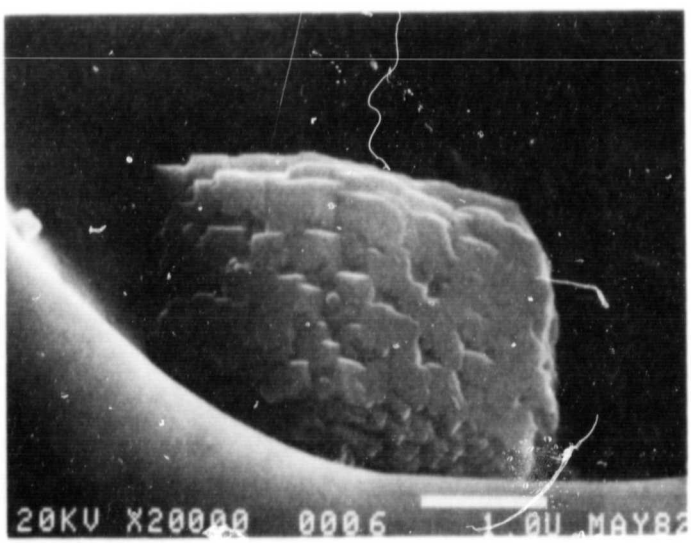

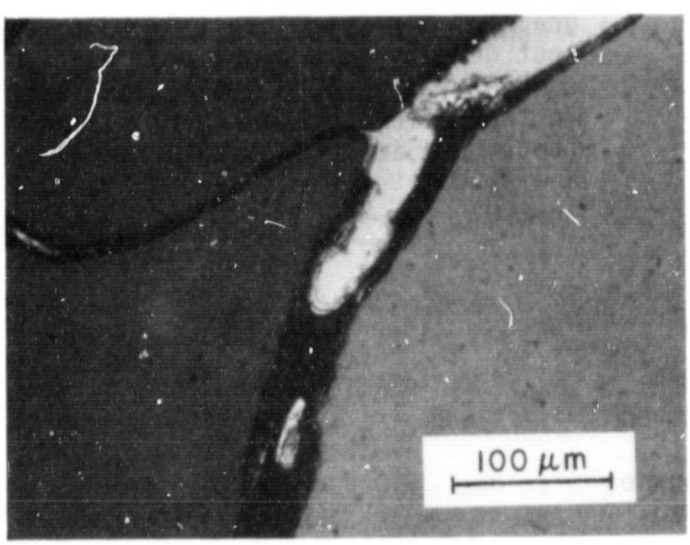

Fig. 2. (Top) A magnesite crystal on the wall of a fluid inclusion in a lherzolite from the Canary Islands. Identification is based on EDS and WDS characteristic x-ray spectra, in which C and Mg are the only major elements. (Bottom) Calcite and basaltic glass (extinct) in a crack between two olivine grains in a lherzolite xenolith from Salt Lake Crater, Hawaii, x-nicols. The glass composition is similar to that of the host basalt. The carbonate was introduced into the xenolith and is not part of its "indigenous" fraction.

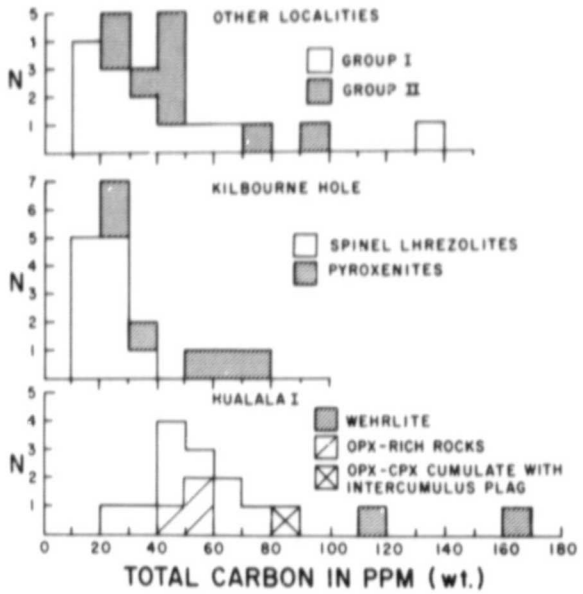

Fig. 3. C abundances for acid-washed xenoliths from alkali basalts. Unlabelled Hualalai samples are dunites.

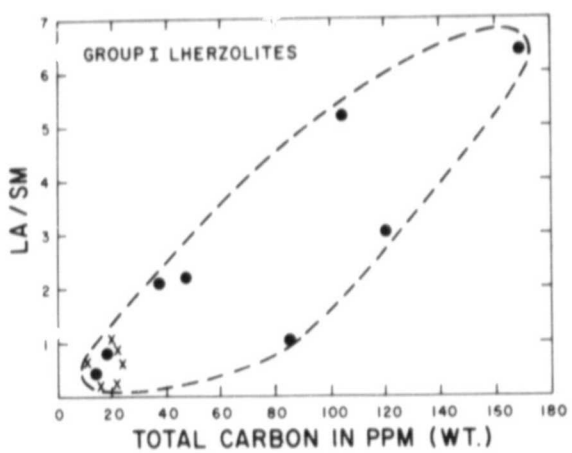

Fig. 4. Variation of C abundances in acid-washed Group I rocks with their degree of LREE enrichment. REE data are from (5) and (11) on unwashed splits. Host rocks include alkali basalts and kimberlites. (X) Kilbourne Hole; (●) other localities.

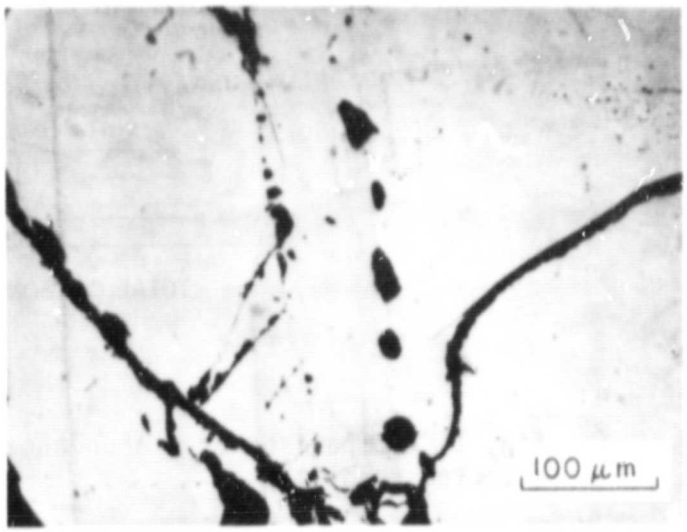

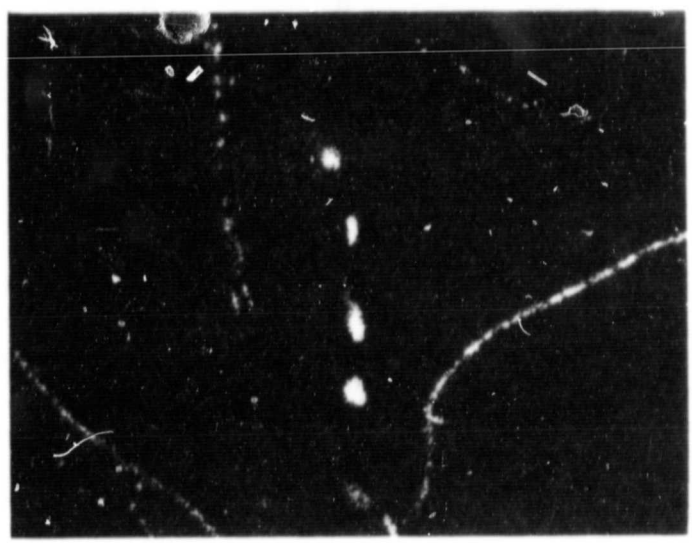

Fig. 5. Beam scanning photomicrograph of C-x-rays (top), in which spot density is proportional to C concentration, over the region shown in the reflected light photomicrograph (bottom). Sample preparation and analytical techniques are summarized in (10).

THE STRUCTURE OF THE PRIMORDIAL ATMOSPHERE AND THE AMOUNT OF GRAINS. H. Mizuno, Carnegie Institution of Washington, Department of Terrestrial Magnetism, 5241 Broad Branch Road, N.W., Washington, D.C. 20015

Two topics on the primordial atmosphere will be presented. First, the structure of the primordial atmosphere of the earth will be described in relation to the dissolution of rare gases. The second topic is an attempt to determine the grain opacity which is an important factor to govern the structure.

According to the theory of planet formation in the solar nebula, the primordial atmosphere forms around the earth and has significant effects on the initial state of the earth both thermally and chemically. One such effect is the dissolution of rare gases contained in the primordial atmosphere into the molten earth material. Numerical calculations show that the amount of dissolved rare gases depends on grain opacity in the atmosphere. The higher grain opacity gives the less amount of dissolved mass (1). The direct cause of this dependence is that the atmospheric pressure is lower in the higher grain opacity model. The computations indicate that the lower atmospheric pressure is a result of the fact that there exists less gaseous mass in the inner region of the atmosphere where the gravity is strong. This is explained in the following way: In general the high grain opacity lengthens the density scale height which gives a measure of density gradient. Moreover the density distribution of the primordial atmosphere is smoothly connected to the density of the solar nebula at the Hill sphere. Therefore, in the higher grain opacity model, we get a lower density or consequently lower gaseous mass in the inner region. Thus the high grain opacity yields the small mass of dissolved rare gases into the molten earth material.

The grain opacity is an important parameter, as seen above, when one considers the structure of the primordial atmosphere. How large is the grain opacity in the primordial atmosphere? What processes determine it? If there are not any sources of grains in the atmosphere, the grain opacity has the value of that for the solar nebula, that is, the order of 10^{-4} cm^2/g. This is because the primordial atmosphere is composed of the nebula gas. However one must not forget a possible source during the accretion phase of the earth. Let us consider a planetesimal which goes into the Hill sphere from near Lagrangian points. The motion of the planetesimal is approximately expressed as Keplerian motion around the earth. The gas drag force acting on the planetesimal gradually changes the orbital elements of the Keplerian motion. For example, the gas drag dissipates the energy and the semi-major axis becomes small. Finally it collides on the earth and contributes to the growth of the earth. While the planetesimal is moving in the primordial atmosphere in this way, it sprinkles its own material as grains into the atmosphere owing to the large relative velocity between the planetesimal and the atmospheric gas and owing to the high gaseous density. This process can be a source of grains during the accretion phase. On the other hand, the grains sprinkled by the planetesimal soon stop the motion relative to the atmospheric

gas because of the strong gas drag, and begin to sink toward the earth owing to gravity. Hence the sedimentation can be a sink of grains in the atmosphere.

These two mechanisms are acting in opposite directions, that is, sprinkle and sedimentation of grains give the actual amount of grains in the primordial atmosphere. The essential parameters to determine the amount are the grain size and the fraction of the energy used to separate grains from the gravity field of planetesimals. Moreover, if a large convective region exists, the convective motion plays a role to retain the grains in the convective region for a longer time compared with the quiet atmosphere. It is found that, in order that the high opacity ($\sim$1 cm^2/g) is realized, the growth time scale during which the grains grow up to about 1 cm in the convective region is necessary to be longer than the time scale of sedimentation for the grains with the size of 1 cm ($\sim 10^{-2}$ yrs).

Reference:

(1) Mizuno, H., Nakazawa, K. and Hayashi, C. (1980) Earth Planet. Sci. Lett. 50, 202-210.

PLANETARY ABUNDANCES OF VOLATILE ELEMENTS: A DATUM FROM THE EARTH'S UPPER MANTLE

John W. Morgan, U.S. Geological Survey, Mail Stop 911, Reston, Virginia 22092

Planetary bulk composition and volatile complement can be examined from two ends of the evolutionary spectrum. The meteorites provide evidence of the material extant in the early history of the solar system and of the compositional range of the accretionary debris that formed the planets. The accessible parts of the planets reveal the end products of accretionary fractionation and of 4.5 b.y. of planetary evolution. Recent measurements of siderophile and volatile trace elements in terrestrial ultramafic xenoliths (1-3) provide a fixed point against which to test model compositions and conversely may be viewed in terms of the general framework of other planets.

Bulk Composition of Terrestrial Planets Estimates of the bulk compositions of the terrestrial planets can be made from the basic premise that planetary matter condensed from a cooling solar gas under equilibrium conditions (4). Three primary components formed sequentially; an early condensate, rich in Ca, Al, and refractories; metallic Ni-Fe; and Mg silicates. Below ~700K, metal and silicates take up volatile elements; metal reacts with H_2S to form a fourth component (FeS) and with H_2O to form FeO that enters the Mg silicates. Evidence from the chondritic meteorites suggests that the three primary components became mutually fractionated. Before or during accretion some material underwent a brief melting episode (analogous to chondrule formation) during which volatile elements were lost from the silicates and FeS was reduced to metal, thus providing two more components; remelted silicate and remelted metal. Finally, the highly volatile elements which were only partially condensed may be assigned to a seventh volatile-rich component. The elements may be divided into major groups on the basis of volatility, and, as members of the groups generally remain in approximately cosmic proportions, one well-chosen indicator element may represent the whole group. Index elements used to calculate bulk compositions of terrestrial planets are summarized in Table 1 (5-7). The index ratios are chosen because these incompatible elements are strongly correlated in crustal processes, but the choices are not unique. In the Earth, for example, Rb/Sr ratios derived from isotopic systematics could equally well be used. Indicator ratios differ significantly between planets. The K/U ratios on Earth and Venus are five or six times lower than they are in chondrites; they are even lower in smaller planets. Indicator ratios show that the more volatile elements are severely depleted on the Moon, Mars (and presumably Mercury). Where Tl abundances have not been measured directly, they may be approximated from data from planetary atmospheres; Ar^{36} on Mars (8), or C and N on Venus.

Table 1 Index elements and ratios for the calculation of terrestrial planet compositions

Component	T_{cond}(K)	Index	Mercury	Venus	Earth	Moon	Mars
Early condensate	>1400	U ppb	11	15	14.3	40	28
Metal	1400-1300	Core %	68	32	32.4	~2	19
Remelted silicate	1400-1300	difference					
Unremelted silicate	1300-600	K/U*	2000	10,000	9440	1900	2200
Volatile-rich material	<600	Tl/U*	0.004	0.27	0.27	0.0023	0.005
Wustite (FeO)	~900-500	$\frac{FeO}{(FeO+MgO)}$‡	0.03	0.07	0.12	0.20	0.23

Values underlined are poorly determined * Weight ratio ‡ Molar ratio

VOLATILE ELEMENTS FROM EARTH'S UPPER MANTLE

Morgan, J.W.

Terrestrial Ultramafic Xenoliths In terrestrial ultramafic xenoliths (garnet lherzolites and spinel lherzolites) the most uniform and well-determined abundances are those of the moderately siderophile elements (2,3): On a C1 chondrite-normalized basis; Ni, 0.20±0.02; Co, 0.22±0.02; Ge, 0.027±0.004. The low Ge/Ni of 0.137 is apparently a reasonable reflection of the volatile depletion of the bulk Earth, and is essentially identical to the terrestrial model value of Ge/Ni = 0.138 (C1 chondrite-normalized) calculated from entirely independent assumptions (6). Absolute abundances of Ni, Co, and Ge in the Earth's mantle are significantly lower than calculated bulk estimates because significant amounts of these elements reside in the Earth's core. It could be argued, therefore, that the low Ge/Ni ratio results from metal-silicate fractionation during core formation. The argument can be countered by estimating the bulk Ni content of the Earth from observed mantle abundances by making the model-dependent, but cosmochemically reasonable assumption that Ge is about as abundant as the moderately volatile lithophile elements. [The assumption seems reasonable because the bulk (total Fe)/Si ratio of the Earth is essentially identical to the cosmic value, indicating little metal-silicate fractionation before or during accretion]. To derive a bulk Ni value from observed mantle xenolith abundances, Ge is scaled to Zn (a well-determined compatible element) to yield Ni = 1.8 percent; a result in excellent agreement with the bulk Earth value of 1.82 percent derived by model calculation (6). Many analysed xenoliths represent depleted mantle which may or may not have been metasomatized. Sheared garnet lherzolite PHN 1611 possibly represents a sample of mantle that is relatively undepleted and not seriously affected by metasomatism. Abundances of lithophile volatile elements in PHN 1611 tend to be higher than those in granular garnet lherzolites and spinel lherzolites, and more uniform when normalized to C1 chondrites. The homologous elements Zn (moderately volatile) and Cd (very volatile) behave as compatible elements in ultramafic xenoliths and observed abundances agree quite well with the model calculations when normalized to C1 chondrites and Si.

	Zn	Cd
Calculated	0.17	0.018
PHN 1611	0.14	0.032

The highly chalcophile elements Se and Te are strongly depleted in mantle xenoliths relative to elements of similar volatility and ~97 percent of the Earth's S, Se, and Te may reside in the outer core. Abundances of Te in the xenoliths are remarkably constant, and closely resemble the C1 chondrite-normalized abundances of such highly siderophile elements as the Pt group metals (PGM). The Te/PGM ratio is 0.8 in PHN 1611 and 0.5 in spinel lherzolites. The PGM's were apparently introduced by a late bombardment of the Earth after core formation (3,9), and if the observed Te/PGM ratio represents that in the bombarding population, then the average composition of the planetesimals may have been as high in volatiles as the C2 chondrites, which contain 8 percent H_2O. The late bombardment could then supply ~135 ppm H_2O, on 15 ppm H. This lower limit may be compared to a calculated value of 33 ppm H (6).

References: (1) Jagoutz, E., Palme, H., Baddenhausen, H., Blum, K., Cendales, M., Dreibus, G., Spettel, B., Lorenz, V., and Wanke, H. (1979) Proc. Lunar Planet. Sci. Conf. 10th, pp. 2031-2051. (2) Morgan, J.W., Wandless, G.A., Petrie, R.K., and Irving, A.J. (1980) Proc. Lunar Planet. Sci. Conf. 11th, pp. 213-233. (3) Morgan, J.W., Wandless, G.A., Petrie, R.K., and Irving, A.J. (1981) Tectonophysics, 75, pp. 47-67. (4) Ganapathy, R., and Anders, E. (1974) Proc. Lunar Planet. Sci. Conf. 5th, pp. 1181-1206. (5) Morgan, J.W., and Anders, E. (1979) Geochim. Cosmochim. Acta, 43, pp. 1601-1610. (6) Morgan, J.W., and Anders, E. (1980) Proc. Natl. Acad. Sci. USA, 77, pp. 6973-6977. (7) Morgan, J.W., Hertogen, J., and Anders, E. (1978) The Moon and Planets, 18, pp. 465-478. (8) Anders, E., and Owen, T. (1977) Science, 198, pp. 453-465. (9) Chou, C.-L. (1978) Proc. Lunar Planet. Sci. Conf. 9th, pp. 219-230.

LOSS OF DEEP MANTLE CARBONIC REDUCED VOLATILES DURING N POLARITY, STORAGE OF THESE VOLATILES DURING R POLARITY; L. O. Nicolaysen*, P. W. Day§, and A. Hoch* *BPI Geophysics, University of the Witwatersrand, Johannesburg, South Africa, 2001 §Jones and Wagener, Inc., Bevan Road, Rivonia, Johannesburg, South Africa, 2128

Recent studies on mantle convection have dealt with the "geochemical model," where a primitive undifferentiated lower mantle and an incompatible element-depleted upper mantle are large-scale reservoirs which convect separately. The model requires an interface boundary layer which acts as a thermal insulator and precludes steady heat transfer between the two reservoirs. Episodic heat transfers (episodic leaks between the two reservoirs) are required. We propose that poroelastic behaviour occurs in the insulating boundary layer, which we equate with the rigid middle mantle or mesosphere of Morgan (1972). Poroelasticity permits a simple physical model for episodic leaks between the two mantle reservoirs. (The model exploits the solution for the stress changes within a porous elastic sphere during consolidation, found by Day, Hoch and Nicolaysen).

The lithostatic load is supported partially by stresses in the crystalline material of the middle mantle carapace, and partially by pressure of its pore fluid. An episodic or "two-stroke" deformation cycle, based on build-up and release of poroelastic stresses, moves fluids and heat through the carapace. Heat is removed from the carapace largely by the transfer of tenuous fluids up the hotspot "pipes", i.e., by mantle degassing.

Poroelastic stresses in the mantle carapace are continuously redistributed to the crystallising core. When the carapace is infiltrated and inflated by elastically stored fluid, the core is subjected to decreasing pressure and it crystallises slag. When the carapace is deflated, by the escape of elastically stored fluid, the core is subjected to increasing pressure and it crystallises Fe metal.

Schloessin and Jacobs (1980) developed a gravity-powered dynamo in which alternating crystallisation of metal (inner-core coundary) and slag (mantle-core boundary) are responsible for the two alternative polarities of the geomagnetic field. Because the episodic mantle degassing system offers a self-consistent physics for modulating the mode of solidification of the core, incorporation of this dynamo theory into our model offers fine opportunities for observational tests.

For a start, this bistable coupled system accounts for the oscillations and rhythms in the magnetic reversal time-scale. Moreover, alternate "strokes", in which the hotspots are either storing or leaking deep carbonic reduced volatiles, should correlate with the alternating reversed and normal polarity of the geomagnetic field: many published papers report observations consistent with this proposition. An accompanying analysis by Nicolaysen shows that polarity-coupled degassing helps us to understand important features of the geological record: (i) Correlation of eras of polarity bias with faunal eras. (ii) Correlation of eras of polarity bias with the phases of the Wilson cycle. (iii) Shock deformation and cratering associated with alkaline ultramafic magma eruptions (e.g., Vredefort structure). (iv) The evidence that the Mesozoic era was terminated by internally-induced cratering event, associated with eruption of alkaline ultramafic magma (like the Vredefort Shock I event). (v) The evidence that tektites formed during violent escape and detonation of deep mantle carbonic reduced volatiles, and are

unrelated to meteorite impact. A short film illustrates the physical principles of this two-stroke model for mantle devolatilisation.

Additional notes on polarity-coupled degassing and the geological record (Nicolaysen)

Hotspots :

The present analysis re-examines several important propositions concerning the global hotspot discharge rate which were made by Vogt (1972). He first suggested that there was episodic but globally synchronous discharge from many hotspots. He noted that hotspot discharge fluctuations appear to mirror the histories of global geological parameters; faunal extinction and global faunal crises were linked to intervals of intense hotspot volcanism, when ecosystems were polluted by trace elements of hotspot origin. Finally, he concluded that there was some connection between intensity of hotspot discharge and reversal frequency in the geomagnetic polarity time-scale. Variations in deep mantle plume discharge rate were believed to correlate with the nature of convection in the core.

Because Vogt was not able to specify the physics responsible for the global correlations in the hotspot discharge rate, his propositions did not receive wide attention. The Biot equation solutions for the deformation of a poroelastic mantle carapace supply a quantitative physics for hotspot discharge, which is episodic, and in which the stresses and strains may be coupled to the stresses and strains of the gravity-powered dynamo. The model is therefore open to many observational tests. Correlations between hotspot opaque mineral oxidation state and remanent polarity, reported by Wilson and Haggerty (1966) and Wilson and Watkins (1967) and others, are accounted for. The model also predicts that certain hotspots should show a Neogene discharge rate which is episodic and broadly correlated with intervals of normal polarity. The observation that much of the upper Cretaceous was a period of sustained kimberlite activity and also widespread hotspot and midplate activity in the Western Equatorial Pacific (on the one hand) and a lengthy interval of quiet normal geomagnetic polarity (on the other) is readily explained.

Sea Level :

The Jurassic and Cretaceous intervals of global sea level elevation correlate strikingly with the longest intervals of quiet normal polarity in the Phanerozoic geomagnetic polarity record. Schlanger, Jenkyns and Premoli-Silva (1981) demonstrated that upper Cretaceous cumulative mid-plate volcanism played a significant part in the elevation of sea level. Many other workers have suggested that increased spreading rates during the upper Cretaceous also contributed to elevation of sea level. In the present physics, a cumulative presentation of the geomagnetic polarity record is linearly related to the cumulative input of deep mantle fluids into the asthenosphere. As predicted by the model, the Phanerozoic cumulative polarity record provides a good indicator of Phanerozoic sea level changes.

Cryptoexplosions :

The sustained effort to understand and incorporate the main features of cryptoexplosions (listed (iii), (iv) and (v) above) arose partly from detailed published sediment core logs, which show that the Ries, Australasian and Ivory Coast cratering events each occurred at a time which was extremely close (within $\sim 10^3$ years) to a switch from reversed polarity to normal polarity. In the new interpretive framework tensile stresses increase in the inflating poroelastic carapace (R polarity), until the instant when it undergoes a puncture. Simultaneously deflation (and a normal polarity interval) begins. Evidently, a tektite-forming blast occurs when such an internally-generated puncture affects a continent-bearing sector of the earth's poroelastic carapace, and a particularly violent outburst of volatile-rich material takes place.

Detailed published geochemical data from sediment cores show that high magnesia microtektites were blasted outwards during the Australasian, Ivory Coast and North American cratering events. Evidently, the puncture referred to above is achieved by a kimberlite-related deep mantle magma. Although crustal ejecta from the ensuing high energy detonation and surficial cratering predominate in the ensuing tektites and microtektites, the high Mg-high Al microtektites are interpreted as contaminated remnants of the kimberlite-related magma. The scenario of Crawford (1979), which emphasizes carbonatite-related 'hypervolcanic' explosions, is in part consistent with the present framework.

REFERENCES

Crawford, A.R. Tektites probably wholly terrestrial and related to continental movement, Geol. Mag., 4, 261-283, 1979.

Day, P.W., Hoch, A. and Nicolaysen, L.O. On the stress changes within a porous elastic sphere during consolidation. Ms. to be submitted for publication.

Morgan, W.J. Plate motions and deep mantle convection, Geol. Soc. Amer. Memoir 132, 7-22, 1972.

Schlanger, S.O., Jenkyns, H.C. and Premoli-Silva, I. Volcanism and vertical tectonics in the Pacific basin related to global Cretaceous transgressions. Earth Planet. Sci. Lett., 52, 435-449, 1981.

Schloessin, H.H. and Jacobs, J.A. Dynamics of a fluid core with inwardgrowing boundaries. Canadian Jour. Earth Sci., 17, 72-89, 1980.

Vogt, P.R. Evidence for global synchronism in mantle plume convection, and possible significance for geology. Nature, 240, 338-342, 1972.

Wilson, R.L. and Haggerty, S.E. Reversals of the earth's magnetic field. Endeavour, v. 25, 104-109, 1966.

Wilson, R.L. and Watkins, N.D. Correlation of petrology and natural magnetic polarity in Columbia Plateau basalts. Geophys. Jour. R. Astr. Soc. 12, 405-424, 1967.

EQUILIBRIUM COMPOSITION OF THE MT. ST. HELENS MAGMATIC VOLATILE PHASE FROM THE PYRRHOTITE-MAGNETITE ASSEMBLAGE

B. E. Nordlie, S. E. Thieben, and D. R. Burggraf,
Department of Earth Sciences, Iowa State University
Ames, Iowa 50011

On October 16, 1980, a pyroclastic eruption initiated the sixth major eruptive phase of Mt. St. Helens since renewed activity began the preceding March. Five eruptive pulses occurred during the period October 16-18; each lasted from five minutes to an hour and produced eruption columns which rose to a maximum height of 14 km (Christiansen and Petersen, 1981, p. 28). The first pulse began at 2158 (PDT) on the evening of the 16th and destroyed the lava dome which had developed since the last significant eruption. A sector to the southwest of the volcano was blanketed with a light ash fall (Sarna-Wojcicki et al., 1981, p. 597). At Cougar, Washington, 15 km SW of the summit, tephra from this pulse accumulated initially as pumice lapilli and later as lithic- and pumice-rich crystal ash.

Approximately 15 minutes after the beginning of the October 16 pyroclastic eruption, dacitic pumice lapilli began to fall on the Cougar area. For several hours after the end of the lapilli fall, lithic- and pumice-rich crystal ash accumulated to a mass concentration of 0.014 g/cm^2, which was collected on a planar aluminum sheet of about 3.3 m^2 area for 9½ hours after the eruption began. Zoned intermediate plagioclase fragments, which are the majority of the crystal fraction, commonly include isolated or concentric micro-laminae of glassy melt inclusions. Of lesser abundance in the crystal fraction are quartz, enstatite, hornblende, magnetite, biotite, ilmenite, and a Fe-Cu sulfide phase.

The coexistence of the sulfide and oxide phases is significant for the present study because the equilibrium formation of these minerals requires known fugacities of S_2 and O_2, respectively, in the magma. This, in turn, sets the fugacities of these species in the volatile phase. The specific values of these fugacities versus temperature are dependent upon the actual compositions of the two mineral phases within their possible solid solution ranges.

SEM and polished section examinations of the sulfides show that the grains are composed of two phases, with the minor phase occurring as exsolution lamellae and overgrowths. Electron microprobe analyses (Fig. 1) give a range of compositions which include a host, end-member pyrrhotite (Po) phase containing about 2% Cu, and a minor, end-member phase with a composition near cubanite. Intermediate compositions in Fig. 1 result from the inability of the microprobe to distinguish the intergrown phases in some areas. The Po end-member composition varies from 37.4 to 38.0 wt. % S.

Magnetite (Mt) grains from the October 16 ash are essentially homogeneous and microprobe analyses give an average composition of 78.88 wt. % FeO and 10.06 Wt. % TiO_2. This composition is nearly identical to the average for magnetites analyzed by Melson and Hopson (1981) for tephra from earlier eruptions of Mt. St. Helens. Based upon this agreement, the O_2 fugacity versus T^{o}C determinations of Melson and Hopson from coexisting magnetites and ilmenites are used in the present study.

Molecular equilibrium calculations in the C-O-H-S gaseous system were carried out using the method of Nordlie (1971). The results were applied to determine: 1) all bulk gas atomic compositions which can be in equilibrium with the Po-Mt assemblage of the October 16 ash; 2) the abundances of the 15-20 most important molecular species and their variations within the field of allowed bulk compositions; 3) the total pressures of the volatile phase throughout the bulk composition field.

A limited range of possible S_2 fugacities is given by the measured range of Po compositions (Toulmin and Barton, 1964). The possible range of O_2 fugacity is taken from Melson and Hopson (1981); near liquidus magmatic temperatures are also given in this paper. The required fugacities of S_2 and O_2 are two constraints which equilibrium volatile molecular compositions must satisfy. Two additional constraints were selected in order to bracket reasonable expected properties of the Mt. St. Helens magmatic volatiles: 1) only those atomic bulk compositions which yield equilibrium contents of 80% H_2O or greater were considered, since no evidence exists for a volatile phase with lower H_2O; 2) atomic C/S was limited to the range 2.0 to 6.0, which brackets measured values in the fume clouds just before and during eruptions (Fig. 2). An initial working temperature of 1050°C was used to anchor computations for all bulk compositions at a common point, so that the changes in molecular compositions with temperature of each bulk composition could be compared. Log O_2 fugacity (oxidation) limits at 1050°C are -9.5 and -10.0. Total pressure was allowed to vary as dictated by those equilibrium compositions which satisfy the above constraints. Calculations were made over the temperature range 1250°C to 650°C to assess higher and lower temperature properties of each bulk composition.

The allowed bulk atomic compositions in equilibrium with the Po-Mt assemblages are severely restricted to a small region of the C-O-H-S tetrahedron. Figure 3 shows two lines which include all of the allowed compositions on the C/S = 6.0 plane of the tetrahedron at the upper and lower limits of possible O_2 fugacities. All possible bulk compositions fall within these two limits. A series of computations for fixed C/S values between C/S = 2.0 and C/S = 6.0 define two planes in the C-O-H-S tetrahedron between which the Mt. St. Helens bulk compositions must lie (Fig. 4).

A projection of either of the planes in Figure 4 to the C-H-S base of the tetrahedron provides a useful display of the total pressures of the volatile phase over the allowed compositional range (Fig. 5). Total pressures are low for most compositions and correspond to Po-Mt formation under conditions just beneath the floor of the St. Helens crater. High pressures are possible only in very sulfur-deficient compositions near the C-H side of the diagram (C-O-H face of the tetrahedron).

Figure 6 shows how O_2 fugacities of equilibrium molecular compositions change with decreasing temperature. Lower temperature O_2 fugacities, for all bulk compositions which satisfy the upper O_2 fugacity limit at 1050°C, fall between the upper two curves. Similarly, O_2 fugacities for all possible bulk compositions satisfying the lower O_2 limit at 1050°C fall between the lower two curves. Thus, the O_2 fugacity changes follow the trend of the data points of Melson and Hopson and, taken together, the equilibrium O_2 fugacities bracket these data. It should be emphasized that the lower temperature fugacity changes shown are independent of the Po-Mt assemblages. The volatile

phases are forced to be in equilibrium with the assemblage at 1050°C, and the curves show how O_2 fugacities change when this requirement is removed and the temperature is decreased. The resulting relationships indicate two viable conclusions: 1) the St. Helens volatile phase buffered the magma and controlled the mineral phase compositions; 2) since the cooling volatiles independently follow the same trends that would be followed if the volatile phase composition were controlled by mineral buffers in the magma, the magma could be the buffering agent, and little or no change of composition of the volatile phase needs to take place to maintain equilibrium. Although the data do not dictate which possibility should be chosen, the extensive degassing that probably occurs at very shallow depths (low total P) could create a large enough volatile volume for the volatile phase to be the buffering agent.

Figure 7 shows changes in S_2 fugacity which correspond to the O_2 fugacity changes of Figure 6. The required S_2 fugacity for the highest temperature Po composition (37.4 wt. %) was used in conjunction with the required lower O_2 fugacity at 1050°C. As an example alternative possibility, an S_2 fugacity 0.5 log units higher was used in conjunction with the upper O_2 fugacity limit. In effect, this maintains S_2/O_2 at the same value for the two O_2 fugacity limiting cases. In either case, the change of S_2 with decreasing temperature is such that it crosses the range of measured Po compositions and shows that the various pyrrhotites in the ash could have formed simultaneously with the range of varying Fe-Ti oxide compositions shown in Figure 6. The alternatives of either the magma or the volatiles acting as the buffering agent also apply to the sulfide phase.

An additional application of Figures 6 and 7 is to consider the two fugacity limits as the effect of different total pressures. The equilibrium S_2 and O_2 fugacities of the lower oxidation limit could be translated to those of the upper oxidation limit by an increase in total pressure of 0.5 log units. Equilibrium proportions of all molecular species would remain the same (assuming ideal gas behavior), although all partial pressures would increase by 0.5 log units. The difference in the two "oxidation" limits can, therefore, be the result of variations in total pressure rather than differences in composition. A variety of paths could be drawn between the limiting curves of Figures 6 and 7 to show a total pressure decrease or increase during cooling and could explain the measured compositional ranges of pyrrhotite and Fe-Ti oxides.

Figures 8 and 9 show the equilibrium molecular compositions of two bulk atomic compositions which are at extreme ends of the allowed composition field. Only the most abundant gas species are shown. H_2O dominates both examples, reflecting the high hydrogen content of all possible compositions (Figs. 3 and 4). SO_2 and H_2S contents vary with both composition and temperature. Bulk compositions with relatively high S and low H have molecular compositions in which SO_2 dominates the sulfur-containing species. Bulk compositions with high H contents (high H_2O) are dominated by H_2S at low temperatures; however, this is reversed at magmatic temperatures where SO_2 is most abundant.

These relationships may explain the differing results obtained in gas collections from Mt. St. Helens. Samples have been analyzed in which either SO_2 or H_2S is the most abundant sulfur gas species. Some researchers have assumed that H_2S is dominant in the magmatic gas on the basis of H_2S dominated gas collections from sources with temperatures near 800°C. Figures 8 and 9

show that such samples have compositions which have "quenched" at sub-magmatic temperatures, and they may give an erroneous indication of magmatic compositions. These samples may all have been dominated by SO_2 when closely associated with the St. Helens magma.

References

Casadevall, T. J., D. A. Johnson, D. M. Harris, W. I. Rose, Jr., L. L. Malinconico, R. E. Stoiber, T. J. Bornhorst, S. N. Williams, Laurel Woodruff, and J. M. Thompson. 1981. SO_2 emission rates at Mount St. Helens, from March 29 through December, 1980. p. 193-200. In Peter W. Lipman and Donal R. Mullineaux (eds.) The eruptions of Mount St. Helens, Washington. USGS Professional Paper 1250.

Harris, D. M., Motoaki Sato, T. J. Casadevall, W. I. Rose, Jr., and T. J. Bornhorst. 1981. Emission rates of CO_2 from plume measurements. p. 201-208. In Peter W. Lipman and Donal R. Mullineaux (eds.) The eruptions of Mount St. Helens, Washington. USGS Professional Paper 1250.

Melson, William G., and Clifford A. Hopson. 1981. Preeruption temperatures and oyxgen fugacities in the 1980 eruptive sequence. p. 641-648. In Peter W. Lipman and Donal R. Mullineaux (eds.) The 1980 eruptions of Mount St. Helens, Washington. USGS Professional Paper 1250.

Nordlie, Bert E. 1971. The composition of the magmatic gas of Kilauea and its behavior in the near surface environment. Amer. Jour. Sci. 271:417-463.

Sarna-Wojcicki, Andrei M., Susan Shipley, Richard B. Waitt, Jr., Daniel Dzurisin, and Spencer H. Wood. 1981. Areal distribution, thickness, mass volume, and grain size of air-fall ash from the six major eruptions of 1980. p. 577-600. In Peter W. Lipman and Donal R. Mullineaux (eds.) The 1980 eruptions of Mount St. Helens, Washington. USGS Professional Paper 1250.

Toulmin, Priestly, III, and Paul B. Barton. 1964. A thermodynamic study of pyrite and pyrrhotite. Geochim. et Cosmochim. Acta 28:641-671.

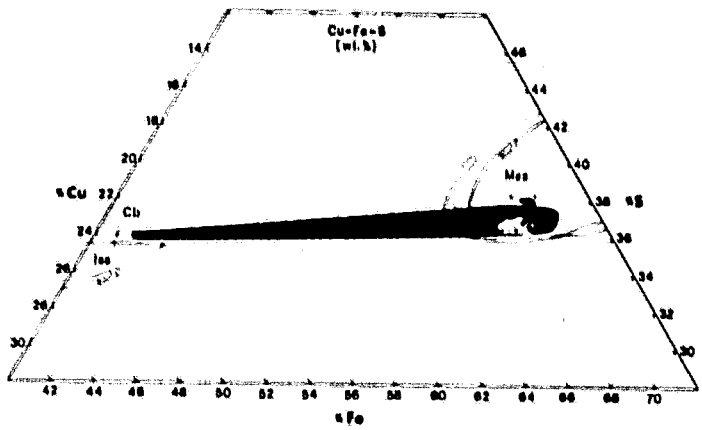

Figure 1. Microprobe analyses of sulfide grains from the October 16 Mt. St. Helens ash. Data points are individual analyses of end-member and mixed phases; shaded fields include all analyses of single mineral grains. End-member Cu-deficient phase is pyrrhotite ranging from 37.4 to 38.0% S and containing approximately 2% Cu. Intermediate solid solution (ISS) and monosulfide solid solution (MSS) fields for temperatures indicated are superimposed on data.

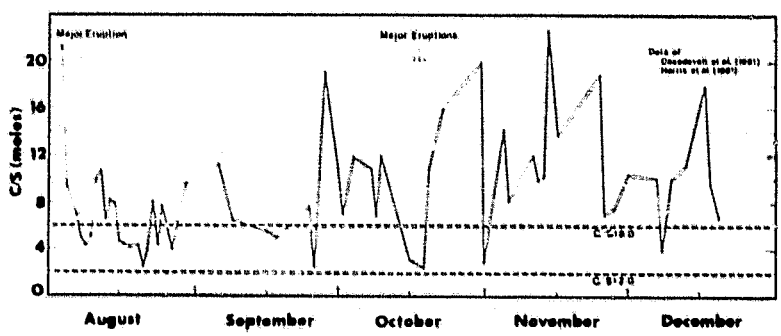

Figure 2. C/S measured in fume clouds above Mt. St. Helens from August to December, 1980. Measurements determined SO_2 and CO_2 in tons/day; the original data are restated as moles and are combined. Dashed lines show C/S compositional limits used in this paper; values were chosen to bracket measured values prior to and during eruptions.

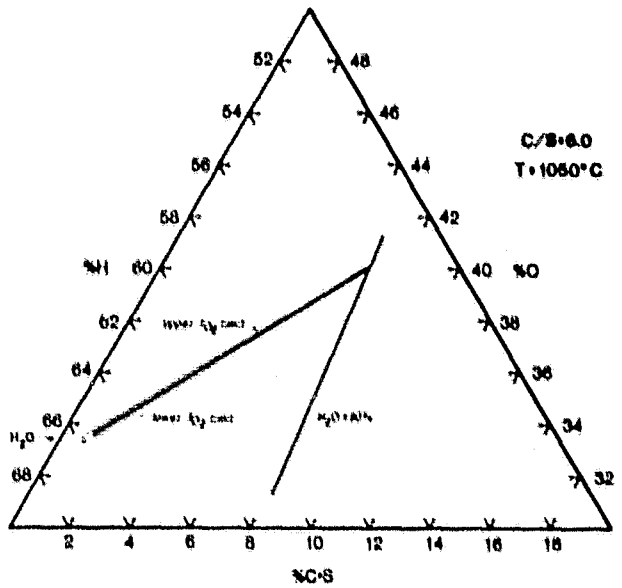

Figure 3. C/S = 6.0 plane of C-O-H-S bulk composition tetrahedron. Lines labeled "upper" and "lower" f_{O_2} limit include all bulk compositions which satisfy compositional and equilibrium constraints at these limits at 1050°C (see text).

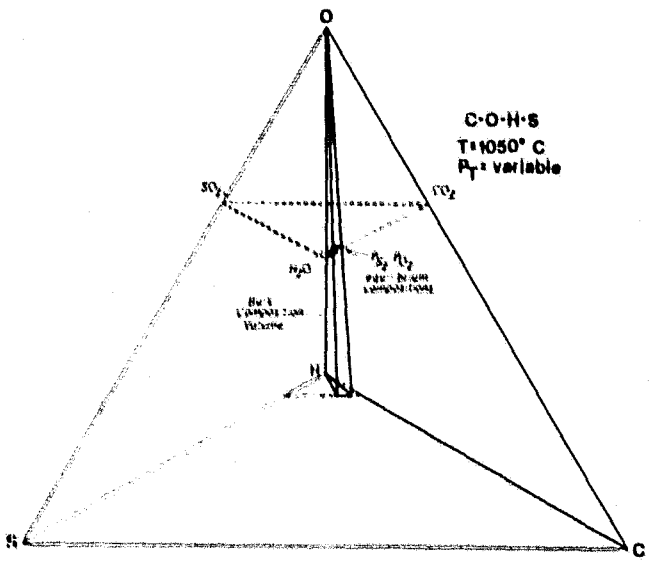

Figure 4. C-O-H-S bulk composition tetrahedron. Heavy lines show composition constraints established for this study (H_2O greater than 80% by volume, C/S = 2.0 to 6.0). Small solid planar volume represents the two planes (upper and lower O_2 fugacity limits) which bracket all possible atomic bulk compositions. The two planes were generated by a series of sections similar to Figure 3. Upper dashed lines show the extension of the solid plane and indicate domination of molecular compositions by oxidized species H_2O, CO_2, SO_2. Dashed lines on tetrahedron base show projection of small solid plane to C-H-S plane.

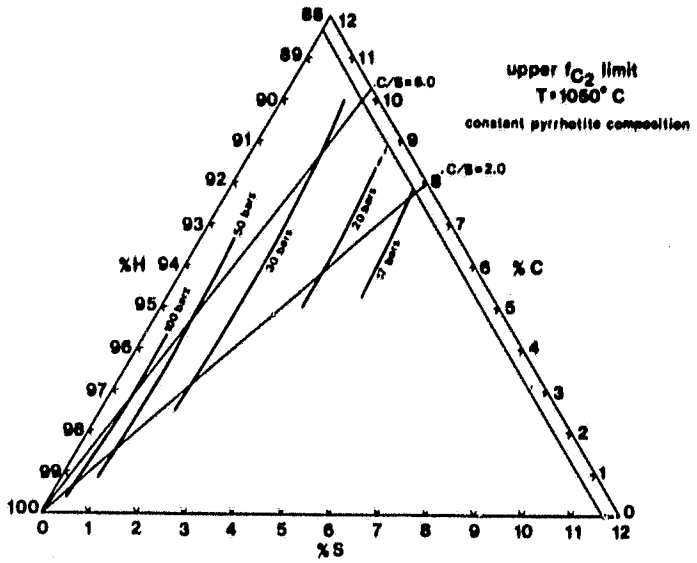

Figure 5. Expanded projection of allowed bulk composition plane of Figure 4 onto C-H-S base of bulk composition tetrahedron. Total volatile phase isobars indicated between C/S = 2.0 and C/S = 6.0 limits. Total pressures are as required for equilibrium molecular compositions which satisfy all required constraints at 1050°C.

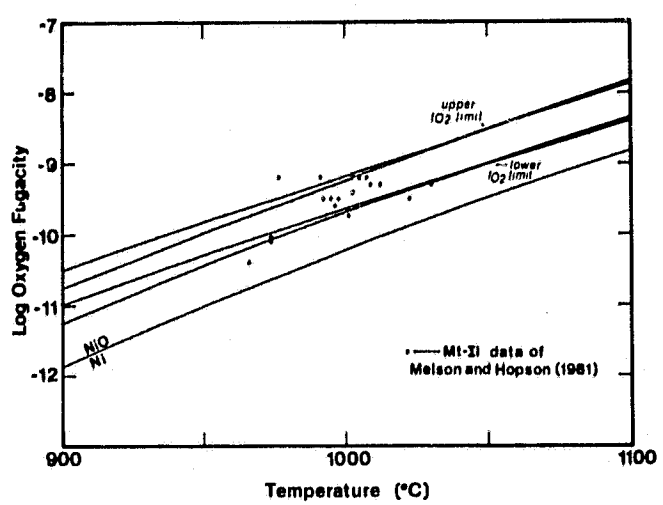

Figure 6. Log oxygen fugacity versus temperature for Mt. St. Helens volatiles. Data points are for coexisting magnetites and ilmenites of pre-October 16 ash deposits. Upper and lower O_2 fugacity limits at 1050°C are required conditions for equilibrium volatile phases; values were selected so that calculated values at lower temperatures bracket Mt-Il data. The two upper limit curves include calculated equilibrium fugacity values of all possible atomic bulk compositions which yield upper limit O_2 fugacity at 1050°C. Two lower limit curves include all values of lower limit bulk compositions.

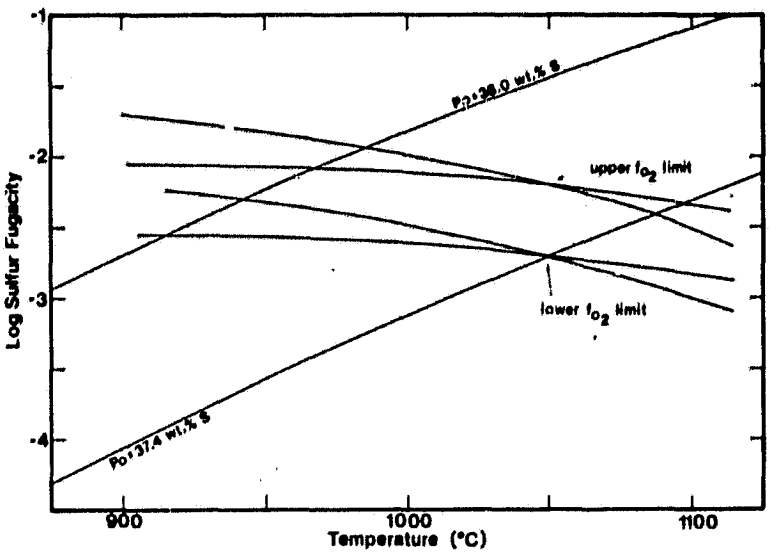

Figure 7. Log sulfur fugacity versus temperature for Mt. St. Helens volatiles. Po = 38.0 and 37.4 curves are S_2 fugacities required at equilibrium with extremes of measured Po compositions (Toulmin and Barton, 1964). Upper and lower O_2 fugacity limit values at 1050°C are established volatile phase requirements which correspond to 1050°C values of Figure 6. Upper and lower limit pairs of curves include lower temperature S_2 fugacities of all possible atomic bulk compositions which satisfy 1050°C requirements (same bulk compositions as those of Fig. 6).

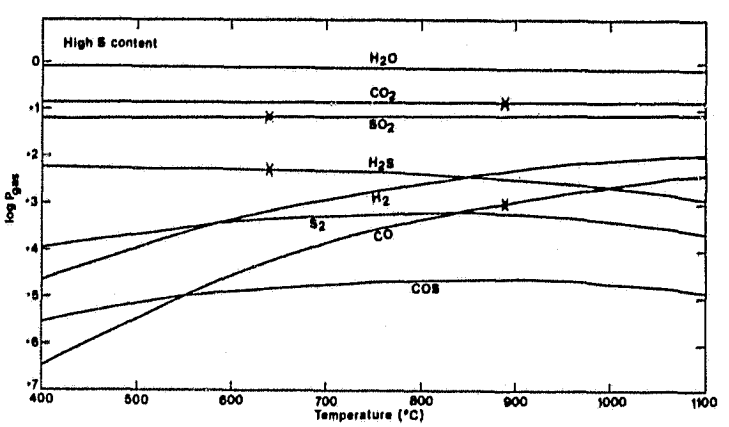

Figure 8. Molecular equilibrium composition of typical volatile phase with relatively low H and high S contents. Total pressure set at one bar for comparison with Figure 9 and analyzed collections. Log gas species pressures given in bars. Marked values (X) show calculated values which equal analyzed amounts in gas collections obtained at one atmosphere total pressure. "X" values indicate temperatures at which gas collection compositions are quenched.

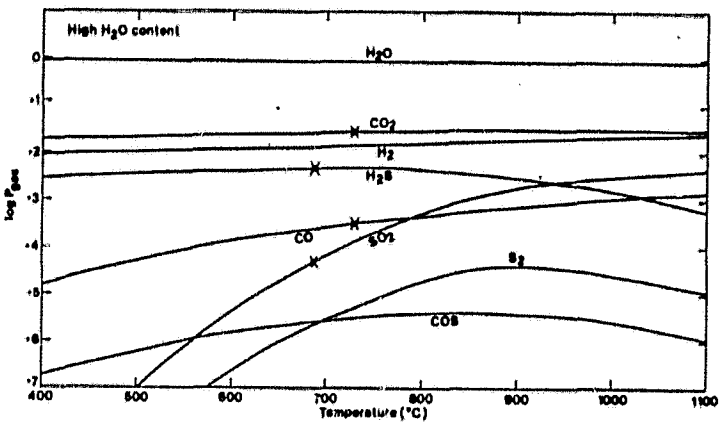

Figure 9. Molecular equilibrium composition of typical volatile phase with relatively high H and low S contents. Total pressure set at one bar for comparison with Figure 8 and analyzed collections. Log gas species pressures given in bars. Marked values (X) show calculated values which equal analyzed amounts in gas collections obtained at one atmosphere total pressure. "X" values indicate temperatures at which gas collection compositions are quenched.

HEAT AND VOLATILE TRANSPORT IN PLANETARY INTERIORS

Richard J. O'Connell, G. A. Houseman, Department of Geological Sciences, Harvard University, Cambridge, Massachusetts.
B. H. Hager, Seismological Laboratory, California Institute of Technology, Pasadena, California

The transport of volatiles within the earth is closely related to heat transport. Thermal convection in the mantle determines large scale mass transport in the interior, and diffusing volatile species should mimic conductive heat losses near the surface. Most of the earth's present day heat loss is associated with magmatic transport of heat at mid-ocean ridges; this process should dominate volatile transport as well. Since the solid state diffusivities of most volatiles are lower than the thermal diffusivity, diffusive transport of volatiles should be slow, and volatile transport should be dominated by motions of volatile rich fluid phases, which may result in a relatively higher effective diffusivity.

Volatile losses at ridges can be modelled from simple numerical convection models that include lithospheric plates. The resulting transport depends on the pattern of thermally driven interior motions that bring material close enough to the surface beneath a ridge for partial melting, and volatile loss, to occur. At the present rates of plate motions, it would require nearly 5Gy to move the entire mantle through a zone 100 km beneath the mid-ocean ridges. This suggests that a substantial fraction of the original volatile inventory has not been lost. If the upper and lower mantle are separated and have non-mixing convection patterns, then volatiles, and heat, must traverse an internal conductive boundary layer to escape the lower mantle. Parameterized convection models can be used to estimate the relation between effective volatile diffusivities and transport across this boundary. Unless volatile diffusivities are comparable to or greater than thermal diffusivities, or direct transport of fluid phases occurs across the boundary, volatile loss from the lower mantle is small.

CURRENT COMPOSITIONS OF PLANETARY ATMOSPHERES. Tobias Owen, Dept. of Earth and Space Sciences, State Univ. of New York, Stony Brook, New York 11794

The successes of Venera 13 and 14 at Venus and Voyagers 1 and 2 at Saturn have led to improved spacecraft data on the composition of the atmospheres of Venus, Saturn, and Titan. These new results can be compared with previous work on these objects and with other studies of Mars and Jupiter. We do not yet have observations from spacecraft of Uranus, Neptune, Pluto, and Triton, but ground-based and near-Earth observations give us a preliminary indication of atmospheric composition for these bodies. It is already clear, for example, that the atmospheres of Uranus and Neptune have different compositions from those of Jupiter and Saturn and from each other. We still need more information about Jupiter and Saturn to see how similar their atmospheres are and how closely their compositions reflect abundances that existed in the primordial solar nebula. Isotopic data will be helpful in this discrimination, but available values for D/H and $^{12}C/^{13}C$ are not completely consistent. Titan offers us an evolved, reducing atmosphere in which some of the chemistry may resemble reactions on the primitive Earth. The origin of that atmosphere seems tied to the formation of clathrate hydrates. This mechanism may also contribute to the incorporation of volatiles in comets, which may in turn provide a pathway for bringing material from the outer solar system to the inner planets.

In the inner solar system, we are seeking to determine just how similar are the volatile inventories of Mars, Venus, and Earth. Rough agreement between the atmospheric C and N on Venus with estimates of outgassed quantities of these elements on Earth has led in the past to the expectation of a common source of volatiles for all the inner planets. Viking studies of the atmosphere of Mars appeared consistent with this hypothesis although this smaller planet has evidently experienced much less outgassing than its larger neighbors. Isotopic information on Martian gases includes a high value of $^{15}N/^{14}N$ attributable to escape of nitrogen and high ^{129}Xe relative to terrestrial xenon. The recent discovery of a non-planetary pattern in the noble gases in the atmosphere of Venus requires a modification of the common reservoir hypothesis. Some local process has evidently enriched the neon and argon in that planet's atmosphere compared with the relative abundances found on Earth and Mars. However, the large amount of primeval water on Venus implied by the huge enrichment of deuterium in the present epoch suggests that distant sources did contribute volatiles to the planet. These sources may again represent the common reservoir, or there may simply be no common reservoir.

A large step toward the resolution of these ambiguities could be made by a coordinated set of atmospheric probes and missions to comets. We may hope for considerable progress from planned investigations of Halley's Comet (Giotto, Vega) and the atmosphere of Jupiter (Galileo).

INTERRELATIONSHIPS OF VOLATILE HISTORY, THERMAL EVOLUTION, AND TECTONICS IN THE TERRESTRIAL PLANETS, R. J. Phillips, Lunar and Planetary Institute, Houston, Texas 77058 and Department of Geological Sciences, Southern Methodist University, Dallas, Texas 75275.

The interrelationships of volatile history, thermal evolution, and tectonics in the terrestrial planets are discussed here under three major themes: viscosity, the effects of volatiles on tectonics (particularly seafloor spreading), and the implications for outgassing of ^{40}Ar for the tectonic evolution of a planet. Below, each of these concepts is discussed.

I. Viscosity

Viscosity has a profound effect on the tectonics of a planet. In turn, given that volatiles might have a strong influence on the activation energy for viscous creep, a potentially strong link exists between volatiles and tectonics.

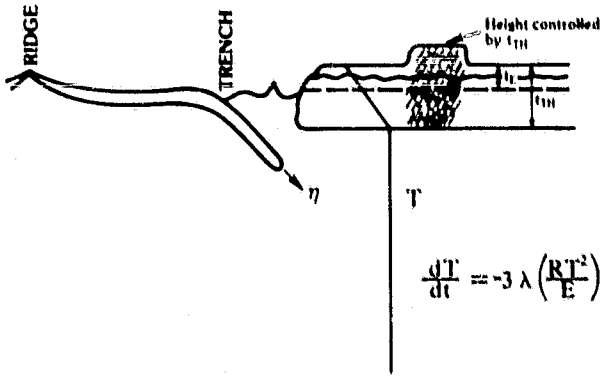

FIGURE 1

Figure 1 illustrates several effects of viscosity on the tectonics of a planet. It is well-known that viscosity modulates convection in the mantles of the terrestrial planets. This is seen in a simple differential equation for the temperature history, T, of a convecting mantle, given by Turcotte and Schubert (1):

$$\frac{dT}{dt} = -3\lambda\left(\frac{RT^2}{E}\right) \qquad (1)$$

where λ is the average decay constant for the mixture of radioactive isotopes in the mantle, R is the universal gas constant, and E is the activation energy for viscous creep. Viscosity also has a direct effect on the descent rate of subducted lithospheric slabs in seafloor spreading.

The thicknesses of the thermal and elastic lithospheres are also controlled by viscosity, and in fact are both defined to be regions of low creep strain. The outer part, the elastic lithosphere, is able to transmit and maintain elastic stress over long intervals of geologic time, while the lower thermal

INTERRELATIONSHIPS OF VOLATILE HISTORY, THERMAL EVOLUTION, AND TECTONICS IN THE TERRESTRIAL PLANETS, R. J. Phillips, Lunar and Planetary Institute, Houston, Texas 77058 and Department of Geological Sciences, Southern Methodist University, Dallas, Texas 75275.

The interrelationships of volatile history, thermal evolution, and tectonics in the terrestrial planets are discussed here under three major themes: viscosity, the effects of volatiles on tectonics (particularly seafloor spreading), and the implications for outgassing of ^{40}Ar for the tectonic evolution of a planet. Below, each of these concepts is discussed.

I. Viscosity

Viscosity has a profound effect on the tectonics of a planet. In turn, given that volatiles might have a strong influence on the activation energy for viscous creep, a potentially strong link exists between volatiles and tectonics.

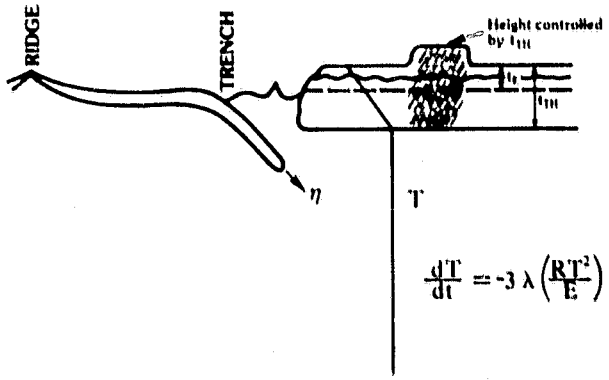

FIGURE 1

Figure 1 illustrates several effects of viscosity on the tectonics of a planet. It is well-known that viscosity modulates convection in the mantles of the terrestrial planets. This is seen in a simple differential equation for the temperature history, T, of a convecting mantle, given by Turcotte and Schubert (1):

$$\frac{dT}{dt} = -3\lambda\left(\frac{RT^2}{E}\right) \qquad (1)$$

where λ is the average decay constant for the mixture of radioactive isotopes in the mantle, R is the universal gas constant, and E is the activation energy for viscous creep. Viscosity also has a direct effect on the descent rate of subducted lithospheric slabs in seafloor spreading.

The thicknesses of the thermal and elastic lithospheres are also controlled by viscosity, and in fact are both defined to be regions of low creep strain. The outer part, the elastic lithosphere, is able to transmit and maintain elastic stress over long intervals of geologic time, while the lower thermal

portion will relax elastic stress but still remains an integral part of the lithosphere. The semi-rigid to rigid behavior of the outer region of the Earth is, of course, an essential feature of plate tectonics.

The height of topography is often controlled by the thickness of the lithosphere, particularly in the absence of significant active horizontal stress, such as that associated with ongoing continental collision. Most topography exists in an isostatic state, for which the maximum shear stress imparted to the interior is directly proportional to topograpic height. The strain rate for viscous creep can be expressed as

$$\dot{\varepsilon} = A\sigma^{n}\exp\ [-(E + pV)/RT] \qquad (2)$$

where A is a constant, σ is deviatoric stress, p is lithostatic pressure, and V is activation volume. One measure of finite strength of a material is that it have low strain rate (high viscosity) over geologic time. Isostatic support implies a state of finite strength (or elastic, not viscous, behavior). Thus equation (2) and the isostatic stress state imply that the strain rate is proportional to the nth power of the topographic height and there is some limiting topographic height such that the strain rate is high enough to preclude isostatic support. There is also some temperature T which leads to a critical strain rate and thus defines a maximum depth of possible isostatic compensation. This depth could encompass the entire thermal or elastic lithosphere or it could be at some intermediate depth such as the crust-mantle boundary. The thermal lithospheric thickness, t_{TH}, may be taken as a convenient measure of maximum topographic height possible under isostatic conditions because the base of this layer is defined to be an isotherm, T_{th} (say 1600 K). Then the temperature gradient, which dictates the temperature and thus the strain rate of any given depth, is to first approximation inversely proportional to lithospheric thickness. With simple Pratt isostasy, lithospheric thickness is a direct measure of maximum topographic height.

It has been suggested (2) that activation energy and volume can be directly related to melting temperature, T_m, via

$$aT_m = (E + pV)/R \qquad (3)$$

where a is a constant. If this relationship is true, then the vast amount of information relating melting temperature of rock to volatile content can be transferred directly to the effects of volatiles on viscosity. It can also easily be shown (1) that the temperature in the convecting mantle is related to the zero-pressure melting temperature, T_{mo}, by

$$\frac{dT}{dt} = -3\lambda\left(\frac{T^2}{aT_{mo}}\right) \qquad (4)$$

A number of authors (e.g., 3,4,5,6,7,8,9,10) have reported creep laws for single crystals and rocks, under both wet and dry conditions. In general, the activation energies are lower in the wet samples, indicating lower viscosities, and casting aspersions of validity on equation (3). The effect of water on lowering the melting points of minerals is clearly an atomic phenomena; i.e., water effects the strength of crystalline bonds. However, Justice et al. (11), on the basis of carefully controlled laboratory experiments, report that: "Single crystal deformation experiments demonstrate no loss in strength for

single crystal olivine specimens deformed in 'wet' relative to 'dry' experimental environments." Chopra and Patterson (12) find that dunites are weaker under wet conditions than dry conditions, but that the weakening effect is mainly in the grain boundaries, and that grain boundary sliding is probably significant under wet conditions. They conclude that: "Water weakening does not appear to be associated with hydrolytic weakening within the olivine grains," in agreement with Justice et al. (11).

Summary

A. Viscosity profoundly affects tectonics.

B. Water weakens rock, lowers viscosity, and thus has a strong effect on tectonics.

C. The water weakening effect appears to be associated with grain boundaries and not with hydrolytic weakening of crystals.

D. The physical basis of relating activation energy to melting temperature deserves careful scrutiny, particularly when volatiles are involved.

E. The tectonics of a planet and the history of water and other volatiles must be considered simultaneously.

II. Effects of Volatiles on Seafloor Spreading

Figure 2 illustrates the effects of volatiles on seafloor spreading and subduction. This is a particularly important issue when considering the case for this type of tectonics on Venus.

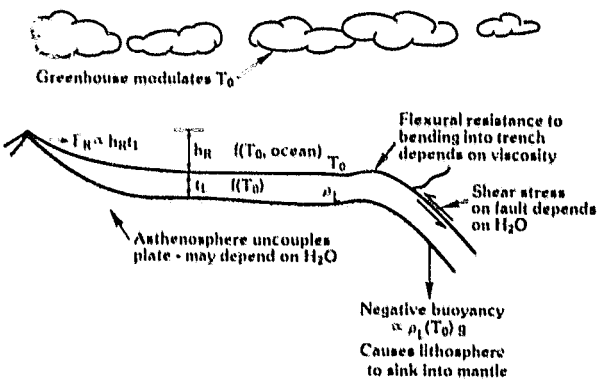

FIGURE 2

An atmospheric greenhouse raises the surface temperature, T_0, of a planet: some several tens of degrees on Earth and several hundred degrees on Venus. The surface temperature, in turn, has a strong effect on the buoyancy of the lithosphere, an important variable in the subduction process. If Venus and

Earth have the same concentration of heat sources, then they will evolve to about the same interior convecting temperature (13) despite the differences in their surface temperature (Venus ∿750 K, Earth ∿273 K). Thus, compared to Earth, the mean temperature of the venusian lithosphere will be greater, and the density less (for equivalent composition), due to the effect of thermal expansion. Since the base of the lithosphere is defined by an isotherm, it is clear that the higher surface temperature of Venus also leads to a thinner lithosphere. The total elevation difference between ridge crest and ocean basin, h_R, depends directly on lithospheric thickness, t_L, and, because of isostatic considerations, also is a function of the density of the overlying material (e.g., ocean). Ridge push forces, F_R, due to the potential energy of the ridge above the basin, may be important to the initiation of subduction. F_R is proportional to the products of h_R and t_L and thus depends on t_L^2 (14). Taking into consideration the thinner lithosphere on Venus implies that F on Venus may be about half that of Earth (15).

Plate motion on Earth appears to be neither helped nor hindered by coupling to the underlying mantle (e.g., 16,17). That is, the lithosphere is likely uncoupled and this takes place at the asthenosphere, which is a low viscosity zone. This may be due to the presence of water, so if water has been outgassed from Venus and not returned (no ocean storage), then Venus may not have an asthenosphere. It is possible, however, that there is a weak viscosity minimum in the upper mantle of the Earth even in the absence of water, due to the behavior of the geotherm (e.g., 1).

Bending of a plate into a trench is resisted by the elastic strength of the lithosphere (i.e., flexure). Since viscosity controls the thickness of the elastic lithosphere, which in turn determines the flexural rigidity, subduction is affected by the volatile influence on viscosity. Subduction at trenches is also resisted by the shear stress on the fault plane at the subduction trench. McKenzie (14) suggests that the low value of shear stress (∿100 bars) on Earth is due to the presence of water and the lack thereof could lead to a different tectonic style on other planets.

Summary

A. The strongest effect of volatiles on the tectonics of a planet may have to do with modulation of the surface temperature by the atmosphere.

B. The direct effect of water on terrestrial seafloor spreading may be important in lithospheric uncoupling, and in flexure and thrust faulting at the trenches.

III. Tectonic Implications of Outgassing

The ^{40}Ar Venus-Earth ratio of ∿ 0.25 has a number of alternate explanations, none provable. Since ^{40}Ar is a decay product of ^{40}K, one explanation is that Venus is depleted in potassium relative to the Earth. This seems unlikely based on both cosmochemical arguments and the Earth-like (crustal) values of the K/U ratio measured by the Venera spacecraft on the surface of Venus. A second explanation is that in order for ^{40}Ar to diffuse effectively out of the interior of a planet, the potassium must be differentiated toward the surface (e.g., in the formation of crust). Thus the ^{40}Ar ratio could imply that Venus is less

differentiated than Earth. A third possibility is that ^{40}Ar transport in the interior of a planet is dominated by solid state diffusion, which is much lower than thermal diffusion. While this certainly may be true for crystal diffusion, diffusivities could be much higher for rocks, where one might expect grain boundary diffusion to dominate. If ^{40}Ar diffusion is much lower than thermal diffusion, then the only way to efficiently remove ^{40}Ar is in a fluid phase (18); e.g., magma transport to the mid-ocean ridges most likely accounts for most of the ^{40}Ar loss from the interior of the Earth. Therefore, a third explanation of the ^{40}Ar ratio is that much less magma has been brought to the surface of Venus compared to Earth. This is consistent with the hot spot tectonic hypothesis for Venus (15,19). Under this scenario, most of the heat delivered to the surface is by localized hot spots; i.e., diffusion across thin thermal boundary layers (with high thermal gradients). The Hawaiian swell is a good example of a terrestrial hot spot, but on Earth most of the heat is delivered by magma at the mid-ocean ridges as part of the seafloor spreading process.

Summary

A. We cannot really decide conclusively between the alternative hypotheses for the Venus-Earth ^{40}Ar ratio of about ~ 0.25.

B. More data would help.

REFERENCES

(1) Turcotte, D. L. and Schubert, G. (1982) Geodynamics, Applications of Continuum Physics to Geologic Problems, John Wiley and Sons.

(2) Weertman, J. (1970) Rev. Geophys. Space Phys., 8, 145-168.

(3) Heard, H. C. and Carter, N. L. (1968) Amer. J. Sci., 266, 1-42.

(4) Carter, N. I and Ave'Lallemant, H. G. (1970) Geol. Soc. Amer. Bull., 81, 2181-2202.

(5) Raleigh, C. B., Kirby, S. H., Carter, N. L. and Ave'Lallemant, H. G. (1971) J. Geophys. Res., 76, 4011-4022.

(6) Post, R. L., Jr. and Griggs, D. T. (1973) Science, 181, 1242-1244.

(7) Kohlstedt, D. L. and Goetze, C. (1974) J. Geophys. Res., 79, 2045-2051.

(8) Carter, N. L. (1976) Rev. Geophys. Space Phys., 14, 301-360.

(9) Parrish, D. K., Krivz, A. and Carter, N. L. (1976) Tectonophysics, 32, 183-207.

(10) Post, R. L. (1977) Tectonophysics, 42, 75-110.

(11) Justice, M. G., Jr., Graham, E. K., Tressler, R. E. and Tsong, I. S. T. (1982) Geophys. Res. Lett., 9, 1005-1008.

(12) Chopra, P. N. and Paterson, M. S. (1981) Tectonophysics, 78, 453-473.

(13) Turcotte, D. L., Cooke, F. A. and Willeman, R. J. (1979) Proc. Lunar Planet. Sci. Conf., Pergamon Press, 2375-2392.

(14) McKenzie, D. P. (1977) in Island Arcs, Deep Sea Trenches and Back-Arc Basins, American Geophysical Union, 57-61.

(15) Phillips, R. J. and Malin, M. C. (1982) in Venus, University of Arizona Press, in press.

(16) Forsyth, D. and Uyeda, S. (1975) Geophys. J. R. Astron. Soc., 43, 163-200.

(17) Carlson, R. L. (1981) Geophys. Res. Lett., 8, 958-961.

(18) O'Connell, R. J. and Hager, B. H. (1983) This volume.

(19) Morgan, P. and Phillips, R. J. (1983) J. Geophys. Res., in press.

THE SEDIMENTARY INVENTORY OF ATMOSPHERIC XENON

F. A. Podosek, T. J. Bernatowicz, M. Honda and F. E. Kramer, McDonnell Center for the Space Sciences, Washington University, St. Louis, MO 63130

Except for gases implanted during direct exposure to the solar wind, trapped primordial noble gases in meteorites occur in a characteristic and well-known elemental abundance pattern designated the "planetary" pattern. The planetary pattern appears in most meteorite classes and characterizes elemental composition across at least 3-4 orders of magnitude variation in total abundance. Several models for the trapping mechanism and the generation of the planetary pattern have been advanced, but none are compelling. Nevertheless, in the absence of contrary evidence it is reasonable to expect that noble gases in the major terrestrial planets, e.g. the earth, should have an origin similar to that for meteorites and should thus occur in planetary proportions.

The meteorite analogy thus suggests that if noble gases in the earth's atmosphere account for most of the total terrestrial inventory, or at least represent an unbiased sample, they too should occur in the relative abundances of the planetary pattern. The gases Ne, Ar, and Kr conform to this expectation quite well, and furthermore their total atmospheric abundances, per unit mass of the earth, fall within the range observed in meteorites. The atmospheric abundance of He is very much lower than extension of the analogy suggests, but this is understandable and does not weaken the analogy because He escapes from the atmosphere on a geologically short time scale. The abundance of Xe in air is also significantly lower, by a factor of about 23, than the analogy suggests, and in this case no straightforward excuse is evident.

A number of views concerning this apparent underabundance of Xe are possible. One is that the analogy with meteorites does not apply, and that the underabundance reflects basically different origins for Xe in the earth and meteorites; this position could also be argued on the basis of prominent isotopic differences between terrestrial and meteoritic Xe which have never been satisfactorily explained. A second is that the atmosphere is not an unbiased sample, and that Xe has been degassed from the solid earth into the atmosphere with a much lower efficiency than have the other gases. Both these views have interesting ramifications, the first for the origin of the earth and the second for its overall chemical evolution.

A third view is that the apparent underabundance is only apparent, i.e. that Xe in planetary proportions was indeed degassed into the atmosphere, but because of its interactions with sediments most of it has not remained in air. The possibility that most of the atmosphere's Xe was subducted in sediments warrants attention, but the usual variant of this "shale hypothesis" is that the apparently missing planetary Xe is still in the generalized atmosphere, but mostly in extant sediments, specifically shales, rather than in air (1,2). This view seems to have been widely adopted as the consensus explanation of the Xe underabundance problem.

The shale hypothesis has been challenged (3-5) on the grounds that neither the previously applied arguments (1,2), nor experimental results subsequently obtained, justify the conclusion that extant shales contain enough Xe to bring the atmospheric inventory up to planetary proportions. The reasoning is straightforward. The <u>average</u> Xe concentration needed for the estimated 10^{24} g of extant shale to account for this much Xe is higher than that found in <u>any</u> sedimentary rock so far. The distribution of available data in fact suggests that the inventory of Xe trapped in sediments is

about an order of magnitude smaller than the air inventory. This assessment is not conclusive since not all potentially important reservoirs or rock types have been surveyed, but the hypothesis that sedimentary rocks account for the missing planetary Xe must be argued in spite of rather than because of available data.

All of the available data are normal trapped gas measurements, and all of them involve days to months of exposure to laboratory vacuum prior to analysis, usually with a day or more at temperatures around 100°C. It could be argued that such analysis grossly underestimates natural gas concentrations because most gas is very "loosely bound" - roughly speaking, merely adsorbed rather than trapped - and is lost during this vacuum exposure.

This possibility may be addressed by consideration of the extent of physical adsorption of Xe or shales. Available data suggest that Xe adsorbed on shales, in equilibrium with modern air, quite possibly makes a bigger contribution to the inventory than Xe trapped in the same shales, perhaps even makes a substantial contribution to the atmospheric inventory, but appears rather unlikely to make a big enough inventory contribution raise atmosphere Xe to the planetary level (5). Another qualification arises, however, in the suggestion (5) that Xe migration in shales might be so slow that laboratory measurements of physical adsorption also greatly underestimate the amount of Xe adsorbed on shales in nature.

These and other ambiquities about how much Xe is actually present in sedimentary rocks in nature can be greatly reduced by a modified experimental procedure now in use in this laboratory. The key step is sealing rock samples in air, with minimal alteration from their natural state, and not breaking the seal until all gas in the sample can be collected for analysis. In our procedure the samples are enclosed in close-fitting Al capsules sealed by pressure on an In gasket. Subsequent mass spectrometer analysis of capsule and contents yields the total gas content of the sample with no intervening loss in the vacuum system and without regard for the physical reasons for the presence of the gas. Preliminary results of such experiment and their relevance to the Xe inventory problem will be presented.

(1) Canalas R.A., Alexander E.C. and Manuel O.K. (1968) J. Geophys. Res. 73, 3331-3334.
(2) Fanale F. P. and Cannon W.A. (1971) Earth Planet.Sci.Lett.II, 362-368.
(3) Bernatowicz T.J. and Podosek F.A. (1978) in Terrestrial Rare Gases (eds. E.C. Alexander and M. Ozima), Tokyo, pp. 99-135.
(4) Podosek F.A., Honda, M. and Ozima M. (1980) Geochim. Cosmochim. Acta 44, 1875-1884.
(5) Podosek F.A., Bernatowicz T.J. and Kramer F.E. (1981) Geochim. Cosmochim. Acta 45, 2401-2415.

NOBLE GASES IN PLANETARY ATMOSPHERES: IMPLICATIONS FOR THE ORIGIN AND EVOLUTION OF ATMOSPHERES. James B. Pollack and David C. Black, Space Science Division, NASA Ames Research Center, Moffett Field, CA 94035

The radiogenic and primordial noble gas content of the atmospheres of Venus, Earth, and Mars are compared with one another and with the noble gas content of other extraterrestrial samples, especially meteorites. The four-fold depletion of ^{40}Ar for Venus relative to the Earth is attributed to the outgassing rates and associated tectonics and volcanic styles for the two planets diverging significantly within the first billion or so years of their history, with the outgassing rate for Venus becoming much less than that for the earth at subsequent times. This early divergence in the tectonic style of the two planets may be due to a corresponding early onset of the runaway greenhouse on Venus. The sixteen-fold depletion of ^{40}Ar for Mars relative to the Earth may be due to a combination of a mild K depletion for Mars, a smaller fraction of its interior being outgassed, and to an early reduction in its outgassing rate. Based on the observed present day flux of ^{3}He from the Earth's interior and the ^{40}Ar content of the atmosphere, we estimate that the current outgassing rate of ^{40}Ar is about 7% of its time averaged value. Venus has lost virtually all of its primordial He and some of its radiogenic He. The escape flux of He may have been quite substantial in Venus' early history, but much diminished at later times, with this time variation being perhaps strongly influenced by massive losses of H_2 resulting from efficient H_2O loss processes.

Key trends in the primordial noble gas content of terrestrial planetary atmospheres include (1) a several orders of magnitude decrease in ^{20}Ne and ^{36}Ar from Venus to Earth to Mars; (2) a nearly constant $^{20}Ne/^{36}Ar$ ratio which is comparable to that found in the more primitive carbonaceous chondrites and which is two orders of magnitude smaller than the solar ratio; (3) a sizable fractionation of Ar, Kr, and Xe from their solar ratios, although the degree of fractionation, especially for $^{36}Ar/^{132}Xe$, seems to decrease systematically from carbonaceous chondrites to Mars to Earth to Venus; (4) and large differences in Ne and Xe isotopic ratios among Venus Earth, meteorites, and the Sun. Explaining trends 2; 2 and 4; and 1 pose the biggest problems for the solar-wind-implementation, primitive atmosphere, and late veneer hypotheses, respectively.

It is suggested that the grain-accretion hypothesis can explain all four trends, although the assumptions needed to achieve this agreement are far from proven. In particular trends 1, 2, 3, 4 are attributed to large pressure but small temperature differences in various regions of the inner solar system at the times of noble gas incorporations by host phases; similar proportions of the host phases that incorporated most of the He and Ne on the one hand (X) and Ar, Kr, and Xe on the other hand (Q); a decrease in the degree of fractionation with increasing noble-gas partial pressure; and the presence of interstellar carriers containing isotopically anomalous noble gases.

Our analysis also suggests that primordial noble gases were incorporated throughout the interior of the outer terrestrial planets, i.e., homogeneous accretion is favored over inhomogeneous accretion. In accord with meteorite data, we propose that carbonaceous materials were key hosts for the primordial noble gases incorporated into planets and that they provided a major source of the planets' CO_2 and N_2.

HELIUM: FURTHER EVIDENCE OF A SIMILAR ORIGIN FOR EARTH AND VENUS

Michael J. Prather, Center for Earth and Planetary Physics, Harvard University, Cambridge, MA 02138

The abundance of noble gases provides clues to the origin and evolution of the terrestrial planets and, in addition, to the interaction of the solid body with the atmosphere through subsequent degassing of volatiles. We focus here on the radiogenic gases ^{40}Ar and ^{4}He. Argon is stored in the atmosphere; whereas escape is important in modifying the atmospheric abundance of helium. The rate for escape of ^{4}He, 10^{6} $cm^{-2}s^{-1}$, is similar for Earth and Venus, indicating like sources of helium from uranium and thorium in their respective crusts. Data on the abundance of crustal potassium and atmospheric ^{40}Ar also point to the basic similarity of the two planets.

NUMERICAL EXPERIMENTS WITH THE GEOCHEMICAL CYCLE FOR CARBON. Steven M. Richardson, Dept. of Earth Sciences, Iowa State University, Ames, IA 50011 and Allen S. Grossman, Lawrence Livermore Laboratory, Livermore, CA 94550

The partitioning of carbon among major geochemical reservoirs is controlled at steady state by a variety of transfer processes, such as volcanism, chemical and mechanical weathering, and limestone deposition. The rates of these processes are, in turn, controlled by parameters such as atmospheric temperature, mean continental elevation, and mean oceanic depth. Over short periods of time, many transfer processes can be described adequately by linear first-order differential equations. Rate constants can often be measured or empirically derived by consideration of the control parameters. Over long periods of time, however, the rates of transfer processes are time-dependent. The carbon cycle attempts to maintain a dynamic steady state during episodic or continual changes in the geological environment. Equations to describe the long-term carbon cycle, therefore, are in general non-linear.

We have begun numerical experiments in which we extend the matrix method of Lasaga (1) to track the evolution of the steady state. For these initial experiments we consider only the simple cycle containing carbon, and do not consider the real world condition in which the carbon cycle is coupled to the cycles for oxygen, sulfur, and other elements, although the matrix method can be modified to treat such non-linear problems. The steady state for a short-term cycle can be described by examining the eigenvectors of a matrix composed of the first-order rate constants. If we treat the long-term cycle as a sum of suitably small short-term steps, between each of which a small change is made in selected rate constants, then the long-term evolution of the cycle can be effectively linearized and followed by this same eigenvector method. Changes of reservoir contents in response to two or more competing time-dependent transfer functions can be examined in this fashion.

1. A.C. Lasaga (1980) The kinetic treatment of geochemical cycles. Geochim. et Cosmochim. Acta: 44, 815-828.

ATMOSPHERIC EVOLUTION DURING ACCRETION: A NUMERICAL MODEL. Steven M. Richardson, Dept. of Earth Sciences, Iowa State Univ.,Ames, IA 50011, Ray T. Reynolds, NASA Ames Research Center, Moffett Field, CA 94035, Allen S. Grossman, Lawrence Livermore Laboratory, Livermore, CA 94550, and James B. Pollack, NASA Ames Research Center, Moffett Field, CA 94035

Models of atmospheric evolution which favor an early "catastrophic" outgassing period are often difficult to reconcile with models of energy and mass deposition during accretion and with models for subsequent differentiation and thermal evolution. For accretionary times on the order of 10^7 to 10^8 years, the energy released by impacts alone is sufficient to cause appreciable planetary melting and may result in a global magma ocean. High planetary temperatures lead to maximum efficiency of outgassing, but may also lead to a dense atmosphere and runaway greenhouse temperatures.

We are investigating model conditions under which a runaway greenhouse can be either avoided or reversed during early outgassing. To do this, we consider a spherically symmetrical planet whose radius increases at a constant rate over a growth period of 5×10^7 years. In a fashion to Kaula (1), we assume that a fraction (μ = 0.1 to 0.5) of the energy of impacting particles is deposited below the surface of the planet, generating a melt zone which we take to be roughly 100 km deep. The melt zone is overlain by a thin, fragmented crustal layer analogous to the solid surface that develops on lava lakes. This crust is subject to puncturing by impacts and to tensional fracturing as the planetary radius increases. It serves as a cap of low thermal conductivity, restricting major heat losses from the melt zone to a small fraction of the total planetary surface. An approximate steady state balance between accretional energy gains and radiative heat losses across the surface is maintained by regulating the fraction of surface area covered by crust.

Heat transfer in the melt zone is convective and can be shown to be rapid relative to the rate of increase of the planetary radius. Hence, the thermal profile of the melt zone with depth is near to the melting curve for the magma. At the base of the melt zone, however, lithostatic pressure is high enough and accretional energy deposition is low enough that magma solidifies at a rate roughly comparable to the planetary growth rate.

Potential atmospheric components are concentrated in the melt zone as the planet grows and are continually expelled from the surface in regions of exposed magma. If the atmosphere is well-mixed and remains nearly in thermal equilibrium with the magma from which it came, then condensation of water vapor is precluded and runaway greenhouse conditions are implied, though they may be reversible once accretion stops and heat losses from the planetary surface become smaller. On the other hand, the atmosphere may attain thermal equilibrium with the larger fraction of the planetary surface, covered by thin crust. If so, condensation of water vapor may be possible, leading to the early formation of an ocean, the removal of carbon dioxide by precipitation of carbonate rocks, and the avoidance of runaway greenhouse conditions.

1. W.M. Kaula (1979) The beginning of Earth's thermal evolution. Proc. Wilson Conf.:"The Continental Crust and Its Mineral Deposits", Toronto.

VOLATILE ELEMENT TRANSPORT FROM THE MANTLE: EXPERIMENTAL SOLUBILITY DATA FOR S- SYSTEM. M.J. Rutherford and M. Carroll, Dept. of Geological Sciences, Brown University, Providence, RI 02912.

INTRODUCTION. The problem to be addressed in this paper is that of the relative degassing rates of C-O-H-S gas species from the mantle of a terrestrial-type planet such as the Earth, Mars or the Moon once the planet has formed a crust. Volatile elements could be brought from the mantle to the surface of such a planet in one of three states. The volatiles could be bound in crystalline phases of sufficiently low S.G. that they would be carried to the surface in magma derived from the mantle. Graphite (1,2) might be such a phase. Alternatively, volatiles could be dissolved in mantle - derived magma and carried to the surface with the magma. The third possibility is that a discreet vapor phase exists in the upper mantle, and this vapor comes up with or through the magma as a separate phase. In order to evaluate these possibilities for any one or a group of volatile elements, it is necessary to know the following: (1) The nature of the volatile-bearing crystalline phases and their stability as a function of depth (P,T,fo_2,etc.)in the mantle (2) The distribution of the volatile element of interest between the crystalline mantle phases and the coexisting magma (if present), and (3) Whether or not a separate vapor phase would coexist with a given mantle assemblage, and if it does, its composition. A considerable body of experimental and observational data has been gathered regarding H_2O and the C-O gases - the purpose of this paper is to present data for the behavior of sulfur.

UPPER MANTLE VOLATILE-BEARING CRYSTALLINE PHASES. On the basis of mantle xenolith studies, it is well established that in addition to the major silicates, the upper mantle of the earth does in places contain phlogopite (3) graphite, diamond (4) and possibly amphibole (3,5,6,7). Apatite is another volatile-bearing phase which may be present, although there is some question whether it is stable at basalt liquidus temperature in the mantle (8). Experimental studies (9,10) verify that these phases are stable under certain upper mantle conditions and also indicate that Ca-Mg carbonates may be present (11), particularly where geothermal gradients are low. Any or all of these phases could be mantle reservoirs of C-O-H gas species. The main reservoir for mantle S appears to be an FeS-rich sulfide based on its common occurrence as inclusions in silicates (12) and diamonds of mantle xenoliths (4).

SOLUBILITY OF C-O-H-S FLUIDS IN BASALTIC MAGMA. Experimental data indicates that the solubility of H_2O in basaltic magmas is large (~10 wt% at 10kb and 1100°C, (13)). As a result there would be no difficulty in transporting H_2O to the surface of a terrestrial-type planet particularly if there were adiabatic mantle upwelling which would tend to carry hydrous phases out of their stability field. The solubility of C-O gas species in basaltic magmas is not likely to be as large as H_2O (14), but it is substantial. Thus there would be no problem bringing C, O or H up from hot mantle regions as species dissolved in basaltic magmas. However, the data on the solubility of S in basaltic magmas indicates that it would be very difficult to transport significant amounts of sulfur from mantle depths in the same way.

Figure 1 shows the data we have collected on S solubility in basaltic magmas under a variety of conditions along with some collected earlier (15) at 1 atm. The new data emphasize the findings of (15) indicating that X_{FeO} and X_{TiO_2} are important variables in determining S solubility. New data for the basalt-C-O-S system (2.7 wt% TiO_2) shows that there is essentially no pressure effect on this solubility up to 5 kb. Wendlandt (16) indicates there is probably a decrease in S-solubility with pressure in this system. Experiments on the same basalt (2.7 wt% TiO_2) in equilibrium with FeS and an

Rutherford, M. J. and Carroll, M.

H-O-S fluid (Fig. 1) show a 30-50% increase in the S-solubility, but the amount of S present is still only 0.20 wt%. On the basis of these data it is concluded that dissolution of S in basaltic melt would not be an effective process for transporting sulfur from the mantle to the surface of terrestrial type planets, particularly in comparison to C,O and H.

DISCUSSION. If S cannot be effectively dissolved in basaltic melts, what is the explanation for the abundance of S gas species in volcanic gases and fluids (17)? Immiscible sulfide is not likely to be carried up in a basaltic melt. Two explanations seem likely. (1) There may actually be a vapor phase in the upper mantle which could come up with or through magmas. The high pressure CO_2-rich fluid inclusions found in many mantle xenoliths (18) often contain sulfide grains (19) indicating the possibility of C-O-S fluid. (2) Possibly S is only slowly removed from upper mantle regions and the sulfur evident in oceanic volcanic regions is largely recycled.

REFERENCES. (1) Sato, M. (1978) LPS, IX, 990-992. (2) Sato, M. (1979) Proc. Lunar Planet. Sci., 10, 311-325. (3) Boettcher, A.L. and O'Neil, J.R. (1980) Am. J. Sci. 280A, 594-621. (4) Gurney, J.J., Harris, J.W. and Rickard, R.S. (1979) Proc. Kimb. Conf., 2,1, 1-15. (5) Wass, S.V. (1979) Proc. Kimb. Conf., 2, 2, 366-374. (6) Irving, A.J. (1980) Am. J. Sci. 280A, 389-427. (7) Wilshire, H.G., Pike, J.E.N., Meyer, C.E. and Schwartzman, E.C. (1980) Am. J. Sci., 280A, 576-594. (8) Green, T.H. (1981) J. Volc. & Geoth. Res., 10, 405-422. (9) Modreski, P.J. and Boettcher, A.L. (1973) Am. J. Sci., 273, 385-414. (10) Eggler, D.H. (1978) Am. J. Sci., 278, 305-343. (11) Wyllie, P.J. (1979) Am. Min., 64, 469-500. (12) DeWaal, S.A. and Calk, L.C. (1975) J. Petrol., 16, 134-154. (13) Hamilton, D.L., Burnham, C.W. and Osborn, E.F. (1964) J. Petrol., 5, 21-39. (14) Eggler, D.H., Mysen, B.O., Hoering, T.C. and Holloway, J.R. (1979) E.P.S.L., 43, 321-330. (15) Haughton, D.R., Roedder, P.L. and Skinner, B.F. (1974) Ec. Geol., 69, 451-467. (16) Wendtlandt, R.F. (1981) GSA Abst. with Prog., 578. (17) Gerlach, T.M. (1980) J. of Volc. and Geoth. Res., 7, 295-317. (18) Roedder, E. (1965) Am. Min., 50, 1746-1782. (19) Moore, J.G., Batchelder, J.N. and Cunninghan, C.G. (1972) J. Volc. Geoth. Res., 2, 301-327.

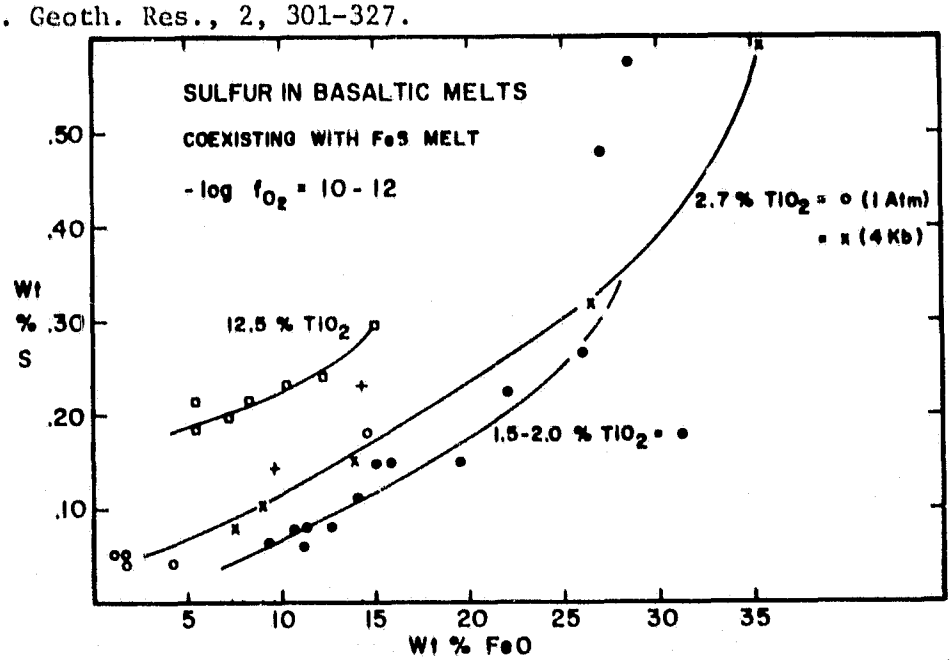

Fig. 1. Sulfur solubility in basalts. Experiments with fluids in the C-O-S system (o,x, ,) and the H-O-S system (+). The ( ) are from (15).

COMPARATIVE Ar-Xe SYSTEMATICS IN THE EARTH'S MANTLE

Ph. Sarda, Th. Staudacher, and C.J. Allègre,
Laboratoire de Géochimie, Institut de Physique du Globe,
4 Place Jussieu - 75230 Paris cedex 05 - France.

Argon and Xenon isotopic ratios and gas concentrations have been measured in glassy rims of dredged MORB samples, using a Reynold-type mass spectrometer, ARESIBO I. Total rock analyses and stepwise heating experiments have been performed.

We have obtained the first systematic ^{129}Xe anomalies even found in MORB with $^{129}Xe/^{130}Xe$ ratios up to 6.94. On the other hand, very high $^{40}Ar/^{36}Ar$ isotopic ratios, as high as 22 000, have been measured. Stepwise heating experiments allow the elimination of atmospheric contamination (by sea water dissolved gases) which drastically lowers the $^{40}Ar/^{36}Ar$ ratio. Our results also indicate large gas losses of the samples during their emplacement.

Such high $^{129}Xe/^{130}Xe$ and $^{40}Ar/^{36}Ar$ ratios are supposed to be close to the isotopic features of the source of MORB. We used them as constraints to study the kinetics of the atmosphere generation, by the way of ^{129}I-^{129}Xe and ^{40}K-^{40}Ar chronometric systems ($T_{1/2}$ = 17 10^6y and 1.25 10^9y respectively).

We describe the outgassing of the Earth's mantle in a two box-model, the only assumption being that the degassing did not grow with time (it is actually not a first order kinetics). The atmosphere is thus found to have a mean age > 4 10^9y using both argon and xenon results. However, a discrepancy does exist between argon and xenon derived mean ages, the latter being slightly older.

Such a difference leads us to consider a back flux of atmospheric gas into the mantle by sediment reinjection. Such reinjection should have a greater influence on the argon isotopic composition of the mantle due to the enormeous difference in the $^{40}Ar/^{36}Ar$ ratios of atmosphere and mantle (295.5 and >22 000 respectively), and thus decrease the argon derived mean age of the atmosphere.

REDOX STATE AND STABLE DISTRIBUTION OF VOLATILES IN PLANETARY INTERIORS

Motoaki Sato, U. S. Geological Survey, Reston, VA 22092

It is a common concept that volatiles were lost in gaseous forms from terrestrial planets because these planets became hot at a certain stage of their evolution while the planets were not massive enough to accquire large enough gravitational fields to hold on to these gases. This may have been true for rare gases and for some elements such as nitrogen, but for many gas-forming elements, the redox state of the interior of a planet palys a a crucial role in determining whether an element exists mainly as gas. For example, carbon forms gases only under oxidizing conditions or H_2-rich reducing conditions; the elemental form is extremely refractory.

The presence of a metallic core is considered to be evidence that the interior of the planet is in a reduced state. One might entertain a notion that perhaps the larger the core is, the more reduced the interior is. Comparison of lunar rocks with terrestrial rocks, however, immediately brings up a seeming paradox. The Moon, which may not even have a core, has rocks ubiquitously containing metallic iron, whereas the Earth, which has a large core, has more oxidized mantle rocks. This paper aims at developing a thermochemical basis to assess the redox state of a planetary interior by extending my preliminary attempt(1) and gaining more insight into the behavior of gas-forming elements at various stages of planetary evolution.

An important factor overlooked by recent investigators of the chmistry of planetary interiors is the effect of gravity on chemical equilibria in the vertical direction. Brewer(2) suggested that the stable distribution of elements in the Earth is such that iron concentrates in the center and oxygen near the surface because of the gravitational contribution to the free energy term. Brewer did not go beyond a statement of the principle, however, because of "mathematical" difficulties for a non-isothermal body. The difficulty can be circumvented as shown below.

For a gas, the gravitational contribution appears as the barometric effect. For an ideal gas at constant temperature and gravitational acceleration, the difference in free energy per mole is given by:

$$G(h_2) - G(h_1) = M g (h_2 - h_1) = - R T \ln (p_2 - p_1) \qquad (1)$$

where g is the gravitational acceleration, M the molecular weight, h_1, h_2, and p_1, p_2 the heights and respective partial pressures, and R the gas constant. For a real gas, fugacities should be used instead of partial pressures. Where T and g vary, as in a planetary atmosphere or within a planetary interior, integration of these parameters as a function of height (=radial diatance) becomes necessary. So we have:

$$\log f_1 - \log f_2 = (M / 2.303 R) \int (g / T)\, dh \qquad (2)$$

The integration term decreases as a homogeneously accreted planet differentiates or its temperature rises; it increases as a planet cools.

The above relation should apply to rare gases as well as to any other gas. As the rare gases cover a wide range of molecular weight, it is evident that rare gases should not degass alike. To escape to the atmosphere, the fugacities of He3, He4, Ne20, Ar36, Kr84 and Xe132 in the present Earth's mantle (100 km, 1500 k) must be 1.25, 1.35, 4.51, 15.1, 562 and $10^{4.32}$ times higher, respectively, than those already in the atmosphere according to equation (2). These numbers suggest that if the material

Sato, M.

that formed the Earth had chondritic abundances, the atmosphere should be increasingly depleted of heavier rare gases. This conclusion is in agreement with the finding of (3).

In the initial stage of homogeneous accretion, the almost ubiquitous presence of metallic iron in chondritic matter presumably buffered the f_{O2} of the accreted matter at values lower than that of the Fe-FeO buffer throughout the interior. The f_{O2} of an oxygen buffer increases as either temperature or pressure increases. As the interior temperature increased due to radioactive decay, adiabatic compression, etc., and as the pressure increased by increased mass and gravity, the f_{O2} of such buffers increased. The fugacity of Fe increases likewise. The increases amounted to orders of magnitude for a planet of the size of the Earth. The increasing fugacities in the interior did not necessarily cause both oxygen and iron to move to the cooler, low-pressure areas, however. Equation (2) stipulates that f_{O2} and f_{Fe} should be orders of magnitude higher in the deep interior to maintain barometric equilibria. Only when corrections for the barometric effect are made, can one judge if the distribution of a volatile element is stable or not. A term called "equigravitational fugacity (symbol $f^{=}$)" to designate the fugacity of a gas which is corrected for the barometric effect has been introduced by (1). The reference datum was chosen at the surface of a planet.

Equigravitational fugacities of O_2, Fe, and gases of the C-S-O system buffered by various mineral assemblages have been computed for homogeneous protoplanets ranging in mass from that of the Moon to that of the Earth for Fe-FeS eutectic and peridotite melting temperature models. These fugacities have been computed also for the differentiated Earth with the known pressure gradient and an estimated temperature gradient.

The results obtained so far suggest the following. (i) In an accreting planetary body of the size of the Moon, very little redox differentiation would occur. Gaseous volatiles would be lost and sulfur would be retained. (ii) In a planetary body of the size of Mars, redox differentiation would be more significant. (iii) By the time a planetary body reaches the size of the Earth, a strong tendency would exist for Fe to concentrate in the core region and oxygen in the upper mantle. The tendency would decrease as the redox differentiation proceeds and the planet becomes stratified in density. (iv) The Earth has not yet reached the most stable state in terms of redox differentiation, because Fe still shows a tendency to move down to the core region from the lower mantle at the expense of FeO. Alternatively, if the Earth was very hot in the early Archean, the stable distribution of iron and oxygen may have once been closely approached and then subsequent cooling may have resulted in increased disequilibria, facilitating production of heat by increased redox differentiation to counter the cooling. (v) Neither sulfur, carbon, nor oxygen is stable in the outer core of the Earth. This suugests that the light element is likely to be silicon.

REFERENCES

(1) Sato M. (1980) In Lunar and Planetary Science XI, p. 974-976, Lunar and Planetary Institute, Houston. (2) Brewer L. (1951) J. Geol., v. 59, p. 490-497. (3) Kaneoka I., Takaoka N., and Aoki K. (1978) In Terrestrial Rare Gases (editors E. C. Alexander and M. Ozima), p. 71-83, Japan Scientific Societies Press, Tokyo.

ARCHAEAN PHOTOAUTOTROPHY: IMPLICATIONS FOR THE EVOLUTION OF THE PHOTOSYNTHETIC OXYGEN BUDGET

M.Schidlowski, Max-Planck-Institut f. Chemie, D-6500 MAINZ, W. Germany

Current photochemical models predict extremely low partial pressures of oxygen in the Earth's prebiological atmosphere, with values ranging between 10^{-8} to 10^{-14} PAL (Present Atmospheric Level) (1, 2). Since the non-biological oxygen source (i.e., photodissociation of water vapor in the upper atmosphere) is basically diffusion-limited (3,4), photochemical oxygen production is determined by the temperature of the tropopause cold trap which prevents any major leakage of water to the stratosphere. Only a substantial rise in the average temperature (195°K over tropical regions) of this cold trap could increase the rate of H_2O transfer to the stratosphere so as to subsequently yield stationary P_{O_2}'s between 10^{-2} to 10^{-3} PAL as a result of inorganic photochemistry (5). Oxygen levels in this range are, accordingly, the maximum expected in any prebiological scenario.

Therefore, it seems reasonable conjecture that oxygen pressures of the order-of-magnitude observed in the Earth's present atmosphere could only be sustained by life processes or, more specifically, by autotrophic carbon fixation. Here, using light as the energy source, carbon dioxide is reduced to the carbohydrate level by water, releasing molecular oxygen as metabolic by-product in a fixed stoichiometric relationship:

$$2\ H_2O^* + CO_2 \xrightarrow{h\nu} CH_2O + H_2O + O_2^* \qquad \Delta G_0' = +470.7\ kJ \qquad (1).$$

Hence, the origin of the Earth's oxygenated atmosphere is ultimately related to the problem of the evolution of photosynthetic carbon fixation. Several lines of evidence suggest that photoautotrophy is a very ancient process. Stromatolite-type biosedimentary structures commonly ascribed to the matting behavior of benthic prokaryotes appear in rocks as old as 3.5 Ga (6, 7, 8), the principal Archaean mat-builders having probably been both phototactic and photoautotrophic (9). Moreover, the content of reduced (organic) carbon in Archaean and Early Proterozoic sediments does not seem to be basically different from that of geologically younger rocks (10). This might indicate that formidable rates of primary production were sustained on the early Earth by prokaryotic microbial ecosystems preceding the advent of eukaryotic life about 1.5 Ga ago (11). Since prokaryotic mat communities have been shown to produce organic matter at rates around 8g C/m^2day approximating those of common agricultural crops (12, 13), these inferences would not seem unreasonable. Additional corroboration for the assumed antiquity of biological carbon fixation comes from the sedimentary carbon isotope record which displays a relatively constant average fractionation between carbonate and organic carbon back to 3.5 Ga ago which time terminates the occurence of unmetamorphosed sediments (14, 15). Since the characteristic enrichment of light carbon (^{12}C) in ancient sedimentary organics is virtually identical with that produced via common photosynthetic pathways (notably the RuBP carboxylase reaction of the Calvin cycle), the sedimentary $\delta^{13}C_{org}$ record bears the isotopic signature of biological carbon fixation (10, 15) which apparently began 3.5 Ga, if not 3.8 Ga, ago (assuming that the isotopic shifts observed in the oldest meta-sedi-

ments from Isua, West-Greenland, are due to metamorphic reequilibration between both sedimentary carbon species (15, 16).

The early appearance of photoautotrophy as both a biochemical process and as a geochemical agent has crucial implications for the oxidation state of the ancient environment. From the point where photosynthesis became quantitatively important on Earth and sizable amounts of organic carbon were incorporated into terrestrial rocks, the corresponding oxidation equivalents were bound to accumulate in the exogenic system in quantities dictated by the stoichiometry of the photosynthesis reaction. The only uncertainty concerns the specific oxidation product released since most forms of bacterial photosynthesis (that substitute different sources of reducing power such as H_2 or H_2S for water) evolve oxidized species other than free oxygen, e.g.,

$$0.5\ H_2S + H_2O + CO_2 \xrightarrow{h\nu} CH_2O + H^+ + 0.5\ SO_4^{2-} \quad \Delta G_0' = +117.2\ kJ \quad (2).$$

Unfortunately, any differentiation between organic carbon derived from splitting water (cf. Eq.1) or from other forms of photosynthesis has to be based on independent evidence which, for the most part, is difficult to obtain. Since there is a broad consensus, however, that the anoxygenic forms of bacterial photosynthesis have preceded the oxygen-releasing reaction (entertained by cyanobacteria and green plants) in the evolution of photoautotrophy, oxidation products other than free oxygen (notably sulfate, see Eq.2) might have been more abundant in the Archaean than during later times. We may, furthermore, assume that prior to the utilization of water as a reductant, proliferation of life was limited by the availability of biologically suitable forms of reducing power. The fact that life ultimately resorted to water-splitting photosynthesis which posed an exorbitant energy requirement (cf. Eq.1) indicates that a formidable evolutionary pressure to find an abundant electron donor had developed (17).

From the stoichiometry of the generalized photosynthetic reaction ($2\ H_2X + CO_2 \xrightarrow{h\nu} CH_2O + H_2O + 2\ X$) we may quantify the accumulation of photosynthetic oxidation products (X) in the exogenic system by tracing the evolution of the organic carbon equivalent back through time. Since almost all organic carbon is stored in the sedimentary shell as kerogen and related substances (the standing surface biomass is smaller by 4 orders of magnitude), we may base our calculation on the quantitative evolution of the sedimentary C_{org}-reservoir. Since organic carbon seems to average about 0.5% already in the oldest sediments and has remained close to this mean during the Earth's later history, only information on the evolution of the total sedimentary mass through time is needed in order to estimate the size of the sedimentary C_{org}-reservoir.

Usually, the evolution of the stationary sedimentary mass is viewed in terms of two limiting scenarios, namely, (i) the constant mass model and (ii) the linear accumulation model both of which are based on respective limits for the terrestrial degassing process (18, 19). Early catastrophic degassing would have yielded a sedimentary mass of the current size within some 10^8 yr after the Earth's formation which was apt to subsequently persist as a quasi-stationary quantity ("constant mass"), while a linear degassing process would have resulted in a linear growth function for the sedimentary shell. With about 0.5% of the sedimentary mass being organic carbon and the linear model defining a lower limit for the buildup of the sedimentary C_{org}-reservoir, the quantity

of sedimentary organics could have been hardly less than 20% of the present one from about 1 Ga after the Earth's formation (i.e. the beginning of the terrestrial degassing process). In accordance with the stoichiometry of the photosynthesis reaction, this percentage must necessarily hold for the corresponding oxidation equivalents released (Fig.1). However, since the growth function most probably followed the "constant mass" or "asymptotic" models (cf. Fig.1), the actual quantities of both C_{org} and photosynthetic oxidation products stored in the exogenic system at that time may well have approached their present reservoirs.

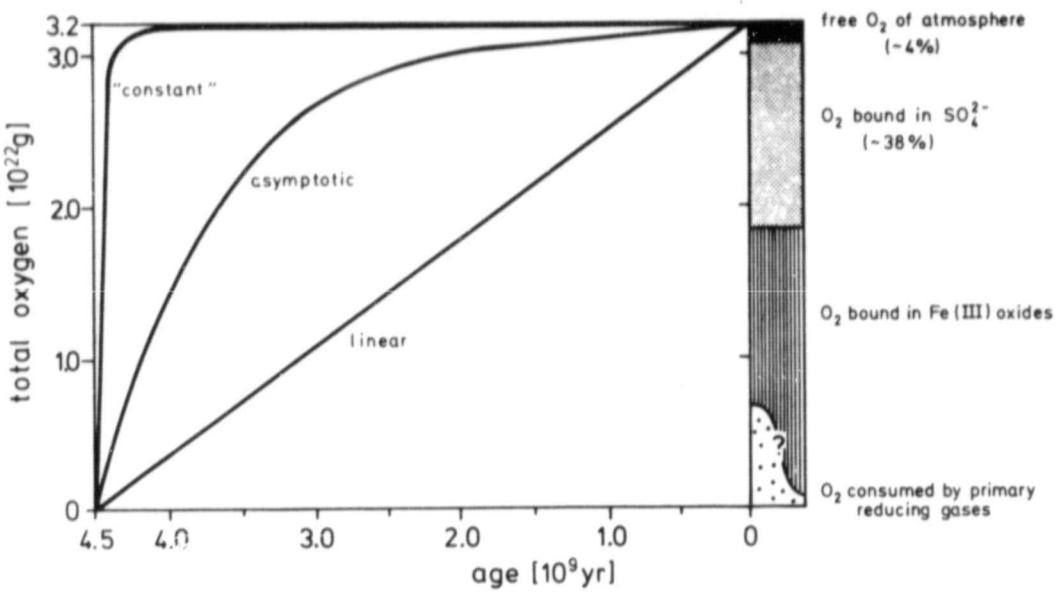

Fig. 1. Evolution of the budget of photosynthetic oxidation equivalents (expressed as O_2) based on different growth models for the sedimentary shell and its organic carbon reservoir (21). The 3.2×10^{22}g oxygen represented by the budget column are the equivalent of 1.2×10^{22}g C_{org} stored in the present sedimentary shell (10, 22). Note that the bulk of photosynthetic O_2 has come to be tied up in sulfate and ferric oxides of the crust and that the 1.2×10^{21}g of free oxygen residing in the atmosphere account for 4% of the total only.

The buildup of a sedimentary C_{org}-reservoir of the order-of-magnitude of the present one is difficult to perceive without photosynthesis resorting to the water-splitting process, simply for want of other forms of biologically suitable reducing power (17, 20). Accordingly, a good case can be made for a very early evolution of O_2-releasing (cyanobacterial) photosynthesis. However, with abundant reducing substances (notably dissolved ferrous iron) present in the ancient environment, the sequestering of major amounts of photosynthetic oxidation equivalents by the atmosphere could be of much younger date. Therefore, the rise of atmospheric oxygen need not necessarily be linked to the onset of photosynthetic O_2-production as such, but was more likely a function of the partitioning of this oxygen among the principal geochemical reservoirs (the style of which could have changed with time). In the present budget, free oxygen makes up the tip of the iceberg with about 4% of the total

(Fig.1) because most O_2-consuming reactions in the exogenic cycle are kinetically retarded. On the other hand, in the absence of a kinetic lag in oxygen consumption, a modern-size reservoir of total photosynthetic oxygen might have been readily coupled with extremely low stationary concentrations in the atmosphere. In general, any accumulation of free oxygen in the atmosphere ultimately results from the failure of thermodynamics to exercise strict control over the redox balance of the atmosphere-ocean-crust system. As is fairly obvious from the nature of free oxygen as a transient and from the comparatively small size of its reservoir, sequestering of photosynthetic oxidation equivalents by the atmosphere represents a minor side show in the global redox cycle, at least from the quantitative point of view.

For a more exhaustive treatment of these questions the reader is referred to a forthcoming publication (21).

References:

(1) Kasting, J.F., Liu, S.C., and Donahue, T.M. (1979) J. Geophys.Res. 84,3097-3107. (2) Kasting, J.F. and Walker, J.C.G. (1981) ibid., 86, 1147-1158. (3) Hunten, D.M. and Strobel, D.F. (1974) J.Atm.Sci.31,305-317. (4) Walker, J.C.G. (1977) Evolution of the Atmosphere (New York: Macmillan). (5) Carver, J.H. (1981) Nature 292,136-138. (6) Lowe, D.R. (1980) ibid. 284,441-443. (7) Walter, M.R., Buick, R., and Dunlop, J.S.R. (1980) ibid 284,443-445. (8) Orpen, J.L. and Wilson, J.F. (1981) ibid. 291,218-220. (9) Walter, M.R.(1983), in: J.W.Schopf (Ed.) The Earth's Earliest Biosphere: Its Origin and Evolution (Princeton, N.J.: Princeton Univ.Press). (10) Schidlowski, M.(1982), in: H.D.Holland and M.Schidlowski (Eds.) Mineral Deposits and the Evolution of the Biosphere, 103-122 (Berlin: Springer). (11) Schopf, J.W. and Oehler, D.Z.(1976) Science 193, 47-49. (12) Cohen, Y., Aizenshtat, Z., Stoler, A., and Jorgensen, B.B. (1980) in: J.B. Ralph, P.A. Trudinger and M.R. Walter (Eds.) Biogeochemistry of Ancient and Modern Environments, 167-172 (Berlin: Springer). (13) Evans, L.T. (1980) ibid. 1-6. (14) Schidlowski, M.(1980), ibid. 47-54. (15) Schidlowski, M., Hayes, J.M., and Kaplan, I.R. (1983) in: J.W.Schopf (Ed.) The Earth's Earliest Biosphere: Its Origin and Evolution (Princeton, N.Y.: Princeton Univ.Press). (16) Schidlowski, M., Appel, P.W.U., Eichmann, R., and Junge, C.E. (1979) Geochim.Cosmochim.Acta 43,189-199. (17) Schidlowski, M. (1978), in: H.Noda (Ed.) Origin of Life, 3-20 (Tokyo: Center Acad.Publ. Japan). (18) Garrels, R.M. and Mackenzie, F.T. (1971) Evolution of Sedimentary Rocks (New York: Norton). (19) Li, Y.H. (1972) Am.J.Sci.272,119-137. (20) Broda, E. (1975) The Evolution of the Bioenergetic Processes (Oxford: Pergamon). (21) Schidlowski, M. (1983) Precambrian Res. (in press). (22) Ronov, A.B. (1980) Osadotchnaya Obolotchka Zemli (Moscow: Izdatel'stvo Nauka).

IMPACT BASINS AND THE STORAGE/RELEASE OF VOLATILES ON MARS.

Peter H. Schultz, Lunar and Planetary Institute, Houston, TX, John L. Rogers, American Petrofina, Houston, TX.

The Hellas and Argyre basins are the most obvious remnants of major impacts on Mars that must have had global effects. In addition, however, there are numerous other subtle impact basins whose deep-seated imprint in the crust not only has controlled volcanic/tectonic processes (in a manner analogous to basins on the Moon) but also influenced the distribution of volatiles. Impact-basin control of volatiles in the crust occurs by three primary mechanisms. First, central basin and concentric ringed depressions provide obvious topographic traps for aeolian or fluvial deposition. Second, the permeable ejecta facies represent significant reservoirs of volatiles whether trapped or precipitated during emplacement. Third, basin-controlled fractures become major release centers of volatile reservoirs during epochs of regional volcanic/tectonic rejuvenation. The expression of these three mechanisms for specific basins provides clues for the timing and style of volatile transfer.

Basin-controlled topographic lows and contained depressions represent one of the most obvious traps for martian volatiles. Recent studies (1) indicate that Mars may not be deficient in the number of major impact basins larger than 300km; rather they were nearly erased by active erosional and depositional processes early in geologic history. Such structures can be recognized on the basis of topography and the concentric arrangement of massifs, fractures, and scarps. Their subtle expression, however, underscores the potential volume of sediments that once were globally redistributed as: aeolian deposits; outwash deposits from fluvial activity indicated by convergent narrow valley networks and channels; widespread fall-out of suspended fine-size ejecta from major impacts accumulated over 4 billion years; and polar deposits trapped during previous locations of the geographic pole (2,3) The last process is active today on the periphery of the present poles where thick layered deposits occur on the floors of large craters.

Ancient martian impact basins typically have a pervasive network of narrow valleys along the outer rings and in the inferred ejecta facies. This selective occurrence, at the very least, indicates the ease with which impact ejecta can be eroded. More importantly the style of erosion suggests a sapping process (4) wherein the highly permeable ejecta facies provide an aquifer during periods of climate change and global heating. In several basins, certain narrow valleys emerge locally along a scarp in a manner consistent with an origin as spring-fed systems. Mapping of characteristic mass-wasting styles of terrains around Isidis, Chryse, Argyre, and Hellas indicates that inferred spring-fed processes are extensive around Isidis and exposed cratered terrains of Chryse but are highly localized around Argyre and Hellas. Although models can be envisioned where a vast aquifer localized volatiles within ejecta deposits well after emplacement, a more direct mechanism simply buries or mixes pre-existing volatile traps, e.g., polar deposits, with basin ejecta early in martian history. The formation of the basin and the passage of ejecta through the martian atmosphere could have had a direct effect on the early climate and the precipitation of certain volatile fractions, such as water. Considerations of more modest-size impacts on the Earth (5) suggest that the re-entry of high-speed ejecta heat the atmosphere and micron-size ablation/spallation products could form important nucleation centers.

Impact basins subsequently have played an important but largely unappreciated role in the release of volatile reservoirs. A recent study indicates that nearly all major outflow channels originate along a basin ring (1). Such occurrences are interpreted as basin-trapped ices that have been hydrothermally

melted along ring fractures during a period of basin-controlled intrusive activity. On the Moon, analogous volcanism resulted in eruptions of basalt and the formation of sinuous rilles. On Mars, volatiles previously trapped in topographic lows were melted episodically and their release produced the major outflow channels. One of the largest systems is related to the Chryse Basin.

1. Schultz, P.H., Schultz, R.A. and Rogers, J.L. (1982) J. Geophys. Res. (in press).
2. Schultz, P.H. and Lutz-Garihan, A.B. (1981), in Papers Presented to the Third International Colloquium on Mars, pp. 229-231.
3. Schultz, P.H. and Lutz-Garihan, A.B. (1982) J. Geophys. Res. (in press).
4. Pieri, D.C. (1980) Science, 210, p. 895-897.
5. Schultz, P.H. and Gault, D.E. (1982) Proceedings of the Conference on Large-body Impacts on the Earth, GSA Special Paper (in press).

MEANDER RELICS: DIRECT EVIDENCE OF EXTENSIVE FLOODING ON MARS

David H. Scott, U.S. Geological Survey, 2255 N. Gemini Dr., Flagstaff, AZ 86001

Introduction

Many morphologic features whose formation is commonly associated with running water also can be duplicated by other processes. On Mars this ambiguity has caused some controversy over the formation of channels (1). Although most planetary investigators now agree on the fluvial origin of the larger channels, there is less evidence and agreement on the extent of floodwaters into the plains beyond the immediate vicinity of channel mouths. Previous studies (2) indicated that alluvial channels within the Chryse basin (lat 20° N., long 40° W.) extended farther into the northern plains than had been mapped. This work was based primarily on the recognition of scour and depositional features commonly associated with the rapid and turbulent flow of water; their identification did not extend much beyond lat 30° N. Additional detailed geologic mapping has revealed new evidence for the past occurrence of running water in the northern plains of Mars.

Morphologic Characteristics and Occurrence

One characteristic that is probably unique to formation by running water is the meander pattern developed along the courses of mature streams and rivers. As rivers swing from side to side in flowing across their flood plains, sinuous channels are formed that gradually migrate downstream as bends in their channels are eroded. Cutoffs are formed where sustained erosion or floodwaters create shorter courses across meander loops. Eventually a pattern of abandoned meanders is marked by scroll-like scars and oxbows on the flood plain. The wavelength of the meander bends become adjusted to the width of the channel and does not increase beyond a limit of about 10 times the width of the river as indicated by the relation: $\lambda = 6.6\ W^{1.1}$ where λ and W are the respective wavelength and width of the stream (3). As a result of this dependence of channel wavelength to width, a freely meandering river flows in a meander belt that is usually about 15 to 18 times its bank-full width (4).

Relict crescentic depressions that are nearly identical both in shape and size to meander patterns of terrestrial streams occur in Chryse Planitia (Fig. 1). These postulated meander scars have widths of about 2-3 km and wavelengths estimated to be approximately 10-20 km. They are especially well developed along the lower course of Ares Vallis, where they are confined within the sculptured banks of the main channel that is about 60 km across. However, the decreasing relief downstream of the channel walls as the meander remnants become more conspicuous suggests that slope gradients had decreased sufficiently to allow a less turbulent type of discharge as floodwaters spread out over the plains. In places, these presumed meander loops appear to terminate near the valley walls, where they may have been covered by slump material or debris flows. In other places within the main channel enclosing the meander belt, streamlined bars partly overlie the loops suggesting that intermittent flooding probably occurred.

Scott, David H.

Elsewhere within the Chryse-Acidalia Planitia region, meander remnants have been buried more completely and do not show such well-developed and integrated forms (Fig. 2). They generally can be recognized, however, by a narrow near-central ridge within the channel troughs, well shown in Figure 1. The origin of these medial ridges is uncertain; they may represent coalesced point bars along the inside bends of meander channels or elongate sandbanks down the middle of the channels, where there is less bottom turbulence. Similar appearing ridges occur in other martian river channels near Deuteronilus Mensae (Fig. 3, lat 35° N., long 340° W.) and in Ma'adim Vallis (Fig. 4, lat -25° S., long 185° W.). On terrestrial flood plains, scroll-like patterns of ridges form where shifting of meander flow channels has occurred.

It may also be that the channel ridges formed in a periglacial environment. Subsurface pore water migrates and accumulates mostly toward the lower-central part of an abandoned river channel. With decreasing temperatures after a warm period that induced flooding, encroaching permafrost would further concentrate the remaining pore water toward the channel center (Fig. 5). Eventual freezing and expansion of the water would create an ice-cored ridge along the valley floor beneath a cover of alluvium. Highly elongate pingos occur in valley-floor sediments on Prince Patrick Island, Northwest Territories, Canada, where they may be related to freeze-thaw processes associated with invasion and retreat of the sea along low-lying inlets (5).

Whatever the origin of the martian ridges, they appear to be diagnostic of meander channels in this region and thus afford a means of identifying fluvial channels from troughs created by tectonic and other processes. Their recognition as far as lat 45° N. in Acidalia Planitia suggests that water flooding was pervasive in the northern plains.

Another occurrence of meander-like patterns is in the southeast part of the Cebrenia quadrangle (Fig. 6) at about the same latitude as those in Acidalia Planitia. They are not associated with any recognizable major outflow channel as are those in the Chryse area, nor are medial ridges common or prominent. Some vague, low-relief, north-trending valley-like features lie to the south of this sinuous trough complex. They appear to be deeply buried by younger deposits of volcanic or eolian materials and their nature or connection with the possible meander channels cannot be established. Here, as in the Acidalia Planitia region of the northern plains (Fig. 2), radar profiles might well reveal buried valleys and stream patterns as they have done beneath the sand sheet of the Eastern Sahara desert (6).

In the Ismenius Lacus quadrangle and to the north and northeast of the large (250 km diameter) crater Lyot (lat 50° N., long 330° W.), a few highly subdued meander remnants with central ridges can be recognized. In places they appear to be overlain by ejecta from Lyot, however, the southern edges of this crater are embayed by material that may have a fluvial origin.

Relative Ages of Fluvial Episodes

Preliminary crater counts made within various channels of the Kasei-Ares Valles drainage system indicate differences in relative ages of the fluvial deposits. On the basis of these counts, the earliest water

flooding appears to have occurred at about the same time as beginning volcanism at Tharsis Montes and Syria Planum (7). The channel deposits of Mangala Vallis to the west of Tharsis Montes are of similar age and support the probability that volcanic and fluvial activity are interrelated. In contrast, the postulated meander remnants in the Cebrenia region are associated with much younger surfaces and thus may not be related to the volcanism in the adjoining Elysium Mons-Hecates Tholus region which is believed to predate the Tharsis eruptions (8).

References:

(1) Carr, M. H. and Clow, G. D. (1981) Icarus 48, 91-117.
(2) Tanaka, K. L. and Scott, D. H. (1980) Proc. Third Colloquium on Planetary Water, 76-79.
(3) Leopold, L. B., and Wolman, M. G. (1960) Geological Society of America Bulletin 71, 769-794.
(4) Holmes, Arthur (1965) Principles of Physical Geology, Second Ed., Ronald Press Co., 528-538.
(5) Embleton, C. and King, C. H. M. (1975) Periglacial Geomorphology, Halsted Press, 1-203.
(6) McCauley, J. F., Schaber, G. G., Breed, C. S., Grolier, M. J. (1982) Reports of Planetary Geology Program 1982, in press.
(7) Scott, D. H., and Tanaka, K. L. (1981) Icarus 45, 304-319.
(8) Scott, D. H., and Carr, M. H. (1978) U.S. Geological Survey Miscellaneous Geologic Investigation Map I-1083.

Fig.1 a - Ares Vallis (Viking frame 864A02). Meander scars (1), channels banks (2), streamlined erosional forms (3). Diagrams b and c show configurations of meanders in Ares Vallis and Missisippi river at same scale; arrows show direction of flow.

Figure 2. Partly buried meander remnants in Chryse-Acidalia region of northern plains. Arrows indicate channels with characteristic central ridges.

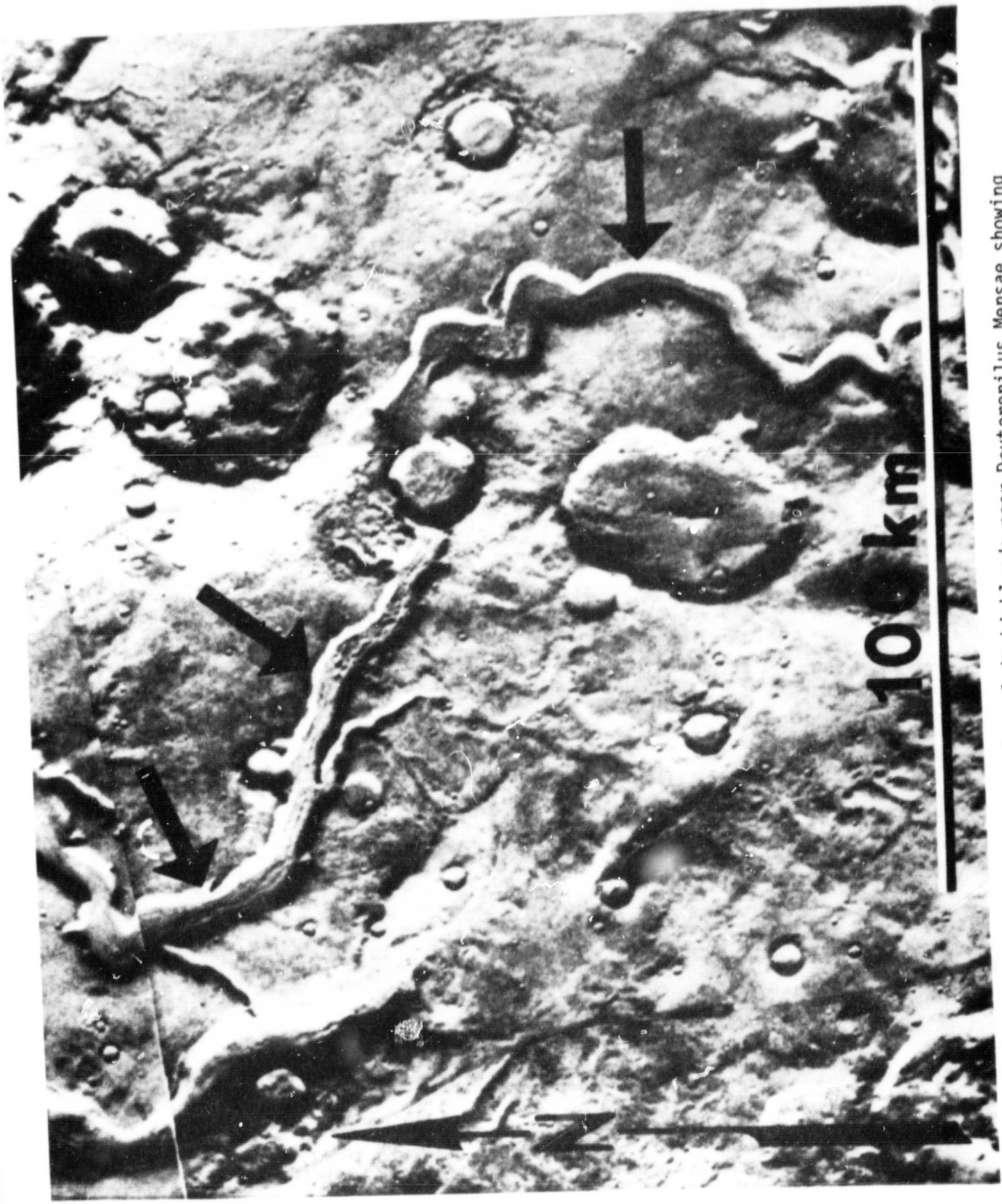

Figure 3. Prominent channel in highlands near Deuteronilus Mensae showing well developed medial ridges.

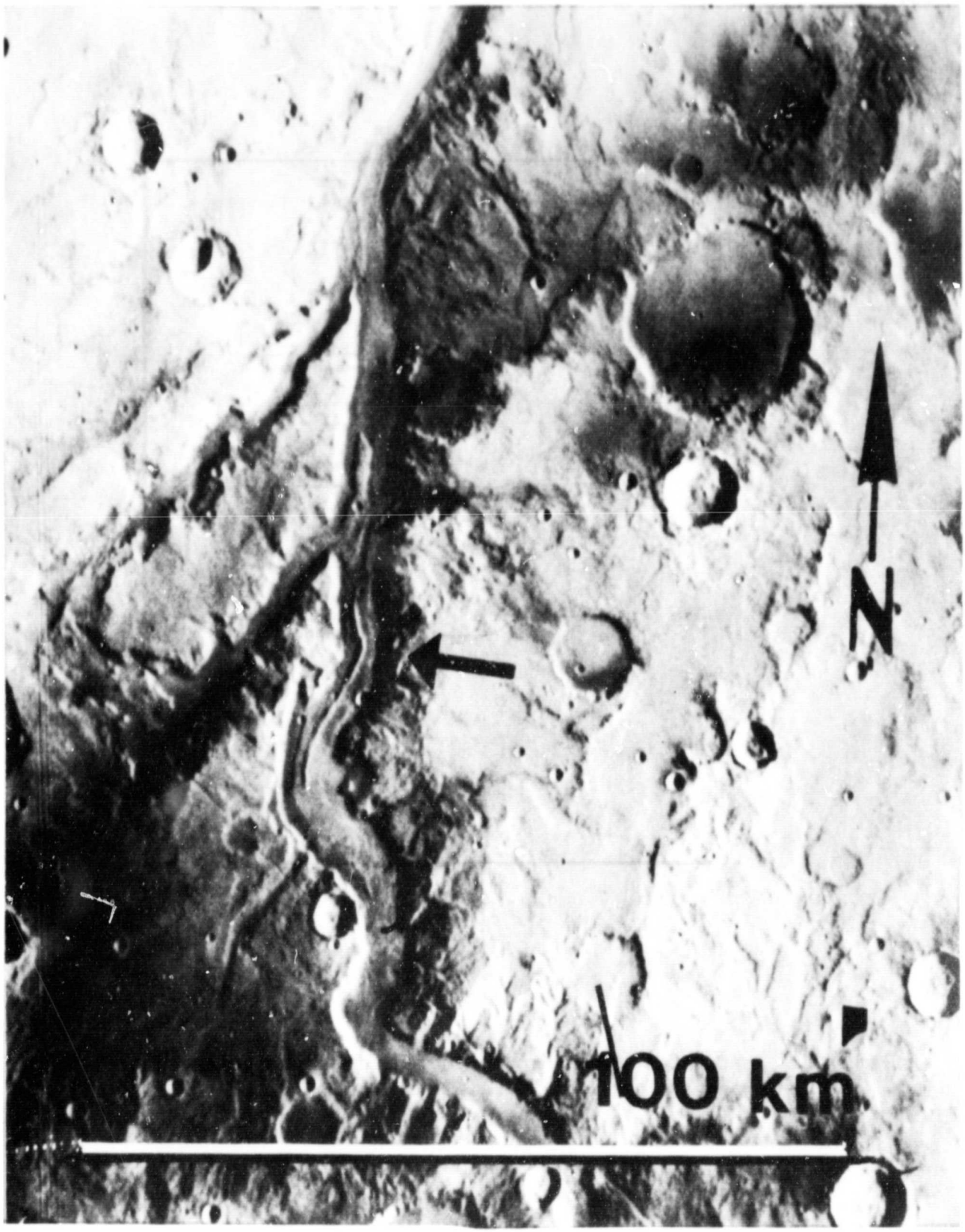

Figure 4. Ma'adim Vallis, a large ancient river channel in the Aeolis quadrangle of Mars. Central ridge shown by arrow.

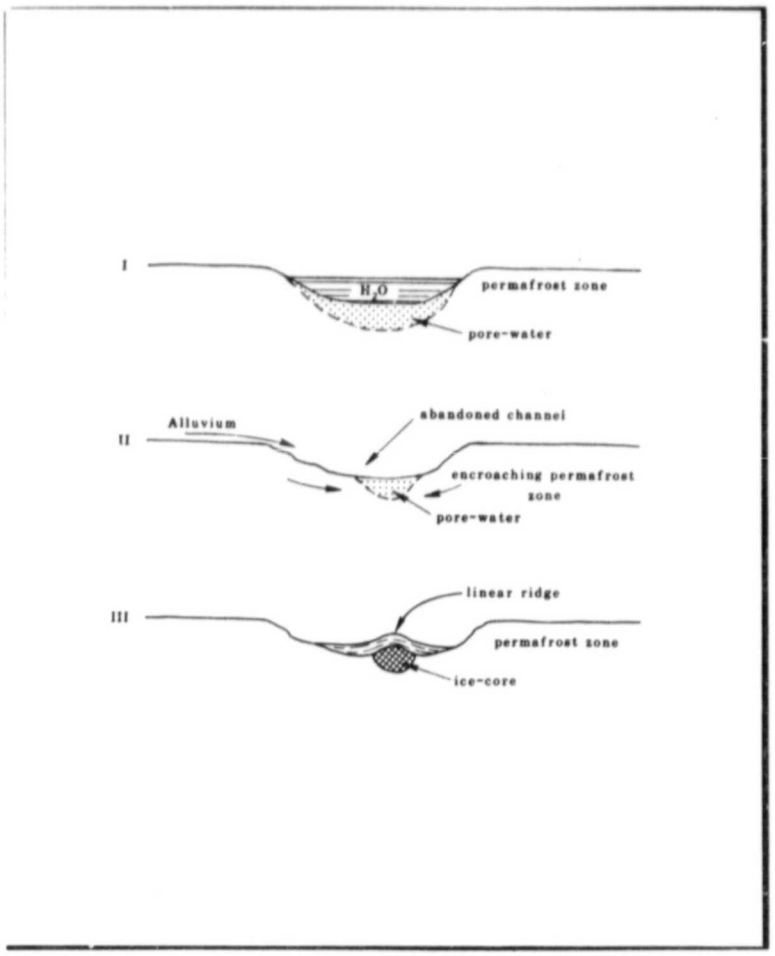

Figure 5. Postulated stages in development of linear pingo ridges along channel floors.

Figure 6. Probable meander remnants in the Cebrenia quadrangle of Mars. Faint central ridges visible in places indicated by arrows.

VOLATILE EXCHANGE WITH THE MANTLE AT MID-OCEANIC RIDGES AND THE THERMAL HISTORY OF THE EARTH'S INTERIOR (Norman H. Sleep, Geophysics Department, Stanford University, Stanford, CA 94305)

Water, CO_2, Cl, and S are cycled into and out of the earth's mantle. About half of the earth's inventory of H_2O, CO_2, and Cl is in crustal reservoirs such as the ocean, limestones, and salt deposits. Sulfur is much less strongly concentrated in the crust. Mid-oceanic ridges are largely a sink of water hydrated into the crust and a sink for free Oxygen. Sulfur from the basaltic crust enters the ocean and sulfate in the ocean reacts to form sulfides in the oceanic crust. The potential for reaction is great as all seawater is cycled through hydrothermal vents once every 10 m.y. (or less). Hydrothermal vents at the ridge axis have been extensively sampled and indicate that the water has extensively reacted with the rock and is quantitatively depleted in some components. Thermal calculations constrained by the shape of the magma chamber (obtained from seismic reflection) indicate that about 1/10 of the circulation is through axial vents. Off-axis circulation probably reacts with the rock to a lesser extent. The correlation of S and C isotopes through the Phanerozoic is compatible with the relatively small chemical exchange with from the thermal models.

The amount of chemical exchange in the past is proportional to the global rate of seafloor spreading because all the reaction occurs within very young crust. Reaction is also favored by shallow water over the ridge axis such as near Iceland. A possible instability is that once the ocean is sufficiently shallow at the ridge axis, hydration would consume much of the remaining water. This never happen on the Earth but may have happen on Venus. The instability also precludes gradual build-up of the ocean through much of Earth history. Large losses of water at mid-oceanic ridges through geological time would change the ratio H_2O : NaCl and H_2O : CO_2. As there is no evidence for this change, the volitile data is most compatible with a gradually cooling interior of the earth and spreading rates comparable to the present through geological observable time.

ORIGIN AND CIRCULATION OF HYDROTHERMAL FLUIDS AT LARDERELLO: CLUES FROM NOBLE GASES. Stephen P. Smith, Dept. of Physics, Univ. of California, Berkeley, CA 94720.

Spatial and temporal variations of the compositions of gases in steam from geothermal fields can be used to constrain models of the fluid circulation in the reservoir (1,2). Elemental and isotopic abundances were measured for noble gases in steam from five wells in the central and southern portions of the Larderello, Italy geothermal field. These data and literature data on the active gases (1,3) and noble gases (2,4) in other wells at Larderello suggest a complex picture of mixing among different components of volatiles from several atmospheric and juvenile sources.

RESULTS OF THIS STUDY. The elemental abundances of the non-nucleogenic gases appear to be dominated by two-component mixing between an air-like component (A) and a heavy-noble-gas-enriched component (HE). No compositions were measured that matched air-saturated water (ASW).

For helium, $^3He/^4He$ (=R) normalized to atmospheric $^3He/^4He$ (R_a=1.4 x 10^{-6}) gives R/R_a = 1.11 to 2.15, well outside of experimental uncertainty. This variation requires the presence of at least two components. High He/Ne ratios (275 to 2900 time atmospheric) rule out a significant atmospheric He component. The likely components present are crustal radiogenic He ($R/R_a \lesssim 0.1$) and a component enriched in ^3He, either primordial mantle He ($R/R_a > 30$) or ^3He from decay of bomb-produced tritium in young groundwater.

Neon yields atmospheric $^{20}Ne/^{22}Ne$ ratios, but 0 to 20 permil enrichments in $^{21}Ne/^{22}Ne$ compared to atmospheric Ne. The ratio of excess ^{21}Ne to ^4He is about 5 x 10^{-8}, consistent with crustal nucleogenic Ne from (α,n) reactions.

Enrichments in $^{40}Ar/^{36}Ar$ range from 0 to 15% over atmospheric reflecting an addition of radiogenic $^{40}Ar^*$ to Ar of atmospheric composition.

Isotopic compositions of Kr and Xe are atmospheric.

GAS COMPONENTS IN LARDERELLO STEAM. Model calculations show that both the compositions and concentrations of the non-nucleogenic noble gases are consistent with generation of the A and HE components from 10°C meteoric groundwater by separate Rayleigh distillation processes. The A component may represent gases from the initial stages of vapor separation at $\lesssim$100°C from an undepleted water body. The HE component appears to be derived at about 200°C from a substantially depleted reservoir (>90% Ar lost). The intersection of the mixing line defined by the sample data with calculated curves of compositions generated by Rayleigh distillation defines the endpoint compositions of the A and HE components ($^{132}Xe/^{36}Ar$ about 1 and 11 times atmospheric, respectively). This allows calculation of the concentration of both components in each sample. For this model, ^{36}Ar from A varies by a factor of about 10, and ^{36}Ar from HE by a factor of about 2.

Variations in the total ^3He concentration of the steam tend to parallel the variations in ^{36}Ar from HE, suggesting a possible genetic link or common mode of transport.

In the four wells containing detectable radiogenic $^{40}Ar^*$, the radiogenic and nucleogenic contributions to ^4He, ^{21}Ne, and ^{40}Ar form a coherent component (NUC). The ratio $^4He/^{40}Ar^*$ is constant (12.6 ± 0.2), as is $^{21}Ne^*/^4He$. Also, the absolute concentrations of ^4He and $^{40}Ar^*$ are constant within experimental uncertainty (0.58 ± 0.04 and 0.045 ± 0.003 ccSTP/kg steam, respectively). These constant concentrations appear to preclude any direct link between the bulk of the NUC gases and any other component showing variable concentrations. For example, The NUC component does not seem to correlate with the CO_2 content of these wells which varies from about 22 to 34 liters/kg steam.

Thus the noble gases in the wells studied appear to comprise a minimum of three independent components; A (air-like non-nucleogenic), HE (heavy-enriched non-nucleogenic; possibly also including ^3He), and NUC (nucleogenic He, Ne, Ar).

PREVIOUS RESULTS; CIRCULATION MODEL. D'Amore and Truesdell (1) present a model for fluid circulation at Larderello in which geographic variations in CO_2, NH_4, H_3BO_3, Cl, and $\delta^{18}O$ are ascribed to outward lateral flow and progressive Rayleigh condensation of steam from central boiling zones. Insoluble gases are concentrated in the uncondensed fraction of the steam - e.g. CO_2 to steam ratios increase by a factor of 5 toward the periphery. Conversely, the soluble constituents are enriched in the liquid condensate.

According to this model, any noble gas components sharing an origin in the central boiling zones with the species listed above should show an enrichment toward the margin by at least a factor of 5. The data reported here serve to define primarily the concentrations in the central part of the field. Limited literature data for the heavier noble gases (2) suggest that a non-nucleogenic component may show a concentration increase parallelling CO_2. Elemental abundance ratios do not show a strong relative enrichment of either A or HE-type gases that might be expected if only one of the two components were radially concentrated. Clarification of this situation requires data from additional wells on the periphery of the field.

Literature data reveals little or no increase (less than x2) in radiogenic ^4He content across the field (2,4). As was suggested from the data on the central wells, CO_2 and ^4He are evidently not closely related. The principal source of steam produced by the wells is evaporation of the liquid condensate in the two-phase region (1). The constant He/steam ratios suggest that the bulk of the radiogenic ^4He in the steam from a given well was originally dissolved uniformly in the condensate and was leached locally from the aquifer.

He isotope data (4; this work) suggest that the $^3He/^4He$ ratio and hence ^3He concentration decrease toward the northern edge of the field. The ^3He and CO_2 appear not to share a common origin or transport mechanism. If the ^3He is of deep mantle origin, it is difficult to see how it could appear in the central Larderello wells without being subject to the same lateral flow that controls the CO_2 distribution. Perhaps this is telling us that the circulation model is incorrect. Alternatively, Torgersen (4) has suggested that the ^3He enrichments at Larderello could be the result of tritium decay in young groundwater such as is known to be recharging the southern part of the field (1). If this is the case, the lack of tritium (5) and very high He/Ne ratios in the wells showing elevated $^3He/^4He$ ratios require that old steam extracted most of the ^3He from the tritiated groundwater without significant hydrogen isotope exchange, and that the young groundwater was almost completely outgassed before the tritium decayed. Model calculations show that this scenario cannot be ruled out at present, although it seems uncomfortably ad hoc. The question of the origin of the ^3He in the Larderello fluids is clearly of great importance.

REFERENCES.

(1) D'Amore F. and Truesdell A.H. (1979) Proc. 5th Stanford Workshop and Geothermal Reservoir Engineering, p.283-297.
(2) Mazor E. (1979) Pageoph. 117, p.262-275.
(3) Truesdell A.H. and Nehring N.L. (1979) Pageoph. 117, p.276-289.
(4) Torgersen T. (1980) J. Geochem. Explor. 13, p.57-75.
(5) Nuti S. (1982) private communication.

IMPORTANCE OF NON-TERRESTRIAL VOLATILES TO FUTURE SPACE OPERATIONS; Robert L. Staehle, Advanced Projects Group, Jet Propulsion Laboratory, California Institute of Technology, Pasadena, California 91109

By 2000 the mass of equipment being placed into geostationary (Clarke) orbits annually may be 10^1-10^2 times the present level[1], making space transportation a multibillion dollar industry in terms of yearly revenues. Assuming advanced hydrogen/oxygen propellant upper stages, nearly 75% of the mass launched from Earth as payloads destined for geostationary orbit will be in the form of propellant[2], with perhaps 300 t/yr of oxygen. In terms of energy required for transport, the Moon is 10 times closer to low Earth orbit (LEO) than the Earth's surface, and several known asteroids are even closer at some times[3,4].

With the future space transportation industry becoming large enough to support its own supplier infrastructure, the possible availability of certain volatile elements on the Moon and some asteroids becomes attractive for reducing the costs of interorbit and other forms of space transportation. While the commercial breakeven point for extraterrestrial vs. terrestrial sources of commodities used in space operations cannot yet be predicted, current estimates of space transportation demand, particularly for civilian communications services, make such a breakeven conceivable within 20-30 years. Because of the lead times required in establishing even terrestrial resource operations, theoretical development and exploration over the next decade is likely to be decisive in choosing the first resource sites used to support space operations.

One important resource, oxygen, is abundant in many lunar minerals, and can be extracted via molten electrolysis[5] and possibly other techniques[6]. Other than oxygen, the key uncertainties for extraterrestrial resource operations involve the reducing agents hydrogen and carbon, the concentrations of which in known lunar materials are insufficient to be economically useful. Consequently, the most important issue for the investigation of planetary volatiles from the point of view of space resources is the possible presence of H and C in concentrations of 1-10 wt % or greater in unexplored regions of the Moon or on accessible asteroids.

The possibility of lunar permafrost in permanently-shaded polar crater floors has been advanced[7], and some meteoritic materials thought to be related to C-type asteroids have been found to have a component of water and carbon with non-terrestrial origin[8]. Limited exploration, combined with sound theoretical development, could result in the discovery of economically important reservoirs of volatile elements on the Moon, asteroids, and elsewhere.

The importance of potential extraterrestrial volatile resources is described, along with possible methods of locating valuable reservoirs. Some areas of scientific consideration are suggested which would be most helpful in determining and advancing the viability of extraterrestrial resources by reducing the costs of certain high-volume space operations.

References

1. Johnson Space Center (Author Unknown), Space Operations Center Presentation to JPL, "STS/SOC Traffic Model-Medium Options: Equivalent STS Flight -- Schedule 100 Baseline," Chart S-81-11734, 9/17/81.

2. Staehle, Rob, "Propellant Estimate for Clarke Orbit Traffic in 2000," Jet Propulsion Laboratory IOM 312/82.3-1972, March 11, 1982.

3. French, J. R., and N. D. Hulkower, "Exploration of the Asteroids," Journal of the British Interplanetary Society, 35, pp. 167-171, 1982.

4. Hulkower, Neal D., "Opportunities for Rendezvous and Round Trip Missions to 1982 DB Based on Update Elements," JPL IOM 312/82.3-2046, June 7, 1982.

5. Kesterke, D. G., "Electrowinning of Oxygen from Silicate Rock," U.S. Bureau of Mines, RI 7587, 1971.

6. Criswell, David R., "Processing of Lunar and Asteroidal Materials," Extraterrestrial Materials Processing and Construction, Lunar and Planetary Institute, 30 September 1978.

7. Watson, K., B. C. Murray, and H. Brown, "The Behavior of Volatiles on the Lunar Surface," J. Geophys. Res., 66, 3033, 1961.

8. Kerridge, J. F., and T. E. Bunch, "Aqueous Activity on Asteroids: Evidence from Carbonaceous Meteorites," in Asteroids, T. Gehrels, ed., The University of Arizona Press, 1979.

Selected Uncited References

Robert L. Staehle, "Small Planetary Missions for the Space Shuttle," American Astronautical Society paper 79-288, 10/29/79.

David F. Bender, "A Suggested Trajectory for a Venus-Sun, Earth-Sun Lagrange Point Mission, VELA," AAS/AIAA Paper 79-112, June 1979.

J. D. Burke, "Where Do We Locate the Moon Base," Spaceflight 19, pp. 363, October 1977.

James R. Arnold, "Ice in the Lunar Polar Regions," J. Geophys. Res. 84, pp. 5659, Paper 9B0581, September 10, 1979.

J. H. Hoffman, et al., "Lunar Atmospheric Composition Experiment," Apollo 17 Preliminary Science Report, NASA SP-330, 1973.

Anonymous, "Soviets Propose Multinational Lunar Mission," Aviation Week and Space technology, p. 26, July 26, 1982.

Barbara M. Middlehurst, "A Survey of Lunar Transient Phenomena," Phys. of the Earth and Plan. Interiors 14, pp. 185, 1977.

Wolfgang H. Steurer, et al., Extraterrestrial Materials Processing, JPL Publication 82-41, April 15, 1982.

(This work was conducted at the Jet Propulsion Laboratory, California Institute of Technology, Pasadena, CA., supported by NASA Contract NAS7-918.)

IMPORTANCE OF NON-TERRESTRIAL VOLATILES

Staehle R. L.

OPERATIONAL USES FOR VOLATILE ELEMENTS

- PROPULSION, ESP, O_2 AND H_2, POSSIBLY WITH C
  - USING LOX/LH_2, 60% OF CLARKE-BOUND LEO MASS IS LOX FOR ADVANCED CHEMICAL PROPULSION
  - LOX/LH_2/CH_x REDUCES TANKAGE MASS, INCREASES PROPELLANT MASS, A POSSIBLE STEP
  - TOTAL MASS 2-3 TIMES USEFUL PAYLOAD MASS FOR MOST COMMON OPERATIONS
  - 100-700 t/yr BY 2000 IF TRAFFIC TRENDS AS PREDICTED
  - POSSIBLE LATER INTEREST IN Ar FOR ELECTRIC PROPULSION
- LIFE SUPPORT
  - 1-2 kg O_2/PERSON/DAY IF CO_2 NOT RECYCLED
  - N_2 LEAKAGE MAKEUP (LESS THAN O_2 CONSUMPTION)
  - 10-20 t/yr BY 2000 IF 40 PEOPLE CONTINUOUS, RECYCLED CO_2
- OTHER
  - PROCESS REAGENTS
  - MILITARY LASERS
  - TBD
  - DEMAND UNCERTAIN

CLARKE ORBIT TRAFFIC

VITAL STATISTICS

- TOTAL 71 TONNES, 131 SATELLITES, 1964-1981, EXCLUDING USSR
- OPERATIONAL CIVILIAN COMMUNICATIONS = 24.6 t
  " MILITARY " = 17.7 t
  } ~ 60%
- 1985 SCHEDULED LAUNCHES ~ 30-40 t TOTAL*
- 1981, 82 ACTUAL AND SCHEDULED ~ 10-12 t TOTAL* EACH YEAR
- COMMUNICATIONS SATELLITE OPERATOR GROUP RAPIDLY GROWING
  - NEW U.S. CORPORATE CARRIERS
  - EUROPEAN GOVERNMENT/CORPORATE CARRIERS
  - DEVELOPING COUNTRIES AND REGIONAL GROUPS

*NOT CONSIDERING ARIANE L-05 FAILURE

172 Staehle R. L.

ANNUAL TRAFFIC TO CLARKE ORBIT

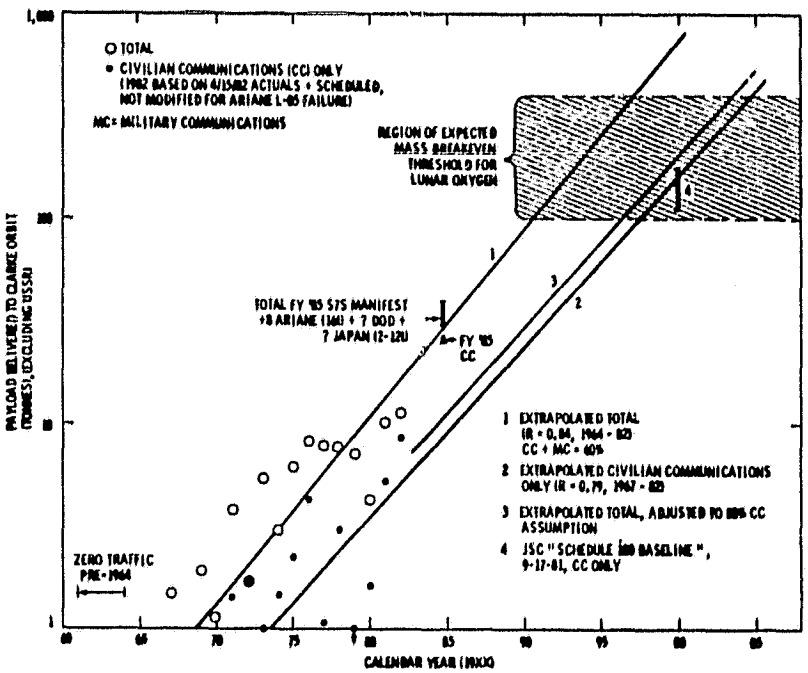

ALL POINTS SHOWN ARE ACTUAL, EXCEPT 1982, AS NOTED. TREND 3 IS SIMPLY TREND 2 WITH 25% ADDED TO ACCOUNT FOR NON-CC TRAFFIC. BAR 4 IS FROM A SPACE STATION TRAFFIC PROJECTION AND IS IN NEAR AGREEMENT WITH OTHER PROJECTIONS FOR 2000. HOWEVER, NO SUCH PROJECTION SHOULD BE TAKEN FOR FACT. GROWTH SHOWN HERE IS SIMILAR TO HISTORICAL GROWTH FOR OTHER NEW COMMUNICATIONS CAPABILITIES, BUT A VARIETY OF CONDITIONS COULD SUBSTANTIALLY INCREASE OR DECREASE ACTUAL TRAFFIC (SEE NEXT 2 CHARTS).

Staehle R. L.

CLARKE ORBIT TRANSPORTATION

- PRESENT OPTIONS (prices dependent on launch year, customer services, use as ROM only)
  - U.S.: Delta (600 kg, $30M), Atlas Centaur (1100 kg, $50M), STS/PAM-D (600 kg, $15-25M), STS/PAM-A (~1200 kg, ~$40-50M), STS/IUS (~2,300 kg, ~$130M)
  - E.C.: Ariane (~1,000 kg, ~$20-30M)
  - JAPAN: DELTA-DERIVATIVE
  - $3,000/kg TO LEO ON STS
- DEVELOPING OPTIONS
  - SHUTTLE: IUS TOO EXPENSIVE FOR COMMERCIAL USERS
    CENTAUR CAPABILITY 5,000-6,000 kg, $ 100M?
  - ARIANE: AGGRESSIVE MARKETING, DEVELOPMENT OF GROWTH CAPABILITY, POSSIBLE COST REDUCTIONS. 2,000-3,000 kg 1986-1988
- FUTURE POSSIBILITIES
  - ORBIT-BASED REUSABLE ORBIT TRANSFER VEHICLE (OTV) } LIKELY TOGETHER
  - AERO-ASSISTED OTV } LIKELY TOGETHER
  - ARIANE TO 5,000 kg
  - SOLAR- OR NUCLEAR-ION LOW THRUST (REVENUE LOSS, SOLAR CELL DEGRADATION)
  - TETHER-ASSIST (>20 y)

FACTORS INFLUENCING CLARKE ORBIT TRAFFIC

- CUSTOMER DEMAND
  - TRADITIONAL POINT-TO-POINT (TELEPHONE, DATA, TV: INTELSAT, COMSAT GENERAL, AT&T, RCA, ANIK, PALAPA, ETC.)
  - MARITIME
  - DIRECT BROADCAST
  - MOBILE SERVICE (LAND COMMERCIAL, AERONAUTICAL)
  - VIDEO TELECONFERENCING
- LAUNCH VEHICLE THROUGHPUT CAPACITY
  - CAPACITY-LIMITED THROUGH 1986-1990
  - POSSIBLE PRIVATE LAUNCH VEHICLES
  - CONGRESSIONAL vs. COMMERCIAL STS FLEET SIZE SELECTION
  - STS UPPER STAGE SELECTION (COST vs. MASS-TO-ORBIT)
  - UPRATED ARIANE (4 AND 5) DEVELOPMENT
- LAUNCH VEHICLE RELIABILITY
  - INSURANCE COSTS, RISK EXPOSURE
  - UNCERTAINTY OF ARIANE L-02, L-05 FAILURES

FACTORS INFLUENCING CLARKE ORBIT TRAFFIC (continued)

- REGULATORY UNCERTAINTY
  - INTERNATIONAL ALLOCATIONS OF SLOTS AND FREQUENCIES
  - DOMESTIC ALLOCATIONS
  - DIRECT TV BROADCAST TREATIES
- OTHER UNCERTAINTIES
  - PETROLEUM PRICES
  - INTEREST RATES
  - TECHNOLOGY ADVANCES

CLARKE ORBIT TRANSPORTATION

- PHYSICAL PARAMETERS
  - LEO ~ 370 km, i = 28.5°; Clarke ~ 35,900 km, i = 0°
  - ΔV_{up} = 4.3 km/sec = characteristic velocity
  - ΔV_{down} = { 4.3 km/sec = all propulsive; 2.0 km/sec = aerobraking (drag only) [best choice]; 1.6 km/sec = aeromaneuvering (lift and drag) }
  - rocket equation:

$$\frac{\text{propellant mass}}{\text{delivered mass}} = \frac{m_p}{m_f} = \exp\left(\frac{\Delta V}{c_{eff}}\right) - 1$$

c_{eff} = effective exhaust velocity ~ 3.4-4.5 km/sec

- ACTUAL STAGES
  - m_f = tankage + guidance + structure + useful payload
  - $\frac{m_{LOX}}{m_{LH_2}} = 6$
  - $\frac{m\ (\text{propellant})}{m\ (\text{useful payload})} \sim$ 2.5 expendable; 3.8 aerobraking, all propellant from LEO; 3.2 aerobraking, return propellant delivered to clarke orbit

Staehle R. L.

ACCESSIBILITY IN THE INNER SOLAR SYSTEM

Location	Min. ΔV to LEO* (km/sec)	Time of flight (ballistic)	Frequency of Opportunity (ballistic)	Distance from Earth (light time)	Distance from Sun (AU)	Rotation Period
1982 DB	0.1-0.5	2-8 mo	2-10 yr	0.5-20 min	0.9-1.2	? hr
Near-Earth Asteroids	0.5-2	2-20 mo	2-5 yr	1-20 min	0.8-2	? hr
Earth Trojans**	≤1.4-2	0.8-2 y	continuous	4-10 min	1	? hr
Phobos Deimos	∿1.5-2	0.5-2 y	1-2 y	5-20 min	1.4-1.7	8-31 hr
Lunar Surface	3.2	3-5 d	continuous	∿ 2 s	1	28 d
Mars Surface	5.6	0.5-2 y	1-2 y	5-20 min	1.4-1.7	25 hr
Earth Surface	8.2	10-15 min	continuous	-	1	24 hr

*With aerobraking in Earth atmosphere prior to orbit insertion
**Speculative

ALL SITES SHOWN ARE OF POSSIBLE INTEREST. IF WATER EXISTS NEAR THE LUNAR SURFACE (SEE LATER CHARTS), THE MOON WILL ALMOST CERTAINLY BECOME THE FIRST SITE OF COMMERCIAL RESOURCE EXTRACTION. THE FIRST THREE ACCESSIBILITY CRITERIA (ΔV, TOF, FOO) ARE THE MOST IMPORTANT, AND SINCE NO BODY EXCELS IN ALL THREE, COMPLEX COMMERCIAL TRADEOFFS WILL EXIST. NOTE THAT TRANSIT ENERGY VARIES AS THE SQUARE OF ΔV, WHILE PROPELLANT REQUIRED IS AN EXPONENTIAL FUNCTION OF ΔV.

CIS LUNAR ACCESSIBILITY
(km/sec)

ORIGINAL PAGE IS
OF POOR QUALITY

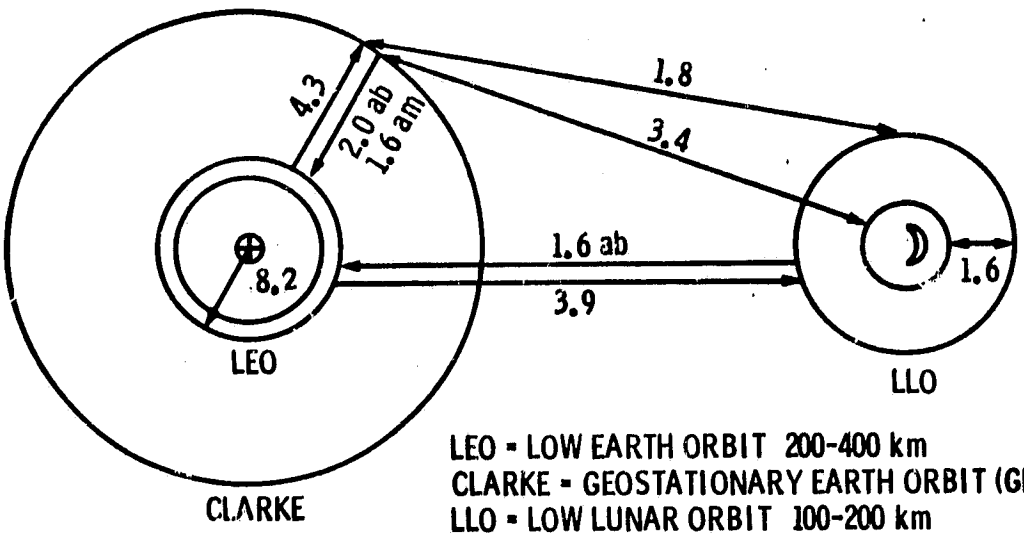

LEO = LOW EARTH ORBIT 200-400 km
CLARKE = GEOSTATIONARY EARTH ORBIT (GEO) 35,900 km
LLO = LOW LUNAR ORBIT 100-200 km
ab = WITH AEROBRAKING (DRAG ONLY)
am = WITH AEROMANEUVERING (LIFT AND DRAG)

CLARKE ORBIT TRANSPORTATION

PROPELLANT REQUIREMENTS

- CIVILIAN COMMUNICATIONS ONLY, c_{eff} = 4.5 km/sec, AERO-ASSIST OTV (4.3, 2.0 km/sec), m_{LOX}/m_{LH_2} = 6, NO BOILOFF PROVISION
- NO TERRESTRIAL PROPELLANTS AFTER INITIALIZATION

YEAR	Useful Payload to Clarke Orbit (t)	Terrestrial LEO LOX (t)	Terrestrial LEO LH_2 (t)	Lunar Hydrogen and Oxygen Production LOX (t)	Lunar Hydrogen and Oxygen Production LH_2 (t)	Lunar Hydrogen and Oxygen to LEO LOX (t)	Lunar Hydrogen and Oxygen to LEO LH_2 (t)	Lunar Hydrogen and Oxygen to Clarke LOX (t)	Lunar Hydrogen and Oxygen to Clarke LH_2 (t)
1995	62	202	33	477	79	160	27	10	1.7.
2000	163	531	88	1260	209	421	70	27	4.4
2005	427	1390	231	3290	547	1100	184	70	11.5

COMPARISON OF TERRESTRIAL vs LUNAR MASSES OF REQUIRED PROPELLANT. PRODUCTION ON LUNAR SURFACE IS GREATER THAN SUM OF PROPELLANTS DELIVERED TO LEO AND CLARKE ORBIT BY AMOUNT EQUAL TO THAT USED IN CIS-LUNAR TRANSPORTATION OF PROPELLANT PRODUCT.

Staehle R. L.

KNOWN VOLATILES SOURCES OF POTENTIAL OPERATIONAL IMPORTANCE

Body	Volatile Elements of Operational Interest				
	O	H	C	N	Ar
Near-Earth Asteroids	probable	?	?	?	no
Earth Trojans*	?	?	?	?	no
Phobos/ Deimos	probable	?	?	?	no
Moon	30-50%	10-100 ppm	trace	no	?[1]
Mars	abundant	polar caps H_2O vapor	CO_2 atmos.	2.7% atmos.	1.6% atmos.
Earth	yes	yes	yes	yes	yes

*not discovered

*** = known quantities have operational potential

[1] See S. Jovanovic and G.W. Reed, Jr., "Trapping of Gases and Low Temperature Volatiles in Lunar Samples," this volume.

IMPORTANCE OF NON-TERRESTRIAL VOLATILES

Staehle R. L.

SPECULATIVE VOLATILES SOURCES OF POTENTIAL OPERATIONAL IMPORTANCE
(ORDERED BY ANTITICPATED OPERATIONAL SIGNIFICANCE IF DISCOVERED)

- LUNAR POLAR WATER (ICE)
  - SUGGESTED BY WATSON, MURRAY, BROWN
  - NO EVIDENCE FOR OR AGAINST
  - DISAGREEMENT ON QUANTITY AND LOSS MECHANISMS
  - "IDEAL" SOURCE FOR H AND O, SIMPLE EXTRACTION AND PROCESSING

- EARTH TROJAN ASTEROIDS
  - EXISTENCE POSTULATED (WEISSMAN AND WETHERILL), THEORETICALLY STABLE ORBITS (DUNBAR)
  - LOW TRAJECTORY ENERGIES, LOW THRUST:WEIGHT
  - LONG TRANSIT TIME BUT CONTINUOUS FLIGHT OPPORTUNITIES

- NEAR-EARTH ASTEROIDS
  - 59-60 KNOWN*
  - AT LEAST 4 WITH ΔV COMPARABLE TO LUNAR SURFACE, PROBABLY DOZENS WITHIN DETECTION LIMITS
  - SPECULATIVE COMPOSITION PARALLELS METEORITES

- LUNAR SUBSURFACE GAS
  - HIGHLY SPECULATIVE AND CONTROVERSIAL
  - H AND C SUGGESTED
  - SPECIFIC SITES SUGGESTED
  - NO HIGH-QUALITY EVIDENCE
  - DIFFICULT EXTRACTION, POTENTIALLY SIMPLE PROCESSING

*AT TIME OF PUBLICATION

RESOLVING THE KEY RESOURCE UNCERTAINTIES

- LUNAR ICE
  - POLAR ORBITER
  - γ-RAY SPECTROMETER, ELECTROMAGNETIC SOUNDER (100-150 MHz)
  - VERY SIMPLE SPACECRAFT, LARGE LAUNCH MASS MARGINS
  - ALTERNATIVE TO INTEGRATE WITH SCIENCE-ORIENTED LPO OR POLO
- EARTH TROJANS
  - ONGOING GROUND-BASED SEARCH (DUNBAR, HELIN)
  - SIMPLE SEARCH SPACECRAFT POSSIBLE IF NO TELESCOPIC SUCCESS
- HELIOCENTRIC, NEAR-EARTH ASTEROIDS
  - ONGOING SEARCH AND DISCOVERY (e.g., HELIN, et al.)
  - ONGOING SPECTRAL CHARACTERIZATION (e.g., McCORD, et al.)
- LUNAR GAS RELEASES
  - GASEOUS ORIGIN OF LUNAR TRANSIENT PHENOMENA NOT CONFIRMED
  - NO ONGOING CONFIRMATION
  - NO ONGOING SPECTRAL INSTRUMENT READINESS

IS THERE WATER AT THE LUNAR POLES?

- NO REAL EVIDENCE, FOR OR AGAINST, EXISTS REGARDING THE PRESENCE OF LUNAR POLAR ICE.
- PERMANENTLY SHADOWED CRATERS EXIST AT LATITUDES HIGHER THAN ~70°, COVERING ABOUT 0.5% OF TOTAL LUNAR SURFACE. SURFACE TEMPERATURES ARE 120°K AND BELOW, AT WHICH SEVERAL METERS OF WATER ICE ARE STABLE OVER BILLIONS OF YEARS (WATSON, MURRAY, BROWN, 1961).
- SOURCE OF WATER: PRESUMABLY OUTGASSING DURING AND AFTER DIFFERENTIATION. RELEASED WATER DOES NOT ACHIEVE ESCAPE IMMEDIATELY, AND SOME MIGRATES TO COLD POLAR SURFACES FROM ALL LATITUDES.
- THEORETICAL LOSS MECHANISMS (SUBLIMATION, METEOROID IMPACT, SOLAR WIND BOMBARDMENT, ETC.) REMOVE A SMALL FRACTION OF TOTAL EXPECTED IF PROPOSED SOURCES ARE ACCURATE.
- IF ICE EXISTS, IT WILL ALMOST CERTAINLY BE ALL H_2O, AND WILL BE PRESENT IN OPERATIONALLY LARGE (i.e. MANY DECADES' SUPPLY) QUANTITIES.

IMPORTANCE OF NON-TERRESTRIAL VOLATILES

180

Staehle R. L.

MISSION CHARACTERISTICS

- SPIN-STABILIZED, 300-kg SPACECRAFT
- 2-MONTH MISSION
- APOLLO SPARE γ-SPECTROMETER, SIMPLE EM SOUNDER
- MINIMAL NEW FACILITIES

COST AND COMPLEXITY

- SINGLE MISSION OBJECTIVE
- TWO INSTRUMENTS, LOW DATA RATE, ON OR OFF, OMNI ANTENNA
- IN-PRODUCTION PAM-D STANDARD INJECTION STAGE, STS-QUALIFIED, LARGE MASS MARGIN (500 kg)
- SHORT MISSION, NO INSTRUMENT SEQUENCE PLANNING
- LOW DATA QUANTITY, MODEST PROCESSING REQUIRED
- FREQUENT LAUNCH OPPORTUNITIES, COMPATIBILITY WITH OTHER SHUTTLE PAYLOADS
- TOTAL PROJECT COST ~ $70 M

(from C. Uphoff, R. Staehle, and D. Skinner)

Staehle R. L.

EARTH TROJAN SEARCH TRAJECTORY

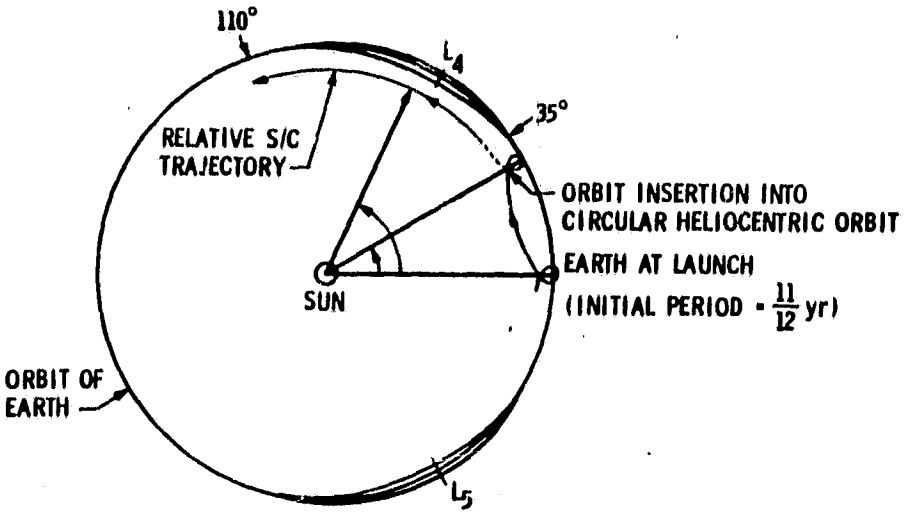

(FROM DAVID F. BENDER)

A GROUND-BASED SEARCH FOR EARTH TROJAN ASTEROIDS IS IN PROGRESS, BUT VIEWING CONDITIONS ARE DIFFICULT. A SIMPLE SPACECRAFT COULD FIND OBJECTS BELOW THE GROUND-BASED DETECTION THRESHOLD, USING A TRAJECTORY SHOWN HERE SCHEMATICALLY.

THE SPACECRAFT (NEXT CHART) CARRIES AN INSTRUMENT TO SLOWLY SCAN THE SKY OUTWARD FROM THE SPACECRAFT ORBIT, ALLOWING NEARLY FULL-PHASE DETECTION OF ANY ASTEROIDS. SPACECRAFT DATA YIELD GROSS DIRECTION AND ORBITAL VELOCITY, FROM WHICH NARROW-FIELD GROUND-BASED INSTRUMENTS SHOULD BE ABLE TO RECOVER NEW OBJECTS.

EARTH TROJAN SEARCH CONCEPT

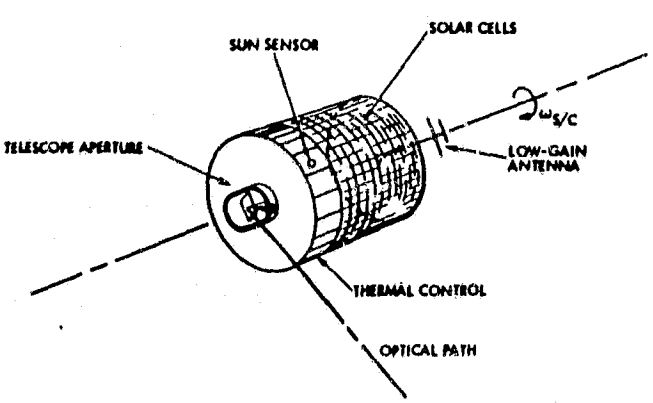

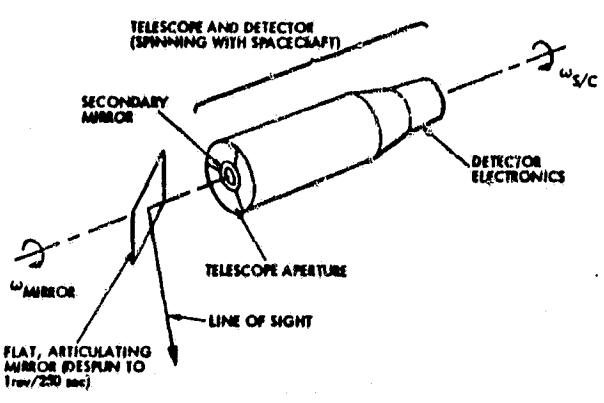

BREAKEVEN THRESHOLD

- OPERATIONAL

$$\left(\begin{array}{l}\text{Earth launch mass to deliver}\\ \text{mass M of equal quality from}\\ \text{non-terrestrial source}\end{array}\right)^{*} < \left(\begin{array}{l}\text{Earth launch mass to}\\ \text{deliver mass M from}\\ \text{ground}\end{array}\right)$$

*Includes "capital" mass invested in exploration, test, setup, and maintenance

- COMMERCIAL

Material of non-terrestrial origin can be delivered to the customer at the customer's specified destination on date specified for a price lower than that for which the customer can obtain the best terrestrial alternative, with the resource system operator able to realize a profit.**

**Profit calculations must include cost of risk, interest on capital, and depreciation, as well as all direct operating cost.

Operational threshold involves a straightforward engineering calculation based on technical assumptions which may be as conservative as desired. Estimate of this region for lunar operations is shown on Annual Traffic chart. Commercial threshold is much more difficult to predict. Analysis is presently focused on narrowing the uncertainty of predicted operational threshold, after which commercial analysis will begin. Commercial breakeven now appears conceivable shortly after 1995, and likely by 2010. In the end, only profitable operations, following years of investment planning, pilot operations and market testing, will prove commercially breakeven.

CONCLUSIONS

- SPACE OPERATIONS ARE EXPANDING RAPIDLY
- SPACE TRANSPORTATION WILL REMAIN COSTLY, PROPELLANT MASS DOMINATES
- GEOPOTENTIAL WELL MAKES TERRESTRIAL MATERIALS EXPENSIVE TO OBTAIN IN SPACE, AND MAKES OTHER SOURCES APPEAR ATTRACTIVE
- VOLATILE ELEMENTS O, H, AND POSSIBLY C OF PRINCIPAL INTEREST
- EMERGING ECONOMIC INCENTIVE TO FIND AND UTILIZE VOLATILE SUBSTANCES ON ACCESSIBLE BODIES
- CERTAIN DISCOVERIES COULD SPEED SPACE RESOURCE UTILIZATION AND CONSEQUENT BENEFITS TO MOST MAJOR SPACE OPERATIONS

IMPORTANCE OF NON-TERRESTRIAL VOLATILES

Staehle R. L.

KEY QUESTIONS

- DO THE FOLLOWING EXIST?
  - WATER ICE AT THE LUNAR POLES
  - EARTH TROJAN ASTEROIDS, WITH O, H, AND/OR C
  - HELIOCENTRIC NEAR-EARTH ASTEROIDS,* WITH O, H, AND/OR C
  - SUBSURFACE LUNAR GAS RESERVOIRS, WITH H OR C
- HOW DO WE FIND THEM, OR CONFIRM THEIR NON-EXISTENCE?

*SUBJECT TO COMPLEX ACCESSIBILITY CRITERIA

Investigators in fields related to planetary volatiles must answer these questions while working with engineers, corporate managers, and financiers, before space resource utilization will become a commercial reality. Directed space science research will become an emerging interest in the business community.

CHEMISTRY AND EVOLUTION OF TITAN'S ATMOSPHERE, Darrell F. Strobel, Naval Research Laboratory, Washington, D.C. 20375

The chemistry and evolution of Titan's atmosphere is reviewed in light of the scientific findings from the Voyager Mission. It is argued that the present N_2 atmosphere may be Titan's initial atmosphere rather than photochemically derived from an original NH_3 atmosphere. The escape rate of hydrogen from Titan is controlled by photochemical production from hydrocarbons. CH_4 is irreversibly converted to less hydrogen rich hydrocarbons, which over geologic time accumulate on the surface to a layer thickness of $\sim$ 0.5 km. Magnetospheric electrons interacting with Titan's exosphere may dissociate enough N_2 into hot, escaping N atoms to remove $\sim$ 0.2 of Titan's present atmosphere over geologic time. The energy dissipation of magnetospheric electrons exceeds solar EUV energy deposition in Titan's atmosphere by an order of magnitude and is the principal driver of nitrogen photochemistry. The environmental conditions in Titan's upper atmosphere are favorable to building up complex molecules, particularly in the north polar cap region.

Planet. Space Sci., 30, 839-848, 1982.

BUBBLE DIFFUSION AND COMPOSITION OF INERT GASES ON VENUS. A.S. Tamhane and G.W. Wetherill, Department of Terrestrial Magnetism, Carnegie Institution of Washington, Washington, D.C. 20015

The inert gases Ne and Ar have been observed to be more abundant on Venus by a factor of about 100 compared to Earth (1). One proposed hypothesis is that the inert gases were implanted, during the waning phase of a T Tauri stage, by an enhanced solar wind bombardment of the inner edge of a protoplanetary swarm. Material from the inner edge was then preferentially incorporated into Venus rather than the Earth (2). The present day solar wind ratio of $^{20}Ne/^{36}Ar$ is, however, $\sim$100 times higher than that observed in the atmosphere on Venus. This implies that a mechanism that would retain argon more efficiently than neon must be identified. Here we investigate the physical conditions under which one such mechanism, bubble diffusion (3), may give rise to fractionations similar to those observed.

Since ^{20}Ne is depleted by a factor of $\sim$100 with respect to ^{36}Ar, it is obvious that more than 99% of ^{20}Ne is lost from the grains. If this loss occurs in the form of bubbles, the bubble precipitation must take place at least up to the depth in the grains which corresponds almost to the end of the range of ^{20}Ne ions. It can occur only when the sputter erosion is low and the grains are saturated with implanted inert gases. This would require a solar wind bombardment of individual members of the <1 cm-diameter debris for a period of $\sim$100 years, assuming a flux enhanced by a factor of 500.

Bubble diffusion leads to fractionations in which heavier nuclides are enriched with respect to lighter ones. Assuming the energy of the primordial solar wind particles were equal to the present values, enrichment of ^{36}Ar by a factor of $\sim$100 with respect to ^{20}Ne would lead to a simultaneous enrichment of Kr with respect to ^{36}Ar by a factor of about 1.4. Analysis of Pioneer data suggests that the upper limit to Krypton mixing ratio most likely represents a measured concentration (4). The value of the most probable mixing ratio for Kr is 47 ppb which, if it is solely of solar wind origin, leads to an enrichment factor of 3.3, in disagreement with the prediction.

If the Pioneer measurement represents an actual detection of Kr, rather than an upper limit, one possible way of accounting for the higher enrichment factor would be to assume that the solar wind energy during the waning phase of the T Tauri stage was different than at present. If a higher energy is postulated, calculations indicate that the energy must have been in the range $20\ \text{Kev/n} < E \lesssim 100\ \text{Kev/n}$. Whether such an assumption can be justified is an open question. Some T Tauri stars exhibit rapid fluctuations in the ultraviolet, which are ascribed to the superposition of many simultaneous small flares (5). A

flare model based on this observation for the T Tauri stars could possibly provide a basis for the assumption (6).

Calculations are being made of the expected $^{36}Ar/Kr$ and $^{22}Ne/^{20}Ne$ fractionation at various energies in order to determine if there is an energy range for which the bubble diffusion mechanism is consistent with observation of inert gas abundances on Venus.

References:

(1) Pollack, J.B. and Black, D.C. (1979) Science 205, 55-99.
(2) Wetherill, G.W. (1981) Icarus 46, 70-80.
(3) Tamhane, A.S. and Agrawal, J.K. (1979) Earth Planet. Sci. Lett. 42, 243-250.
(4) Donahue, T.M., Hoffman, J.H. and Hodges, R.R., Jr. (1981) Geophys. Res. Lett. 8, 513-516.
(5) Kuan, P. (1976) Astrophys. J. 210, 129-136.
(6) Ulrich, R.K. (1978) in Protostars and Planets, T. Gehrels (ed.) 718-733.

WHAT ARE THE VOLATILES LIKE INSIDE THE EARTH? Karl K. Turekian, Department of Geology and Geophysics, Yale University, Box 6666, New Haven, CT 06511.

If we start with the premise that the carrier of volatiles to the accumulating earth was similar to C-1 carbonaceous chondrites, then the determination of the distribution of volatiles in the earth can be made based on measurements made at the earth's surface. Heat flow measurements, Nd, Sr and Pb isotope systematics, and radiogenic and stable isotopic abundances of some of the rare gases combined with the oxidation state of mantle-derived rocks yield information for a moderately self-consistent picture of the rare gas, water and carbon content of the earth's interior.

ANCIENT ATMOSPHERIC ARGON IN CHERTS.

G. Turner, C.M. Jones and A.W. Butterfield, Physics Department, Sheffield University, Sheffield S3 7RH, U.K.

The outgassing rate of atmospheric noble gases can in principle be inferred from a knowledge of the variation of the atmospheric ($^{40}Ar/^{36}Ar$) ratio as a function of time. In an attempt to determine the composition of atmospheric argon in the past we are carrying out an analytical programme involving the analysis of argon extracted from cherts and silicified plants. The samples analysed include ones which have been subjected to neutron irradiation in order to use the ^{40}Ar-^{39}Ar technique to correct for in situ decay of ^{40}K in addition to providing chronological information. As well as attempting to determine the ($^{40}Ar/^{36}Ar$) ratio our aims have been to provide a systematic understanding of the way in which atmospheric gases are incorporated in chert and to investigate the likelihood of inferring sensible values for the isotopic composition.

In our preliminary work we have analysed twenty discrete samples from ten individual specimens. The specimens consisted of four silicified plants and two cherts with ages ranging from Permian to Eocene, and four ancient cherts from the Precambrian. The rationale behind the analysis of the recent cherts (in addition to seeking to demonstrate the presence of atmospheric argon) was to see whether they would indeed yield a sensible value for the composition of the (modern) atmosphere, or whether they would be seriously affected by such processes as mass fractionation or the incorporation of excess radiogenic argon. Clearly if it is not possible to use cherts to determine the (known) composition of today's atmosphere there is little point in making strenuous efforts to use them to determine the composition of the ancient atmosphere.

The 'recent' specimens have ages ranging from 50 Ma to 250 Ma and all contain significant amounts of dissolved argon. Concentrations of ^{36}Ar range from 7×10^{-9} ccSTP/g to 3×10^{-8} ccSTP/g. For comparison Cadogan (1977) observed a concentration of 2.5×10^{-8} ccSTP/g in Rhynie chert. The equilibrium solubility of atmospheric argon in terrestrial surface waters corresponds to concentrations roughly a factor of 100 greater than this (i.e. from 10^{-6} to 2×10^{-6} ccSTP/g). Since cherts typically contain structural and non structural water at the 1% level it seems likely that the argon we find in the cherts was originally dissolved in the ground water responsible for the silicification and was simply trapped during silicification.

The argon has been analysed during stepped heating experiments and shows a characteristic bimodal release pattern with major release (75%) at temperatures in excess of 1200°C, indicative of the fact that a major component of the gas is very strongly bound within the chert, and is not (for example) simply adsorbed from the present day atmosphere. Cadogan's Rhynie chert data shows a similar release pattern which may be a useful diagnostic feature in future attempts to identify ancient atmosphere in Precambrian samples. Estimates of diffusion coefficients and activation energies suggest that argon should be retained in cherts for times of the order of 1000 Ma or greater provided they are not subjected to temperatures in excess of 2 - 300°C. Interpretation of diffusion data in a simple minded way is clearly suspect, nevertheless the analysis does suggest, qualitatively at least, that dissolved atmospheric argon is only likely to be found in those Precambrian samples which have escaped all but the mildest metamorphism.

Neutron activation provides a means of determining concentrations of K, Ca and Cl, by way of neutron reactions which produce ^{39}Ar, ^{37}Ar and ^{38}Ar respectively. K concentrations in the modern cherts are all low, from 40 to 220 ppm. Corrections for radiogenic argon are therefore small. The ^{38}Ar data is of interest since it provides a possible way of investigating the palaeoenvironment of the samples, by way of the $^{Cl}/^{36}Ar$ ratio. In modern sea water this ratio is around $(5 - 10)\times10^6$ at/at. In four of the samples analysed the measured ratio covers the range $(1 - 2)\times10^6$, while in the remaining two Eocene samples (a silicified peat from the Albany coal basin, and Quincyte, a dolomite replacement chert from Mehun sur Yeure, France) the ratio was much lower, 0.14×10^6 and 0.13×10^6 respectively. If the 'solubility/trapping' mechanism postulated to account for the amounts of dissolved argon is correct, one might expect a similar mechanism to operate for chlorine though possibly with somewhat different efficiency due to chemical and ionic radius differences. This being so we are led to interpret the high $^{Cl}/^{36}Ar$ ratios as an indication of silicification under saline or marine conditions and the low ratios as an indication of freshwater conditions. This interpretation is consistent with our present knowledge of

the palaeoenvironments of the samples analysed.

The recent samples were, apart from a silicified fern stem from the Permian of Autun in France, confined to a narrow age range from 50 to 150 Ma. A global plot of all the data gave a best fit ($^{40}Ar/^{36}Ar$) ratio of 296.2 + 1.5 which is within error the same as the modern atmospheric value of 295.5. The Permian sample contained the smallest amount of gas and the ($^{40}Ar/^{36}Ar$) ratio of 293 + 14 is far too imprecise to distinguish between the modern value and a value of 294.0 + 1.5 for the Permian which is implied by Cadogan's data. While it is not possible to make any inferences about the rate of change of ($^{40}Ar/^{36}Ar$) from these measurements they are encouraging in that they appear to indicate that effects of mass fractionation or the incorporation of excess radiogenic argon are unlikely to be a major problem and provided the appropriate samples can be located there appears to be no fundamental obstacle in the way of using cherts to determine the isotopic composition of ancient atmospheric argon.

The Precambrian samples analysed in the preliminary study, a stromatolite from the Gunflint, and three black cherts (Bangemall, Hamersley and Onverwacht), gave no indication of dissolved atmospheric argon, and provided some limited chronological information only. The Gunflint sample from the Mink mountain area contained 43ppm K and based on a rather imprecise isochron had apparently been outgassed 1180 + 100 Ma ago. Three Onverwacht samples gave apparent ages close to 4000 Ma, considerably higher than the published Sm-Nd age of 3540 + 30 Ma (Hamilton et al., 1979). An examination of previously published $^{40}Ar/^{39}Ar$ ages of cherts (Alexander, 1975) revealed a similar tendency towards higher than expected ages and lead us to suspect the possibility of ^{39}Ar loss due to recoil during neutron activation. This effect has been confirmed by our most recent experiments in which samples of Gunflint from the Schreiber Beach locality were irradiated in evacuated quartz ampoules. Analysis of the argon in the ampoules indicated that around 12% of the ^{39}Ar was lost from the samples during irradiation.

In this most recent study seven samples of Gunflint have so far been analysed, two unirradiated and five irradiated. Stepped heating of the unirradiated samples revealed the 'diagnostic' high temperature release of ^{36}Ar and a concentration of around 4x10-9 ccSTP/g. Because of recoil loss it is clearly not meaningful to attempt to interpret stepped heating analyses of irradiated samples. Potentially the only meaningful data to use in isotope mixing diagrams (in order to separate radiogenic and atmospheric ^{40}Ar) are 'total gas' ratios or possibly 'total gas' less a (small) correction for low temperature release of modern air argon. Unfortunately the data so far obtained does not indicate a simple binary mixture of radiogenic and atmospheric. Two samples from the same chert cobble show clear indication of excess argon (high $^{40}Ar/^{36}Ar$ ratio). Excess argon is less evident in the two unirradiated samples and the other three irradiated samples, nevertheless it is not possible to infer a unique age and $^{40}Ar/^{36}Ar$ ratio. Based on the samples with the least evidence of excess argon we can infer an $^{40}Ar/^{36}Ar$ ratio based on an assumed age for the Gunflint. The ratio inferred is in the range 296 (i.e. modern), for an assumed age of 1900 Ma, to 260, for an assumed age of 2200 Ma. These values are only consistent with low rates of outgassing of ^{40}Ar over the past 2000 Ma, viz. <3.3x105 atoms/cm2/sec. Cadogan's data on Rhynie chert corresponds to a mean outgassing rate of (2.5 + 1.0)x105 atoms/cm2/sec over the past 400 Ma. Until the source of excess argon in the Gunflint samples is isolated the calculated ratios can only be regarded as upper limits. Work is continuing on this problem.

References.

Cadogan, P.H. (1977). Paelaeoatmospheric argon in Rhynie chert. Nature, 268, 38.

Hamilton, P.J., Evenson, N.M., O'Nions, R.K., Smith, H.S. and Erlank, A.J. (1979). Sm-Nd dating of the Onverwacht Group volcanics, southern Africa. Nature 279, 298.

Alexander, E.C.Jr. (1975). ^{40}Ar-^{39}Ar studies of Precambrian cherts: an unsuccessful attempt to measure the time evolution of the atmospheric $^{40}Ar/^{36}Ar$ ratio. Precambrian. Res. 2, 329.

GEOLOGIC BUFFERING OF THE HYDROSPHERE-ATMOSPHERE SYSTEM IN POST-HADEAN TIMES. J. Veizer, University of Ottawa, Canada K1N 6N5.

The kinetic steady state, buffering the composition of the present day oceans, is controlled by the following fluxes: (a) continental river discharge-F_C; (b) interaction between seawater and basalts of the oceanic crust predominantly, but not exclusively, in hydrothermal cells on mid-oceanic ridges-F_M; and (c) efflux via, and interaction with, sediments-F_S. Today, despite claims to the contrary, F_C likely outweighs F_M as the most important controlling factor of seawater composition. This is well demonstrated for tracers with differing signatures for these two fluxes. For example, the $^{87}Sr/^{86}Sr$ of F_C is 0.711 and of F_M is 0.703. Thus, a relative F_C:F_M intensity of $\sim$4.1 is required to produce the seawater ratio of 0.709. In geological past the intensity of F_C was proportional to the size of the continents, whereas that of F_M to the terrestrial heat flow. Consequently, the relative F_C:F_M intensities varied during terrestrial evolution, with the early stages being dominated by F_M and the subsequent evolution by F_C. Sr isotope data suggest that the crossover interval between a mantle (F_M) and continentally (F_C) dominated steady states was the late Archean-early Proterozoic period. Such an evolving scenario can explain the observed chemical (Fe, Fe^{2+}/Fe^{3+}, Mn, Ba, Sr ?) and isotopic ($^{87}Sr/^{86}Sr$, $\delta^{34}S$, $\delta 18O$) secular trends observed for chemical sediments. Furthermore, the observed sedimentological (e.g. Archean volcaniclastics vs. Proterozoic shelf sequences), geological (greenstones vs mobile belts) and metallogenetic (base metals; Fe, U, Au ores) patterns are entirely consistent with this outline.

The recent discoveries of direct evidence for existence of life since at least 3.5 Ga ago, coupled with the modern type carbon isotope record, attest to the great antiquity of life and possibly oxygen generating photosynthesis. Thus the emergence of the highly oxygenated atmosphere at $\sim$2.0 Ga ago may be a consequence of the diminishing effectiveness of oxygen sinks (reduced gases, Fe, Mn) due to declining F_M. This is in contrast to conventional explanation, which relates the event to the emergence and rapid evolution of oxygen generating biota during the early Proterozoic.

In addition to the first order evolution of the hydrosphere-atmosphere, from an F_M dominated, to the F_C dominated system, second order perturbations ($\leq 10^7$-10^8 a) are being established for the Phanerozoic. The covariance of seawater $^{87}Sr/^{86}Sr$, $\delta^{13}C_{bicarbonate}$, $\delta^{34}S_{sulfate}$ and sea level curves provides the first direct evidence for interactions of organic and inorganic cycles on geological time scales. Although a unifying model integrating all these parameters is not yet available, the results strongly suggest that this coupling is the real controlling factor of oxygen atmospheric levels.

Seawater is a medium which integrates and records global

responses to evolution and perturbations of the past geological steady states. This record, inscribed in chemical sediments, deserves attention commensurate with its potential and significance.

COMETARY IMPACTS ON THE TERRESTRIAL PLANETS, Paul R. Weissman, Earth and Space Sciences Division, Jet Propulsion Laboratory, Pasadena, CA 91109.

Long and short-period comets are the major source of solar system volatiles still actively interacting with the terrestrial planets. The cometary nuclei have been stored in the Oort cloud at distances up to 10^5 AU from the sun since the formation of the solar system. Stellar perturbations from random passing stars bring the cometary perihelia into the planetary region where perturbations by Jupiter and Saturn then control their further orbital evolution. According to Whipple's (1950) icy conglomerate model the nuclei are heterogeneous mixtures of roughly equal amounts of frozen volatiles (predominantly H_2O) and dust, a few kilometers in diameter.

Impact rates for long and short-period comets are calculated for each of the terrestrial planets. Impact probabilities are found using the standard Öpik (1976) formulae for encounters with planets in near-circular orbits. For the long-period (LP) comets a hypothetical distribution of near-parabolic orbits, uniformly distributed in perihelion distance and randomly oriented over the celestial sphere, is assumed. For the short-period (SP) comets the impact probabilities are based on the known sample of SP comets. Marsden (1979) has catalogued 113 SP comets of which 2, 9, 20, and 59 are Mercury, Venus, Earth, and Mars crossers, respectively. Results are shown in the table below.

	Long-period Comets		Short-period Comets				
	$\bar{p}$	$\bar{v}$ km s^{-1}	N_c	N_1	$\bar{p}$	$\bar{p}_y$ yr^{-1}	$\bar{v}$ km s^{-1}
Mercury	2.1×10^{-9}	81.2	1	1	2.4×10^{-9}	5.5×10^{-10}	41.5
Venus	3.7×10^{-9}	60.2	5	4	1.3×10^{-8}	2.0×10^{-9}	39.6
Earth	2.2×10^{-9}	51.7	13	7	6.6×10^{-9}	8.1×10^{-10}	37.4
Mars	6.8×10^{-11}	41.1	35	24	1.5×10^{-10}	2.2×10^{-11}	20.9

For the LP comets, $\bar{p}$ is the mean impact probability per comet per perihelion passage and $\bar{v}$ is the mean impact velocity. For the SP comets, N_c is the number of known planet-crossers of more than one apparition, N_1 is the number of one apparition planet-crossers, $\bar{p}$ is the mean impact probability per perihelion passage, $\bar{p}_y$ is the mean per year, and $\bar{v}$ is the mean impact velocity. There is some uncertainty in the SP impact rates due to small number statistics, particularly for Mercury and Venus.

The dynamical evolution of comets in the Oort cloud and the flux of comets entering the planetary region has been modeled by Weissman (1982a) using Monte Carlo simulation techniques. If comets originated in the Uranus-Neptune zone and were subsequently ejected to the Oort sphere, then they rapidly diffused back into the inner solar system with flux rates during the first 5×10^8 years of the solar system's history up to 200 times the current flux. However, if comets originated farther from the sun on the fringes of the primordial solar nebula or even in satellite fragments of the nebula, then the enhanced early flux would be considerably less, possibly even less than the present observed flux. The integrated average flux over the history of the solar system could be as high as 30 times the current value for an origin in the Uranus-Neptune zone, or as little as 0.66 times the current flux for origin in nebula fragments at 10^4 AU from the sun.

The total mass of LP and SP comets impacting the terrestrial planets can be found by multiplying the impact probabilities found above by the observed planet-crossing flux rate, the age of the solar system, the mass of the average

visible cometary nucleus (7.3×10^{15} g), and a completion factor of 1.12 to account for small, unobservable nuclei less than 0.9 km in diameter (Weissman, 1982c). For the LP comets Everhart's (1967) flux of ~16 comets/AU/year brighter than absolute magnitude $H_{10} = 11.0$ (diameter > 0.9 km) was used. For the SP comets Weissman's (1982b) estimate of ~229 earth-crossing SP comets with nucleus diameters > 0.9 km was used. The mass of impacting SP comets was decreased by 10% to account for sublimation mass loss during their orbital evolution. Results are shown in the table below.

	Long-period Comets		Short-period Comets	
	M_{max}	M_{min}	M_{max}	M_{min}
Mercury	1.4×10^{19}	3.1×10^{17}	4.9×10^{19}	1.1×10^{18}
Venus	4.7×10^{19}	1.0×10^{18}	3.3×10^{20}	7.3×10^{18}
Earth	3.8×10^{19}	8.5×10^{17}	1.8×10^{20}	4.1×10^{18}
Mars	1.8×10^{18}	4.0×10^{16}	7.6×10^{18}	1.7×10^{17}

The columns M_{max} and M_{min} correspond to the case of maximum average flux from the Oort cloud over the history of the solar system: cometary origin in the Uranus-Neptune zone; and the minimum flux case: origin in satellite fragments of the solar nebula. All masses are in grams. About 50-60% of the impacting mass can be assumed to be volatile ices.

The mass estimates have a probable error of plus or minus one order of magnitude. The chief error source is the mass distribution for the cometary nuclei. Uncertainties in the mass distribution result from the poor knowledge of cometary surface albedos and bulk nucleus densities, and observational selection effects acting on the brightness distribution. The current work assumes an albedo of 0.03 for LP comets and a nucleus density of 1.0 g cm^{-3}. In paticular, significantly lower cometary albedos such as those used by Shoemaker and Wolfe (1982) could result in a substantially greater total mass of comets impacting the terrestrial planets. In addition, there is no good way of estimating whether the present cometary flux through the inner solar system is indeed typical for the current Oort cloud. Lastly, cometary impacts may not be a highly efficient means of adding to a planet's volatile inventory since the impact events may possibly result in substantial atmospheric blow-off.

It should be noted that the term "comets" is used here to denote objects derived from the Oort cometary cloud. Icy planetesimals perturbed directly into the region of the terrestrial planets during the early history of the solar system have not been included in the calculation. Such objects probably provided a significant source of volatiles during the accretion of the terrestrial planets.

References:

Everhart, E. 1967. Astron. J., 72, 1002.

Marsden, B. G. 1979. Catalogue of Cometary Orbits, Smithsonian Astrophysical Observatory, 88 p.

Öpik, E. J. 1976. Interplanetary Encounters, Elsevier, Amsterdam, 155 p.

Shoemaker, E. M., and Wolfe, R. 1982. in The Satellites of Jupiter, D. Morrison, ed., Univ. Arizona Press, Tucson, pp. 277-339.

Weissman, P. R. 1982a. in Comets, L. L. Wilkening, ed., Univ. Arizona Press, Tucson, pp. 637-658.

Weissman, P. R. 1982b. in Geol. Soc. Amer. Special Paper No. 190, in press.

Weissman, P. R. 1982c. Astron. & Astrophys., in press.

Whipple, F. L. 1950. Astrophys. J., 110, 375.

THE USE OF TEPHRA STUDIES TO DETERMINE VOLATILE RELEASE DURING LARGE EXPLOSIVE VOLCANIC ERUPTIONS.

J.A. Wolff, Dept. of Geology, Imperial College, London SW7, U.K. & M. Storey, Geology Dept., Bedford College, Regent's Park, London NW1, U.K.

Outgassing at volcanoes occurs in two principal ways; via fumarolic activity and by direct release of magmatic volatiles during eruptions. Significant quantities of volatiles are released at the earth's surface by large-volume (defined for present purposes as $>10^7 m^3$ magma expressed as dense rock equivalent) explosive eruptions. Such events are characteristic of salic volcanoes in many tectonic situations, but are of infrequent occurrence (typically less than one per century per volcano). Thus in order to estimate the outward volatile flux due to eruptions at a given centre, it is necessary to employ methods applicable to the pyroclastic deposits which have resulted from prehistoric eruptions. This contribution describes a geological/petrological approach to the estimation of volatile output due to plinian eruptions, which produce extensive air-fall pumice deposits (1).

Accurate mapping of individual air-fall tephra blankets, to obtain a value for the total erupted volume of magma, is a necessary preliminary to the determination of total released volatiles. Volumes of air-fall pyroclastic deposits are usually estimated by means of an isopach map. However few deposits, unless erupted very recently, can ever be traced beyond the 10cm isopach, thus allowing no direct means of quantifying the considerable proportions of fine ash released during plinian eruptions to accumulate at considerable distances from source. Walker (2,3) has estimated the total erupted volumes of three large air-fall pumice deposits in New Zealand by a crystal concentration method. These estimates are matched by extrapolating mapped isopachs to a limiting thickness of 1mm, at a thinning rate given by the volume determination, as shown in Fig. 1 for the Taupo deposit. This thinning rate is found to be near-identical for the three New Zealand cases, and provides a method of estimating the volume of any plinian or similar deposit given sufficient near-source isopach data (e.g. ref. 4). This is particularly valuable as the more rigorous crystal concentration method can only be applied to optimum cases. We have therefore taken data on several deposits and plotted them on an area vs. thickness diagram (examples shown in Fig. 1) in order to obtain total erupted magma volume figures which take the fine ash component into account.

For fall deposits it is possible to estimate magmatic volatile contents from field data. Wilson and co-workers (5,6) have shown that the "muzzle velocity" of an explosive eruption depends on the mass eruption rate and magmatic volatile content (Fig. 2). However, dependence on eruption rate is very weak for the range of plinian eruption conditions (p on Fig. 2), and thus volatile content, assumed to be entirely water, can be estimated from muzzle velocity. The error due to variations in the volatile component composition is negligible if H_2O is >80% of the total. Muzzle velocity, μ, is given by (ref. 7): $(8gr_o\sigma_o)/(3C\rho) = \mu^2$ where r_o, σ_o are respectively the radius and density of the largest erupted clast, C is the drag coefficient, and ρ is the effective gas density in the volcanic vent (values of ρ are tabulated by Wilson, ref. 7). The required data,

the size and density of the largest erupted clast, may be found by extrapolation of the range dependence of clast size. Data on the three largest accessory lithic fragments (for which σ = 2.5 gcm^{-3}) at any one locality exist for several mapped deposits in the literature and an example is given in Fig. 3. The extrapolation is of the largest measured fragments. The proportion of very large fragments in these deposits is often small and thus there is a considerable error on this extrapolation. Experience shows that an error of ± a factor of 4 on the estimated largest clast size is applicable, giving an uncertainty of ± 30% relative on the final deduced volatile content of the magma. Where the field data points are closely spaced, the error is reduced. Results for selected pumice deposits are given in Table 1.

A petrological method of determining pre-eruptive magmatic volatile species in the system H-O-S in equilibrium with the phenocryst assemblage of the pumice has also been used. We have described this method, and presented data for pumice layers on some Atlantic Ocean alkaline volcanoes, elsewhere (8); the essentials are summarised here. T and fO_2 are calculated from coexisting Fe-Ti oxide compositions. fH_2O is estimated from the reaction between biotite, sanidine and magnetite, while pyrrhotite composition yields a value for fS_2. fH_2, fH_2S, fSO_2 and fSO_3 are then found by combining data on the other gas species. Magmatic water content was estimated assuming PH_2O = Ptotal; agreement with values derived from field data is good (8).

The quantitative volcanological data required for calculation of volatile output rates exist for very few salic volcanoes. We have calculated first-approximation magmatic water output rates for three volcanic islands in the Atlantic Ocean (Table 2). A possible correlation between total salic magma output (lavas, essentially water-free at eruption, plus pyroclastics) , water output, and magma composition (specifically, the degree of silica saturation) is apparent. Realisation of the significance of this correlation must await the acquisition of similar data from other centres, but Table 2 gives us a tantalising hint of the fundamental connection between availability of volatiles and the nature and intensity of volcanism.

REFERENCES

(1). Wright, J.V. et al., 1980. J. Volcan. Geotherm. Res. 8, 315-336.
(2). Walker, G.P.L., 1980. J. Volcan. Geotherm. Res. 8, 69-94.
(3). Walker, G.P.L., 1981. N.Z. J. Geol. Geophys. 24, 305-324.
(4). Walker, G.P.L. et al., 1981. Geol. Rundsch. 70, 1100-1118.
(5). Wilson, L., 1980. J. Volcan. Geotherm. Res. 8, 297-313.
(6). Wilson, L. et al., 1980. Geophys. J. R. Astron. Soc. 63, 117-148.
(7). Wilson, L., 1976. Geophys. J. R. Astron. Soc. 45, 543-556.
(8). Wolff, J.A. & Storey, M., in press. Contrib. Mineral. Petrol.
(9). Booth, B. & Walker, G.P.L., in preparation.
(10). Bloomfield, K. et al., 1977. Geol. Rundsch. 66, 120-146.
(11). Self, S., 1976. J. Geol. Soc. Lond. 132, 645-666.
(12). Booth, B. et al., 1978. Phil. Trans. R. Soc. Lond. A288, 271-319.
(13). Walker, G.P.L. & Croasdale, R., 1971. J. Geol. Soc. Lond. 127, 17-55.
(14). Wilson, L., 1978. in Thera and the Aegean World, Proc. 2nd Int. Conf., pp.221-228.

Table 1. Magmatic water contents and total water released during eruption*

Deposit	muzzle velocity, m/s	weight % magmatic water	erupted magma volume, km^3	total water released, kg
Fogo A	520	6.5	0.55	8.9×10^{10}
Fogo B	470	5.7	0.14	2.0×10^{10}
Fogo C	400	4.5	0.05	5.6×10^{9}
Fogo 1563	415	4.8	0.14	1.7×10^{10}
Fogo Congro	460	5.5	0.01	1.4×10^{9}
Terceira B	500	6.3	0.27	4.3×10^{10}
Terceira E	460	5.5	0.08	1.1×10^{10}
Terceira F	390	4.3	0.04	4.3×10^{9}
La Primavera B	>340	>3.5	14	$>1.2 \times 10^{12}$
La Primavera D	>250	>2.5	0.6	$>3.8 \times 10^{10}$
La Primavera J	>210	>2.0	3.4	$>1.7 \times 10^{11}$
Upper Toluca	500	6.3	2.7	4.2×10^{11}
Minoan	300	2.9	16	1.0×10^{12}

*for several pumice deposits from Fogo volcano, Sao Miguel and Terceira, Azores (11-13), La Primavera and Toluca, Mexico (4, 10) and the Minoan eruption, Santorini (14). The quoted volume for the Minoan pumice includes ignimbrites and pyroclastic surge deposits formed during the same eruption. Water contents estimated on the basis of field data only.

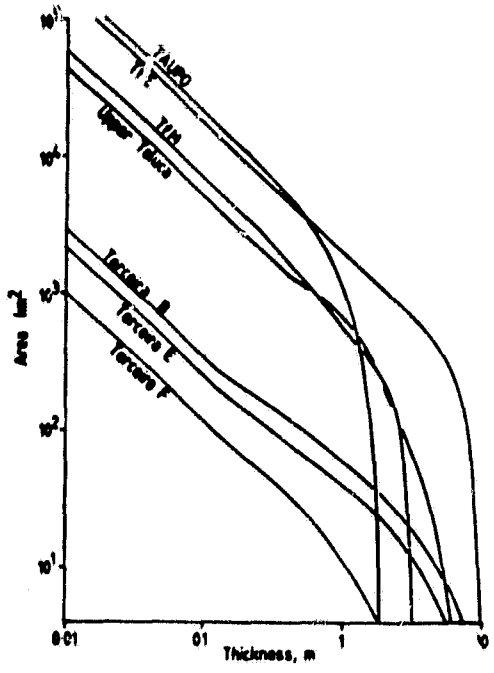

Fig. 1. Area vs. thickness plot for pumice fall deposits, the basis of the volume determinations. Taupo line is from Walker (2); distal portions of other deposits are extropolated parallel to Taupo. Tfe, Tf are from Tenerife, Canary Islands (9); Upper Touluca is from Mexico (10); Terceira B, E, F are from Terceira, Azores (11).

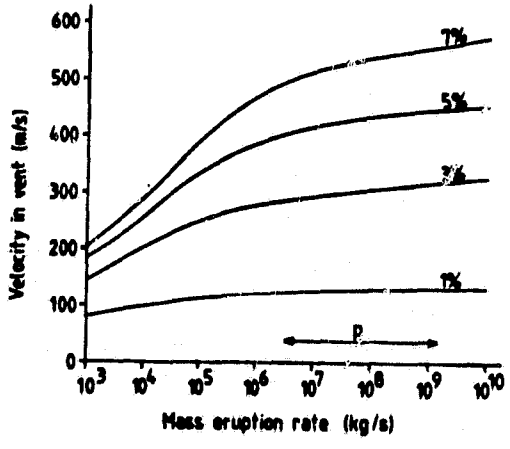

Fig. 2. Relationship between muzzle velocity and mass eruption rate of explosive eruptions for four values of magmatic water content, taken from Wilson et al. (6). p indicates range of plinian mass eruption rates.

Table 2. Magma and magmatic water output rates*

Island	Tenerife	Sao Miguel	Terceira
Salic magma type	Phonolite	Trachyte-comenditic trachyte	Comenditic trachyte-pantellerite
Salic magma output rate, km^3/century	0.13	0.059	0.023
Water output rate, liquid km^3/century	0.017	0.007	0.0007
Volume ratio pyroclastics/(pyroclastics lavas) for salic magma	0.8	0.88	0.23

*for Tenerife, Canary Islands and Sao Miguel and Terceira, Azores, based on field and petrological data given in refs. 8,9,11,12,13. Figures for Tenerife are approximate.

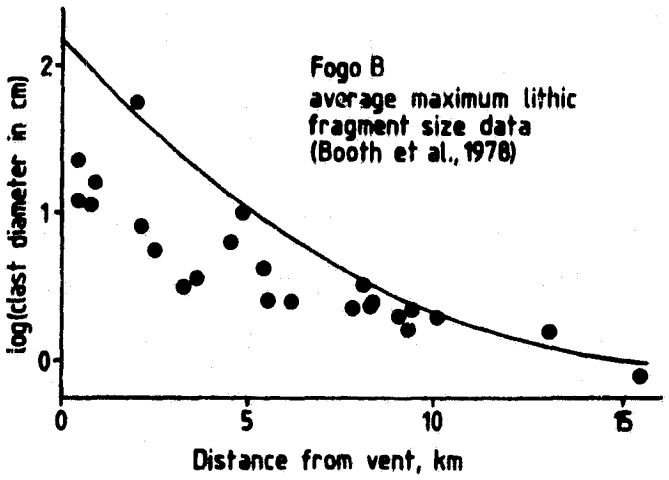

Fig. 3. Average of the three largest accessory lithic fragments found at a given locality plotted against distance from source, for a single pumice fall deposit from Sao Miguel, Azores (12). The largest measurements are extrapolated (solid line) to zero range to yield a value for the largest lithic clast which can just be supported by the eruption column at the vent; this forms the basis for the muzzle velocity calculation (7).

EVOLUTION OF SOLAR ULTRAVIOLET LUMINOSITY, K. J. Zahnle and J. C. G. Walker, Department of Atmospheric and Oceanic Science, The University of Michigan, Ann Arbor, Michigan 48109.

A wealth of astronomical evidence indicates that the young sun was much more active than it is today; i.e., it was a much greater source of energetic particles and radiation. Here we restrict our attention to a tentative history of the solar UV derived from observations of solar analogs, as being both better constrained and obviously consequential to a conference on solar system volatiles.

Solar UV evolution naturally divides into an earlier "T Tauri" stage and a later "main-sequence" stage - the transition occurring some 10^7 years after the sun's formation.

For main-sequence stars, relationships have been established between 1) stellar activity and stellar rotation, 2) activity and age, and 3) rotation and age. Here we combine the observed relation between rotation and age with the various relations between activity and rotation to build our history.

Figure 1 presents our much simplified history of the various source regions that give rise to the solar UV. The relation between x-ray emission (i.e., the corona) and rotation velocity is valid for a wide range of stars, and takes the form $L_X \propto v_r^2$. The transition region is the source of line radiation by highly ionized species such as CIV λ1549. The relations between these lines and rotation take the form $L_t \propto v_r^s$, where $1.5 \lesssim s \lesssim 2.0$. The importance of the transition region should also roughly correlate with the helium lines and the Ly continuum - i.e., it should reflect the EUV ($\lambda \lesssim 1000$Å) flux (this radiation is astronomically unobservable owing to interstellar H). The chromospheric relationship ($L_c \propto v_r^{1.0}$), which is established both from UV and visible light observations, best describes UV from ~2000 >λ>~1500Å. Lyα (1216Å) is generated both by the chromosphere and the transition region, and hence its evolution should be somewhere in between curves 'c' and 't'. The photospheric evolution is indicative of solar flux for $\lambda \gtrsim 2000$Å.

Sunlike stars rotate more slowly as they age; empirically this has been described as $v_r \propto t^{-1/2}$, the angular momentum flowing away with the solar wind. This relation is implicit in the structure of fig. 1. It may be that only the outer layers of the star are effectively spun-down. Gough (1982) reviews evidence that the solar core rotates some six times faster than does the surface. If we assume that the sun once rotated rigidly at the core's angular velocity, an equatorial rotation velocity $v_r \approx 14$ km/sec is inferred and is indicated in fig. 1.

The extrapolation of solar activity back to its T Tauri stage (see fig. 1) is made simply by choosing representative observations of T Tauri stars made by the Einstein and IUE satellites. It is clear that the T Tauri sun would have had a profound impact on the evolving "solar" nebula and/or the evolving planetary atmospheres, if either existed at the time. In particular, EUV fluxes 10^4 times larger than those produced by the modern sun would have been very efficient at fueling the escape of massive hydrogen-rich atmospheres (e.g. Sekiya et.al.) or at fueling the removal of the leftover material in the solar nebula, performing a function once ascribed to the T Tauri wind.

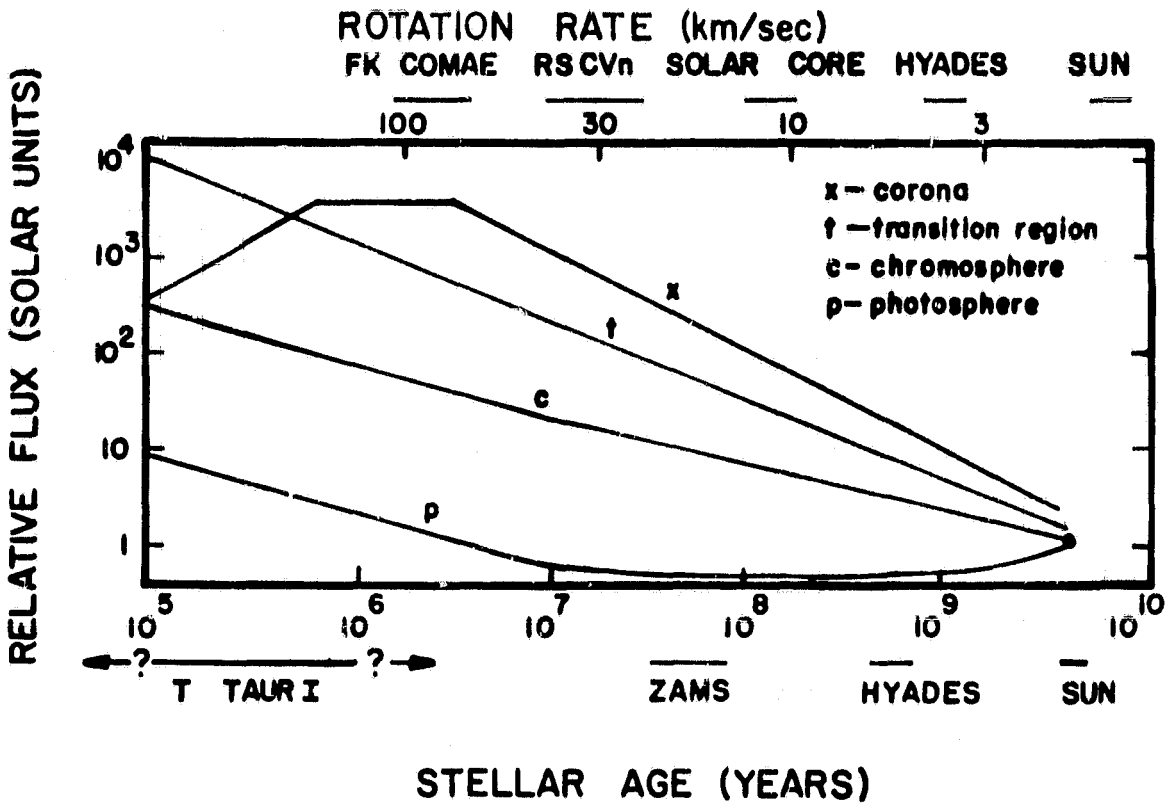

Figure 1. Simple picture history of solar ultraviolet. Labels on top axis refer to types of stars from which the rotation-activity relation has been derived, labels on bottom axis refer to types of stars for which the age-activity relation is found directly. ZAMS refers to the zero-age main-sequence sun.

References

Zahnle, K. J. and Walker, J. C. G. (1982) Rev. Geophys. and Space Phys., 20, p. 280-292.

Newkirk, G. (1980). The Ancient Sun, p. 293-320.

Gaustad, J. and Vogel, S. (1982). Origins of Life, in press.

Feigelson, E. (1982). Icarus, in press.

Gough, D. O. (1982). Nature, 298, p. 334-339.

Sekiya, M., Nakazawa, K., and Hayashi, C. (1982). Prog. Theor. Phys., 64, p. 1968-1985.

MANTLE DIFFERENTIATION AND CRUSTAL GROWTH: AN ISOTOPIC VIEWPOINT.

Alan Zindler[1], Steve Goldstein[1], and Emil Jagoutz[2] (1-Lamont-Doherty Geological Observatory of Columbia University, Palisades, New York 10964; 2-Max Planck Institute fur Chemie, Saarstrasse 23, Mainz, West Germany.)

Recent geochemical modelling of mantle differentiation and crustal growth (1-5) has suggested that Nd and Sr isotopic variations in young mantle-derived rocks may be explained by mixing of two mantle components, "MORB-type" or depleted mantle material and undifferentiated or slightly enriched mantle material. In this context, apparently enigmatic variations in Pb isotope ratios have been interpreted as indicating that the U-Th-Pb system has undergone a more complex evolution in the earth than either Sm-Nd or Rb-Sr. As an alternative, we have suggested that variations in Nd, Sr, and Pb isotopic compositions of mantle-derived rocks indicate the existence of at least three chemically independent mantle components (see (6) for a detailed discussion of some of the ideas presented here).

The first order difference between the two and three component models is not simply the number of mantle components invoked, for any subdivision of the mantle into two, three, or n components is necessarily a simplification of the real situation. The basic difference lies in the nature of the mechanisms which must be called on to explain the differentiation of the mantle into its major observable components. Processes which involve the mobilization of silicate liquids or silica-rich fluids within the mantle are thought to fractionate parents from daughters in each of the isotope systems under consideration. Therefore, to propose that, in a gross sense, Nd and Sr isotopic variations may be explained by two mantle components while three or more components are required by Pb isotope variations is to imply that some geochemically active mantle process causes severe fractionations of U and Th from Pb without significantly affecting Rb/Sr and Sm/Nd ratios, and furthermore, that this process is not one governed solely by solid-liquid-fluid equilibria in a silicate system. Based on this kind of reasoning, several authors (1, 9-11) have proposed that Pb has been transferred from the mantle to the core in a sulfide phase throughout geologic time, causing a progressive increase in mantle U/Pb and Th/Pb ratios. Because the other elements under consideration are not chalcophile in nature, their relative abundances in the mantle will not have been affected by this process. In contrast, if Nd, Sr, and Pb isotopic variations support the existence of more than two mantle components, then fractionations of all three parent-daughter systems may conceivably be in response to magmatic or metasomatic processes operating within the mantle without calling on a special process to fractionate U and Th from Pb.

We have examined mantle Nd, Sr, and Pb isotopic variations in multi-dimensional space in order to investigate systematics which may be obscured in two-dimensional variation diagrams. In three, four, or five dimensions, average isotopic compositions for individual ocean islands or island groups and mid-ocean ridges define a planar array with a high degree of precision (Fig. 1) and indicate that mantle isotopic variations are best described by mixing between three chemically independent mantle components. These results suggest that: 1) processes which involve the mobilization of silicate liquids or silica-rich fluids within the mantle, such as metasomatism or magma generation, can account for differentiation of the three isotope systems without calling on a special process to produce apparently complex Pb isotope variations; and 2) mass-balance arguments which have been used to support convective isolation of the lower mantle (2-4) (and the resulting chemical stratification of the mantle) are not valid, due to the positive identifica-

tion of an additional important mantle component.

Recognition of these systematics in the mantle places important constraints on the evolution of the crust-mantle system. A model has been developed which describes transport between a depleting MORB-type mantle component, the continental crust, and a high U/Pb mantle component, most clearly observed at St. Helena. An additional mantle component is assumed to be relatively undifferentiated. A Monte Carlo approach is used to investigate the effects of varying input parameters through geochemically reasonable ranges.

This modelling has shown that: 1) successful solutions may be generated with the total mass of interactive mantle ranging from 0.3 to 1.0 times the total mantle (Fig. 2; this is independent of the mass assigned to the high U/Pb component); 2) the high U/Pb component is chemically similar to basalt (Fig. 3) and must be generated primarily during the latter half of earth history (if this component is subducted ocean crust, the oldest portion must have been efficiently re-mixed into the mantle; and 3) "J-type" or future leads observed in oceanic basalts may be generated by mixing "B-type" depleted mantle with "J-type" (high U/Pb) mantle and with undifferentiated mantle which lies along the geochron.

References: 1. Allegre, C.J. (1982) Tectonophysics 81, 109; 2. O'Nions, R.K. et al. (1979) J. Geophys. Res. 84, 6091; 3. Jacobsen, S.B. and Wasserburg, G.J. (1979) J. Geophys. Res. 84, 7411; 4. DePaolo, D.J. (1980) GeochimCosmochim. Acta 44, 1185; 5. Anderson, D.L. (1982) Earth Planet. Sci. Lett. 57, 1; 6. Zindler, A. et al. (1982) Nature, in press; 7. L-DGO unpublished data; 8. White, W.M. and Hofmann, A.W. (1982) Nature 296, 821; 9. Vidal, P. and Dosso, L. (1978) Geophys. Res. Lett. 5, 169; 10. Dupre, B. and Allegre, C. J. (1980) Nature 286, 17; 11. Allegre, C.J. et al. (1980) Phil. Trans. R. Soc. Lond. A. 297, 447.

Fig. 1

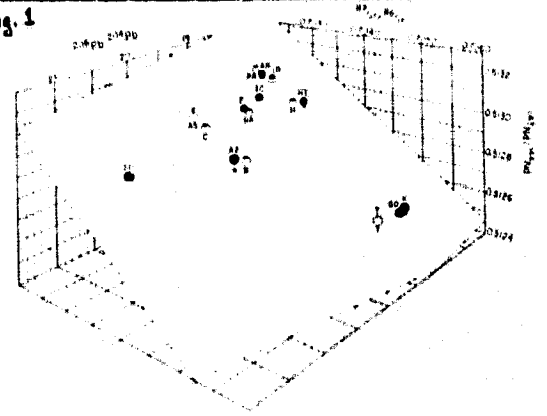

FIGURE 1. THREE-DIMENSIONAL PLOT OF AVERAGE SR, ND, AND PB ISOTOPE RATIOS FOR BASALTS FROM OCEAN ISLANDS AND RIDGES. THE BEST-FIT PLANE IS SHOWN. CLOSED AND OPEN SYMBOLS LIE ABOVE AND BELOW THE "MANTLE PLANE", RESPECTIVELY. LINES CONNECTING THE POINTS TO THE PLANE ARE PARALLEL TO THE ND AXIS AND INDICATE THOSE POINTS WHICH DO NOT INTERSECT THE PLANE. LOCALES ARE AS FOLLOWS: AR = MAR; PR = EPR; IR = INDIAN OCEAN RIDGES; IC = ICELAND; HI = HAWAIIAN ISLANDS; H = HAWAII; E = EASTER ISLAND; GA = GALAPAGOS; AS = ASCENSION; C = CANARIES; AZ = AZORES; R = REUNION; SH = ST. HELENA; T = TRISTAN; GO = GOUGH; K = KERGUELEN. DATA ARE FROM THE LITERATURE.

FIGURE 2. VARIATION DIAGRAM OF ND VS. SR ISOTOPE RATIOS. FIELD OCCUPIED BY AVERAGE DATA POINTS IS SHADED AND SHOWN FOR REFERENCE. SUCCESSFUL SOLUTIONS FROM MONTE CARLO MODELLING ARE SHOWN TO BE COMPATIBLE WITH MANTLE ARRAY OF DATA, REGARDLESS OF THE PERCENTAGE OF INTERACTIVE MANTLE SPECIFIED.

FIGURE 3. CONCENTRATION RESULTS FROM MONTE CARLO MODELLING SHOWING FIELDS FOR THIS CONTINENTAL CRUST AND MANTLE COMPONENTS. DATA ARE NORMALIZED TO C1 CHONDRITE VALUES. A FIELD FOR AVERAGE MORB IS SHOWN TO COINCIDE WITH THE MODEL RESULTS FOR COMPONENT 3, THE HIGH U/Pb MANTLE COMPONENT, PROVIDING SUPPORT FOR THE SUBDUCTED OCEAN CRUST AS COMPONENT 3 HYPOTHESIS.

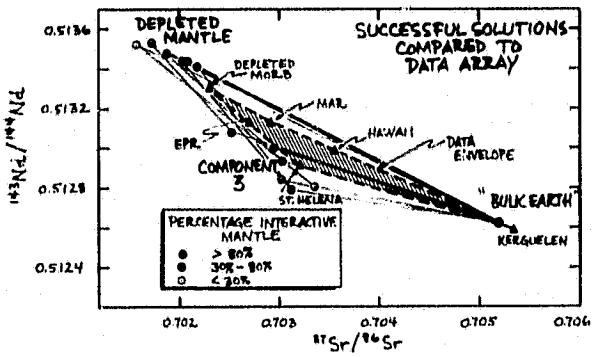

Fig. 2

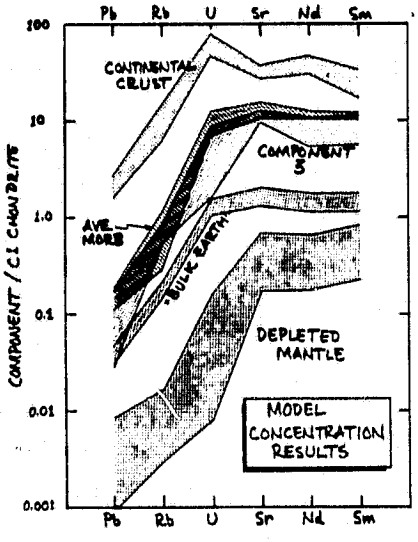

Fig. 3

List of Registered Attendees

Thomas J. Ahrens
California Institute of Technology

E. C. Alexander
University of Minnesota

C. J. Allègre
Université de Paris

Lewis D. Ashwal
Lunar and Planetary Institute

B. Barraclough
University of California, Los Angeles

M. E. Baur
University of California, Los Angeles

W. Beck
University of Minnesota

Richard H. Becker
University of Minnesota

T. J. Bernatowicz
Washington University

David C. Black
NASA Ames Research Center

Art Boettcher
University of California, Los Angeles

Penelope J. Boston
University of Colorado

Y. Bottinga
Université de Nice

G. W. Brass
University of Miami

Henry Brinton
NASA Headquarters

Kevin Burke
Lunar and Planetary Institute and
State University of New York, Albany

A. G. W. Cameron
Harvard University

Michael Carr
United States Geological Survey

Patrick M. Cassen
NASA Ames Research Center

Sherwood Chang
NASA Ames Research Center

Robert N. Clayton
Enrico Fermi Institute

Stephen M. Clifford
University of Massachusetts

M. Condomines
University of Cambridge

P. Dawson
Iowa State University

David J. Des Marais
NASA Ames Research Center

L. Dosso
University of Minnesota

Alfred G. Duba
Lawrence Livermore National Laboratory

P. England
Harvard University

Fraser P. Fanale
Hawaii Institute of Geophysics

Bruce Fegley
Massachusetts Institute of Technology

David E. Fisher
University of Miami

J. Fox
Smithsonian Astrophysical Observatory

Urs Frick
University of Minnesota

Everett K. Gibson, Jr.
NASA Johnson Space Center

P. K. Haff
California Institute of Technology

Michael D. Higgins
McMaster University

Sarah Hoffman
Oregon State University

R. D. Holmes
Australian National University

Donald M. Hunten
University of Arizona

G. Huss
University of Minnesota

William M. Irvine
University of Massachusetts

E. Ito
University of Minnesota

Bruce M. Jakosky
California Institute of Technology

W. J. Jenkins
Woods Hole Oceanographic Institute

D. Johnston
University of Minnesota

James F. Kasting
NASA Ames Research Center

John F. Kerridge
University of California, Los Angeles

S. Kumar
USC Center for Space Sciences

M. D. Kurz
Université de Paris

Philippe Lambert
NASA Johnson Space Center

Manfred A. Lange
California Institute of Technology

R. Luth
University of California, Los Angeles

Oliver Manuel
University of Missouri, Rolla

Kurt Marti
University of California, San Diego

T. Masterson
Iowa State University

E. A. Mathez
University of Washington

C. McKay
NASA Ames Research Center

H. Mizuno
Carnegie Institution of Washington

John W. Morgan
United States Geological Survey

C. Nelson
St. Cloud State University

L. Nicolayson
University of Wittwatersrand

A. Nier
University of Minnesota

Bert E. Nordlie
Iowa State University

Thomas L. Norris
Los Alamos National Laboratory

Richard J. O'Connell
Harvard University

Tobias Owen
State University of New York, Stony Brook

Robert O. Pepin
University of Minnesota

Roger J. Phillips
Lunar and Planetary Institute and
Southern Methodist University

Frank A. Podosek
Washington University

James B. Pollack
NASA Ames Research Center

Michael J. Prather
Harvard University

George W. Reed, Jr.
Argonne National Laboratory

Steven M. Richardson
Iowa State University

M. Rodin
University of Minnesota

Malcolm J. Rutherford
Brown University

Motoaki Sato
United States Geological Survey

M. Schidlowski
Max-Planck-Institut fur Chemie

Peter H. Schultz
Lunar and Planetary Institute

T. J. Shankland
Los Alamos National Laboratory

Norman H. Sleep
Stanford University

Stephen P. Smith
University of California, Berkeley

S. Soter
Cornell University

Robert L. Staehle
Jet Propulsion Laboratory

Carol Stoker
University of Colorado

M. Storey
Bedford College, London

Darrell F. Strobel
Naval Research Laboratory

S. Ross Taylor
Australian National University

S. F. Trieben
Iowa State University

Karl K. Turekian
Yale University

G. Turner
Sheffield University

Paul R. Weissman
Jet Propulsion Laboratory

George W. Wetherill
Carnegie Institution of Washington

Jan Veizer
University of Ottawa

G. Visconti
University Dell'Aquila

K. J. Zahnle
University of Michigan

Alan Zindler
Lamont Doherty Geological Observatory

☆ U.S. GOVERNMENT PRINTING OFFICE: 1983 - 559 013-1834